
In-Situ Burning of Water-In-Oil Emulsions

**Chantal Guénette
Per Sveum
Sintef Applied Chemistry**

**Ian Buist
S. L. Ross Environmental Research**

**Torre Aunaas
Lina Godal
Sintef Applied Chemistry**

**Technical Report Series
94-001**

**Reprint of
Sintef Applied Chemistry
Report STF21 A94053**

DISCLAIMER

This report was prepared under a contract between NOFO and SINTEF Applied Chemistry. Funding partners with NOFO were The Marine Spill Response Corporation, Alaska Clean Seas, Chemische Betriebe Pluto, and AMOCO Eurasia. Publication of this report does not necessarily imply that the contents reflect the views and policies of MSRC, nor are there any MSRC endorsements.

REPORT AVAILABILITY

Copies of this report may be obtained from the Marine Spill Response Corporation at the following address:

Marine Spill Response Corporation
Research & Development
1350 I Street N.W., Suite 300
Washington D.C. 20005

CITATION

Suggested Citation:

Guénete, C., Sveum, P., Buist, I., Aunaas, T., and Godal, L. 1994 In-Situ Burning of Water-In-Oil Emulsions. SINTEF Report STF21 A94053, Reprinted as MSRC Technical Report Series 94-001, 139p.

**SINTEF Applied Chemistry**

Address: N-7034 Trondheim, Norway
Location: Gryta 2, Brattøra
Phone Aquaculture group:
+47 73 59 63 75
Phone Environmental group:
+47 73 59 20 80
Fax: +47 73 59 63 63
Telex: 55 620 sintf n

Enterprise no.: 948007029

REPORT

TITLE

IN-SITU BURNING OF WATER-IN-OIL EMULSIONS

AUTHOR(S)

Chantal Guénette, Per Sveum, Ian Buist,
Tore Aunaas and Lina Godal

CLIENT(S)

NOFO, ACS, MSRC, Pluto, Amoco

FILE CODE

CLASSIFICATION

CLIENT'S REF.

Unrestricted**Andersen, McKenzie, Simmons, Tölle, Vanderkoy**

ELECTRONIC FILE CODE

PROJECT NO.

NO. OF PAGES/APPENDICES

9402131.rap

215283

139+app.

ISBN

PRICE GROUP

DISCIPLINARY SIGNATURE

82-595-8023-3

5

Per Sveum

REPORT NO.

DATE

RESPONSIBLE SIGNATURE

STF21 A94053

1994-06-10

Karl A. Almås, Division Director**ABSTRACT**

This report describes an experimental program on the in-situ burning of emulsions. This study is the third in a series of experimental studies on the in-situ burning of water-in-oil emulsions. The main objective of this study was to improve the capabilities and reduce the limitations of existing systems for igniting water-in-oil emulsions. A secondary objective was to study the feasibility of ferrocene as a soot reducing agent for oils and emulsions, and was incorporated into the experimental program. The experimental work for this research project was accomplished by conducting small-scale laboratory burns and heat transfer experiments, and by conducting meso-scale field experiments under Arctic springtime conditions.

Experiments conducted to study emulsion burning processes revealed that: in order to ignite and burn the emulsion, water is first removed from the emulsion and released mainly through evaporation and that the temperature of the water-in-oil emulsions does not exceed approximately 100°C.

Improvements were made to an existing igniter technology. It was found that the addition of emulsion breakers to gelled crude oil can increase the effectiveness of this igniter when dealing with emulsions with water contents greater than 50%.

Experiments with ferrocene show this compound to be an effective soot inhibitor when mixed with oil or emulsions at concentrations as low as 0.13 wt%. Ferrocene may have some effect on the burning process but further testing is required to confirm this.

KEYWORDS	ENGLISH	NORWEGIAN
GROUP 1	Environment	Miljø
GROUP 2	Oil spill	Oljeforurensning
SELECTED BY AUTHOR(S)	<i>In-situ</i> burning	Brenning
	Ignition	Antennelse
	Emulsions	Emulsjoner

PREFACE

This report describes an experimental program on the *in-situ* burning of emulsions. It is a technical report describing the work performed and the conclusions arising from the findings of this work.

This project was jointly funded by NOFO in Norway, Alaska Cleans Seas and Marine Spill Response Corporation in the United States, CHEMISCHE BETRIEBE PLUTO in Germany and AMOCO Eurasia in Canada.

The experimental work undertaken in this study was conducted by the Environmental Technology Group of SINTEF Applied Chemistry in Norway and by S.L. Ross Environmental Research Ltd, in Canada at the following three locations: the SINTEF Applied Chemistry laboratories in Trondheim, Norway, the S.L. Ross Environmental Research Ltd. laboratory in Ottawa, Canada and at the SINTEF Applied Chemistry field/laboratory facilities in Sveagruva, Svalbard.

ACKNOWLEDGEMENTS

The authors would like to thank the clients for their invaluable assistance in making this research program possible. In particular, thanks are extended to Aage Bjørn Andersen and Vidar Skogly of NOFO, Bruce McKenzie of Alaska Clean Seas, James Simmons of Marine Spill Response Corporation, Christian Tölle of PLUTO, Nick Vanderkooy of AMOCO Eurasia and Jack R. Gould for their support and advice during this research program.

We gratefully acknowledge the dedication and technical support received from Bror Johansen, Lillian Nergaard and Vigdis Kvam Johnsen of SINTEF Applied Chemistry and Jake Morrison of S.L. Ross Environmental Research Ltd.

Thanks also go to Jeff Woods, James McCourt and Tony Francelj who provided technical assistance during their university work-terms at S.L. Ross Environmental Research Ltd.

EXECUTIVE SUMMARY

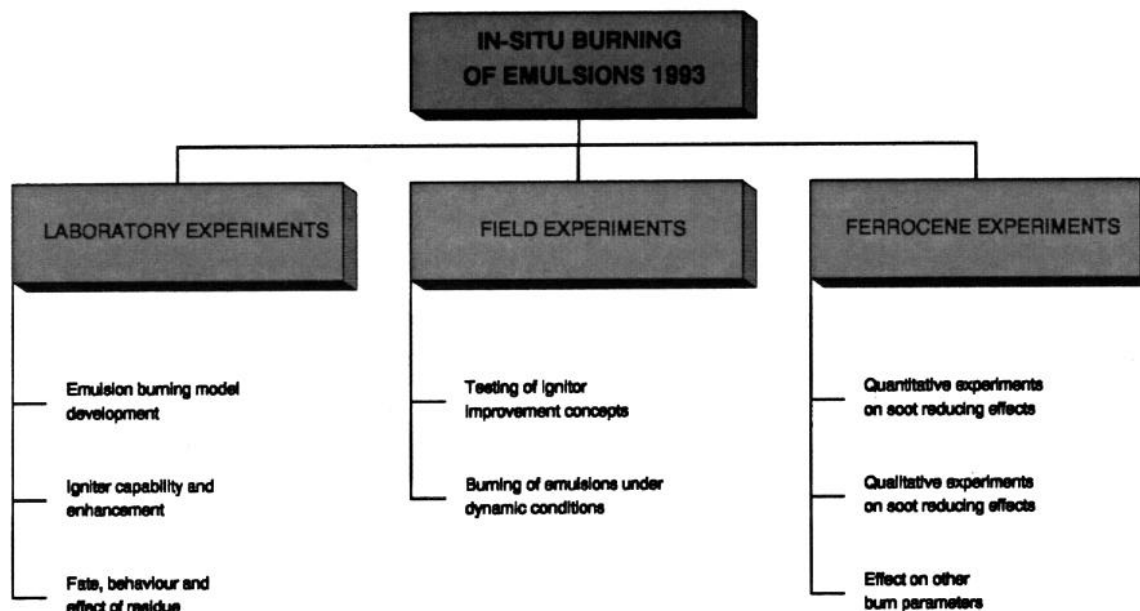
This study is the third in a series of experimental studies on the *in-situ* burning of water-in-oil (w/o) emulsions. The program was initiated in 1990 by NOFO and focused on the *in-situ* burning of oils in ice-infested waters. This program, starting with a comprehensive literature search on *in-situ* burning, provided some basic knowledge concerning *in-situ* burning with respect to feasibility and limitations. The first experimental study took place in 1991 and investigated the effects of varying water content and degree of evaporation on the *in-situ* burning of emulsions. The 1992 program expanded on the knowledge gained in the previous years by studying the effect of waves, ice and scaling on burning emulsions. The focus of the 1993 burning experiments was on methods of improving the capabilities and on reducing the limitations of the existing systems for igniting heavily emulsified water-in-oil emulsions *in-situ*.

The methods, experimental design, results, discussion and conclusions are presented and discussed in the report. Based on the findings from this study, recommendations concerning the future direction of research and development in the area of *in-situ* burning are put forward.

The main objective of this study was to improve the capabilities and reduce the limitations of existing systems for igniting water-in-oil emulsions. A secondary objective was to study the feasibility of ferrocene as a soot reducing agent for oils and emulsions, and was incorporated into the experimental program. These objectives were met by:

- 1./ developing models and conducting laboratory experiments to determine the physical processes involved in the *in-situ* burning of water-in-oil emulsions;
- 2./ conducting laboratory experiments to determine the capabilities and limitations of existing methods for igniting water-in-oil emulsions *in-situ*;
- 3./ conducting laboratory experiments to determine the effects of using gelled crude oil as an igniter for emulsions;
- 4./ conducting laboratory experiments to assess the efficiency of demulsifier addition (either prior to or during ignition); and,
- 5./ conducting field trials to confirm the laboratory findings.
- 6./ conducting laboratory experiments to quantitatively assess the effectiveness of ferrocene as a soot reducing agent, and determine if there are any impact on the burn process;
- 7./ conducting field experiments to confirm laboratory findings regarding the use of ferrocene on a meso-scale; and
- 8./ testing the toxicity of burn residues.

Due to the magnitude of this project and to the various areas of *in-situ* burning addressed in this work, this project was undertaken as five sub-projects. They are listed below with a brief description of each. The following chart depicts the project organization.



SUB-PROJECT 1: EMULSION BURNING MODEL DEVELOPMENT

This sub-project involved developing models of the *in-situ* burning of water-in-oil emulsions, testing their validity and refining them based on simple laboratory tests. Static (no burning) and dynamic (small-scale burns) experiments were carried out to generate data so that the models could be verified. The static experiments, conducted in a sealed aluminum metal box, consisted of exposing the surface to a constant heat source and recording the resultant change in temperature, water content and density. Ignition was prevented by purging the air from the apparatus with nitrogen. Statfjord crude was used for these experiments. Small-scale burns on the order of 40 and 75 cm² in diameter were conducted. Water, slick and air temperatures were recorded during these burns, and burn residue was collected and analyzed for its physical properties. Statfjord, Alaska North Slope and Avalon crudes were used at several degrees of evaporation and water contents. Conceptual, mathematical and statistical models were developed in this task, which describe the physical/chemical processes involved in the *in-situ* burning of emulsions on water.

SUB-PROJECT 2: IGNITER CAPABILITY AND ENHANCEMENTS

Existing methods for igniting oil on water were reviewed and the most promising one selected for testing and further improving. The selected method was the use of a Helitorch and gelled gasoline system. The experiments focused on improving the ignition capability of the ignition source itself - gelled gasoline, by testing the effect of using various additives (emulsion breakers and ferrocene) with the gasoline and by replacing the gasoline with crude oil. A series of small-scale experiments using heavily emulsified Statfjord, Avalon and Alaska North Slope crude oils were conducted.

SUB-PROJECT 3: EXPERIMENTAL FIELD WORK

The experimental work was undertaken in two parts:

i) Meso-scale field experiments were conducted in the frozen fjord near Sveagruva, Svalbard to test the improved igniter concepts studied in the laboratory and to verify the emulsions burning processes described in the modelling sub-project. The capabilities of these improved igniters were tested on evaporated Statfjord crude oil emulsions with water contents of 50 and 60%. The type and amount of additive combined with the gelled oil were varied and evaluated for their effectiveness in enhancing ignition and flame spreading.

ii) The second part of the field work, was a study of the ignition, combustion and residue remaining from a continuous burn of weathered crude oil and emulsions in a dynamic situation. Of particular interest, was the determination of whether or not heat radiated from a fire could ignite an otherwise unignitable emulsion drifting towards the fire. The fate and behaviour of the burn residue was also investigated. Experiments were conducted in a circulating flume cut into the ice, and fitted with a wave maker and current generator, which along with the presence slush ice, could simulate a range of environmental conditions. Metal and wood represented barriers.

SUB-PROJECT 4: EFFECT OF FERROCENE ON *IN-SITU* BURNING OF OILS AND EMULSIONS

One of the main restrictions for using *in-situ* burning as an operational tool to combat oil spills has been the problem of smoke production. Large amounts of dark smoke are generated when burning crude oil on water. In order for this method to be generally accepted as a countermeasure, this problem needs to be addressed and a solution found. Ferrocene has been widely used as a combustion promoter and soot reducing agent in diesel engines and home heating furnaces for many years and has recently been shown to be an effective soot suppressant in small-scale pool burning of crude oil experiments. Ferrocene was included in this experimental program both as a soot inhibitor and as a possible tool for enhancing the emulsion burning process. In this sub-project, a quantitative analysis of the effectiveness of ferrocene was made with fresh and emulsified crude oils. Field experiments were also conducted to qualitatively test the efficiency of ferrocene on a larger scale. The effects of ferrocene on other burn parameters, such as burn efficiency and ignition time were also studied. In addition, the toxicity of burn residue from crude oil and emulsion burns with ferrocene was determined.

SUB-PROJECT 5: FATE, BEHAVIOUR AND EFFECT OF BURN RESIDUE

The final acceptance of *in-situ* burning as a countermeasure for oil spills on water will not only depend on the feasibility of this clean-up technique, but also on the fate, behaviour and effect of the burn residue remaining following a burn operation. In this sub-project, burn residue collected during the laboratory and field experiments was characterized in terms of physical and chemical properties, as a function of both burn efficiency and the properties of the original oil. Selected residue samples were then subjected to toxicity analysis using the Skeletonema test, a routine test for evaluating the toxicity of drilling muds and chemical compounds used in the off-shore oil industry.

The general findings from this experimental program are summarized in the table below:

Major conclusions from the 1993 *in-situ* burning of emulsions program.

OBJECTIVE	CONCLUSIONS
<ul style="list-style-type: none"> conduct laboratory tests to determine physical processes involved when burning water-in-oil emulsions <i>in-situ</i>. 	<ul style="list-style-type: none"> water must be removed from the emulsion before ignition can occur; water is released mainly through evaporation; the temperature of w/o emulsions does not exceed approximately 100°C.
<ul style="list-style-type: none"> conduct laboratory tests to determine the capabilities and limitations of existing methods (i.e. Helitorch) for <i>in-situ</i> ignition of w/o emulsions. 	<ul style="list-style-type: none"> gelled gasoline is not an effective igniter for w/o emulsions, particularly when water content exceeds 50%; addition of emulsion breakers to gelled gasoline enhanced its ignition capability.
<ul style="list-style-type: none"> determine the effect of using gelled crude oil as an igniter for emulsions, and the effect of demulsifier addition. 	<ul style="list-style-type: none"> emulsion stability is a key factor; gelled crude oil is an effective igniter for emulsions with less than to 50% water; and with the addition of emulsion breakers up to 75% water (lab); the use of emulsion breakers enhances ignition and flame spreading (lab and field).
<ul style="list-style-type: none"> determine whether radiated heat from a burning slick is sufficient to ignite emulsions drifting towards a burn. 	<ul style="list-style-type: none"> a Statfjord crude emulsion with a water content of 50% was successfully ignited, at wind speeds of 10 m/s and in currents of up to 0.3 m/s.
<ul style="list-style-type: none"> determine the fate, behaviour and toxic effect (Skeletonema test) of burn residue. 	<ul style="list-style-type: none"> burn residue density does not exceed that of water; residue is not likely to sink due to inherent density properties but may be entrained under barriers and remain neutrally buoyant below the water surface; there were great difference in the toxicity between residue from different oil sources, but <i>in-situ</i> burning likely reduces or does not affect the toxicity of the oil or emulsions.
<ul style="list-style-type: none"> test ferrocene as a soot inhibitor for the <i>in-situ</i> burning of oil and emulsions. 	<ul style="list-style-type: none"> ferrocene is an effective soot inhibitor when mixed with oil or emulsions at concentrations as low as 0.13% by weight.
<ul style="list-style-type: none"> study the effect of ferrocene on other burn parameters and residue properties. 	<ul style="list-style-type: none"> ferrocene reduces the duration of the burn, but its effect on other burn parameters is not clear; ferrocene increases the viscosity and density of the burn residue but does not alter its toxicity.

TABLE OF CONTENTS

PREFACE

EXECUTIVE SUMMARY

	Page
1 INTRODUCTION	1
1.1 BACKGROUND	1
1.2 STUDY OBJECTIVES	2
1.3 PROJECT ORGANIZATION	2
2 MATERIALS AND METHODS	4
2.1 INITIAL OIL PROPERTIES	4
2.2 EMULSION PREPARATION FOR LABORATORY BURN EXPERIMENTS	4
2.3 EMULSION PREPARATION FOR FIELD EXPERIMENTS	10
2.4 METHODS FOR PHYSICAL-CHEMICAL ANALYSIS	11
3 MODEL DEVELOPMENT	13
3.1 METHODS AND EXPERIMENTAL DESIGN	13
3.1.1 Static heat transfer experiments	13
3.1.2 Small-scale burning experiments	18
3.1.3 Meso-scale model verification experiments	22
3.2 RESULTS AND DISCUSSION	22
3.2.1 Conceptual model	22
3.2.2 Mathematical model for steady state emulsion slick burning	26
3.2.3 Static heat transfer experiments	32
3.2.4 Small scale burning experiments	36
3.2.4.1 Ignition and burning of Avalon crude emulsions	36
3.2.4.2 Ignition and burning of Statfjord crude emulsions	47
3.2.4.3 Ignition and burning of Alaska North Slope emulsions	60
3.2.5 Statistical model	67
4 LABORATORY STUDIES ON THE LIMITATIONS OF AND IMPROVEMENTS TO EXISTING IGNITION TECHNIQUES	72
4.1 METHODS	72
4.2 RESULTS AND DISCUSSION	72
4.2.1 Laboratory evaluation of selected techniques	72
4.2.2 Recommended improvements	73
4.2.3 Laboratory tests of igniter capability and enhancement	76
4.2.3.1 Gelled gasoline capabilities and limitations	76
4.2.3.2 Gelled crude capabilities and limitations	76
4.2.3.3 Emulsion breaker addition to the slick prior to ignition	76
4.2.3.4 Emulsion breaker addition to the igniter	77
4.2.3.5 Ferrocene addition to the igniter	78
4.2.3.6 Emulsion breaker plus ferrocene addition to the igniter	78
4.2.3.7 Igniter flame temperatures	78
4.2.3.8 Summary	80

5 FIELD EXPERIMENTS	81
5.1 METHODS AND EXPERIMENTAL SET-UP	81
5.1.1 Verification of laboratory results	81
5.1.2 Burning of emulsions under dynamic conditions	84
5.2 RESULTS AND DISCUSSION	87
5.2.1 Verification of laboratory results	87
5.2.1.1 Emulsion burning process	87
5.2.1.2 Ignition improvement experiments	88
5.2.2 Burning emulsions under dynamic conditions	93
5.2.2.1 Ignition success	95
5.2.2.2 Effect on burning process	98
 6 EFFECT OF FERROCENE ON <i>IN-SITU</i> BURNING OF OILS AND EMULSIONS	 102
6.1 METHODS	102
6.1.1 Preliminary assessment of the use of ferrocene for <i>in-situ</i> burning	102
6.1.2 Quantitative laboratory tests of the smoke reducing effects of ferrocene	102
6.1.3 Field experiments with ferrocene as a soot inhibitor	105
6.2 RESULTS	106
6.2.1 Quantitative assessment of the smoke reducing effects of ferrocene	106
6.2.2 Qualitative assessment of the smoke reducing effects of ferrocene	108
 7 BURN RESIDUE	 113
7.1 METHODS	113
7.1.1 Fate and behaviour of residue in a current	113
7.1.2 Physical-chemical properties of burn residue	116
7.1.3 Toxicity of burn residue	116
7.2 RESULTS	118
7.2.1 Fate and behaviour of residue in a current	118
7.2.2 Physical-chemical properties of burn residue	122
7.2.3 Toxicity of burn residue	124
 8 CONCLUSIONS AND RECOMMENDATIONS	 135
8.1 CONCLUSIONS	135
8.2 RECOMMENDATIONS FOR FUTURE WORK	135
 9 REFERENCES	 137
 APPENDIX A	
Laboratory burn results	
APPENDIX B	
Ignition experiment results	
APPENDIX C	
Emulsion breaker experiment results	
APPENDIX D	
Results from laboratory burn experiments with ferrocene	

LIST OF FIGURES

	Page
Figure 1.1 Overview of emulsion burning project	3
Figure 3.1 Heat transfer apparatus	14
Figure 3.2 Thermocouple and sample port locations	15
Figure 3.3 Experimental set-up for laboratory burns	19
Figure 3.4 Laboratory burn	20
Figure 3.5 Thermocouples in flames	20
Figure 3.6 Thermocouple arrangement for small-scale laboratory burns	21
Figure 3.7 Requirements for ignition of an oil slick	23
Figure 3.8 Heat balance during <i>in-situ</i> burning	23
Figure 3.9 Heat balance on burning emulsion	25
Figure 3.10 Emulsion burning process	25
Figure 3.11 Model of emulsion burning illustrating processes considered in the heat balance	27
Figure 3.12 Temperature development and water content in the emulsion layer during the heat transfer experiment no. 22	33
Figure 3.13 Temperature development and water content in the emulsion layer during the heat transfer experiment no. 24	34
Figure 3.14 Heat transfer experiments: multiple regression models for water content in emulsions	35
Figure 3.15 Heat transfer experiments: multiple regression models for water content in emulsions	35
Figure 3.16 Ignition time vs. weathering - Avalon crude	37
Figure 3.17 Ignition time vs. emulsification - Avalon crude	38
Figure 3.18a Temperatures for emulsified Avalon burns	39
Figure 3.18b Temperatures for unemulsified Avalon burns	39
Figure 3.19 Burn efficiency vs. weathering - Avalon crude	41
Figure 3.20 Burn efficiency vs. emulsification - Avalon crude	43
Figure 3.21 Burning rate vs. fire diameter	44
Figure 3.22 Burn rate vs. weathering - Avalon crude	45
Figure 3.23 Burn rate vs. emulsification - Avalon crude	46
Figure 3.24 Ignition time vs. weathering - Statfjord crude	48
Figure 3.25 Ignition time vs. emulsification - Statfjord crude	49
Figure 3.26 Temperatures for emulsified Statfjord burns	52
Figure 3.27 Temperatures for emulsified Statfjord crude stabilized with Bunker C	53
Figure 3.28 Burn efficiency vs. weathering - Statfjord crude	55
Figure 3.39 Burn efficiency vs. emulsification - Statfjord crude	56
Figure 3.30 Burn rate vs. weathering - Statfjord crude	57
Figure 3.31 Burn rate vs. emulsification - Statfjord crude	59
Figure 3.32 Ignition time vs. weathering - Alaska North Slope crude	61
Figure 3.33 Ignition time vs. emulsification - Alaska North Slope crude	62
Figure 3.34 Burn efficiency vs. weathering - Alaska North Slope crude	63
Figure 3.35 Burn efficiency vs. emulsification - Alaska North Slope crude	64
Figure 3.36 Burn rate vs. weathering - Alaska North Slope crude	65
Figure 3.37 Burn rate vs. emulsification - Alaska North Slope crude	66
Figure 3.38 Multiple regression models for burn efficiency for Statfjord crude oil	69
Figure 3.39 Multiple regression models for burn rate for Statfjord crude oil	69
Figure 3.40 Multiple regression models for ignition time for Statfjord crude oil	70
Figure 3.41 Multiple regression models for time for initiation of the intense burn for Statfjord crude oil	70
Figure 3.42 Multiple regression models for the time for extinction of the burn for Statfjord crude oil	71

Figure 4.1	Burn efficiency vs. emulsification Alaska North Slope crude	74
Figure 4.2	Burn efficiency vs. emulsification Statfjord crude	75
Figure 4.3	Flame temperatures of various gelled fuel igniters	79
Figure 5.1	Large basin (20m ²) for 2000 l burns	83
Figure 5.2	Fresh Statfjord crude (100 l) used as igniter	83
Figure 5.3	Circulating flume tank with current and wave generators	85
Figure 5.4	Circulating flume schematic	85
Figure 5.5	Wave generator	86
Figure 5.6	Hydraulic power pack	86
Figure 5.7	Temperature profiles for experiment L1	89
Figure 5.8	Temperature profiles for experiment L2	90
Figure 5.9	Placement of igniters on 50% w/o emulsion slick	94
Figure 5.10	Comparison of demulsifier concentration in gelled oil igniters	94
Figure 5.11	Feeding emulsion to the burning slick	96
Figure 5.12	Burning of emulsion against a barrier	96
Figure 5.13	Burning of emulsion against a barrier - side view	97
Figure 5.14	Close-up of advancing emulsion drifting into ignited crude oil (Note release of water vapour from edge of ignited slick)	97
Figure 5.15	Temperature profiles for experiment F2	99
Figure 5.16	Temperature profiles for experiment F3	100
Figure 6.1	Preliminary burns with Statfjord crude and ferrocene	103
Figure 6.2	Air sampling arrangement	104
Figure 6.3	Filter samples from experiments 4.29 (top) and 4.30 (bottom)	104
Figure 6.4	Soot reducing effect of ferrocene	107
Figure 6.5	Effect of ferrocene on Statfjord crude burns	107
Figure 6.6	Effect of ferrocene on different burn phases	107
Figure 6.7	Small-scale burns with ferrocene (top:0% ferrocene; middle:0.25% ferrocene; bottom:2% ferrocene)	110
Figure 6.8	Experiment L1: 25% evaporated, 50% water-in-oil emulsion, 0% ferrocene	111
Figure 6.9	Experiment L2: 25% evaporated, 50% water-in-oil emulsion, 0.20% ferrocene	112
Figure 7.1	Circulating flume for the study of behaviour of residue in a current against a barrier	114
Figure 7.2	Circulating flume with residue	115
Figure 7.3	Exp. 4.01 - burn residue in flume at 0.25 m/s	120
Figure 7.4	Exp. 4.01 - burn residue in flume at 0.33 m/s	120
Figure 7.5	Exp. 4.61 - burn residue in flume at 0.2 m/s	121
Figure 7.6	Exp. 4.61 - burn residue in flume at 0.25 m/s	121
Figure 7.7	Growth inhibition (%) and calculated EC-values for the <i>in-situ</i> burn residue S1	126
Figure 7.8	Growth inhibition (%) and calculated EC-values for the <i>in-situ</i> burn residue S2	127
Figure 7.9	Growth inhibition (%) and calculated EC-values for the <i>in-situ</i> burn residue S3	128
Figure 7.10	Growth inhibition (%) and calculated EC-values for the <i>in-situ</i> burn residue S4	129
Figure 7.11	Growth inhibition (%) and calculated EC-values for the <i>in-situ</i> burn residue S5	130
Figure 7.12	Growth inhibition (%) and calculated EC-values for the <i>in-situ</i> burn residue F1	131
Figure 7.13	Growth inhibition (%) and calculated EC-values for the <i>in-situ</i> burn residue F2	132
Figure 7.14	Growth inhibition (%) and calculated EC-values for the <i>in-situ</i> burn residue F3	133

LIST OF TABLES

		Page
Table 2.1	Initial physical-chemical properties of test oils	4
Table 2.2	Emulsion formation tendency and stability test results at room temperature	5
Table 2.3	Physical/chemical properties of Statfjord crude oil and emulsions used in the small-scale laboratory burns	7
Table 2.4	Physical/chemical properties of Alaska North Slope crude oil and emulsions used in the small-scale laboratory burns	8
Table 2.5	Physical/chemical properties of Avalon crude oil and emulsions used in the small-scale laboratory burns	9
Table 2.6	Density of Statfjord crude oil and emulsions used in static heat transfer experiments	10
Table 2.7	Physical/chemical properties of Statfjord oils and emulsions used in the field experiments	11
Table 3.1	Experimental design in the static heat transfer experiment with radiant heat input of 3000 watts	17
Table 3.2	Experimental design in the static heat transfer experiment with initial slick thickness of 6 cm	17
Table 3.3	Comparison of Statfjord emulsion burn data with and without Bunker C added	51
Table 3.4	Statistical parameters for the multiple regression models; with emphasis on the statistically significant parameters	68
Table 5.1	Summary of experiments conducted to study the limitations and improvements of existing ignition techniques for water-in-oil emulsions	82
Table 5.2	Summary of field experiments to study emulsions burning against a barrier	84
Table 6.1	Summary of field experiments with ferrocene	105
Table 6.2	Results from small scale field experiments with ferrocene	108
Table 7.1	Burn residue selected for laboratory flume experiments	113
Table 7.2	Barrier depth and current velocity at which burn residue samples were lost beneath the barrier	119
Table 7.3	Density and viscosity of residue samples from selected field experiments with Statfjord crude oil	123
Table 7.4	Median effective concentrations (EC_{50}) for different <i>in-situ</i> burn residues on algae (<i>Skeletonema costatum</i>) growth rate inhibition	125
Table 7.5	Inhibition of the growth rates of <i>Skeletonema costatum</i> with residue from <i>in-situ</i> burn experiment S1	126
Table 7.6	Inhibition of the growth rates of <i>Skeletonema costatum</i> with residue from <i>in-situ</i> burn experiment S2	127
Table 7.7	Inhibition of the growth rates of <i>Skeletonema costatum</i> with residue from <i>in-situ</i> burn experiment S3	128
Table 7.8	Inhibition of the growth rates of <i>Skeletonema costatum</i> with residue from <i>in-situ</i> burn experiment S4	129
Table 7.9	Inhibition of the growth rates of <i>Skeletonema costatum</i> with residue from <i>in-situ</i> burn experiment S5	130

Table 7.10	Inhibition of the growth rates of <i>Skeletonema costatum</i> with residue from <i>in-situ</i> burn experiment F1	131
Table 7.11	Inhibition of the growth rates of <i>Skeletonema costatum</i> with residue from <i>in-situ</i> burn experiment F2	132
Table 7.12	Inhibition of the growth rates of <i>Skeletonema costatum</i> with residue from <i>in-situ</i> burn experiment F3	133

GLOSSARY

Burn efficiency: This is defined as the initial mass percent of oil (excluding water in the case of emulsions) consumed during a burn and can be expressed as:

$$\text{burn efficiency(\%)} = (\text{initial oil mass} - \text{residue mass}) / \text{initial oil mass} \times 100$$

Burn rate: The regression rate of oil burning from a slick (i.e., mm of oil per minute) is defined as the thickness of oil consumed during a burn (excluding emulsion water) less the thickness of residue remaining after a burn divided by the length of the burn.

Extinction: The moment when all flames have extinguished.

Extinction time: The elapsed time to extinguishment of the burn.

Igniter (or ignition source): The heat and flame source used to ignite the oil or emulsion slick

Ignition time: The ignition time for an experimental burn was defined as the time for the flames to cover the entire slick surface area.

Intense burn phase: This phase is characterized by vigorous burning of the oil slick, a noticeable increase in flame height, an increase in noise level and bright droplets ejected into the flame.

Preheat time: The time from igniter ignition to the beginning of flame spread away from the igniter edge.

Emulsion stability: Emulsions were considered stable if they did not break and separate into two phases within one week.

Wind herding effect: Increase in slick thickness resulting from the wind pushing oil towards a barrier.

1 INTRODUCTION

1.1 Background

The development of systems for igniting oil on water has been an ongoing process for many years. Efforts began in Canada in the mid-70s with studies of oil burning on Arctic melt pools in springtime and the testing of various ignition compounds (Energetex 1977 and 1978). These efforts resulted in the development of the "Dome" igniter produced by Energetex Engineering (Energetex 1980). About the same time the "DREV" igniter was developed (Meikle 1981, Twardawa and Couture 1980). Both of these were hand-held devices designed to be initiated then thrown from a slowly-moving helicopter onto oiled melt pools on ice. Although effective, their high unit and storage costs and finite shelf life (approximately 5 yrs) were drawbacks to their widespread use; only the "Dome" igniter is still commercially available.

The Alaskan oil industry, in a 1986 study of the state-of-the-art (Allen 1986), assessed five aerial ignition systems and concluded that the "Helitorch" manufactured by Simplex in Seattle, showed considerable promise. The device was originally designed for and used in fighting forest fires. The system consists of a drum, pump, nozzle and propane ignition system slung beneath a helicopter and controller by the pilot; the fuel is gelled gasoline (napalm).

Subsequently, the Helitorch was extensively tested on oil spills and slightly modified for operational use (Spiltec 1987). Tests showed that the Helitorch could successfully ignite 2-week weathered (but unemulsified) Prudhoe Bay crude oil at sub-freezing temperatures in winds up to 30 km/hr (Spiltec 1987). Other tests with igniters simulating the Helitorch (Buist 1989) showed that the upper limit for igniting Hibernia crude oil emulsions was between 25 and 50% water content.

A plastic bag containing gasoline gelled with Simplex's "Surefire" gelling agent was used to ignite 30 to 40 hr weathered, 20 to 30% (estimated) water-in-oil emulsion during the early stages of the response to the "Exxon Valdez" spill; subsequent attempts at ignition of heavily emulsified "Exxon Valdez" oil failed (Allen 1990).

Field experiments in June 1992 at Sveagruva, Svalbard, Norway have indicated that the use of gelled crude oil instead of gelled gasoline as the fuel may enhance capabilities for igniting emulsions because crude oil burns much hotter than gasoline (Bech et al. 1992) and that the inclusion of demulsifying surfactants in the gelled fuel may promote emulsion breakage and even better ignition performance (Sveum and Buist 1991). The concept of applying emulsion breakers to a spill *in-situ*, then igniting it (the so-called "break-and-burn" approach) has been suggested before during a workshop sponsored by ESRF in Canada as a promising area requiring R&D (S.L. Ross 1990).

In addition to knowledge about burn processes and the operational aspects connected with *in-situ* burning, the authorities and the public also need to know about possible environmental consequences. Of concern, are the air emissions from burning crude oil and the fate and behaviour of the burn residue.

To study the production and effects of the smoke a series of projects have been conducted, and are still going on, predominantly in North America. In the late 70's and early 80's some research was conducted on the properties and characteristics of the residue remaining on the water after an *in-situ* burn of oil in ice. These burns involved slick thickness on the order of 1 cm. With the development of fire containment booms it is now possible to conduct burns with oil thicknesses of 10 or more centimetres. The residue from this thickness may be different from the residue from 1 cm burns. The properties and characteristics of this type of residue needs to be studied to determine its fate (i.e. sinking and possible environmental effects). Residue that is not collected will ultimately either sink (Lee et al. 1989), degrade or reach a coast and contaminate a shoreline. The rate of residue biodegradation and physical removal

of the sticky oil from a beach is slow. Beach material will adhere to the oil and be incorporated into it which might promote burial of the oil. Once buried in the sediment, biological activity is further reduced due to lower oxygen availability and the possibility of physical removal due to wave activity is limited.

In connection with the M/T Haven accident in 1991 large amounts of oil burned on or near the vessel. After the clean-up operations it was reported that large amounts of oil and burn residue had sunk and burned and unburned oil was discovered along the French and Italian coasts (Moller 1992).

One of the disadvantages of *in-situ* burning as a clean-up technique for oil spills is the copious amount of dark smoke generated. This has been one of the major factors in preventing this method from being accepted on an operational basis. Over the past few years, soot reducing agents have been investigated to reduce the smoke emissions during *in-situ* burning of oil slicks. Ferrocene was included as part of the emulsion burning program for 1993, and experiments were conducted using this product both in the laboratory and field studies.

A comprehensive state-of-the art review on *in-situ* burning is given by Buist et.al (1994, in prep).

1.2 Study objectives

The objectives of the proposed project were to study the burning of water-in-oil emulsions and research techniques for extending the existing capabilities for igniting them successfully *in-situ*. In addition the composition, properties and fate and behaviour of burn residues from laboratory experiments was studied.

1.3 Project organization

This study encompasses a broad range of issues dealing with the *in-situ* burning of oil on water as a response to oil spills. In order to achieve the objectives set out at the beginning of this project, the work was undertaken in six interrelated sub-projects. The six sub-projects, are shown in Figure 1.1.

The laboratory work comprised several detailed activities, some of them strongly integrated with the field activities. They included:

- conducting laboratory experiments to determine the physical processes involved in the *in-situ* burning of water-in-oil emulsions;
- conducting laboratory experiments to determine the capabilities and limitations of existing methods for igniting water-in-oil emulsions *in-situ*; efforts were made to categorize burning effectiveness with oil properties;
- conducting laboratory experiments to determine the effects of using gelled crude oil as an igniter for emulsions;
- conducting laboratory experiments to assess the efficiency of demulsifier addition (either prior to or during ignition);
- conducting medium-scale field experiments to extend the laboratory findings to a larger scale;
- measuring oil/emulsion slick temperatures and underlying water temperatures during selected experiments in both the laboratory and field studies;
- performing physical-chemical analyses of burn residues;
- testing the toxicity of burn residues;
- laboratory studies of the physical/chemical fate of burn residues;
- determining whether radiated heat from a burning slick is sufficient to ignite emulsions drifting towards the burn; and

- studying the fate and behaviour of residue in a current.

The following study goals were common to all field experiments:

- conduct experiments in open systems without artificial closed vessel heating effects;
- study heat transfer and measure heat transfer through the slick and underlying water;
- test residue for toxicity analysis; and
- study the smoke reducing effects of ferrocene.

In the study on the use of ferrocene during *in-situ* burning of oil and water-in-oil emulsions, the following goals were set:

- quantitatively assess the effectiveness of ferrocene as a soot reducing agent for the burning of fresh, weathered and emulsified crude oils in a controlled laboratory environment;
- qualitatively observe the effectiveness of ferrocene on smoke reduction of fresh, weathered and emulsified crude oils in small and meso-scale open system environments;
- assess the effect of ferrocene on other burn parameters such as ignition time, time to intense burn, burn rate and burn efficiency;
- study the effect of ferrocene on the heat transfer characteristics of burning crude oil and emulsions;
- test ferrocene as a potential additive to enhance the efficacy of igniters for use with water-in-oil emulsions; and
- compare the toxicity of residue generated from burns with ferrocene to that of residue generated from burns without ferrocene.

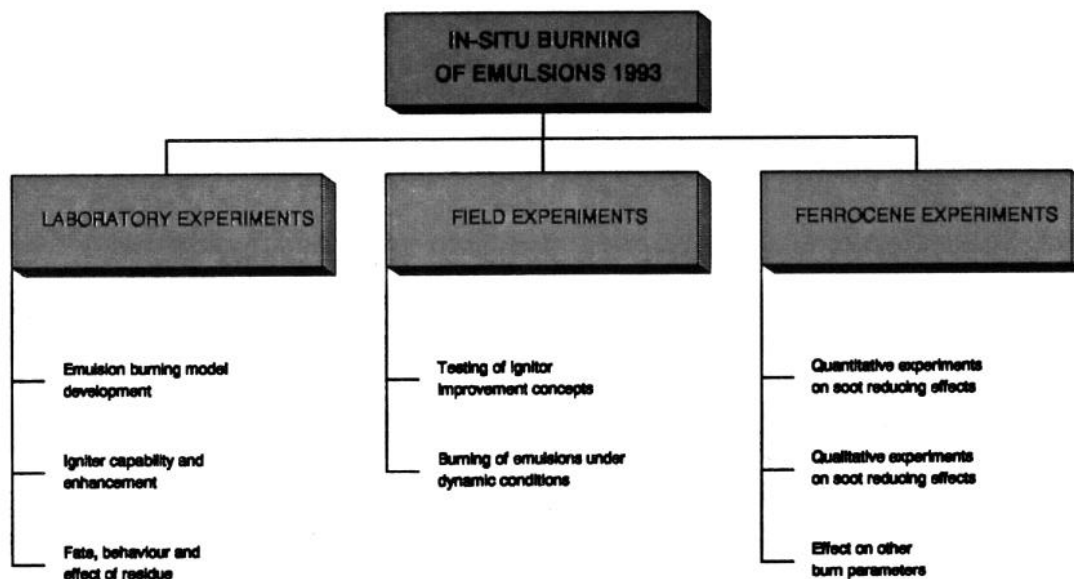


Figure 1.1 Overview of emulsion burning project

2 MATERIALS AND METHODS

This section gives the physical-chemical properties of the oils and emulsions used in all sub-projects. The methods of weathering and emulsifying the parent oils are described as well as the standard analytical methods used for all oil, emulsion and residue property analysis. These properties and methods are presented in this one section as they are shared by each sub-project. This is to avoid repetition from one sub-project to another. The methods and experimental designs particular to a given sub-project will be dealt with in each respective section.

2.1 Initial oil properties

Three different crude oils were used in this project. Avalon, Statfjord and Alaska North Slope crude were used for the small-scale laboratory burning experiments. Statfjord crude was used for the static heat transfer experiments and for the field trials. The following table gives the initial physical-chemical properties of these crude oils.

Table 2.1: Initial physical-chemical properties of test oils.

Test Oil	Density (g/cm ³)	Viscosity (cP at 6.5s ⁻¹)	Flash Point (°C)	Interfacial Tension (mN/m)	
				Oil/Water	Air/Oil
Avalon fresh	0.883 at 14.1°C	230 at 13.5°C	-3	16.4	38.9
Statfjord fresh	0.844 at 13.0°C	17 at 12.3°C	<-10	21.7	29.8
Alaska North Slope fresh	0.878 at 16.1°C	22 at 14.1°C	<-10	4.0	30.1

The test oils used in this project were prepared in such a way as to simulate slick conditions likely to be encountered on the sea surface at various times following a spill. In order to accomplish this, the oils were evaporated and emulsified using the methods described in the following sections.

2.2 Emulsion preparation for laboratory burn experiments

Three oils, Statfjord crude, Alaska North Slope and Avalon were used for the small-scale laboratory burn experiments. Each test oil was artificially evaporated to two or three degrees of weathering by sparging compressed air into the bottom of a 205 l drum containing the oil. The Avalon and Alaska North Slope oils were evaporated to approximately 10 and 20% loss by volume evaporated (12.7% and 20% and 10.8% and 17.4% respectively - the differences being due to the volatility of the oils). The Statfjord crude oil was weathered to 12.9%, 19.6% and 30.9% loss by volume.

Each of the fresh and weathered oils was subjected to a standardized emulsification tendency and stability test (Zagorsky and Mackay 1983, Environment Canada 1992). The results are shown in Table 2.2.

Table 2.2: Emulsion formation tendency and stability test results at room temperature ($\approx 20^{\circ}\text{C}$)

Oil	Volume % Evaporated	F_o	F_{∞}
Alaska North Slope	0	0.0	0.0
	10.8	0.0	0.0
	17.4	0.0	0.3
Avalon	0	1.0	1.0
	12.7	1.0	1.0
	20.0	1.0	1.0
Statfjord	0	0.0	0.0
	12.9	0.0	0.0
	19.6	0.0	0.13
	30.9	1.0	1.0

These results were interpreted using the following guidelines. For emulsion formation tendency, a value of F_o between 0 and 0.25 indicates a low tendency to form emulsions; a value of 0.25 to 0.75 indicates a moderate tendency; and, a value of 0.75 to 1.0 indicates a high tendency. For emulsion stability a value of F_{∞} between 0 and 0.25 indicates a low stability (i.e., the emulsion "breaks" quickly); a value between 0.25 and 0.75 indicates a moderate stability; and, a value between 0.75 and 1.0 indicates a high stability.

The high tendency and stability results for the Avalon oil are consistent with other studies (e.g. S.L. Ross and Mackay 1988) as is the trend that the Statfjord oil needs to be weathered above about 20% loss for a stable emulsion to form in this apparatus (Daling and Brandvik 1988). The results for the Alaska North Slope oil are anomalous and contradict both previous laboratory work (i.e., Mackay et al. 1983; Environment Canada 1992) and experience at the *Exxon Valdez* spill. It may be that there are production, emulsion-breaking chemicals added at the wellheads on the North Slope to enhance removal of produced water. These chemicals may remain with the oil and affect its emulsion-forming characteristics (Ross and Maharaj 1993).

It should be noted that these test results may not be indicative of emulsion stability at colder temperatures or in higher mixing energy regimes. Cooler temperatures, which will increase the parent oil's viscosity and may promote precipitation of emulsion-stabilizing waxes or asphaltenes, will enhance emulsion stability. High mixing energies will also promote emulsion stability by creating smaller water droplets in the emulsion which are less likely to coalesce and may create a more viscous emulsion for a given water content (which further inhibits emulsion separation).

Emulsions for the small-scale laboratory burns were created by adding the required volume of saltwater to crude oil in a 20 l container and mixing the contents with a high energy impeller until a stable emulsion was obtained. Emulsions with water contents of 0, 12.5, 25, 40, 60 and 75% by volume were created.

These were prepared by slowly adding the required volume of 35 ‰ salt water to oil in a 20 l container being stirred at high speed by a four-bladed impeller with a diameter of approximately 80 mm. Emulsion aliquots for tests were taken only after 10 minutes of mixing following saltwater addition. The mixer was left running at all times to enhance emulsion consistency.

Tables 2.3, 2.4 and 2.5 show the physical properties of the weathered oils and emulsions. The properties of the Avalon emulsions are as expected for an oil that forms very stable water-in-oil

emulsions. The notations relating to emulsions breaking in the flash point column relate to the fact that the emulsions broke and free water was visible in the cup after the flash point test.

The properties of the Statfjord emulsions indicate increasing stability with increasing weathering; for the fresh oil, no stable emulsion could be formed. For the 12.9% evaporated oil the emulsions were only stable for more than an hour at 12.5% water content. Emulsions prepared with the 19.6% evaporated oil were stable for more than an hour only with water contents up to 40%; for a 60% water emulsion it was necessary to add 5% by volume Bunker C as a stabilizer to the crude prior to mixing the emulsions. The 30.6% evaporated Statfjord crude produced emulsions that were stable for more than an hour at 13°C with water contents up to 75%.

It was almost impossible to form a stable emulsion with the Alaska North Slope crude. Fresh and 10.8% evaporated crude would form marginally stable (i.e., lasting a few minutes) emulsions up to about 40% water. The 17.4% evaporated would form marginally stable emulsions up to 60% water content. This unusual behaviour (for Alaska North Slope crude) may be related to the presence of production surfactants added to the oil as discussed above.

The Statfjord crude oil used in some of the static heat transfer experiments was weathered and emulsified according to procedures similar to those describe above. The Statfjord crude oil was weathered to 10%, 18% and 26% loss by volume. Emulsions were created in a similar way as for the laboratory burns. The emulsions used for some of these experiments contained 0, 20 and 40% water by volume. The densities of these emulsions are given in Table 2.6.

Table 2.3: Physical/chemical properties of Statfjord crude oil and emulsions used in the small-scale laboratory burns

OIL NAME: STATFJORD										
Emulsion	Density		Viscosity (cP) @ Shear Rate (s ⁻¹)				Flash Point		Interfacial Tension	
	Density (g/cm ³)	Temp. (°C)	13.5 (s ⁻¹) (cP)	6.5 (s ⁻¹) (cP)	2.5 (s ⁻¹) (cP)	Temp. (°C)	Temp. (°C)	(°C)	Oil/Water (dynes/cm)	Air/Oil (dynes/cm)
Fresh										
0.0%	0.844	13.0	16	17	20	12.3	<-10	21.7	29.8	
12.9% Evap.										
0.0%	0.857	13.0	53	74	124	13.6	20	15.4	30.1	
12.5%	0.875	13.2	13	12	13	16.0	24			
25.0%	*0.898	13.0	*30	*35	*38	15.5	30			
40.0%	*0.914	13.0	*45	*41	*39	15.4	**			
60.0%	*0.945	13.1	*130	*135	*150	14.5	**			
19.6% Evap.										
0.0%	0.866	13.0	55	120	183	13.0	49	12.0	30.3	
12.5%	0.889	13.0	78	88	113	15.9	51			
25.0%	0.908	13.0	315	440	780	14.7	50			
40.0%	0.925	13.9	470	729	1214	12.1	**			
60.0%	0.946	13.1	***1117	***1392	***2105	13.1	**			
30.6% Evap.										
0.0%	0.881	13.0	-	655	1557	12.0	89	8.8	31.0	
12.5%	0.894	13.0	1361	2115	4234	13.0	92			
25.0%	0.906	14.0	-	2692	5178	14.0	93			
40.0%	0.921	14.3	1724	2680	-	12.8	**			
60.0%	0.952	13.1	1875	2893	5000	14.0	**			
75.0%	0.970	13.4	2000	2900	4750	14.4	**			

Comments:

* emulsion was unstable; test results may not represent actual emulsion water content

** emulsion broke during testing; water was present in flash cup after test

*** emulsion contained 5% (of the volume) Bunker C to maintain stability

Table 2.4: Physical/chemical properties of Alaska North Slope crude oil and emulsions used in the small-scale laboratory burns

OIL NAME: ALASKA NORTH SLOPE										
Emulsion	Density		Viscosity (cP) @ Shear Rate (s ⁻¹)				Flash Point		Interfacial Tension	
	Water Content	Density (g/cm ³)	Temp. (°C)	13.5 (s ⁻¹)	6.5 (s ⁻¹)	2.5 (s ⁻¹)	Temp. (°C)	(°C)	Oil/Water (dynes/cm)	Air/Oil (dynes/cm)
Fresh										
0.0%	0.878	16.1	22	22	22	20	14.1	<-10	4.0	30.1
12.5%	0.905	12.9	30	29	29	27	14.2	<-10		
25.0%	0.922	13.0	52	51	51	51	13.8	**		
40.0%	0.936	14.4	-	115	112	112	13.4	**		
60.0%	*0.948	13.0	*35	*53	*60	*60	14.0	**		
75.0%	*0.970	11.0	*27	*42	-	-	14.1	0		
10.8% Evap.										
0.0%	0.907	13.1	53	53	53	52	14.7	26	6.0	30.4
12.5%	0.915	12.0	81	81	81	81	14.8	29		
25.0%	0.926	13.2	-	123	123	123	14.7	31		
40.0%	0.943	12.5	154	166	166	218	14.7	**		
60.0%	*0.963	13.1	*372	*485	*453	*453	15.8	**		
17.4% Evap.										
0.0%	0.916	13.0	104	101	101	101	14.4	52	10.3	31.9
12.5%	0.925	11.3	147	148	148	148	13.8	**		
25.0%	0.938	13.6	217	216	216	225	14.3	**		
40.0%	0.945	11.8	385	382	382	387	14.4	**		
60.0%	0.967	12.4	-	840	840	925	14.2	**		
75.0%	*0.973	11.2	*1200	*1360	*1600	*1600	13.7	**		
Comments:										

* emulsion was unstable; test results may not represent actual emulsion water content
** emulsion broke during testing; water was present in flash cup after test

Table 2.5: Physical/chemical properties of Avalon crude oil and emulsions used in the small-scale laboratory burns

OIL NAME: AVALON										
Emulsion	Density		Viscosity (cP) @ Shear Rate (s ⁻¹)				Flash Point		Interfacial Tension	
	Density (g/cm ³)	Temp. (°C)	13.5 (s ⁻¹) (cP)	6.5 (s ⁻¹) (cP)	2.5 (s ⁻¹) (cP)	Temp. (°C)	Oil/Water (dynes/cm)	Air/Oil (dynes/cm)		
Fresh										
0.0%	0.883	14.1	178	230	275	13.5	-3	16.4	38.9	
12.5%	0.903	11.6	141	142	175	14.1	*<0			
25.0%	0.920	13.0	426	542	763	13.1	*<2			
40.0%	0.941	13.1	930	1172	1700	12.6	*<5			
60.0%	0.967	12.6	1505	1890	2600	12.0	*<11			
75.0%	1.003	12.5	4900	6080	8500	13.1	*<14			
12.7% Evap.										
0.0%	0.894	17.5	942	1230	1808	19.1	37	13.2	30.8	
12.5%	0.905	19.4	285	310	315	12.2	24			
25.0%	0.924	12.5	2640	3650	5500	12.2	40			
40.0%	0.941	14.7	1975	2800	4250	12.0	**27			
60.0%	0.962	17.5	3130	3200	4000	13.8	**24			
75.0%	0.978	13.0	8725	10500	15000	14.5	**			
20.6% Evap.										
0.0%	0.904	13.0	240	450	800	25.0	65	8.3	29	
12.5%	0.913	13.5	580	1280	2150	20.4	58			
25.0%	0.920	13.8	1290	1800	5100	19.3	64			
40.0%	0.942	13.0	2700	3600	9500	18.0	57			
60.0%	0.962	13.1	5675	7900	8400	16.7	34			
75.0%	0.978	13.0	-	-	38700	15.4	**			

Table 2.6: Density of Statfjord crude oil and emulsions used in static heat transfer experiments

WATER (%)	EVAPORATION (%)	DENSITY (g/ml)
0	10	0.860
0	26	0.880
20	18	0.871
40	26	0.892

2.3 Emulsion preparation for field experiments

Statfjord crude oil was used for the field experiments at three degrees of evaporation (0%, 18% and 25% by volume) and five degrees of emulsification (0%, 12%, 25%, 50% and 60% by volume).

The fresh Statfjord crude was evaporated in a cylindrical 4500 l tank by sparging compressed air into a known volume of oil and measuring evaporative loss. During the air stripping process the contents of the tank were recirculated using a pump with a flow rate of 400 l/min. This caused the temperature of the oil to increase to roughly 50 °C. The loss of volume due to evaporation was measured by periodically measuring the height of the oil in the tank.

The stable emulsions were produced in the following way:

1) Small batches (< 600 l):

The required amount of evaporated oil and seawater was transferred to a 600 l tank and the contents recirculated using a pump rated at 25 l/min for a period of 10 to 20 hours depending on the water content of the emulsion. A sample of the emulsion was removed and the stability verified before drumming. The drums of emulsions were stored in a heated warehouse at approximately 15 °C in order to keep the emulsions above their pour point. The drums of emulsion were transported to the experimental site shortly before each experiment.

2) large batches (< 4000 l):

A 50% water emulsion was prepared by mixing 2000 l of 25% evaporated oil with 2000 l of sea water in the 4500 l tank. The contents were recirculated using a gear pump rated at 400 l/min for a period of 24 hours. This tank, mounted on skids, was pulled out to the experimental site before the experiments.

The initial physical-chemical properties of the oils and emulsions used in the field experiments are given in Table 2.7. These emulsions were also used for some of the static heat transfer experiments.

Table 2.7: Physical/chemical properties of Statfjord oils and emulsions used in the field experiments.

Oil	Density at 19°C (g/cm ³)	Viscosity (cP at 0.2 s ⁻¹)	Interfacial Tension (dynes/cm)	
			Oil/Water	Air/Oil
0% evap 0% water	0.844	17 at 12.3°C (6.5 s ⁻¹)	21.7	29.8
18% evap 0% water	0.868	12.5x10 ³	n.m.	
18% evap 12% water	0.886	25x10 ³	23.5	31.7
25% evap 0% water	0.876	12.5x10 ³	n.m.	
25% evap 25% water	0.935	25x10 ³	27.9	32.4
25% evap 50% water	0.952	60x10 ³	27.5	32.3
25% evap 60% water	0.971	70x10 ³	31.1	31.6

n.m.=not measured.

The stability of emulsions created for the field work was verified by taking a sample of the emulsion, placing it in a clear glass jar and allowing it to stand at room temperature for several hours. In all cases the emulsions did not break. Samples of these emulsions were brought to Trondheim following the field work and remained stable for several months thereafter.

2.4 Methods for physical-chemical analysis

The following analytical equipment and methods were used to determine the physical-chemical properties of the oils, emulsions and residue samples from this project.

Temperature

All physical property measurements were made as close as possible to 13°C; temperature was measured with a Fluke Model 52K digital thermometer with a Type K probe.

Density

Density was measured using a Anton Parr Model DMA35 digital densiometer. ASTM D4052-91 procedures were followed.

Viscosity

Oil viscosity at different shear rates was measured using a Brookfield Model LVT dial reading viscometer with the IV-series spindles. Portions of ASTM D2983-87 were used as the measurement

procedure. It is difficult to compare viscosities measured at different shear rates, for non-Newtonian liquids. As a guideline, readings can be compared by multiplying the reading by ≈ 3 for each increase in order of magnitude in the shear rate (Daling 1994).

Flash Point

Flash point was measured using a Pensky-Martens Model 74537 closed cup flash tester. ASTM D93-90 procedures were followed.

Interfacial Tension

A Central Scientific Company Model 70545 DuNuoy ring tensiometer was used. ASTM D971-82 procedures were used.

Water Content

The water contents of some emulsions was determined by extracting the oil from a carefully weighed aliquot of the emulsion with toluene. The oil concentration in the toluene was determined spectrophotometrically at a 405 nm wavelength by comparing the sample to a known calibration curve. The mass of oil in the emulsion was then back calculated and the water contents was determined by subtraction.

The Karl-Fischer Titrator method was also used for water content analysis as described by Bobra (1990). The instrument used was a Metrohm KF Titrino 701 titrator.

Emulsion Breaker Testing

As part of the small-scale testing program, the efficiency of four commercial emulsion breakers was determined with the emulsions used in this study. The procedures used were a slight variation of those used as a standard test by Environment Canada (Fingas 1993).

3 MODEL DEVELOPMENT

During the experiments carried out in recent years as part of the NOFO Arctic Program, it became clear that *in-situ* burning of emulsions was different from *in-situ* burning of unemulsified oil on water. It became evident that the "emulsion burning process" was a more complex process involving several more steps than the burning of unemulsified oil. From the field studies conducted in earlier years, and general knowledge about emulsions and heat transfer, it was possible to construct a conceptual model. However, the data obtained in field studies from previous years needed to be interpreted together with data from more detailed designed laboratory studies in order to be used for verification of the model.

The conceptual model for emulsion burning was refined and formulated in mathematical terms. To verify the model, extensive laboratory experiments were performed; i.e. small-scale burns and heat transfer experiments. The data from these experiments were also used for statistical modelling.

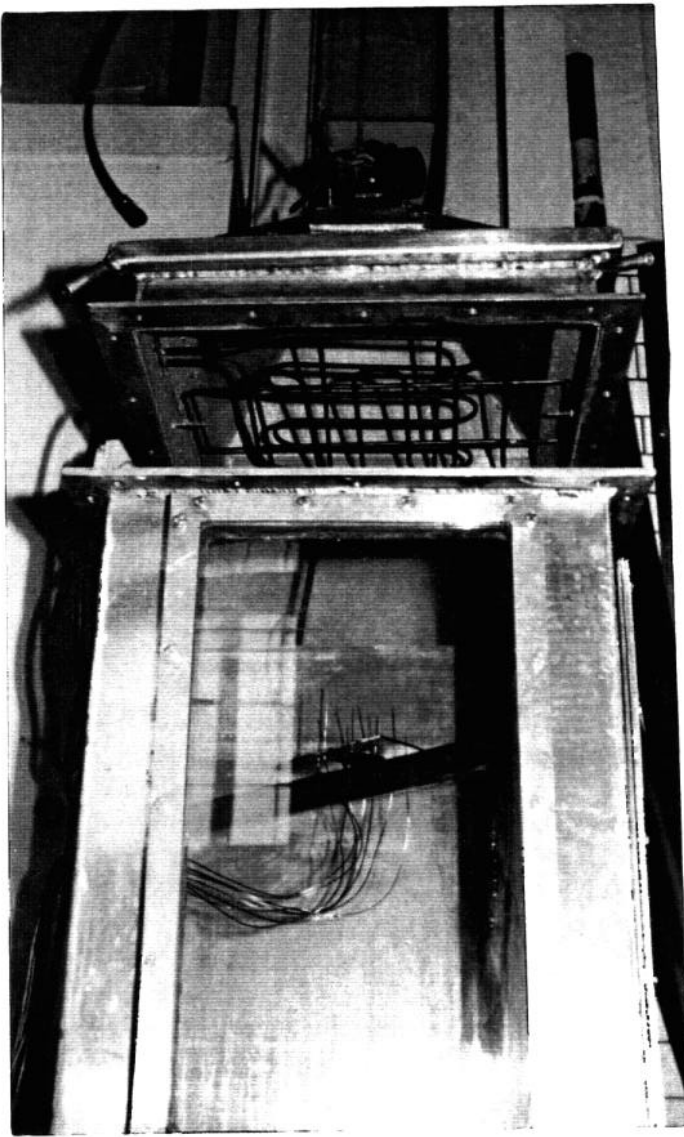
3.1 Methods and Experimental Design

3.1.1 Static heat transfer experiments

A device was designed and built to study the physical and chemical processes occurring in oils and emulsion slicks floating on water when heated at the surface and the heat transfer in oil and emulsion slicks on water. In these experiments, oil and emulsions were subjected to a constant heat flux using a radiant heat source placed above the slick. The purpose of these experiments was to investigate heat transfer through emulsions as a function of slick thickness, emulsion water content, degree of evaporation and heat input. The data generated were used to verify the proposed conceptual models describing the heating and burning of water-in-oil emulsions. A statistical analysis of this data was also performed to obtain information on the effect each parameter had on the heat transfer characteristics of emulsions.

The heat transfer box consisted of a 0.5 m by 0.5 m by 1.4 m high aluminum box with a detachable lid and two side viewing windows. The device is shown in Figure 3.1. Two heating elements were installed in the lid providing a maximum energy output of 3000 watts. Up to eight thermocouples (Type K) could be placed throughout the emulsion layer to measure slick temperatures during the experiment. The emulsion could be sampled at any given time during an experiment using any combination of the 11 available sample ports located on the side of the box. Syringe needles were permanently positioned in these ports, located at different slick depths with the attachment end for the syringe located on the outside of the box. This enabled the slick to be sampled while the box was closed. Figure 3.2 shows the thermocouple and sample port location and distribution throughout the slick.

The box was filled with water to a predetermined height (81, 83 and 85 cm depending on slick thickness) so that the oil or emulsion surface was at the same distance from the heating elements for each experiment. The emulsion was poured onto the water surface using a spill plate to prevent dispersion of the oil into the water. The thermocouples were evenly distributed from top to bottom in the emulsion layer and adjusted according to the emulsion thickness. The upper and the lower thermocouples were positioned at the air/oil and oil/water interfaces, respectively, so that they were just inside the oil or emulsion layer. Thermocouples were also placed 1 cm below and 1 cm above the emulsion. The lid was securely attached to the box using bolts and sealed using a heat resistant gasket. Air was purged from the system using nitrogen to prevent ignition of the oil vapours. The water temperature below the slick was kept constant by recirculating the water through cooled copper piping using a small pump. Cooling water was sprinkled on the lid of the box to condense the vapours forming inside. These vapours, condensing on the underside on the box lid, were collected along the bottom edges of the lid inside the box and funnelled through a small length of pipe to a collection cylinder located outside the box.



← heating elements
in lid

← thermocouples

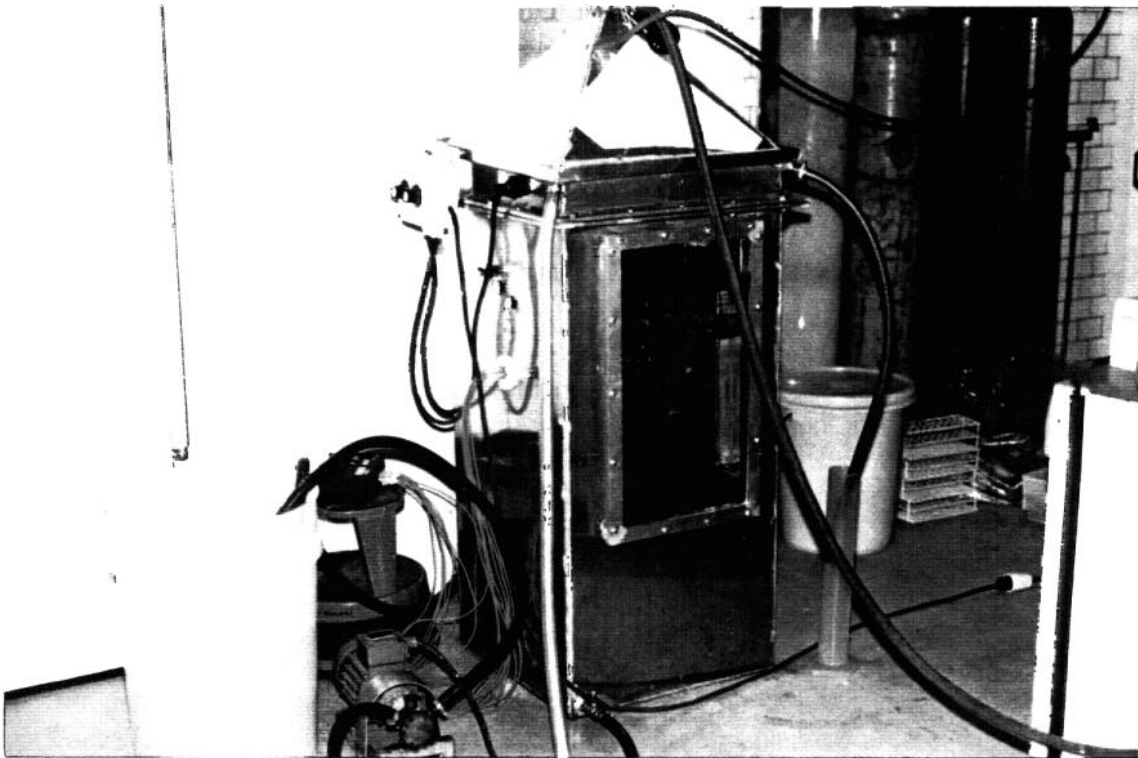
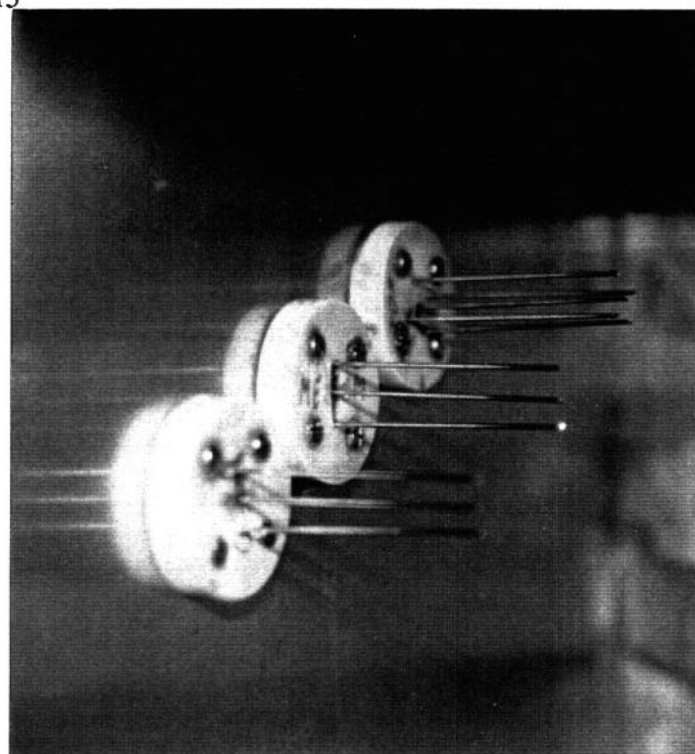
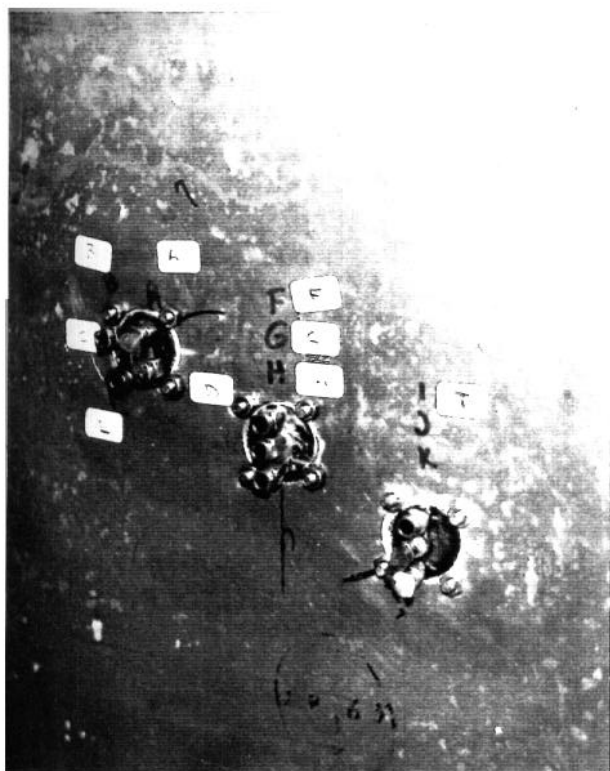


Figure 3.1: Heat transfer apparatus



↑ sample ports
left: outside of box
right: syringes inside box

← thermocouples
↓

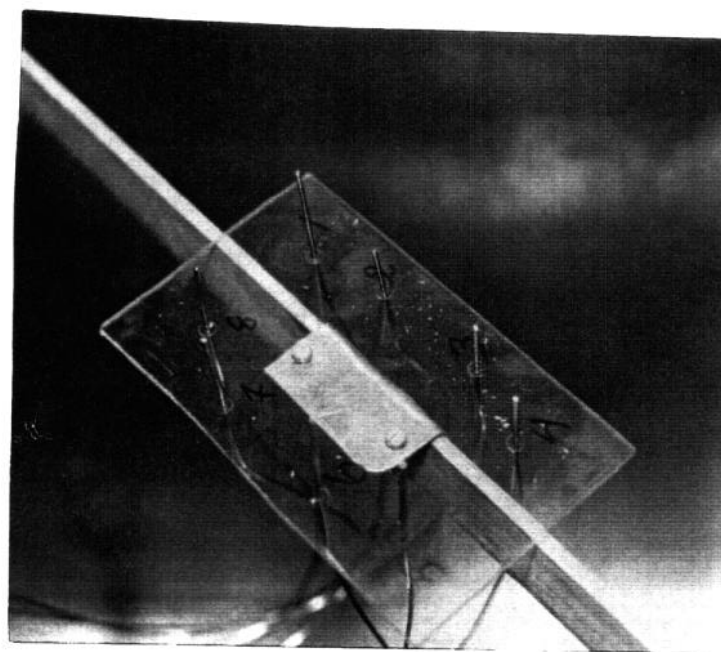
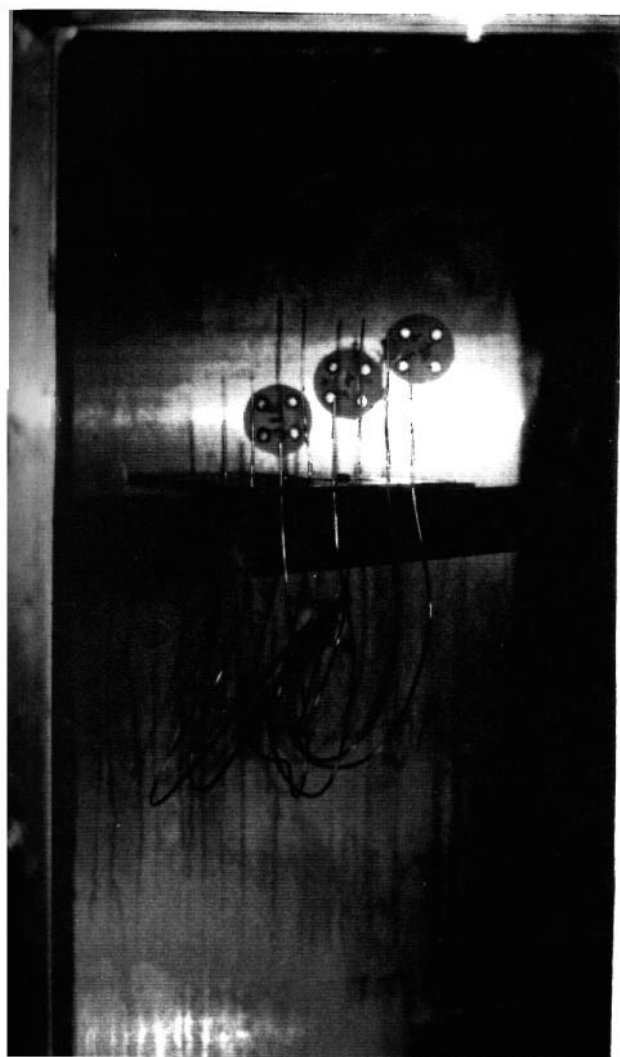


Figure 3.2: Thermocouple and sample port locations

Temperatures were measured and samples of emulsion/oil were collected throughout each experiment:

- Temperature data was collected using data logger or with an A/D board, through a multiplexer connected to a computer. The measurement frequency was once every 15 seconds. Ambient and cooling water temperatures were also monitored throughout the experiments.
- Initial samples of the oil or emulsion were taken before each run and analyzed for water content, viscosity and density. Subsequent samples of the emulsion layers were taken once the surface temperature of the emulsion had reached at least 100°C. These samples were later analyzed for water content and density.

The slick was observed through the glass windows at the end of each experiment. The final slick thickness was measured, and any changes in the emulsion appearance noted.

Tables 3.1 and 3.2 describe the experimental design matrices used in these static heat transfer experiments. In the first set of experiments, heat input was kept constant at 3000 watts, while the emulsion water content, the degree of evaporation and the emulsion slick thickness were varied. Water contents of 0, 20 and 40% were used. The degrees of evaporation were 10, 18 and 26%. Oil or emulsion slick thicknesses of 2, 4 and 6 cm were used. In the second set of experiments, the slick thickness was kept constant at 6 cm. Emulsion water contents of 12.5, 25, 50 and 60% and evaporation degrees of 18 and 25% were studied. This second series of experiments was conducted in the laboratory at Sveagruva. An effort was made to use the same emulsions as in the field experiments during the second experimental series. The heat input used for this second series of experiments was 1500 or 3000 watts. A total of 16 experiments were conducted.

Table 3.1 **Experimental design in the static heat transfer experiment with radiant heat input of 3000 watts**

WATER (%)	EVAPORATION (%)	THICKNESS (cm)
0	10	2
0	10	6
0	26	2
0	26	6
40	26	2
40	26	6
20	18	4
20	18	4
20	18	4

Table 3.2: **Experimental design in the static heat transfer experiment with initial slick thickness of 6 cm.**

WATER (%)	EVAPORATION (%)	HEAT INPUT (watts)
12.5	18	1500
50	18	1500
50	25	1500
25	25	3000
25	25	3000
25	25	3000
60	25	3000

3.1.2 Small-scale burning experiments

The small-scale test burns involved a test matrix of the three crude oils at three degrees of weathering (four for the Statfjord oil), up to 6 water contents (0, 12.5, 25, 40, 60 and 75%) and three initial thicknesses (5, 10 and 20 mm).

The burns were conducted in a water-filled circular steel pan measuring 120 cm in diameter and 32 cm in height. The test oils and emulsion were contained in either 40 cm or 75 cm diameter rings supported at the water's surface by four metal rods. Two 30 cm square mirrors were placed in the tank and angled so that the burning slick could be also viewed from below. A 150 W floodlight was directed into one of the mirrors to illuminate the bottom of the slick. A fume hood was suspended 145 cm above the test ring and connected to a fan (200 m³/min) via 60 cm diameter flexible aluminum ducting. The smoke generated during the burns was exhausted outside the laboratory. An additional 60 cm duct was installed to allow clean air to enter the lab. The experimental set-up is shown in Figures 3.3 and 3.4.

During these burns, temperatures were measured at three flame heights, at eight locations throughout the slick layer and at three depths in the water below the slick using the thermocouple arrangement shown in Figures 3.5 and 3.6. The thermocouples (Type K) were connected to an A/D board, through a multiplexer to a computer. Temperatures were recorded every 3 seconds. The thermocouples were arranged in such a way as to allow a set of those located in the slick to be adjusted vertically to permit consistent placement with respect to the surface for different slick thicknesses. All thermocouples measurements in the slick and underlying water were duplicated.

The pan was filled with water to a height of 20 mm above the highest, fixed thermocouple. The water temperature was adjusted to approximately 10°C. The volume of oil (or emulsion) required to create a slick thickness of 5, 10 or 20 mm was weighed in a tared graduated cylinder or pitcher. The oil was carefully poured onto the water surface of the inner ring using a spill plate to prevent dispersion of the oil or emulsion into the water column. The moveable thermocouples were adjusted so that the tips of the highest two were just below the oil surface. This was done by raising the thermocouples until they formed a meniscus on the surface then the thermocouples were lowered until the meniscus disappeared. The air temperature just above the slick surface and the water temperature in the outer ring was recorded using a digital thermometer.

In this series of burn experiments, the oils and emulsions were ignited using four different ignition sources, each providing an increasing amount of heat input to the slick. They were: 1) 25 cm² gasoline saturated sorbent pad; 2) 25 cm² crude oil saturated sorbent pad; 3) 100 ml of fresh crude oil; 4) 200 ml of fresh crude oil. The gasoline or crude oil soaked sorbent pads were placed in the center of the test slick and ignited using a propane torch. The fresh oil was poured over the slick surface and ignited using a gasoline soaked sorbent pad and propane torch.

For each run the preheat time (the time from igniter placement to the beginning of flame spread away from the igniter edge); the ignition time (time for igniter placement to the time when the entire slick surface was aflame); the time to intense burn (time from igniter placement to that point near the end of the burn when the vigorous burn phase is underway - usually signified by a noticeable increase in flame height, an increase in noise level and bright droplets ejected into the flame); and the time to extinction. For later tests involving high water content emulsions and enhanced ignition techniques a "stable burn time" was also recorded. This was the time from igniter placement to when the flame stabilized and began to grow away from the igniter.

The residue from each burn was collected and weighed to determine burn efficiency and overall burn rate. A sample of the residue was stored for toxicity and physical-chemical analysis. Video records of all laboratory burns were taken from different angles and archived for future reference.

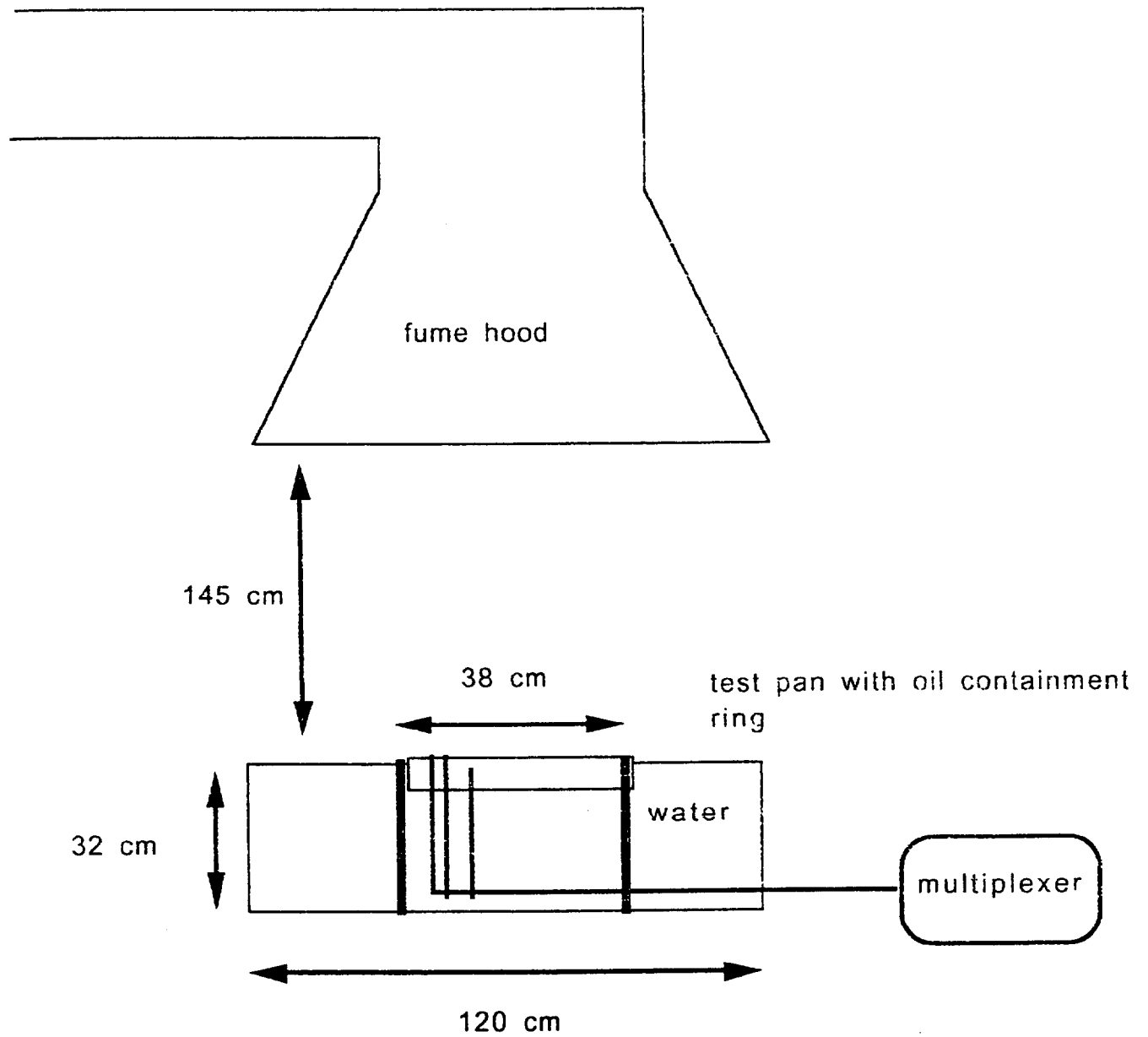


Figure 3.3: Experimental set-up for laboratory burns

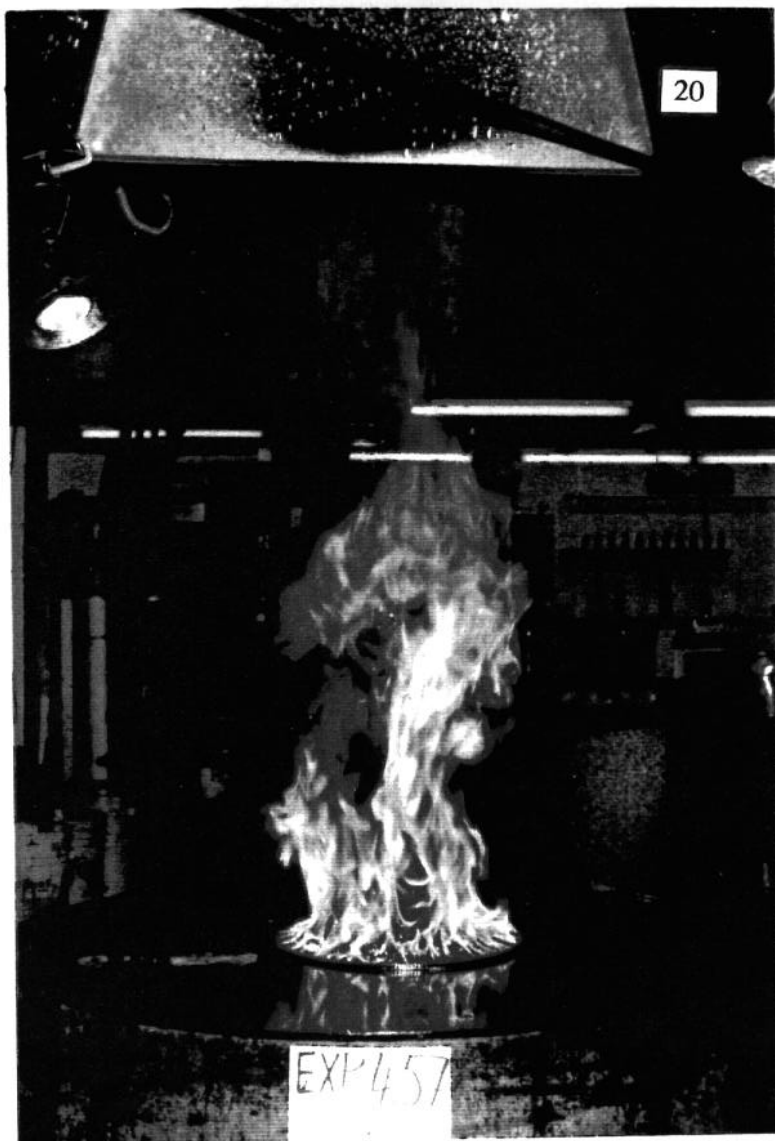


Figure 3.4:
Laboratory burn



Figure 3.5: Thermocouples in flames

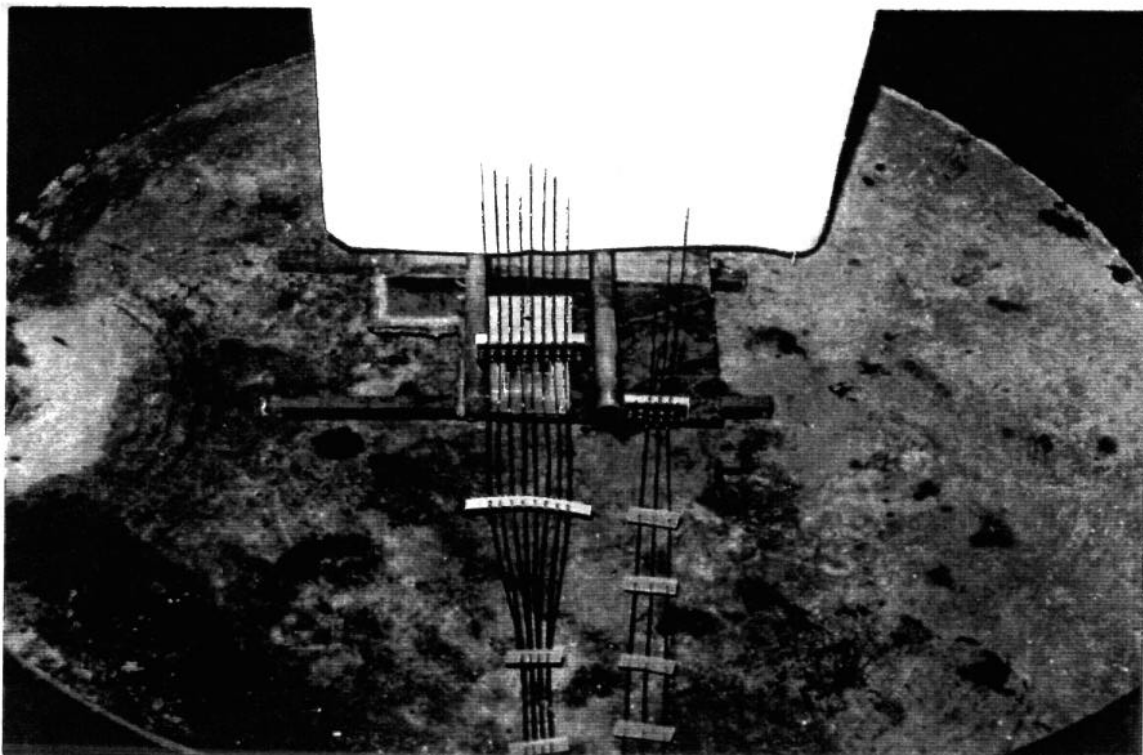
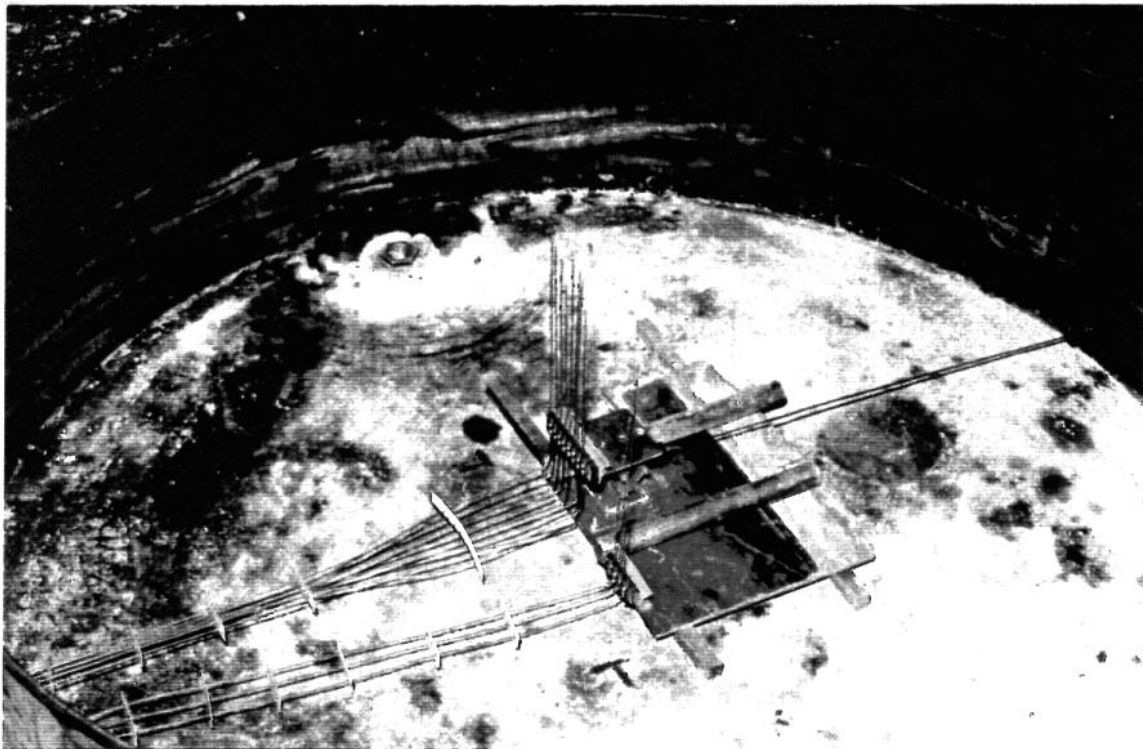


Figure 3.6: Thermocouple arrangement for small-scale laboratory burns

3.1.3 Meso-scale model verification experiments

During selected tests in the field experiments, oil/emulsion slick temperatures, underlying water temperatures and flames temperatures were measured in order to make a comparison with those temperatures measured in the laboratory experiments.

3.2 Results and discussion

3.2.1 Conceptual model

The basic premise of the conceptual model of emulsion slick burning is based on that postulated by Bech et al. 1992 and 1993. This is that, it is not the emulsion that burns, but rather it is a layer of oil floating on the top of the emulsion that supports combustion.

Emulsion Ignition

For ignition of an oil slick to occur (Figure 3.7), the heat supplied by an ignition source must be sufficient to raise the temperature of the adjacent slick surface above the oil's fire point. If the oil is too thin (<1 mm for fresh crude and <3 to 5 mm for weathered crude) the heat escapes into the underlying water. The slick's surface temperature never exceeds the fire point and ignition does not occur. Once approximately 1 m² of slick area is on fire, the burn is considered to be underway.

In the case of water-in-oil emulsions, an additional heat sink exists (the heat required to boil off the water contained in the emulsion) and a ceiling exists for the emulsion temperature (approximately 100°C = the boiling point of water). It is likely that the process of ignition of an emulsion involves the thermal breaking of the emulsion, or boiling off the emulsified water, to produce a layer of relatively water-free oil lying on top of the emulsion (itself floating on water). As such, there are different and/or additional thermal and kinetic processes to account for in a model of emulsion ignition.

Sustained Burning

Once ignition has taken place, sustained burning of an unemulsified oil (Figure 3.8) requires that the heat radiated back to the slick (about 3% of that generated by combustion) be sufficient to maintain the temperature of the surface of the slick at, or above, the oil's fire point. The heat available to raise the oil's temperature is that radiated down from the flame minus the amount conducted through the slick into the underlying water. Because, oil is a relatively good insulator (compared to water) and, once ignition has taken place, sustained burning usually continues easily until the slick thins to near its extinction thickness.

Emulsions, because of their water droplets, will not be as good an insulator as oil and would transfer more heat through the slick to the underlying water. As noted above, the maximum temperature that an emulsion can reach is approximately 100°C. In order for an emulsion to burn, the entrained water must first be removed and only then will the oil heat up and burn. It does not seem likely that this water removal can take place by the emulsified water droplets coalescing and then separating out of the bulk emulsion slick; the underlying, colder slick viscosity would be too high for this to occur at rates sufficiently high to provide a sustained source of oil for combustion (Figure 3.9). More probably, the emulsified water is evaporated (i.e. boiled off).

Whether or not an emulsion will burn as easily as an oil is not clear from a modelling standpoint; more heat is required (to break the emulsion) but the burning of the oil from the broken emulsion may proceed faster because its underlying substrate is emulsion, not just water. Another complicating factor is the observed phenomenon that higher water content emulsions, when they do burn, do so quite

MINIMUM THICKNESS

- determined by heat transfer through slick and fire point of oil

For Slick Ignition

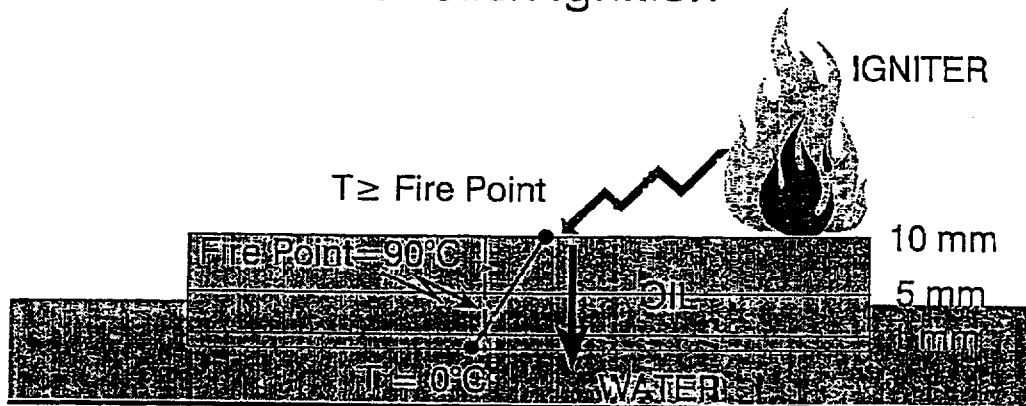


Figure 3.7: Requirements for ignition of an oil slick

HEAT BALANCE

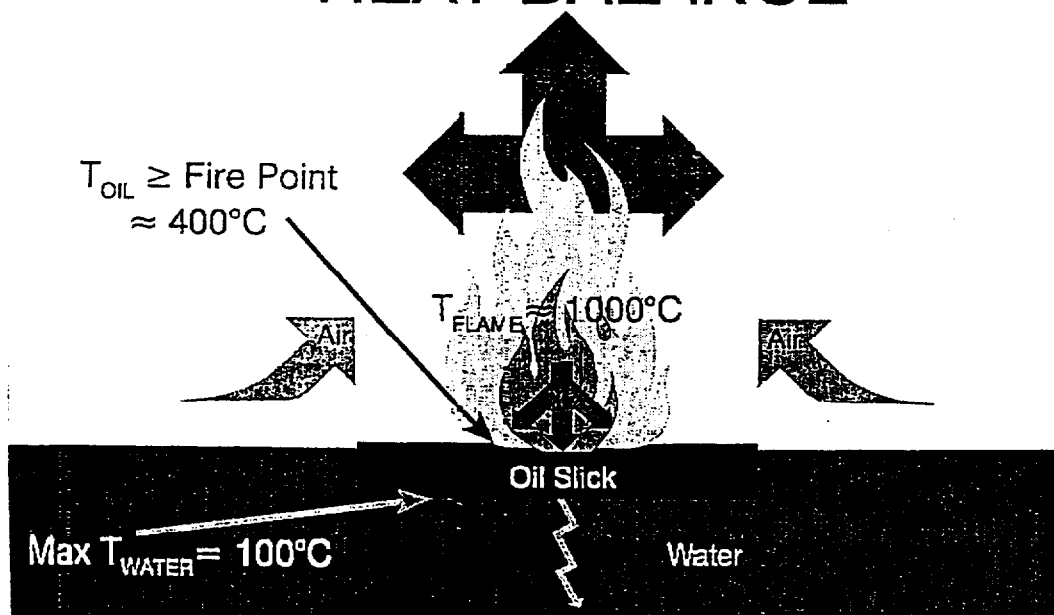


Figure 3.8: Heat balance during *in-situ* burning

This is a very different process of burning that an oil slick undergoes, although it may be similar to the violent burning phase that an unemulsified oil undergoes near the end of a burn, when the heat transferring through the thinner slick increases to a point where the water begins to boil violently.

Extinction

As shown in Figure 3.10, the temperature profile through a burning emulsion slick is quite steep. The surface of the oil beneath the flame is very hot but the temperature drops rapidly with depth in the oil (oil is a relatively good insulator, certainly better than water). At the bottom of the slick, the emulsion temperature approaches that of the underlying water (somewhere between 0° and 100°C). As the burning progresses two things occur: the slick gets thinner and the achievable surface temperature of the oil slowly declines (because more heat is conducted through the slick and the fire point of the remaining oil slowly increases). At the point where the heat conducted through the slick becomes so great as to reduce the achievable oil surface temperature to below the fire point of the remaining oil the combustion stops. This thickness, for most oils, is about 1 mm. Since emulsions have different heat transfer characteristics than oils and the burning process is likely different for emulsions, the extinction model for emulsions will likely also be different. It is possible that the extinction of burning emulsion slicks may involve reaching the point where the rate at which burnable oil is produced by the breaking emulsion falls below the oil removal rate required to sustain combustion of the oil on top of the emulsion. The burning oil slick on top of the emulsion thins to below the minimum thickness required to keep its surface temperature above its fire point and the fire extinguishes. Earlier field trials at Spitsbergen have indicated that emulsion fires are more easily extinguished by waves than raw oil fires (Bech et al., 1993). This lends credence to the theory that the emulsion burning process is different than that for pure oil and is more sensitive to oceanographic conditions.

Foaming

Foaming of a burning emulsion may also be related to the water loss mechanism (boiling vs breaking), rate of breaking or the presence of film-stabilizing chemical species in the oil. Foam is created by the intense mixing of a gas and liquid. The liquid contains surface acting chemicals that stabilize the thin film of liquid around the gas bubble. In the case of burning emulsions that foam, the gas is likely steam (with some combustion byproducts and air) and the liquid is likely oil (it is probably not emulsion since the ambient temperatures would quickly boil any water). It may be that foaming is initiated by the development of a condition of increased pressure in the liquid water in the emulsion.

EMULSION BURNING PROCESSES

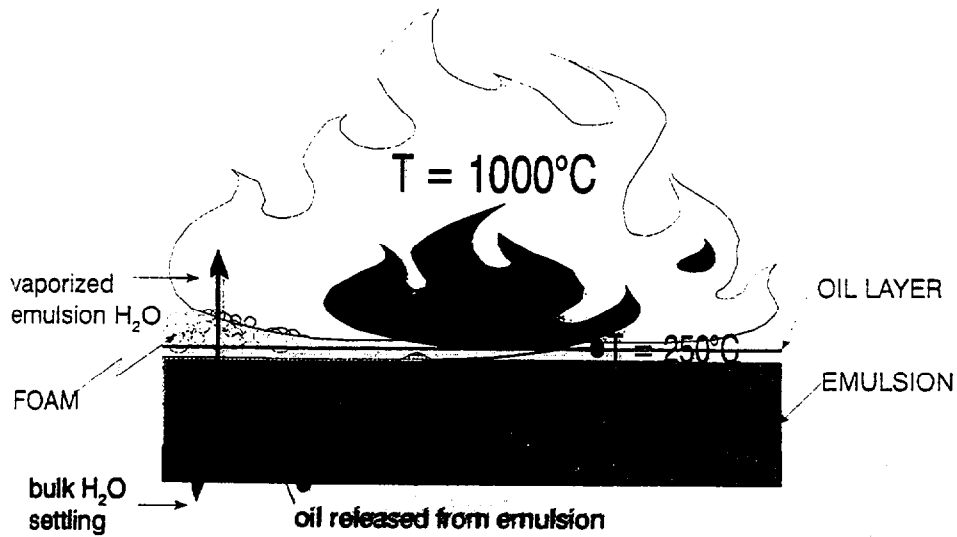


Figure 3.9: Heat balance on burning emulsion

HEAT BALANCE ON BURNING EMULSION

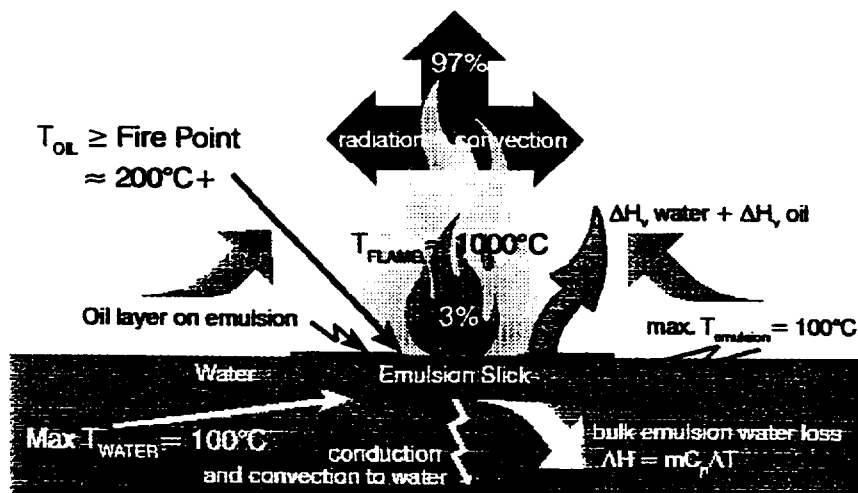


Figure 3.10: Emulsion burning process

The water droplets in the "hot zone" of the emulsion could be heated above 100°C without boiling; the oil film surrounding them may retain the increased pressure in the water required for this to occur. For example, pure water at a pressure of 101.325 kPa boils at 100°C; an increase in pressure of 17.2 kPa (2.5 psi) increases the boiling point to 104.4°C. As the temperature of the water droplets increases the vapour pressure increases until a point is reached when the oil "skin" ruptures. Suddenly the ambient pressure around the droplet reduces and the liquid water flashes. This flashing of the water involves the rapid evolution of vapour from the liquid to reduce the temperature of the liquid to its normal boiling point. The resultant vapour may produce the mechanical energy necessary to produce the foam.

Once the flashing process is completed the boiling rate of the water reduces and the foaming dies down (this would explain the transient nature of foaming). It may also be that the rupture of one water droplet initiates the rupture of nearby droplets and so on. This would explain the rapid appearance and growth of foam in discrete regions of a burning slick.

When the foam is generated it extinguishes the fire locally by either smothering, insulating the oil layer or a combination of the two. After the foam breaks, if another area of the slick is still on fire, the affected area can reignite and burn. The foaming process may be one whereby pure oil is delivered to the surface at a faster rate than by slower boiling of the water out of the underlying emulsion.

3.2.2 Mathematical model for steady state emulsion slick burning

The following mathematical representation of steady state burning of an emulsion builds upon the models proposed by Twardus and Brzustowski (1981) and Brzustowski and Twardus (1982).

The model assumes that the entire slick area under consideration is on fire and that the various heat and mass transfer processes have reached a quasi-steady state. This means that, although these processes are changing with time, the changes are slow enough that, for all intents and purposes, the processes can be considered to be time invariant. This assumption is necessary to keep the mathematics tractable. This means that the model cannot be used to describe the initial stages of burning (ignition and flame spreading) or the final stages (foaming, vigorous burning or extinguishment). The basis of the model is a unit area of emulsion slick that has been ignited and burned for some time. The approach taken to build the model was to balance all the heat inputs to the slick with all the heat sinks in the slick. After this, simplifying assumptions are made to reduce the complexity of the model.

For a quasi-steady state heat balance on the burning oil layer (see Figure 3.11):

$$\text{heat in} = \text{heat out}$$

convection from flame + radiation from flame = heat of vaporization of oil + heat of vaporization of emulsion water boiled + heat to warm oil from emulsion to fire point + heat radiated through slick to emulsion + heat transferred through emulsion slick to water. The heat to warm water from the underlying emulsion temperature to 100°C is ignored at present because it makes up only a small fraction of the heat of vaporization of water.

OR

$$q_{conv}'' + q_r'' \cos \delta = r \rho_o \Delta H_{v,o} - f_w(t) \frac{dZ_{v,s}}{dt} \rho_w \Delta H_{v,w} \quad (1)$$

$$-(1-f_w(t)) \frac{dZ_{v,s}}{dt} \rho_o C_{p,o} (T_e - T_o) + (1-\alpha(Z_o)) q_r'' \cos \delta$$

$$+ U_o \Delta T$$

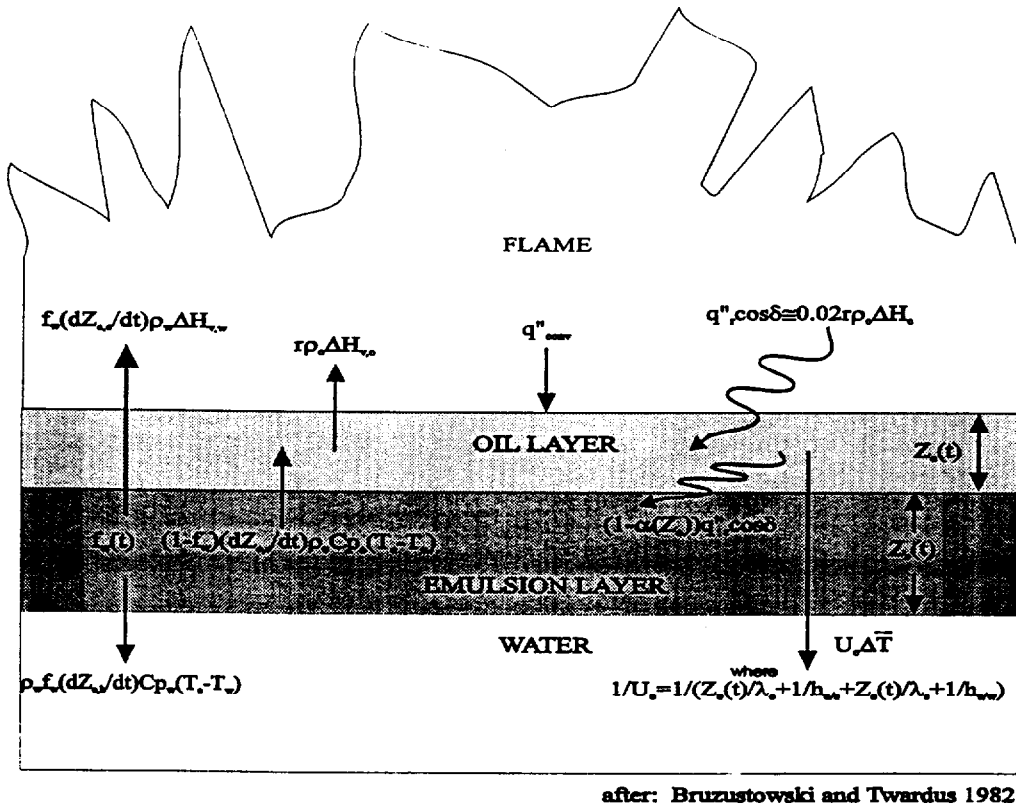


Figure 3.11 Model of emulsion burning illustrating processes considered in the heat balance

where:

q''_{conv}	\equiv convective heat transfer from flame to oil layer [kJ/m ²]
q''_r	\equiv radiative heat transfer from flame to oil layer [kJ/m ²]
δ	\equiv angle of flame bent over by wind
$\alpha(Z_o)$	\equiv function of oil layer thickness that defines what fraction of q''_r is absorbed by the oil layer
r	\equiv burning rate of oil layer [m/s]
ρ_o	\equiv density of oil [kg/m ³]
$\Delta H_{v,o}$	\equiv heat of vaporization of oil [kJ/kg]
$f_w(t)$	\equiv fraction of water in emulsion at time t
Z_o	\equiv oil layer thickness on emulsion [m]
Z_e	\equiv emulsion thickness beneath oil layer [m]
$\frac{dz_e}{dt}$	\equiv rate of change of emulsion thickness due solely to evaporation of water [m/s]
$\frac{dz_{e,b}}{dt}$	\equiv rate of change of emulsion thickness due solely to breaking [m/s]
ρ_w	\equiv density of water [kg/m ³]
$\Delta H_{v,w}$	\equiv heat of vaporization of water [kJ/kg]
$C_{p,o}$	\equiv heat capacity of oil [kJ/kg°C]
T_e, T_o, T_w	\equiv temperature of emulsion, oil and water respectively [°C]
U_o	\equiv overall heat transfer coefficient [kJ/m ² s°K]
ΔT	\equiv average temperature drop across slick (definition depends on U_o) [°C]
λ_e, λ_o	\equiv thermal conductivity of emulsion and oil respectively [kJ/ms°K]
$h_{o/e}, h_{e/w}$	\equiv local heat transfer coefficients for oil/emulsion and emulsion/water interfaces, respectively [kJ/m ² s°K]

The process whereby the emulsion breaks and loses water physically defines f_w as a function of time.

In order to solve equation (1) it is necessary to make some simplifying assumptions; namely:

$$\frac{dz_{e,b}}{dt} = 0 \quad \text{that is no breaking of the emulsion during the burn process.}$$

This means that $f_w(t)$ is a constant and, at steady state it implies that:

$$r = -(1-f_w) \frac{dz_e}{dt} = -(1-f_w) \frac{dz_e}{dt} \quad (2)$$

or the burning rate of the oil layer is directly related to the rate of change in emulsion thickness. The proportionality is the initial fraction of oil in the emulsion (or constant).

With this assumption equation (2) becomes:

$$\begin{aligned} q''_{conv} + \alpha(Z_o) q''_r \cos\delta &= \frac{dz_e}{dt} \rho_o \Delta H_{v,o} (1-f_w) - f_w \frac{dz_e}{dt} \rho_o \Delta H_{v,w} \\ &\quad - (1-f_w) \frac{dz_e}{dt} \rho_o C_{p,o} (T_e - T_o) + U_o \Delta T \end{aligned} \quad (3)$$

grouping the right hand side gives:

$$q_{conv}'' + \alpha(Z_o) q_r'' \cos\delta = \rho_o \frac{dZ_o}{dt} (1-f_w) \Delta H_{v,o} - (1-f_w) C_{po} (T_e - T_o) - f_w \rho_w \Delta H_{v,w} / \rho_o + U_o \Delta T \quad (4)$$

if $f_w = 0$ (i.e. no emulsion) then $T_e = T_o$; and, if the major resistance to heat transfer is conduction through the slick then:

$$U_o \Delta T = \frac{\lambda_o T_o - T_w}{Z_o}$$

which for $f_w = 0$ (i.e., $T_e = T_o$ and $Z_e = Z_o$) is the same as:

$$\dot{Z}_o = \frac{\lambda_o T_o - T_w}{Z_o}$$

equation (3) under these conditions, becomes,

$$q_{conv}'' + \alpha(Z_o) q_r'' \cos\delta = -\rho_o \frac{dZ_o}{dt} \Delta H_{v,o} + \frac{\lambda_o T_o - T_w}{Z_o} \quad (5)$$

which is identical to Brzustowski and Twardus' (1982) equation (2).

Rearranging (4) yields:

$$\frac{dZ_o}{dt} = \frac{q_{conv}'' + \alpha(Z_o) q_r'' \cos\delta - U_o \Delta T}{\rho_o [(f_w - 1) \Delta H_{v,o} + (f_w - 1) C_{po} (T_e - T_o) - f_w \rho_w \Delta H_{v,w} / \rho_o]} \quad (6)$$

This equation has the following correct properties:

- as heat transfer through the slick to the underlying water increases ($U_o \Delta T$), the rate of combustion decreases;
- as the absorptivity of the oil layer to flame radiation decreases ($\alpha(Z_o) q_r$), the rate of combustion decreases; and,
- as the wind speed increases the flame angle (δ) from vertical increases and the contribution to heating of the oil layer from radiation decreases.

For representative oil and water properties ($\rho_o = 850 \text{ kg/m}^3$; $C_{p,o} = 2 \text{ kJ/kg}^\circ\text{C}$; $k_o = 0.13 \text{ J/ms}^\circ\text{K}$; $\Delta H_{v,o} = 250 \text{ kJ/kg}$; $\Delta H_c = 4.5 \times 10^5 \text{ kJ/kg}$; $\rho_w = 1000 \text{ kg/m}^3$; $\Delta H_{v,w} = 2300 \text{ kJ/kg}$; $k_w = 0.7 \text{ J/ms}^\circ\text{K}$) and $T_e = 50^\circ\text{C}$, $T_o = 200^\circ\text{C}$ equation (5) becomes:

$$\begin{aligned} \frac{dZ_e}{dt} &= \frac{q_{conv}'' + \alpha(Z_o)q_r'' \cos\delta - U_o\Delta T}{850(f_w-1)250 + (f_w-1)2(200-50) - f_w(1000)2300/850} \\ &= \frac{q_{conv}'' + \alpha(Z_o)q_r'' \cos\delta - U_o\Delta T}{850(550(f_w-1) - 2700f_w)} \\ &= \frac{q_{conv}'' + \alpha(Z_o)q_r'' \cos\delta - U_o\Delta T}{-4.675 \times 10^5 - 1.8275 \times 10^6 f_w} \end{aligned} \quad (7)$$

In this form, it is easier to determine the effect of various factors on the burning rate.

As f_w increases in equation (7) (assuming that this does not greatly affect U_o), r declines due to the increasing amount of heat required to boil water as well as oil. This general trend is confirmed by the data of S.L. Ross (1989) and Bech et al. (1992).

Several additional simplifying assumptions can be made for special cases; namely:

- after Babrauskas (1988) pool fires greater than 0.2 m in diameter are dominated by radiative not convective heat transfer (this may not be strictly true in winds where the contributions of convective heat transfer are enhanced - there are conflicting data on whether or not wind speed increases or decreases burn rates and why - Babrauskas 1988)
- assume the oil layer absorbs all incident thermal radiation (i.e. $(Z_o) = \text{constant} = 1$)
- assume no wind, i.e. $\cos\delta = 1$

Equation (6) then simplifies to:

$$\frac{dZ_e}{dt} = \frac{q_r'' - U_o\Delta T}{\rho_o((f_w-1)\Delta H_{v,o} + (f_w-1)C_{p,o}(T_e-T_o) - f_w\rho_w\Delta H_{v,w}/\rho_o)} \quad (8)$$

in order to integrate and solve for $Z_e(t)$ it will be necessary to obtain reasonable expressions for q_r'' , U_o and ΔT . Wakamiya et al. 1982 give a simple expression for q_r'' as:

$$q_r'' = 0.02 r \Delta H_c \rho_o \quad (9)$$

which basically states that 2% of the heat of combustion of the oil is radiated back to the slick. This expression can be written as:

$$q_r'' = -0.02 \rho_o(1-f_w) \frac{dZ_e}{dt} \Delta H_c \quad (10)$$

and incorporated into equation (8).

Equation 8 can also be written in its rate form (i.e., substituting from equation (2) as):

$$r = \frac{q_r'' - U_o \Delta t}{\rho_o \Delta H_{v,o} + \rho_o C_{p,o} (T_e - T_o) - \rho_w \Delta H_{v,w} fw / (1 - fw)} \quad (11)$$

or, substituting from equation 13:

$$r = \frac{0.02 r \Delta H_c \rho_o - U_o \Delta T}{\rho_o \Delta H_{v,o} + \rho_o C_{p,o} (T_e - T_o) + \rho_w \Delta H_{v,w} fw / (1 - fw)} \quad (12)$$

In order to further simplify this it is necessary to determine the proper relationship for U_o (i.e., whether or not it involves slick thickness).

It is thus necessary to obtain the correct form of the heat transfer coefficient, which is expressed in its "resistances in series" form as:

$$\frac{1}{U_o} = \frac{1}{\frac{Z_o}{\lambda_o} + \frac{1}{h_{so}} + \frac{Z_e(t)}{\lambda_e} + \frac{1}{h_{se}}} \quad (13)$$

If the interfacial heat transfer coefficients are the major resistances, then the expression for U_o will not involve $Z_e(t)$ and equations 8 or 12 can be easily solved; if the major resistance to heat transfer is the conduction of heat through the oil or emulsion layer the expression for U_o could involve $Z_e(t)$ complicating the integration (see, for example, Brzustowski and Twardus 1982).

The correct expression for ΔT , which will not affect integration, depends on the form chosen for U_o .

3.2.3 Static heat transfer experiments

Figures 3.12 and 3.13 shows data from two of the heat transfer experiments. The temperature graphs show that the temperature in the emulsion slick only does not exceed 100°C, except for in the top layer of the oil. The bar charts both demonstrates that there is a relation between the water content in the oil and to the temperature in the oil slick. With an increase in depth, the rise in temperature is a dynamic process whereby the temperature does not seem to rise above 100°C until the water is removed (evaporated) out of the slick.

A statistical analysis of the data from the of experiments was done to see how the heat transfer through the slick influenced the physical-chemical properties of the emulsion. This analysis was done using linear and full factorial multiple regression models. The parameters considered in this analysis were the water content of the emulsion, the degree of evaporation of the oil, and the slick thickness.

All of the data on oil properties from all the experiments have been treated as one data-set. Thus changes in water content and density of the oil could be studied as a function of initial water content, and evaporation of the oil/emulsion, the initial thickness, and the depth location in the slick; as well as time.

JMP, the statistical program used produces leverage graphs for each factor and combination of factors included. These graphs illustrate the significance of a given effect on the model. The type of leverage plot shown in Figure 3.14 and 3.15, called the "Whole Model Test", plots the experimental values of the response against the model-predicted values. An effect can be tested for significance by comparing the sum of R-squared residuals to the sum of R-squared residuals of the model with that particular effect removed. If residual errors are much smaller when the effect is included in the model, than that effect is a significant contribution to the fit. The horizontal line in the leverage plot represents the mean response of the partially constrained model if the given effect or parameter were constrained to zero. The line of fit is shown with confidence curves indicating whether the test is significant at the 5% level. When the confidence region contains the horizontal line, the effect is not significant. If the confidence curves cross the horizontal line, then the effect is significant at the 5% level. Details on the statistical methods can be found in SAS (1989).

Figures 3.14 and 3.15 show the multiple regression models for water content and density.

The statistical model for the water content in the emulsion shows that the water content at any time, for any sample location in the emulsion layer can be explained by the time elapsed, the initial degree of evaporation, the initial slick thickness and the depth of the sample point in the emulsion layer. None of the factors represented statistically significant explanations indepently, but depth without the selected significant level (i.e. 90%) has the highest explanation level as an independent explanatory factor. The combined factors all contain, depth and time, clearly demonstrating that these two factors are the most important ones. This statistical model indicates that the water loss is a time and depth dependent process, when an emulsion is exposed for radiated heat.

Density was used here to express the degree of evaporation of the oil. As could be expected, the degree of evaporation at any time can be explained both by the initial evaporation, the initial thickness, the time and the depth (i.e. the sample location).

The models for water content and for density are in accordance with each other and are also in accordance with the assumptions made in the conceptual model for burning. The heat transfer experiment can then serve as a verification of this model.

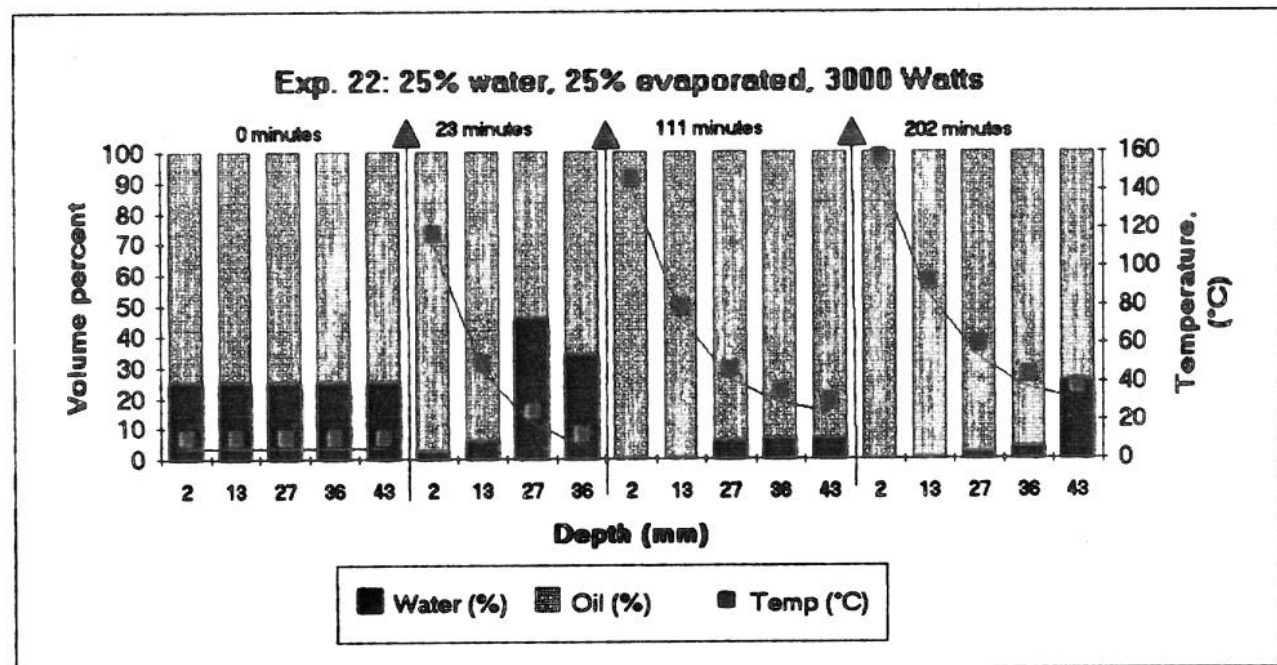
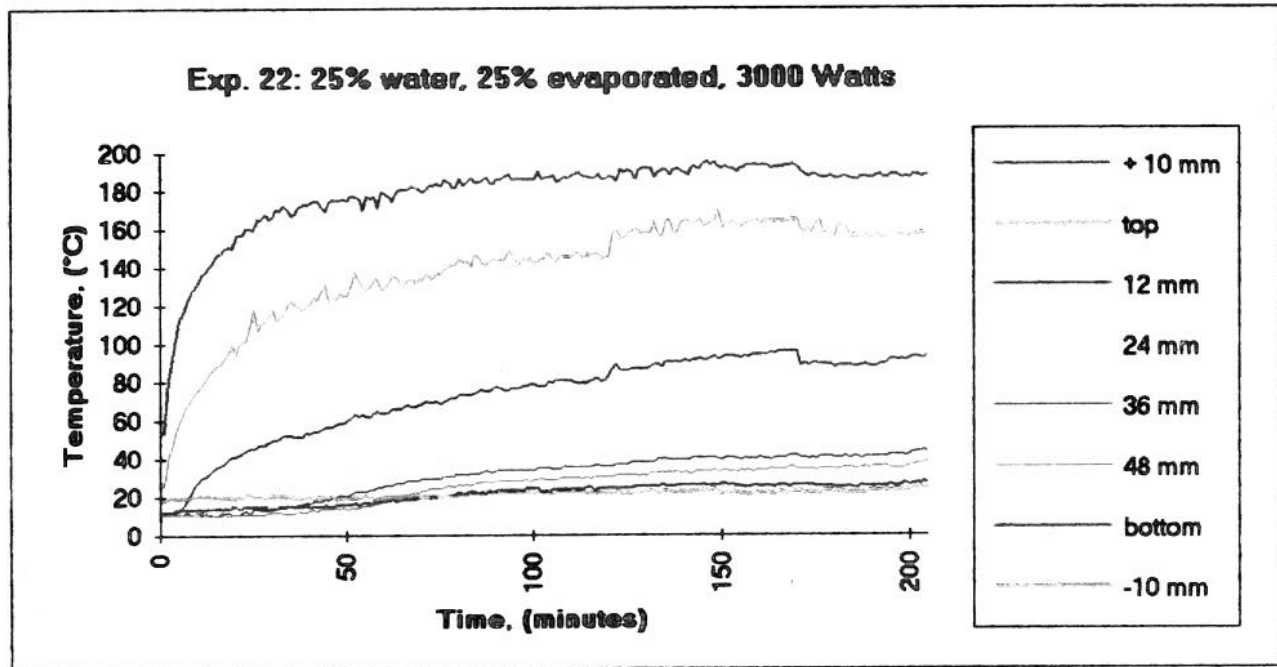


Figure 3.12: Temperature development and water content in the emulsion layer during the heat transfer Experiment No. 22.

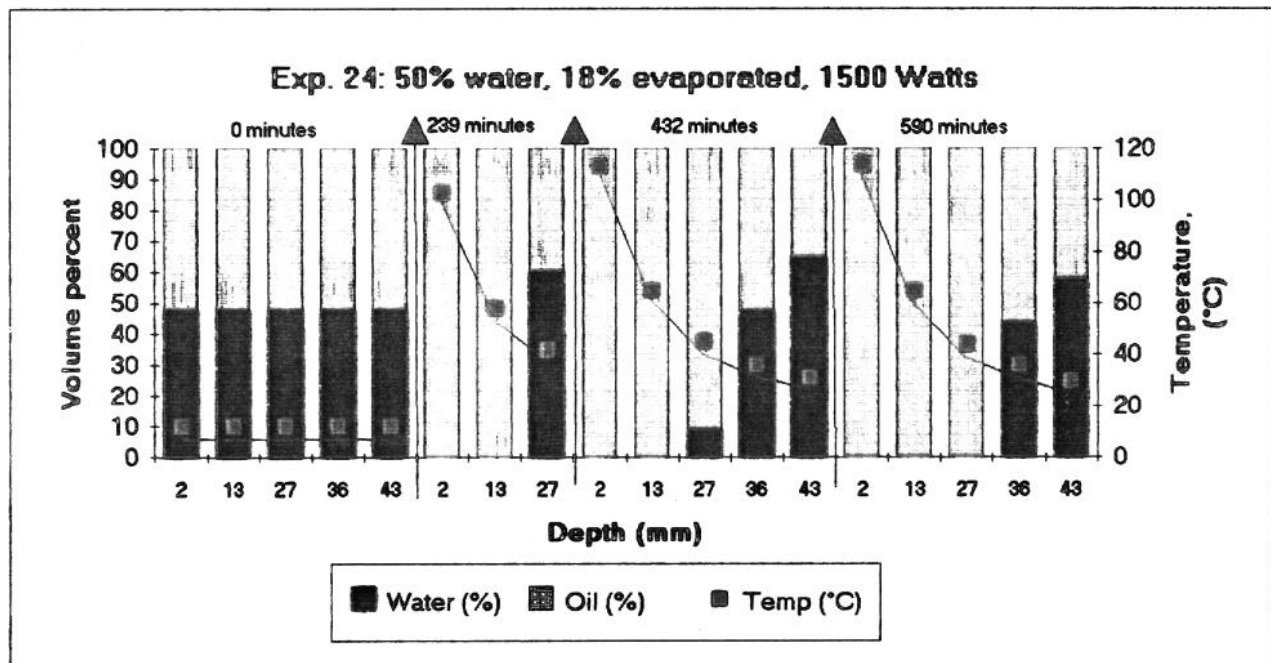
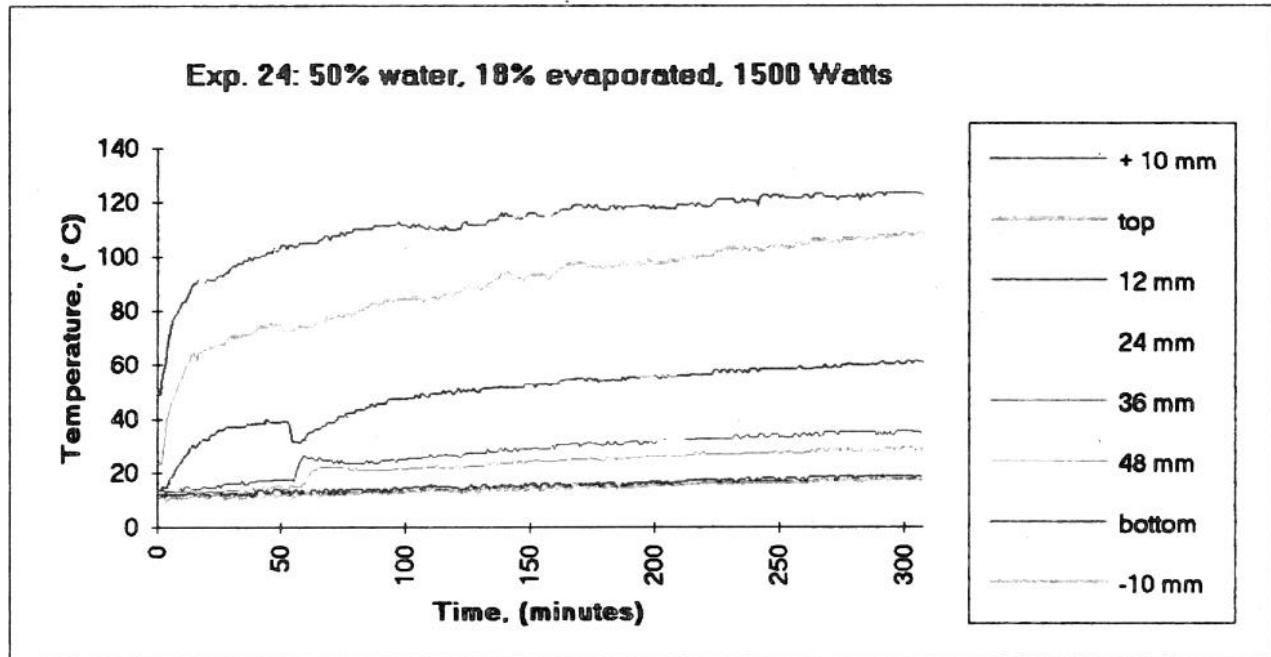
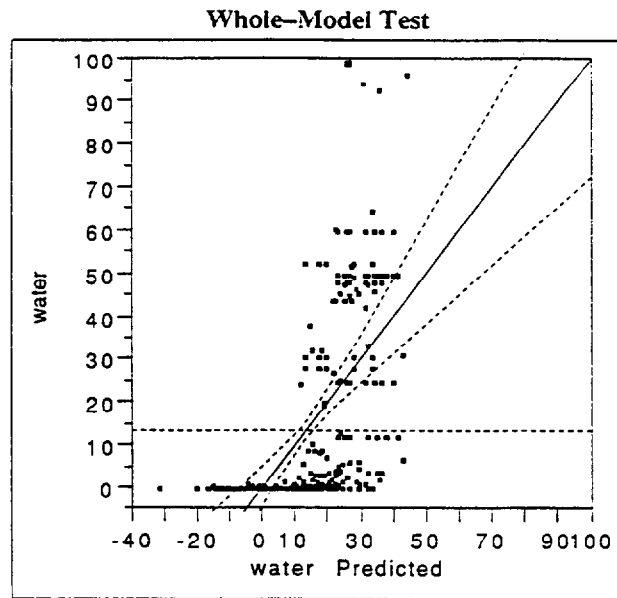
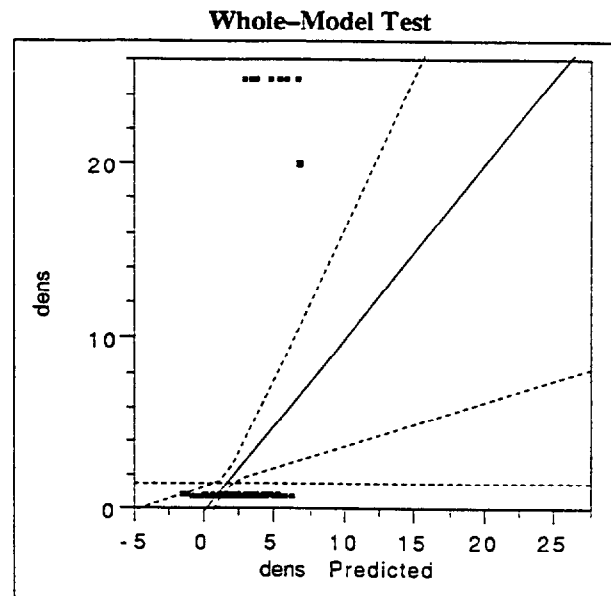


Figure 3.13: Temperature development and water content in the emulsion layer during the heat transfer Experiment No. 24.



Analysis of Variance				
Source	DF	Sum of Squares	Mean Square	F Ratio
Model	15	68556.67	4570.44	16.2586
Error	330	92766.02	281.11	Prob>F
C Total	345	161322.69		0.0000

Figure 3.14 Heat transfer experiments: multiple regression models for water content in emulsions.



Analysis of Variance				
Source	DF	Sum of Squares	Mean Square	F Ratio
Model	15	615.8720	41.0581	3.0763
Error	277	3696.9622	13.3464	Prob>F
C Total	292	4312.8341		0.0001

Figure 3.15 Heat transfer experiments: multiple regression models for water content in emulsions.

3.2.4 Small scale burning experiments

3.2.4.1 Ignition and burning of Avalon Crude emulsions

Ignition

Figure 3.16 shows the relationship between ignition time (using only a 25 cm² gasoline-soaked sorbent as an igniter) and degree of evaporation for 0, 12.5 and 25% water content emulsions of the Avalon crude oil. Three least-square best fit lines are shown on each graph: the solid line relates to the 5 mm initial slick thickness (circle symbols); the short-dash line describes the relationship for the 10 mm initial slick thickness experiments (square symbols); and, the long-dash line applies to the 20 mm initial slick thickness data (triangle symbols).

For unemulsified oil slicks (the top left graph on Figure 3.16) there was a perceptible increase in ignition time with increasing evaporative loss. Although the 5 mm, unemulsified slicks do appear to have taken longer to ignite, there does not appear to be a strong relationship between initial slick thickness and ignition time for the thicknesses studied here. The ignition times for the 12.5% (upper right graph) water content emulsions increased more rapidly with evaporation than for the unemulsified oil; again, the 5 mm thick slicks show a greater dependence than either the 10 mm or 20 mm thick slicks. Only the fresh oil could be ignited for the 25% water content emulsions. These trends are consistent with those found by other researchers (Energetex 1979, S.L. Ross 1989, Bech et al. 1992, Cabioc'h 1993).

Figure 3.17 shows the trends in ignition time (using only a gasoline-soaked sorbent igniter) with increasing water content for a fixed degree of evaporation. For fresh oil (top left graph) the ignition time increased with increasing water content up to 25%; there appears to have been a dependence on thickness but this may just be due to data scatter. The maximum ignitable water content for the fresh Avalon crude was 25%. For the 12.7% evaporated crude (top right graph) the dependence of ignition time on water content is stronger than for the fresh crude; the 5 mm thick slicks were more affected than either the 10 or 20 mm thick slicks. The maximum ignitable water content for the 12.7% evaporated crude was 12.5%. No emulsions of the 20.6% evaporated Avalon crude (lower graph) could be successfully ignited. These results are consistent with those obtained previously for oils that form very stable emulsions (Energetex 1980, S.L. Ross 1989, Bech et al. 1992, Cabioc'h 1993).

Burn Process and Temperatures

Figure 3.18a compares the thermocouple readings from three 10 mm thick, fresh Avalon oil burns. From left to right the water content increases from 0% to 12.5% to 25%. Two interesting aspects of highly stable emulsion burning can be gleaned from this figure. First, as the water content increased the flame temperatures decreased (note the scale differences on the ordinate of the three graphs). Visual observations also confirmed that as the water content increased for this oil the flames became weaker. Second, the rise in surface oil temperature was slower and peaked at lower temperatures as the water content increased. For the unemulsified oil, a peak near surface slick temperature of almost 300°C was reached; for the 12.5% water content slick the peak was 200° C and 100°C was the peak for the 25% water slick. The maximum surface slick temperature reached was also observed to be a function of slick thickness. As shown on Figure 18b, this increased from about 150°C for the 5 mm unemulsified slick (Exp. 2.1) to almost 300°C for the 10 mm unemulsified slick (Exp. 2.2) and reached about 375°C for the 20 mm unemulsified slick.

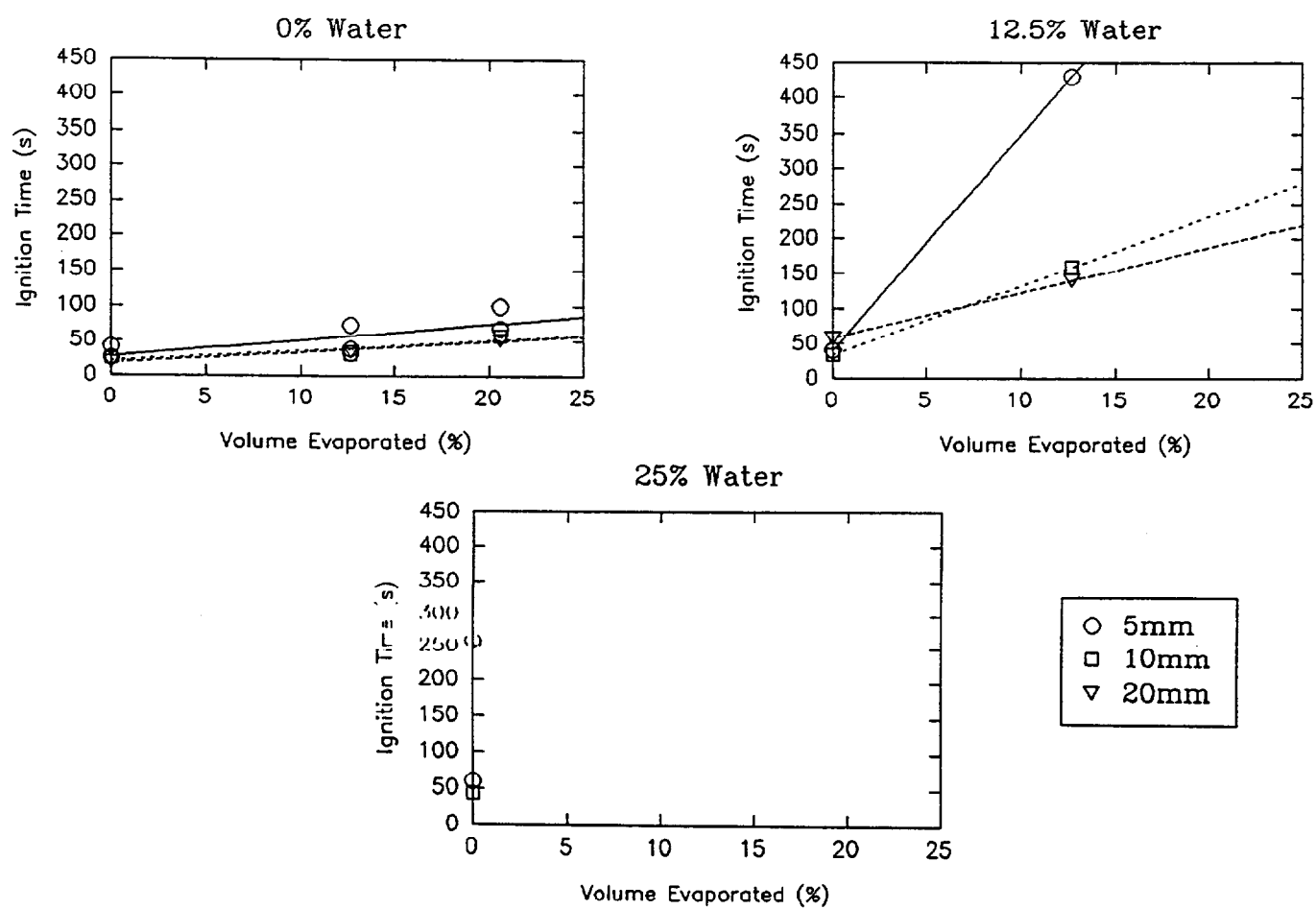


Figure 3.16 Ignition time vs. weathering - Avalon crude

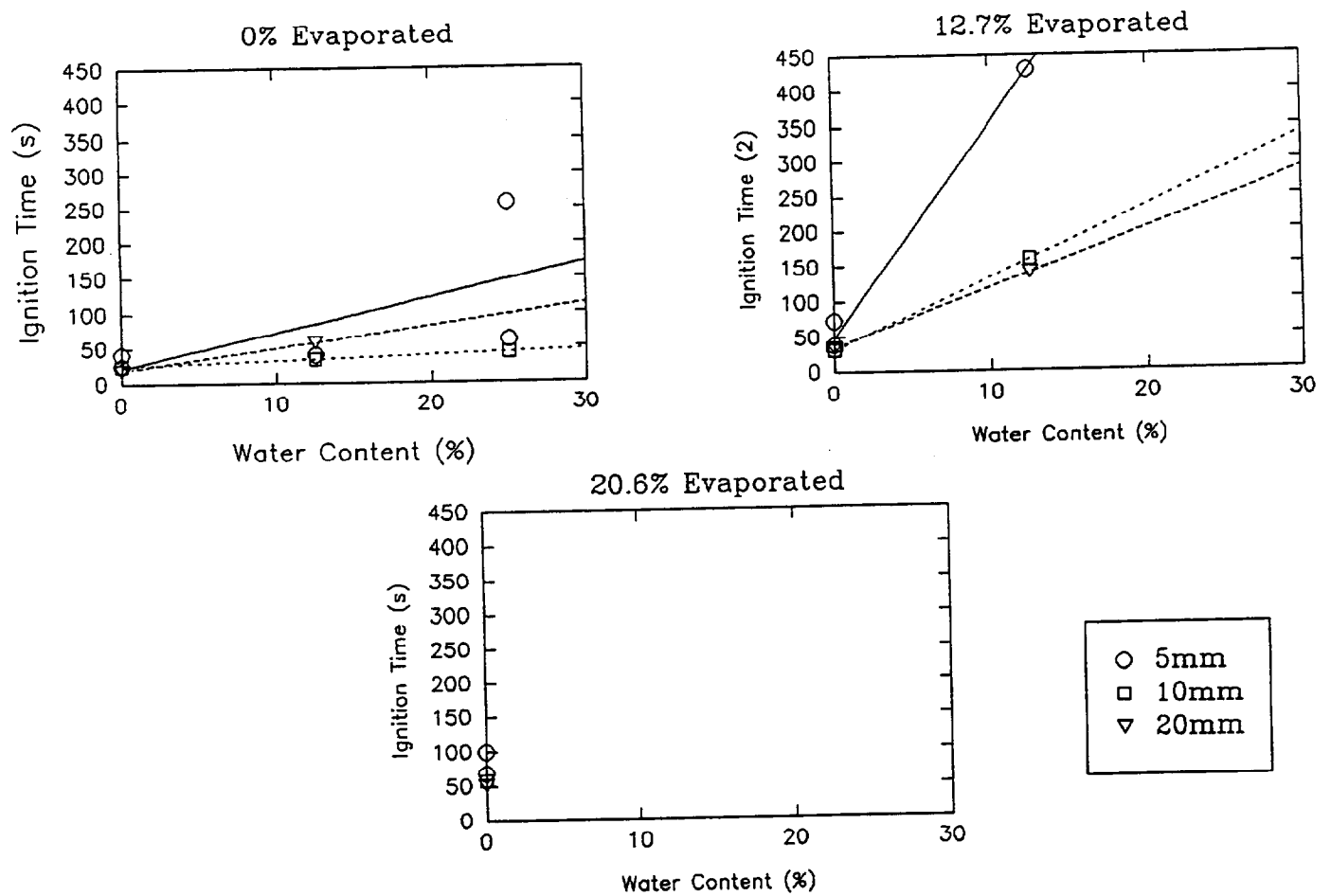


Figure 3.17 Ignition time vs. emulsification - Avalon crude

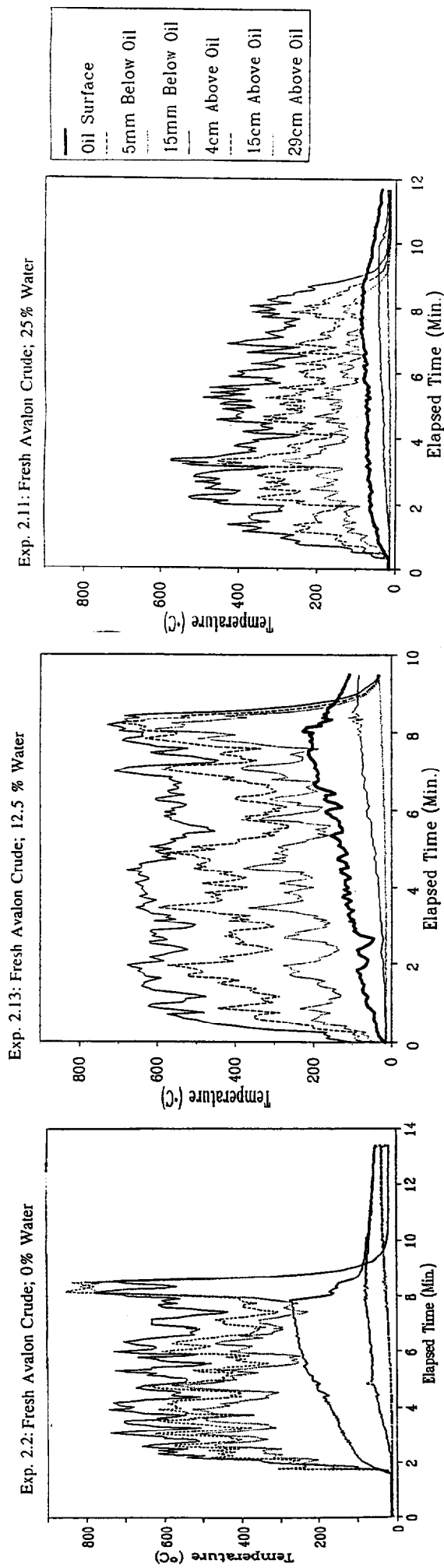


Figure 3.18a Temperatures for emulsified Avalon burns

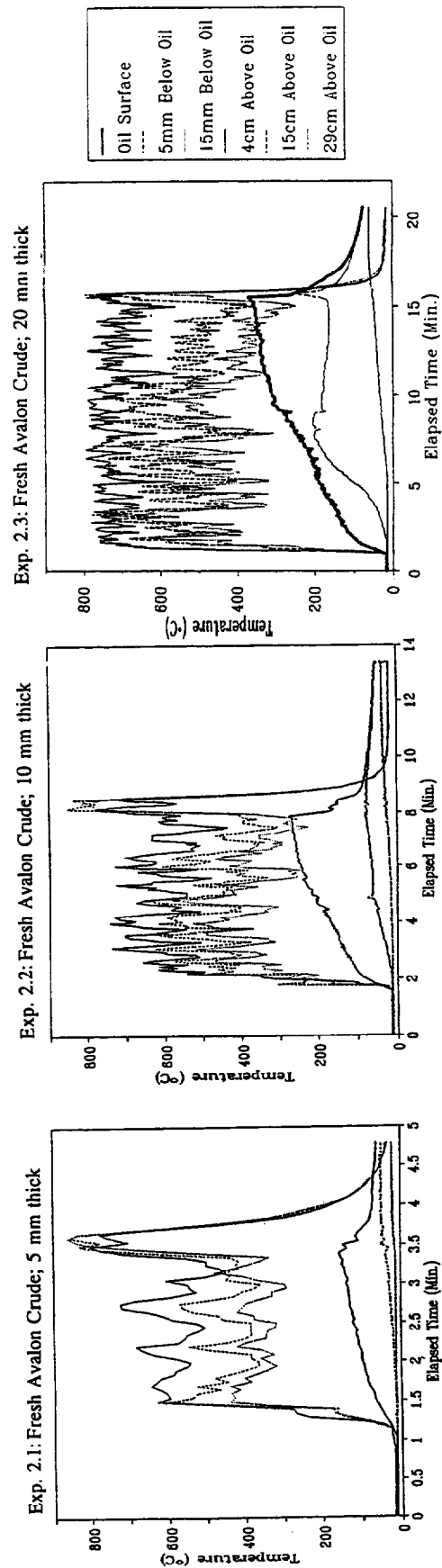


Figure 3.18b Temperatures for unemulsified Avalon burns

It may be that somewhere between 12.5% and 25% water is the maximum water content that permits water to boil out of the emulsion faster than the oil can vaporize and burn. Cabioc'h 1993 reports that for high asphaltene emulsions (very stable) the maximum burnable water content is 20%. At water contents in excess of this maximum, the slick temperature would be restricted to no higher than about 100°C by the presence of liquid water.

Burn Efficiency

Figure 3.19 shows the effect of degree of evaporation on burn efficiency for various water contents. On this, and subsequent graphs the method of ignition is noted. These series of graphs look at burn efficiency, independent of ignition technique; the burn could have been initiated with a 25 cm² gas-soaked sorbent, a 25 cm² fresh crude-soaked sorbent, or thin layers of fresh crude oil spread over the surface. Unsuccessful ignition attempts were not included in the least-squares correlations. In instances where multiple ignitions were required to initiate burning the attempts are assigned a letter code (data points with no letter code nearby were successfully ignited with a 25 cm² gasoline-soaked sorbent). Unsuccessful ignition attempts for a particular test are denoted by the appropriate slick thickness symbol on the abscissa with the failed ignition technique letter code(s) printed directly above. If a subsequent ignition technique was successful, another slick thickness symbol showing the burn efficiency achieved is shown on the graph with the successful ignition source denoted by the letter code to the right of the symbol.

For unemulsified oil (top left graph) there is little effect of evaporation on burn efficiency, as noted by others (e.g., S.L. Ross 1989, Cabioc'h 1993). The interesting point to note on this graph is the relationship between initial slick thickness and burn efficiency. As expected, for a constant residue thickness of about 1 mm, the burn efficiency for the 5 mm thick slick is about 80% $((5-1)/5)$ and the efficiency for the 10 mm thick slicks was about 90% $((10-1)/10)$; however, the efficiency of the 20 mm thick burns was only 75% not 95% $((20-1)/20)$ as expected. This was because the 20 mm burning slicks foamed up and extinguished. The likely explanation for this result is that, for the thickest slicks, the hot zone grew deep enough to initiate turbulence beneath the burning oil while there was still a thick layer of oil remaining. The ensuing turbulence (observable at the underside of the slicks through the underwater mirrors) resulted in emulsification of this highly emulsifiable crude which resulted in both the foaming phenomenon and a residue weight greater than expected because of entrained water. The phenomenon of emulsified residue after a burn of unemulsified oil has been noted by other researchers (Energetex 1979, S.L. Ross and Energetex 1986). The fact that the time to intense burn for the 20 mm thick slicks of Avalon crude was approximately twice that of the corresponding 10 mm burns, lends credence to the residue emulsification theory. It would be unusual for unemulsified oil burn rates to be a strong function of thickness at this scale of tests, thus a burn that lasts twice as long should consume twice as much oil and leave behind much less residue than the amounts actually measured; residue emulsification would explain the discrepancy.

Figure 3.18b in the previous section shows the temperature data measured during burns of unemulsified, fresh Avalon crude with initial thicknesses of 5, 10 and 20 mm (Experiments 2.1, 2.2 and 2.3 respectively). Note the differences in time scale on the abscissa. In the case of the Exp 2.3 the thermocouple 5 mm below the initial oil surface indicates an initial rise in temperature to about 200°C over the first 10 minutes of the burn, then a slow decline (as the oil burns the water level inside the ring rises from below bringing the thermocouple nearer to the oil/water interface). Just before the fire extinguishes a spike occurs in the temperature that may signal the descent of the "hot-zone" to the water surface initiating foaming and residue emulsification. This spike is not apparent in the 10 mm thick slick temperatures. This spike appear consistently for each of the 20 mm, unemulsified Avalon burns (i.e., the 12.7% evaporated and 20.7% evaporated).

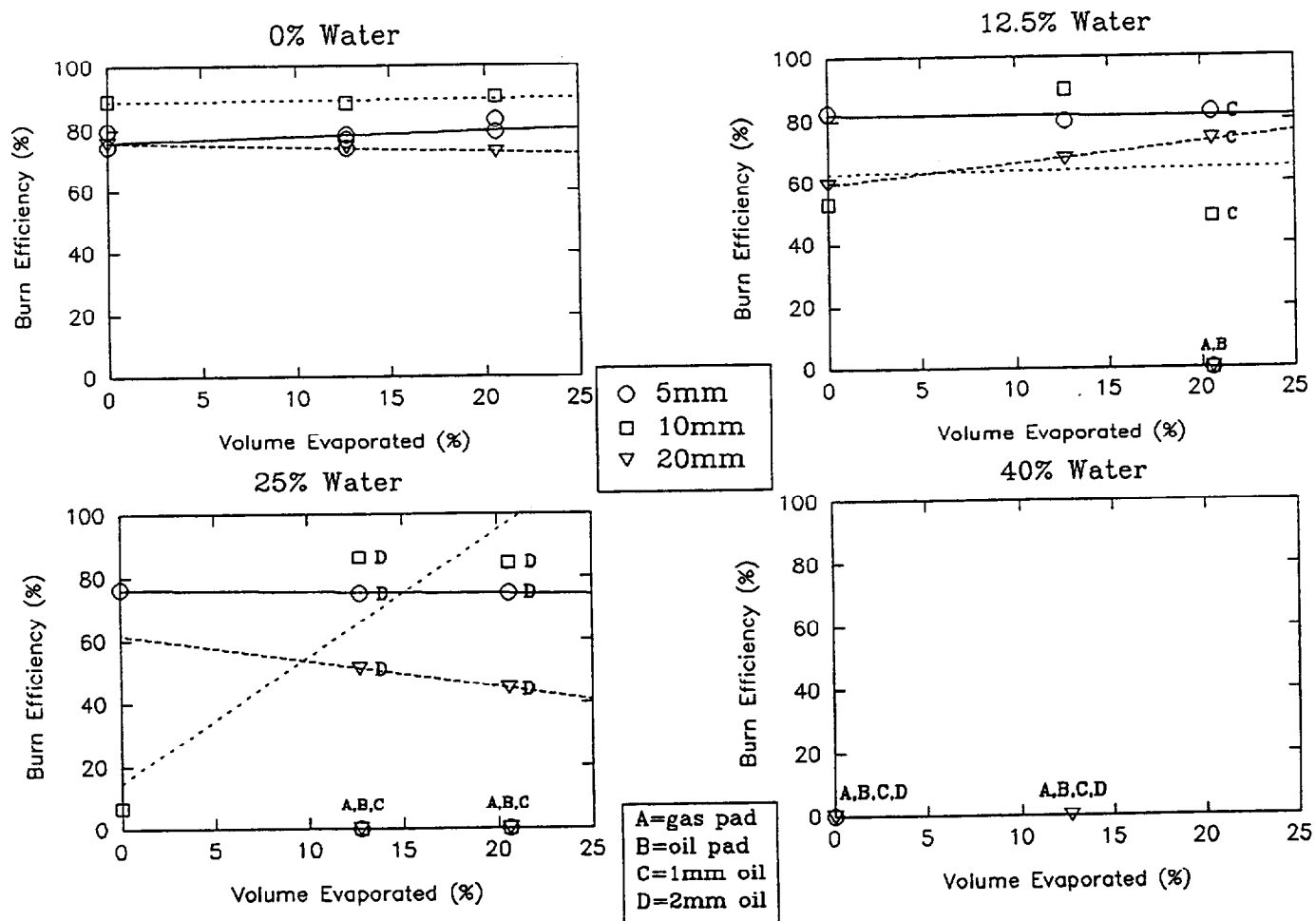


Figure 3.19 Burn efficiency vs. weathering - Avalon crude

The trends in Figure 3.19, excepting the residue emulsification anomaly for the 20 mm slick thickness, are clear: degree of evaporation has little or no effect on burn efficiency. The unusual trend for the 10 mm thickness in the bottom left graph was felt to be due to a poor test result for the fresh oil/25% water content combination.

Figure 3.20 shows the effect of water content on burn efficiency for the three degrees of evaporation of the Avalon crude. Although there is considerable scatter in the data, the general trend seems to be little or no effect on burn efficiency for the 5 and 10 mm thick slicks up to about 25% water content and a steady decline in efficiency for the 20 mm thick slicks with increasing water content. Foaming of the 20 mm slicks was exacerbated by increasing water content. None of the 40% water content slicks could be ignited; attempts were not made to ignite 40% water content slicks of 20.6% evaporated Avalon because neither 12.7% evaporated nor fresh slicks at this water content could be ignited.

Burn Rate

Figure 3.21 shows the range of burn rates determined for all the unemulsified crude oil types as compared to the work of previous researchers. The burn rates determined in this study were within the expected range for the size of the burns.

Figure 3.22 shows the relationship of burn rate (oil only - water excluded) to degree of evaporation for various water content Avalon slicks. It should be noted, particularly for the unemulsified slicks, that the foaming phenomenon and possible emulsification of the burn residue introduces an error into these data points. For the three water contents that could be successfully ignited, neither degree of evaporation nor initial thickness (over the range of these parameters tested) played a strong role in determining oil burn rate.

Figure 3.23 shows that water content strongly affected burn rate for the very stable Avalon crude emulsions. The burn rate for all thicknesses and degrees of evaporation declines rapidly with increasing water content. Emulsions of even fresh Avalon crude with water contents in excess of 25% would not burn. These results are broadly consistent with those of other researchers who have burned highly stable emulsions (Energetex 1980, S.L.Ross 1989, Bech et al. 1992, Cabioc'h 1993).

Summary

In summary, the highly stable emulsions formed by salt water in Avalon crude oil are difficult to ignite and burn at water contents above 12.5% and impossible to ignite at water contents above 25%. The only route by which emulsion water escapes from the emulsion appears to be by vaporization. For the 20 mm thick slicks of Avalon oil or emulsion foaming was the method of extinguishment and residue emulsification may have occurred; thinner slicks were extinguished by transition to vigorous burning followed by extinction via cooling at a residue thickness of about 1 mm.

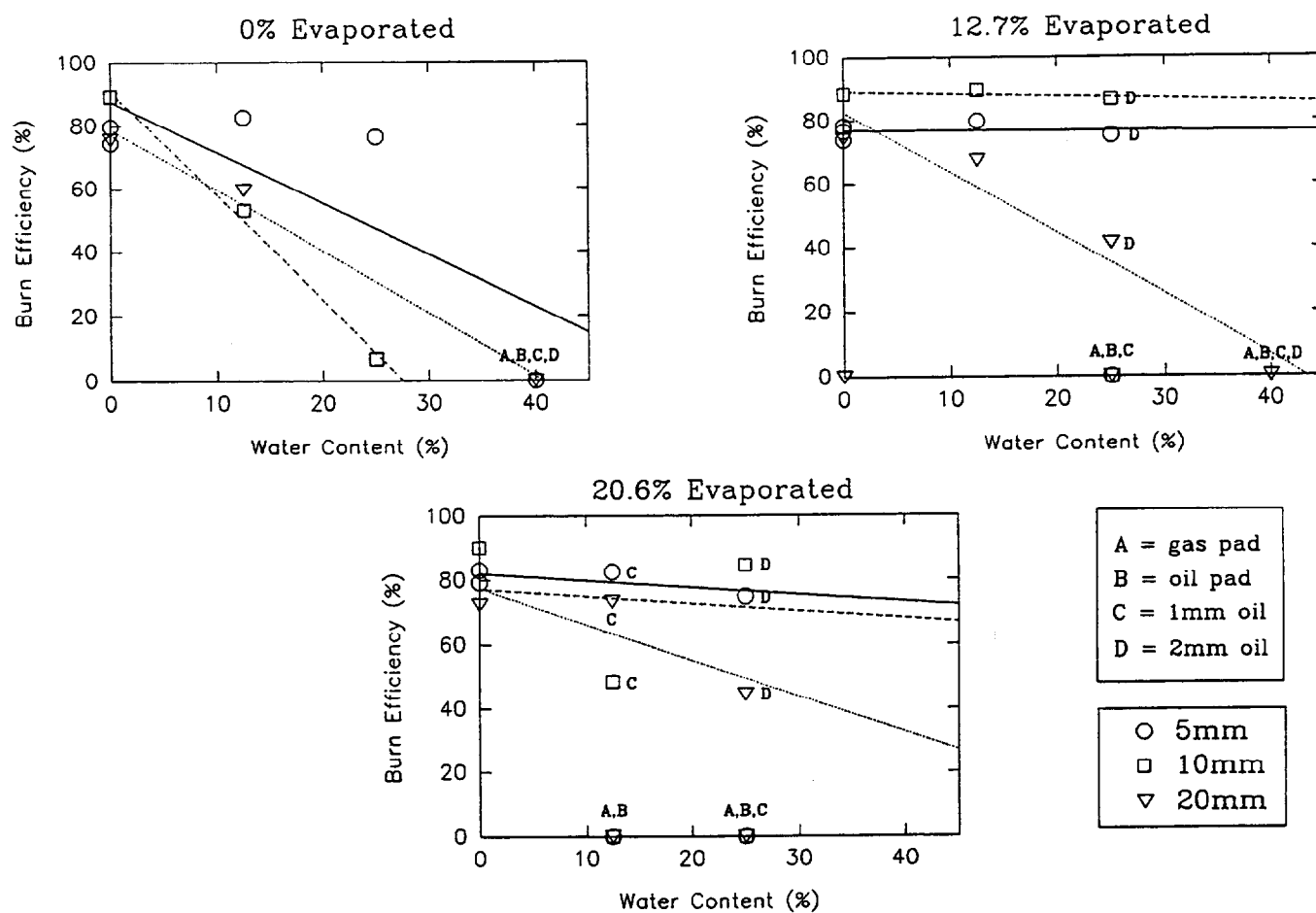


Figure 3.20 Burn efficiency vs. emulsification - Avalon crude

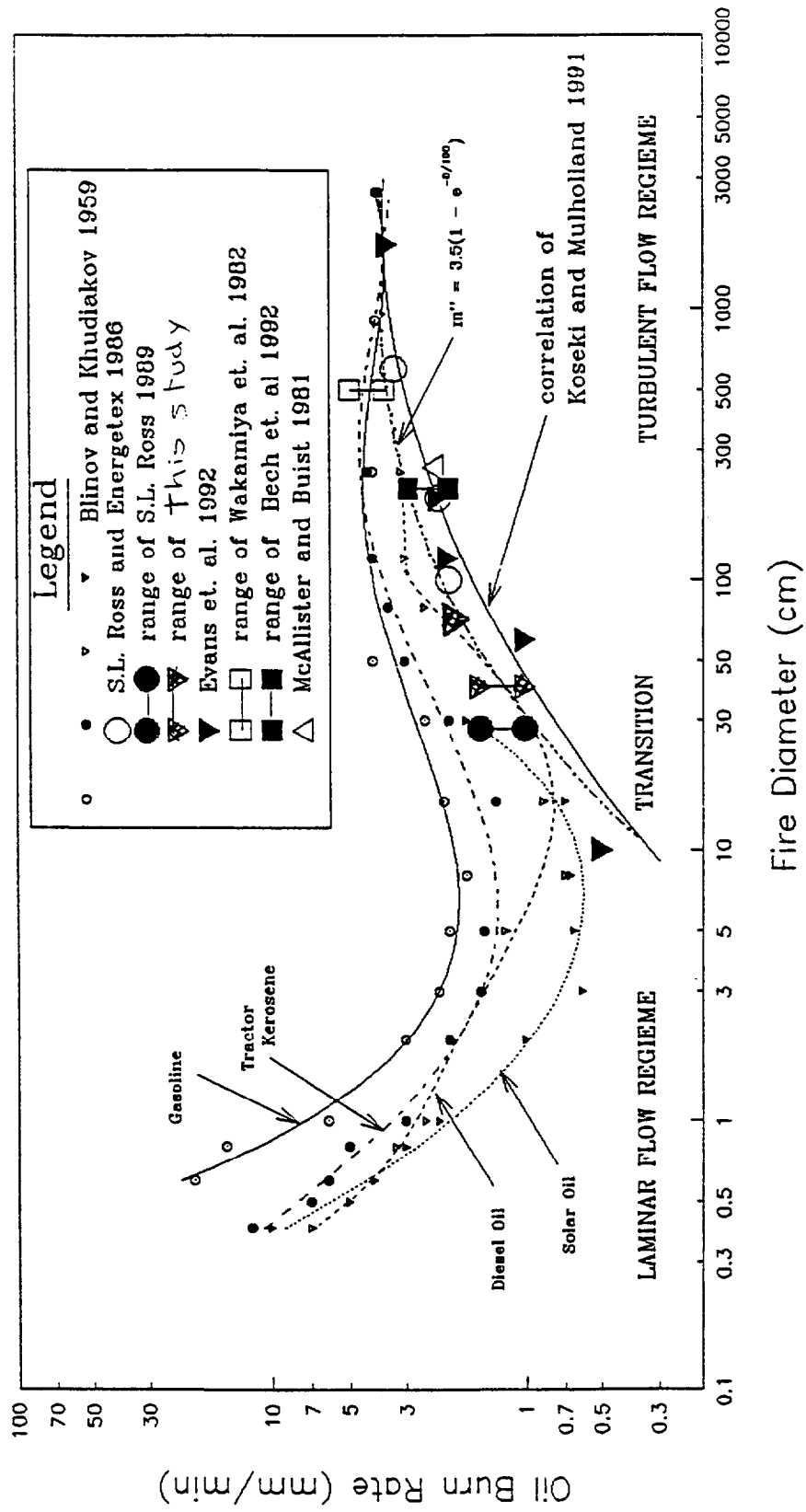


Figure 3.21 Burning rate vs. fire diameter

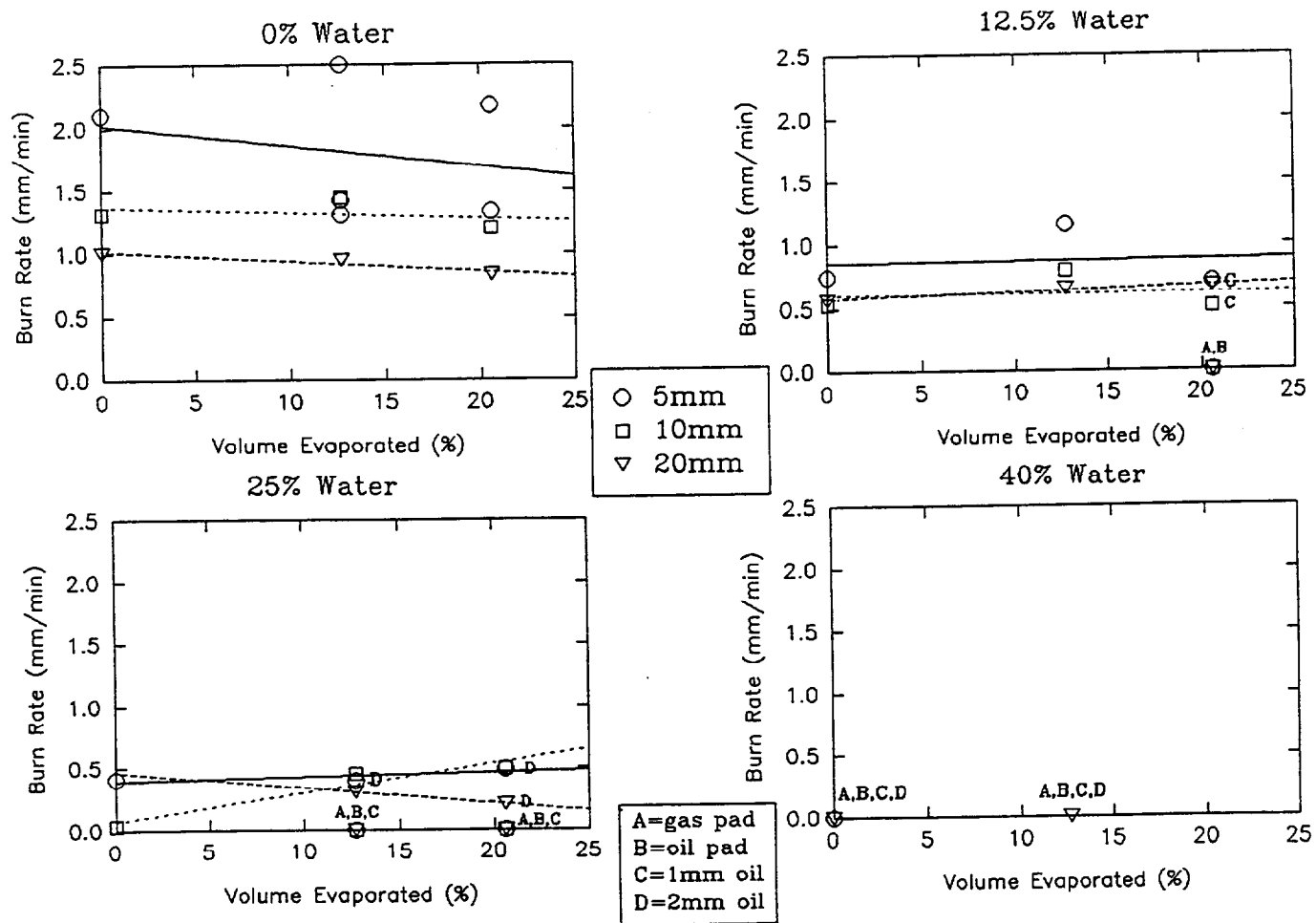


Figure 3.22 Burn rate vs. weathering - Avalon crude

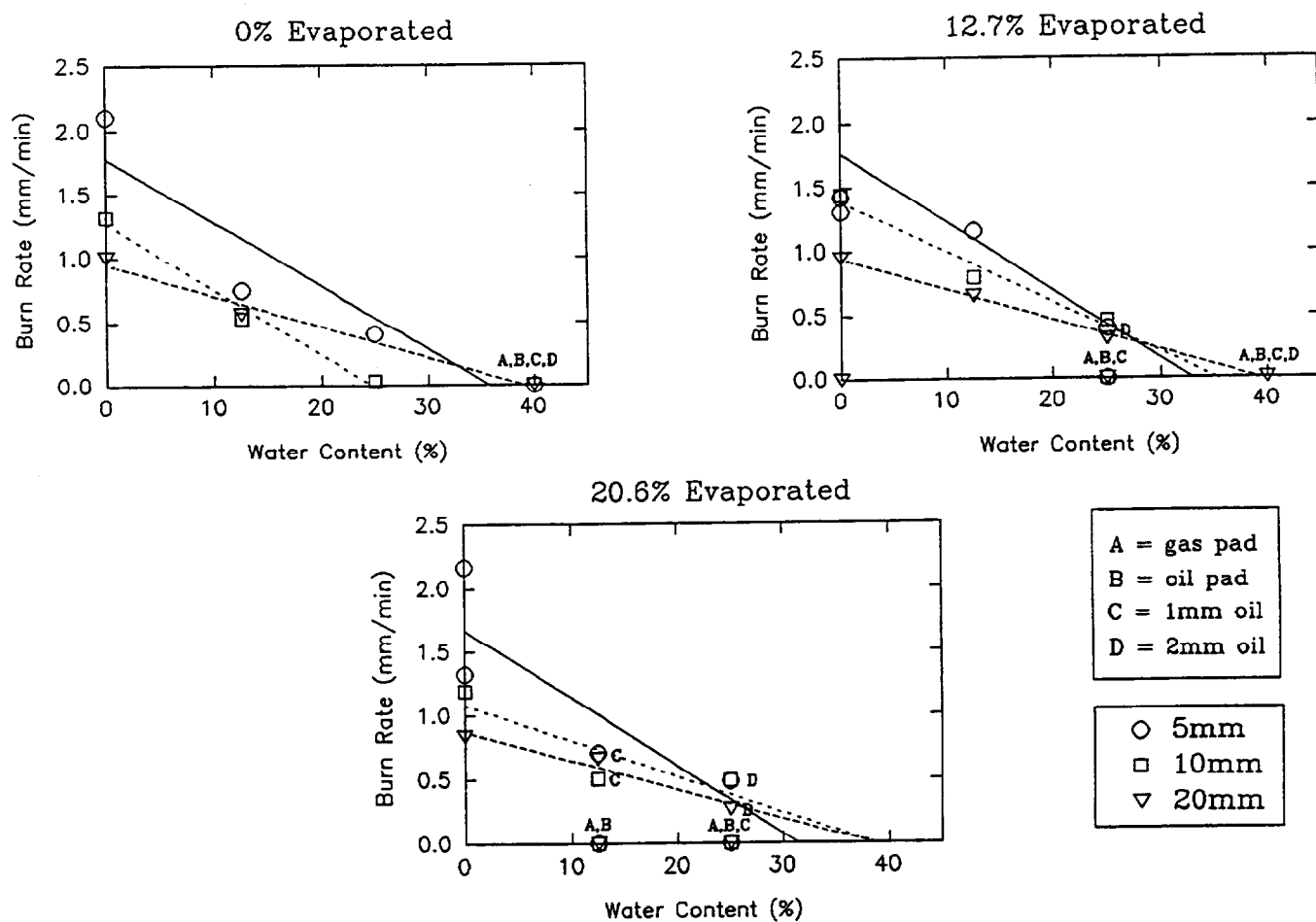


Figure 3.23 Burn rate vs. Emulsification - Avalon Crude

3.2.4.2 Ignition and burning of Statfjord crude emulsions

This section presents and discusses the results of the small-scale experimental burns with salt-water emulsions of fresh and weathered Statfjord crude oil (data can be found in Appendix A). More experiments (89) were conducted with this oil than the other oils because it was the oil available for the mesoscale field burns at Sveagruva and thus most of the small-scale igniter capability and enhancement tests were conducted with this oil. In addition, some burns with additives were conducted with 30 mm thick slicks to give longer soot sampling times (see section 6). The impeller technique of producing emulsions with the Statfjord oil was not capable of producing highly stable emulsions with high water contents at room temperature with degrees of evaporation less than 20% (see Section 3.1.2). For this reason, several experiments were conducted with 5% by volume Bunker C (also known as Number 6 Fuel Oil) added to the oil prior to emulsification. The presence of the asphaltenes in the Bunker C served to help stabilize otherwise unstable emulsions.

Ignition

Figure 3.24 shows the effect of evaporation on ignition time (using only a 25 cm² gasoline-soaked sorbent) for five water contents (0%, 12.5%, 25%, 40% and 60% by volume). It can be seen that, for the unemulsified oil, an increase in evaporation resulted in an increase in ignition time; the rate of increase (about 40 seconds for a 20% evaporative loss) is similar to that measured for the unemulsified Avalon oil (see Figure 3.16). There did not appear to be any measurable effect of slick thickness on the ignition time. As the water content increased the slope of the least squares best fit lines generally increased; it appears that increasing water content accentuates the effect of weathering on ignition time. This is consistent with the results for the Avalon oil and previously reported field burn results for Statfjord crude (Bech et al. 1992). The higher degree of data scatter in the graph for 60% water content emulsions (Figure 3.25, right hand side) may be due to the moderate stability of the emulsions created containing this amount of water.

Figure 3.25 shows the relationship between ignition time and water content for the four fixed degrees of evaporation. The data for the fresh crude (top left graph) reflects the fact that it was not possible to emulsify fresh Statfjord crude with the impeller technique at ambient temperatures. The trend for the 12.9% evaporated emulsions (top right graph), which indicates little or no dependence of ignition time on water content, is likely also an artifact of low emulsion stability at this degree of weathering. It is worthy of note; however, that Bech et al. 1992 report little or no dependence of ignition time on water content for emulsions of fresh and topped Statfjord/Gullfaks mixed crude created using a high speed gear pump.

The trend for the 19.6% evaporated oil shows a slow increase in ignition time with increased water content. For the 30.6% evaporated Statfjord crude (bottom right graph) there is a clear trend in increasing ignition time with increased water content. The emulsions created in the lab using the impeller with this evaporated oil were the most stable ones produced. Emulsions of this oil, with water-contents of 40% and greater, could not be ignited with the 25 cm² gasoline-soaked sorbent pad.

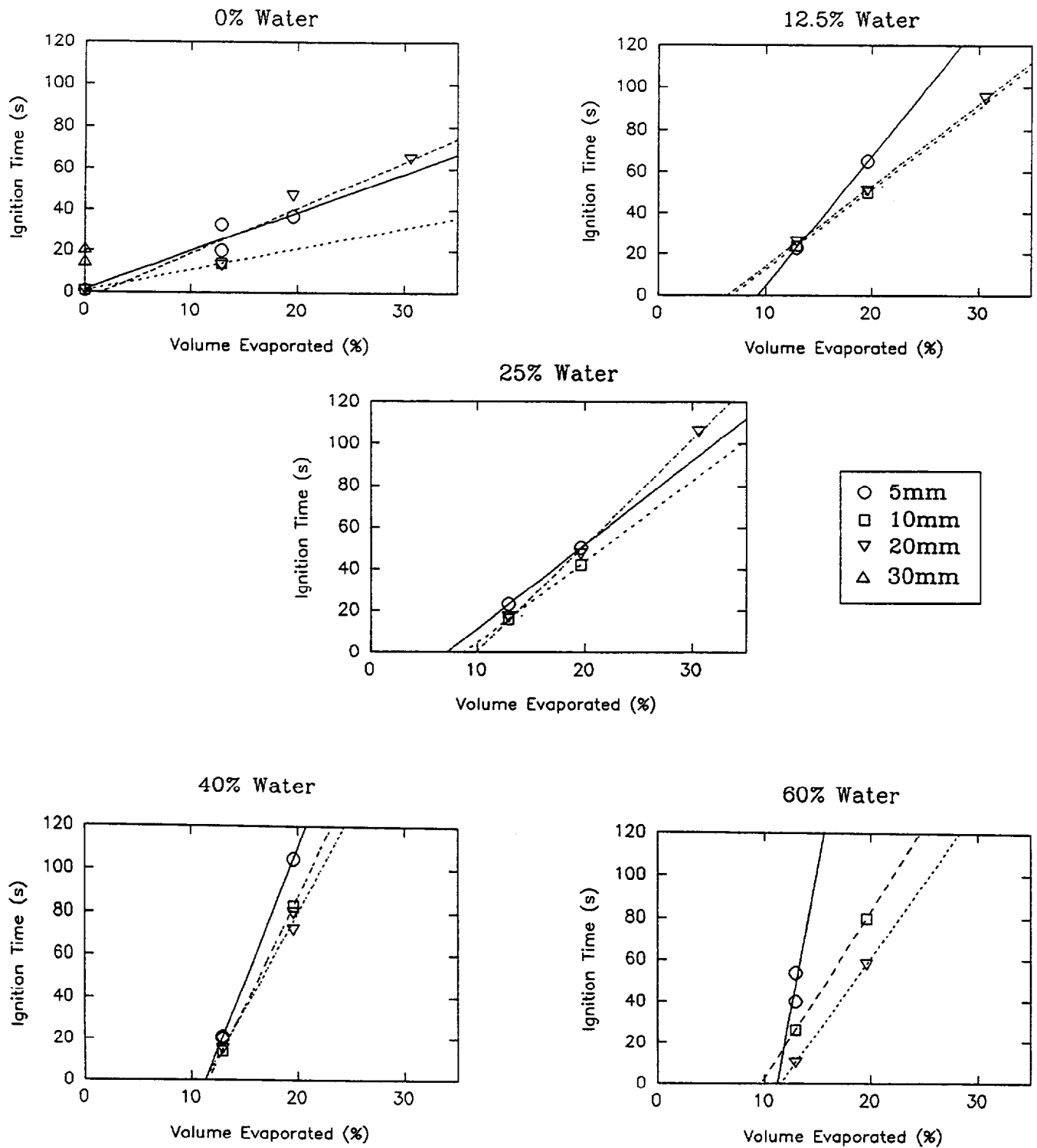


Figure 3.24 Ignition time vs. weathering - Statfjord crude

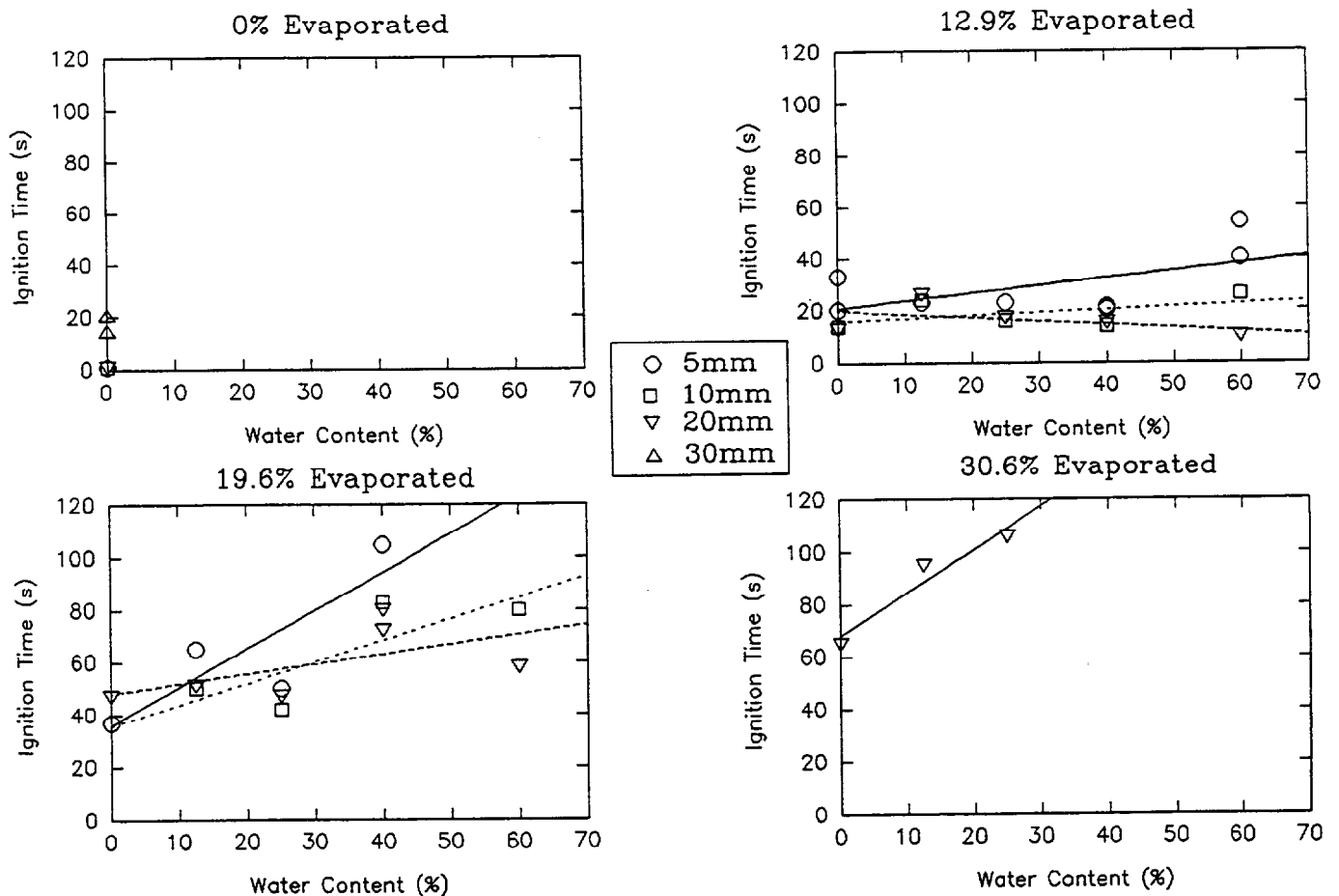


Figure 3.25 Ignition time vs. emulsification - Statfjord crude

Burn Process and Temperatures

During burns with emulsions of Statfjord crude oil with higher water contents an interesting process was observed. As the burn progressed, large bubbles several cm in diameter were observed to appear on the underside of the slick. These bubbles were surrounded by a brown skin and would either break and release a clear liquid or break away from the slick and slowly sink in the fresh water of the test pan. It was concluded that these bubbles contained salt water that had separated out of the slick under the influence of heating. Two experiments (4.47 and 4.48 in Appendix A) were run with 35‰ salt water in the pan; in these the slick did not produce bubbles but did have holes in its underside that appeared to eject water.

This phenomenon is believed to be evidence of another water removal process that affects *in-situ* burning of water-in-oil emulsions, namely the bulk removal of emulsion water by breaking and separation, as opposed to boiling. It appears that for oils that are susceptible to breaking at elevated (but below 100°C) temperatures it is possible for water to be physically removed from the emulsion by breaking. This phenomenon may partially explain the wide range (20 to 70%) of "unignitable" emulsion water contents reported in the literature. Oils that form very stable emulsions at elevated temperature (e.g., Avalon crude) can only lose emulsion water and produce a layer of pure oil for burning by vaporization of the water; these oils may be the ones that have unignitable water contents at the low end of the range. Other oils that form less stable emulsions at elevated temperatures could break on ignition and physically release water; these oils may be the ones that are ignitable at the high end of the water content range.

It is known that the addition of Bunker C to moderately stable emulsions can result in increased stability (Gåseidnes 1993). Several burn experiments with Statfjord emulsions were undertaken with Bunker C added to the oil (4.48 to 4.54). Table 3.3 shows a comparison of these with the corresponding "undoped" experiments. It is clear that artificially enhancing the stability of the emulsions dramatically increases ignition times and reduces burn efficiencies. It is worthy of note that even stabilization of the Statfjord emulsions with Bunker C does not render them as unignitable as the Avalon crude emulsions. It is also worthy of note that few bubbles of emulsion water were produced by the burning emulsions that had been stabilized by Bunker C.

One feature of emulsion burning noted by others (Energetex 1980, S.L. Ross 1989, Bech et al. 1992) is that the oil burns quite violently with much spattering (similar to the vigorous phase of burning of an unemulsified slick). This phenomenon was quite apparent when burning the Statfjord emulsions with 25% water content or more. It is probable that the phenomenon relates to vigorous boiling of the emulsion droplets as they are heated; the steam produced likely ejects oil (or emulsion) droplets from the slick into the flame.

Figure 3.26 compares the temperatures recorded for experimental burns with the 30.6% evaporated Statfjord crude (see Table 3.3 for details). Each burn was initially 20 mm thick (except for Experiment 4.71 which was only 17 mm thick to start). The water content of the emulsion increases (from 0% to 12.5%, 25%, 40% and 60%) with succeeding experiments.

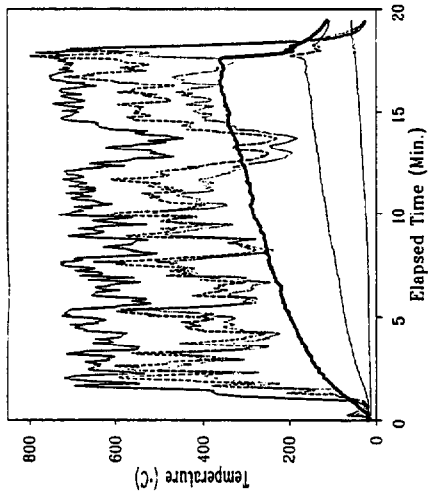
For the unemulsified oil, the surface temperature increased slowly over the burn to reach nearly 350°C near the end. The characteristic temperature spike in the 5 mm depth thermocouple data associated with foaming (which occurred near the end of the burns) is also apparent. As the water content increases to 12.5% and 25% the surface oil temperatures climb somewhat more slowly and peak at lower temperatures. The 5 mm deep temperatures rise more rapidly than for the unemulsified oil (perhaps due to increased thermal conductivity of the slick) then begin to decline. This decline may be due to the rise of the lower slick surface as it is floated up to replace burned oil. It is interesting to note that the salt water bubbles began appearing underneath the slick between 3 and 6 minutes after ignition; this process may have something to do with the decline in internal slick temperatures that is occurring at about the same time.

TABLE 3.3 - Comparison of Statford emulsion burn data with and without Bunker C added

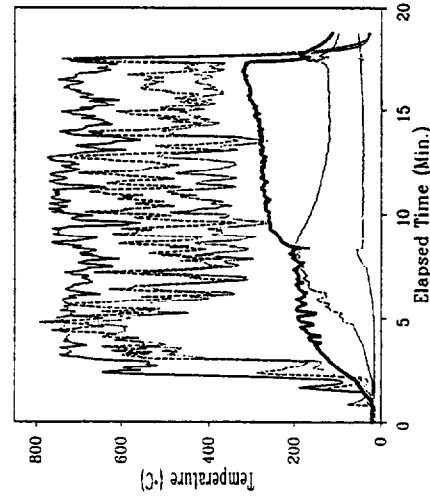
TEST WITH NO BUNKER C STABILIZATION						CORRESPONDING BUNKER C STABILIZED TEST			
Exp. No.	Vol. Evap. (%)	Water Content (%)	Thickness (mm)	Ignition (s)	Burn Eff. (%)	Exp. No.	Ignition (s)	Burn Eff. (%)	
4_46	19.6	70	20	78	80.1	4.48	never	0	
4_40	19.6	40	20	72	89.7	4.52	165	65.8	
4_41	19.6	40	10	83	84.0	4.50	163	52.0	
4_43	19.6	60	20	58	88.1	4.51	never	0	
4_43	19.6	60	20	58	88.1	4.53*	never over entire area	47	
4_43	19.6	60	20	58	88.1	4.54*	562	oil burned slowly for 17 minutes but more residue remained than oil in initial emulsion.	

* involved successive ignition attempts with other igniter types; see Appendix A for details

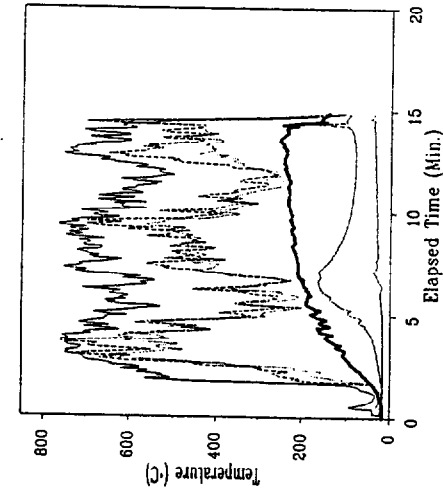
Exp. 4.67: 30.6 % Evaporated Statfjord; 0 % Water



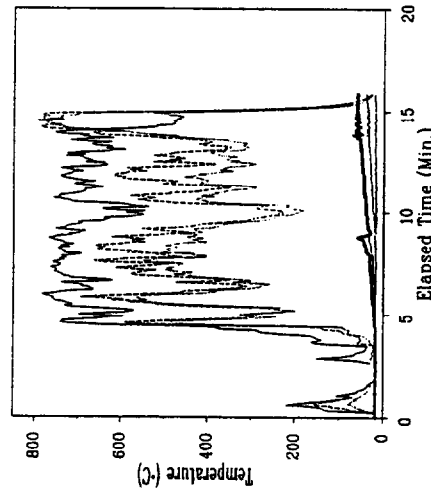
Exp. 4.68: 30.6 % Evaporated Statfjord; 12.5 % Water



Exp. 4.69: 30.6 % Evaporated Statfjord; 25 % Water



Exp. 4.70: 30.6 % Evaporated Statfjord; 40 % Water



Exp. 4.71: 30.6 % Evaporated Statfjord; 60 % Water

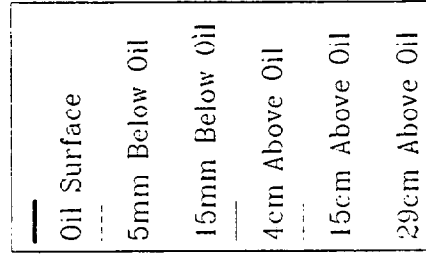
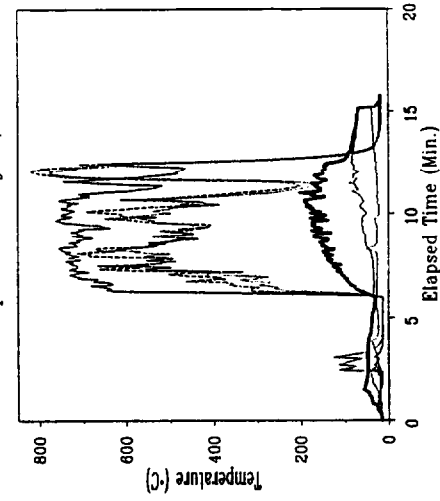


Figure 3.26 Temperatures for emulsified Statfjord burns

The slick thermocouples appear to have not been correctly placed for the 40% water burn (Exp. 4.70). A very interesting fact is apparent in the data from the 60% water burn; the slick surface temperature still reaches almost 200°C, a full 100° above the boiling point of water. This confirms that a layer of oil is being produced that floats on top of the emulsion. This is different from the temperature data for the Avalon burns (Figure 3.18 in Section 3.2.4.1) which indicated that even for the 25% water emulsion the slick surface temperature did not exceed 100°C. This lends credence to the fact that the two oil's emulsions burn differently.

For the 40% and 60% water content emulsions (Experiments 4.70 and 4.71 respectively on Figure 3.26) the flame temperatures remain about the same as for the lower water content tests (the small flame temperature peaks early in the test for these two graphs are unsuccessful ignition attempts with 25 cm² gasoline-soaked sorbent). This is different from the Avalon flame temperatures which showed a decline with increasing water content to 25%. It is likely that this difference between the two oils is also related to the mechanism by which they lose water from their emulsions during the combustion process and to the stability of the emulsions created for these experiments. For comparison Figure 3.27 shows the temperature data from a 20 mm thick test burn with 19.6% evaporated Statfjord crude and 60% water content stabilized with Bunker C (equivalent to Exp. 4.71 on Figure 3.26). In this case, the combustion is less intense than without the stabilizing agent and the oil's surface temperature only reaches about 100°C.

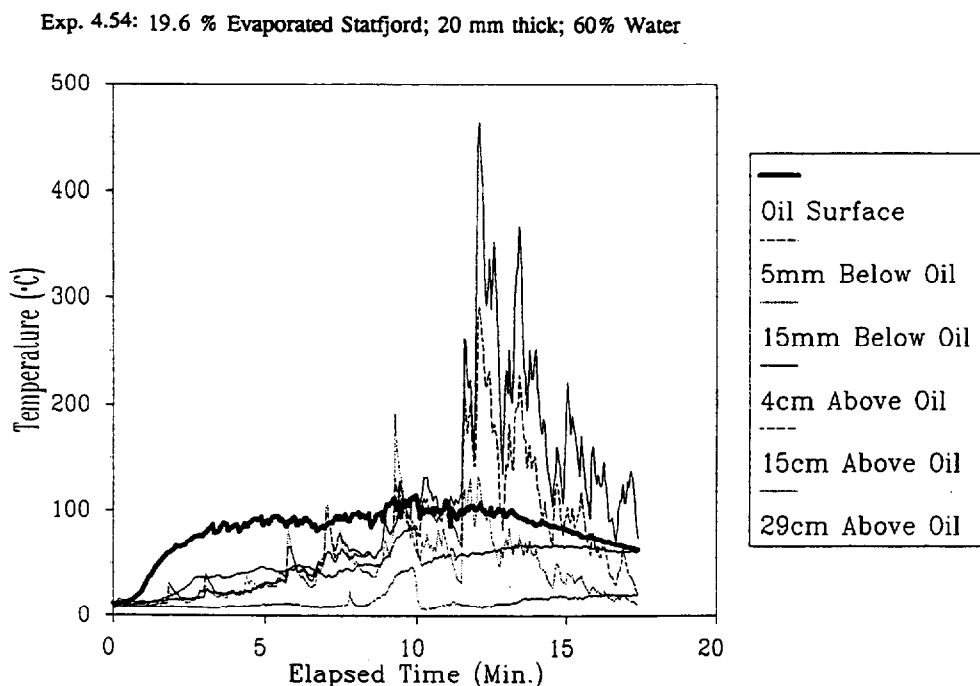


Figure 3.27 Temperatures for emulsified Statfjord crude stabilized with bunker C

Internal slick temperatures in the higher water content Statfjord emulsions (Experiments 4.70 and 4.71 - in Figure 3.26) never exceeded 100°C. This was probably due to the presence of water in the bulk emulsion.

Another interesting feature of Figure 3.26 is the decline in burn time with increasing water content; this is easily explained by examining the amount of oil (excluding water) available for burning. For the 60% water emulsion, only 40% of the fluid is oil, available for burning. All other factors being equal, the 60% emulsion burn should only last about 7 minutes compared to the burn time for the water free oil ($(18-1) \times 0.4$ from Exp. 4.67). This is the case (Exp. 4.71).

Burn Efficiency

The maximum surface temperatures of the fresh, unemulsified Statfjord oil increased from about 150°C with a 5 mm thick slick to approximately 200°C for a 10 mm thick slick, about 325°C for the 20 mm thick slick and approximately 450°C for a 30 mm thick slick.

Figure 3.28 shows the effect of degree of evaporation on burn efficiency for fixed water content emulsions. The data for unemulsified oil (top left on Figure 3.28) indicates that there was little effect of weathering on efficiency. For the fresh and 12.9% evaporated oil the trend of increasing efficiency with increasing thickness was as expected; for the more heavily evaporated oil foaming occurred which may have resulted in emulsified residue (reference to Appendix A) indicates that the burn times were approximately constant or even increased slightly with increased weathering for the unemulsified slicks). As the water contents increased there was little change in the effect of weathering on burn efficiency, except for the 60% water content, 5 mm slicks. For these, 12.9% evaporated was the only degree of evaporation that could be ignited. Most of these emulsions foamed at the end of the test burn.

Figure 3.29 shows the effect of emulsification on burn efficiency for constant degrees of evaporation. Note that the fresh oil (top left graph) would not form emulsions using the impeller technique. For the evaporated oils it is clear that water content had little effect on burn efficiency (except for perhaps the 5 mm thick slicks). This was most likely due to the phenomenon of the emulsions physically losing water by breaking during the burn. This is in sharp contrast to the results for the Avalon oil which showed a decline in burn efficiency with increasing water content for fresh oil. A decline in burn efficiency for weathered Avalon (12.7% and 20.6% evaporated) was also observed for a slick thickness of 20 mm. Bech et al. 1992 also show a decline in burn efficiency with increasing water content (up to 40%) for 28% and 37.5% evaporated Statfjord/Gullfaks mixed crude, but no effect of water content for fresh or 18% weathered. S.L. Ross (1989) shows a decline in efficiency with increasing water content for two different Hibernia crudes. Obviously, crude oil factors play a strong role in determining the effect of water content on burn efficiency.

Burn Rate

Figure 3.30 shows the effect of degree of evaporation on burn rate at constant water content. There was considerable scatter in the data. At lower water contents (25% and less) there did not appear to be any effect (as was the case for the Avalon oil); however, at higher water contents there did appear to be a trend in declining removal rate with increasing evaporation. These results are consistent with those of Bech et al. (1992).

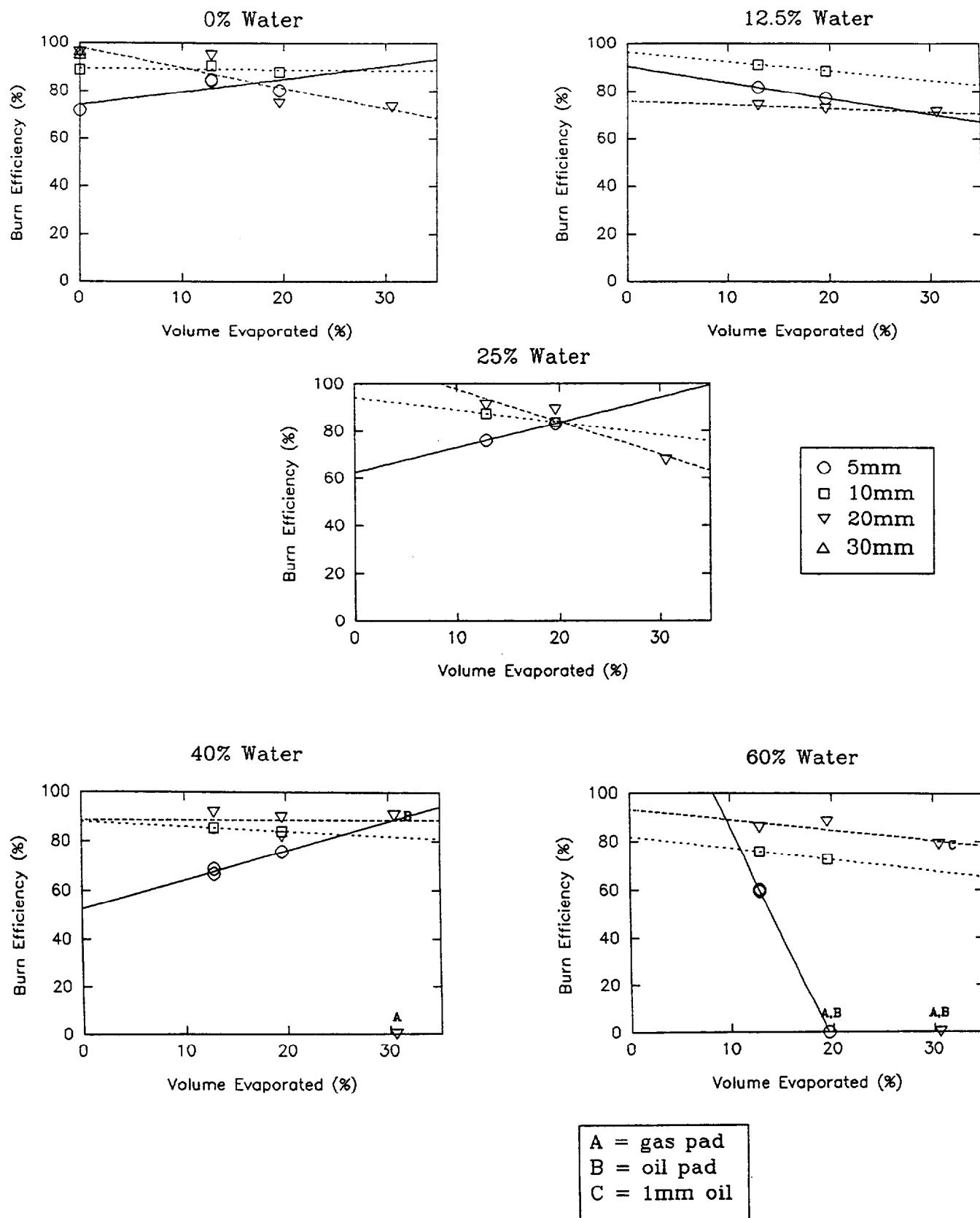


Figure 3.28 Burn efficiency vs. weathering Statfjord crude

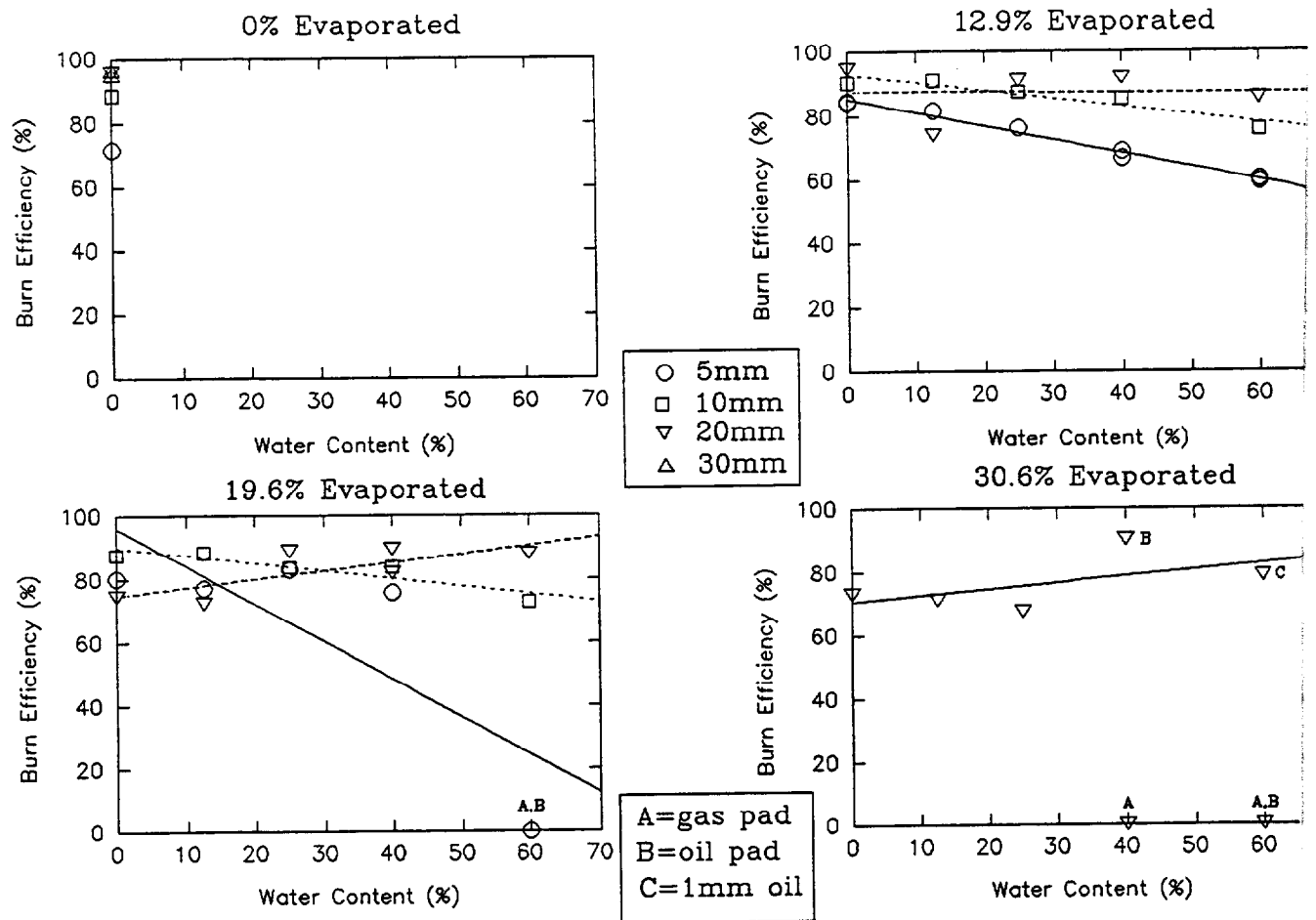


Figure 3.29 Burn efficiency vs. emulsification Statfjord crude

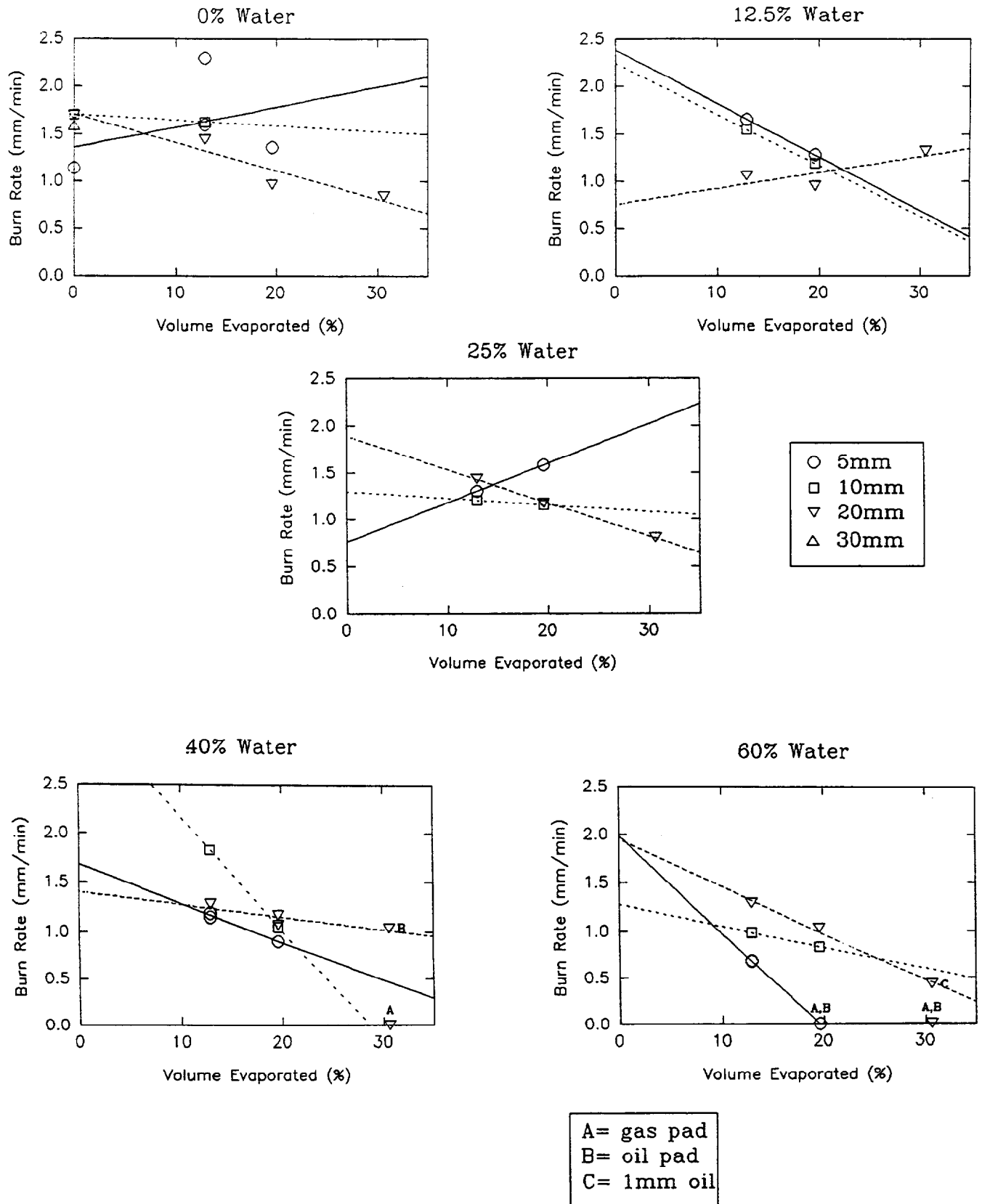


Figure 3.30 Burn rate vs. weathering Statfjord crude

Figure 3.32 shows the effect of water content on burn rate for specific degrees of weathering. The fresh oil (top left graph) would not form an emulsion using the impeller apparatus. Although the trend appears to be less than the data scatter, burn rate seems to have declined with increasing water content. This is consistent with other's data (Bech et al. 1992, S.L. Ross 1989) and the results for the Avalon oil.

Summary

The burning of emulsions of Statfjord crude appears to be easier to initiate and maintain than some other oils. It appears that this is due to a process whereby the emulsion breaks on heating and loses water physically. This may however be due to moderately stable emulsions produced with this oil using the impeller mixing method. This water removal mechanism appears to greatly augment vaporization as a water removal process and generates water-free oil to support combustion at a rate much greater than otherwise possible. Emulsion of 30.6% evaporated Statfjord crude containing 60% water were successfully ignited and burned.

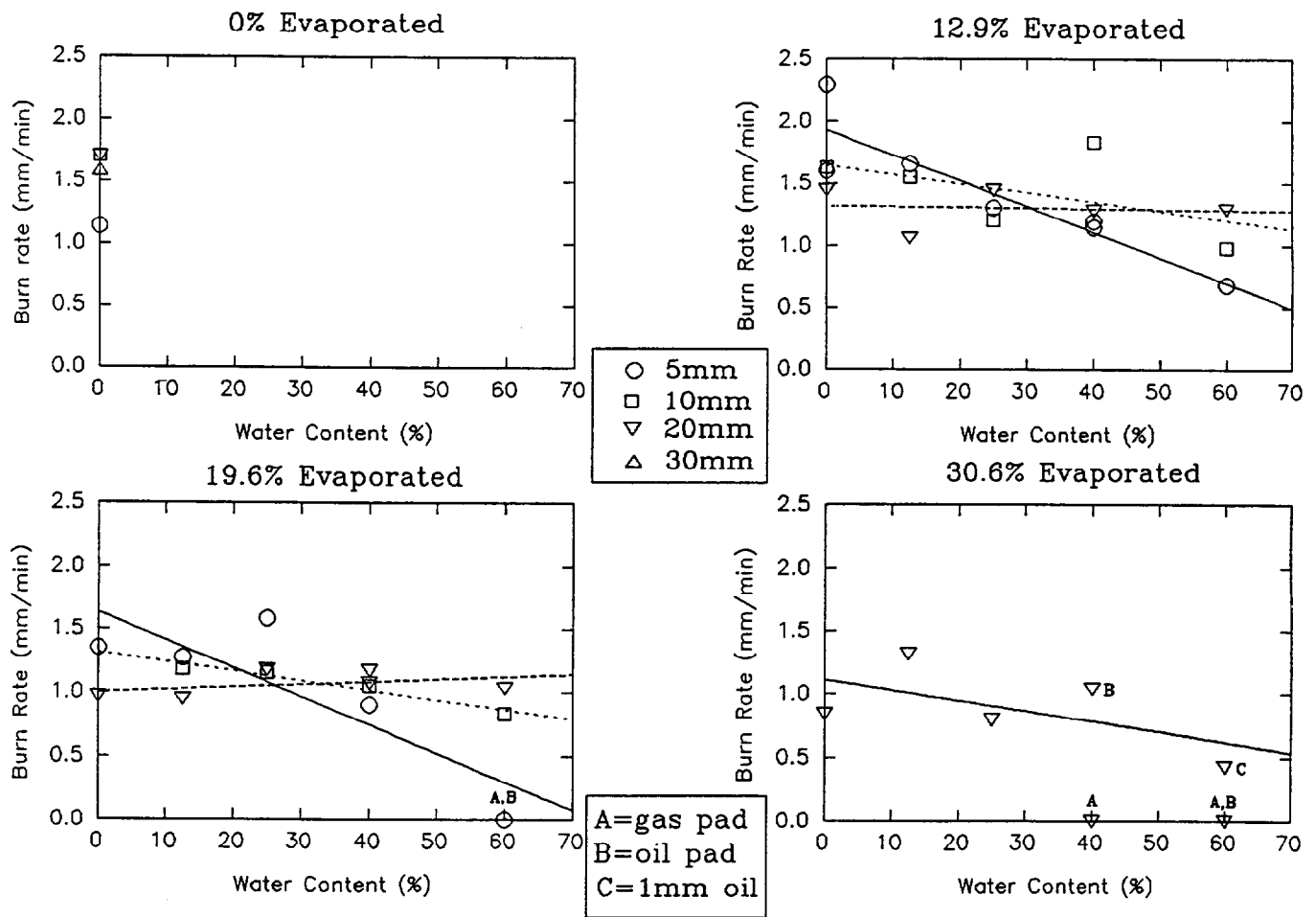


Figure 3.3.1 Burn rate vs. emulsification Statfjord crude

3.2.4.3 Ignition and burning of Alaska North Slope emulsions

Before presenting the results of the test burns with the Alaska North Slope oil it is necessary to point out that the crude sample received contained one or more unknown surfactants that reduced the oil/water interfacial tension of the oil from a normal 20-25 mN/m down to approximately 4mN/m. The fresh and weathered crudes would also not form stable emulsions using the impeller technique. This effect was so pronounced that, at higher water contents (60% and 75%) the water would not combine with the oil but inverted the emulsion to create a dispersion (an oil-in-water emulsion) in the mixing bucket. As well, the burns of Alaska North Slope emulsion were unusual in that they often involved surging flames whereby the combustion would initially be normal, then die down to a weak, lazy flame, then suddenly surge back to normal intensity. It was also noted that the vigorous burn phase was completely absent for some burns while in others it dominated for the entire burn. Often, after the burn extinguished, the residue layer would be found herded against the inside circumference of the ring with one or more large, circular, clear patches of water inside the residue slick.

Since Alaska North Slope has been known to be a strong emulsifier (Environment Canada 1992) in the past the anomalous behaviour of this sample means that the test results must be treated with great circumspection. It is not at all clear whether the sample of Alaska North Slope received for these tests represents an anomaly or is representative of a new "generation" of Alaska North Slope due to production or pipelining additives programs initiated recently. Until this is clarified, no conclusions regarding the *in-situ* burning of Alaska North Slope crude can be drawn from the test results.

In the interest of completeness, the data obtained is presented below and briefly discussed. Appendix C contains this data.

Ignition

Figure 3.32 presents the data obtained for the effect of degree of evaporation on ignition time for fixed water contents. Figure 3.33 presents the data for the effect of emulsion water content on ignition time at the three degrees of evaporation.

Burn Efficiency

Figure 3.34 gives the data that show the dependence of burn efficiency on evaporation at fixed water contents. Figure 3.35 shows the effect of water content on burn efficiency for the three degrees of evaporation tested.

Burn Rate

Figure 3.36 shows the data correlating burn rate with evaporation for fixed water contents; Figure 3.37 shows the relationship between burn rate and emulsification for the three degrees of evaporation.

Summary

Since the sample of Alaska North Slope oil received for these tests had an unusually low interfacial tension and did not form stable emulsions as previously reported samples have, no conclusions as to the *in-situ* combustion of this oil can be drawn. If, in fact, this sample is representative of a "new generation" of Alaska North Slope (because of changes in production or pipelining operations) then the new oil will be much more amenable to *in-situ* burning than the old oil.

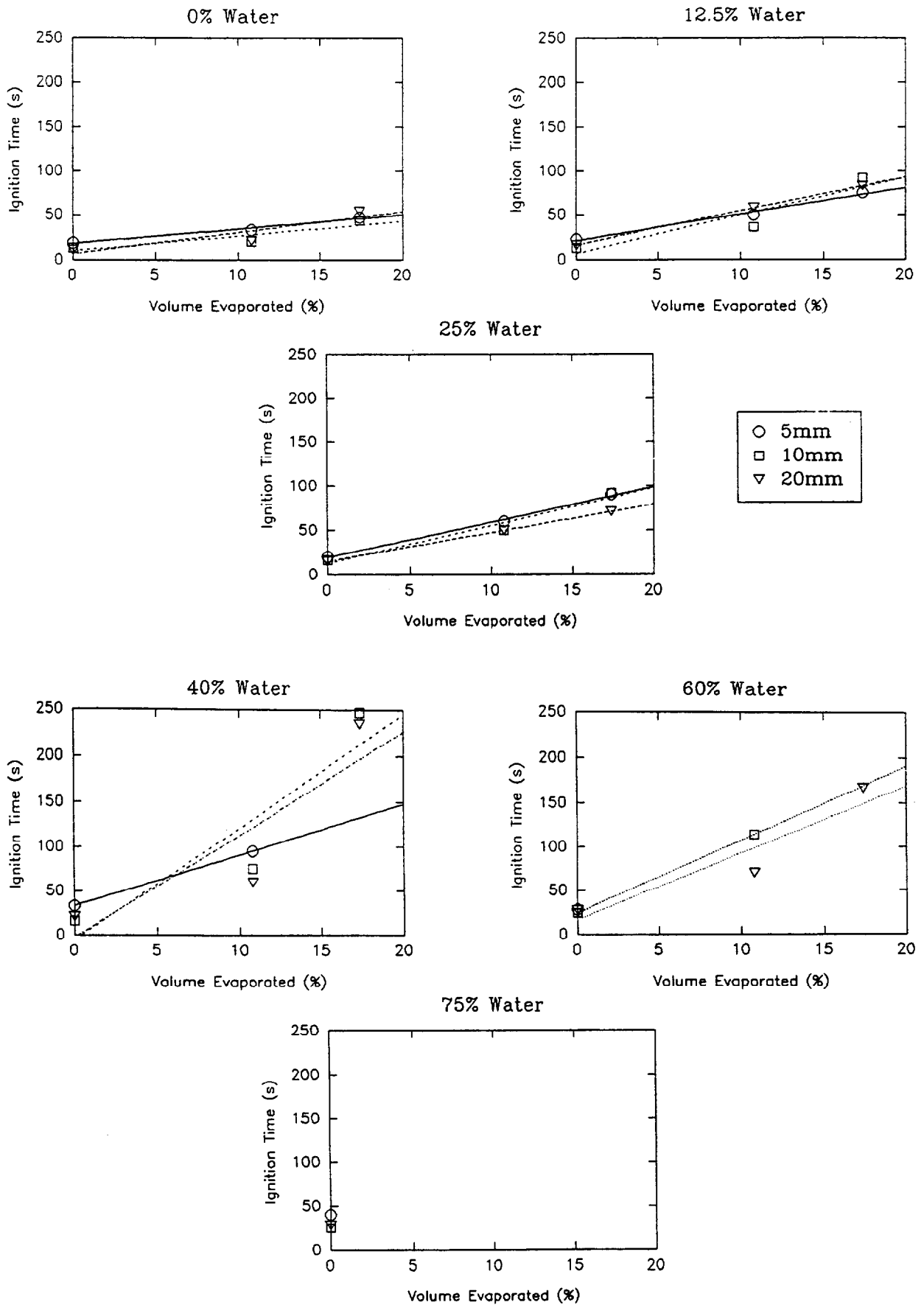


Figure 3.32 Ignition time vs. weathering - Alaska North Slope crude

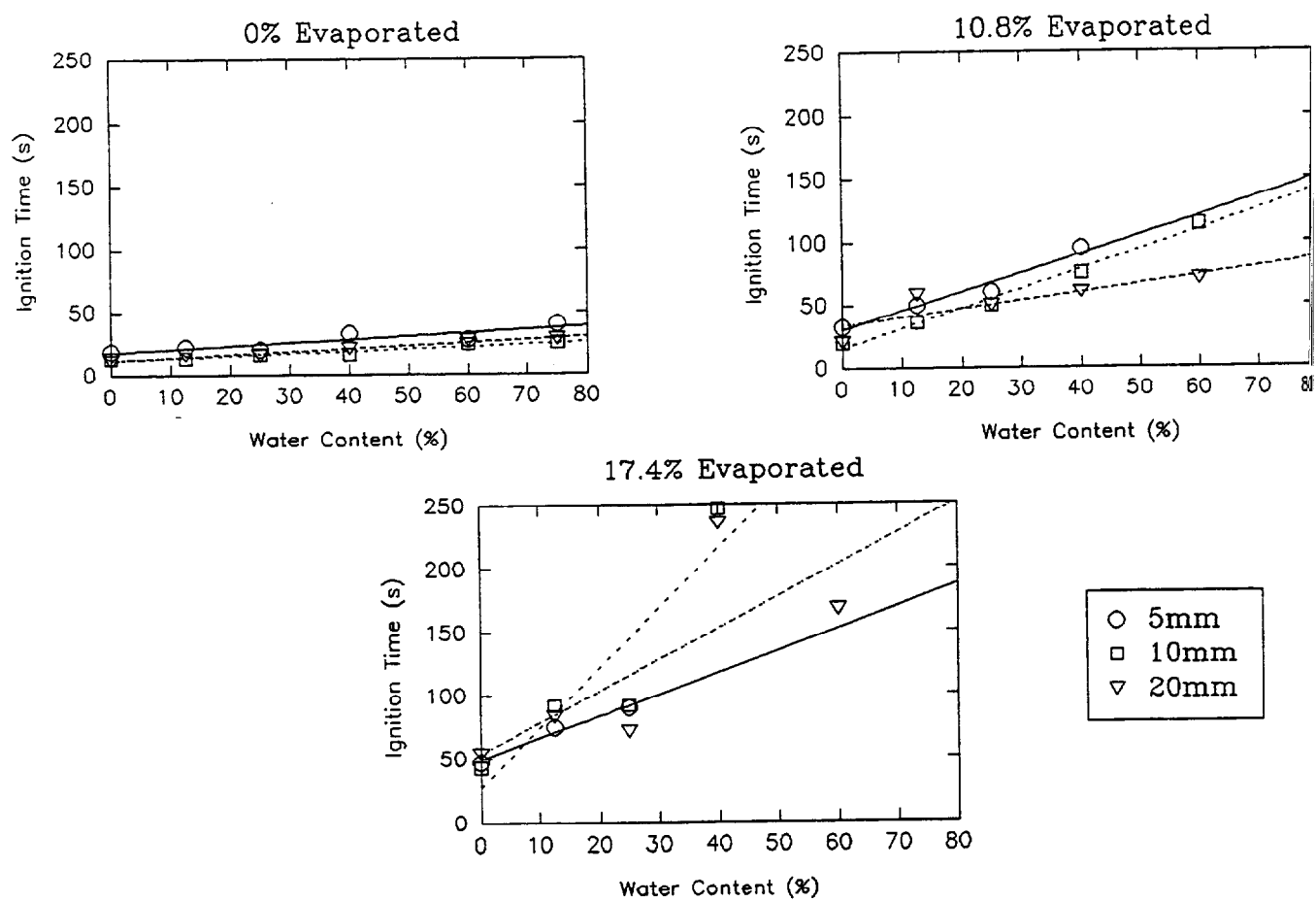


Figure 3.33 Ignition time vs. emulsification - Alaska North Slope crude

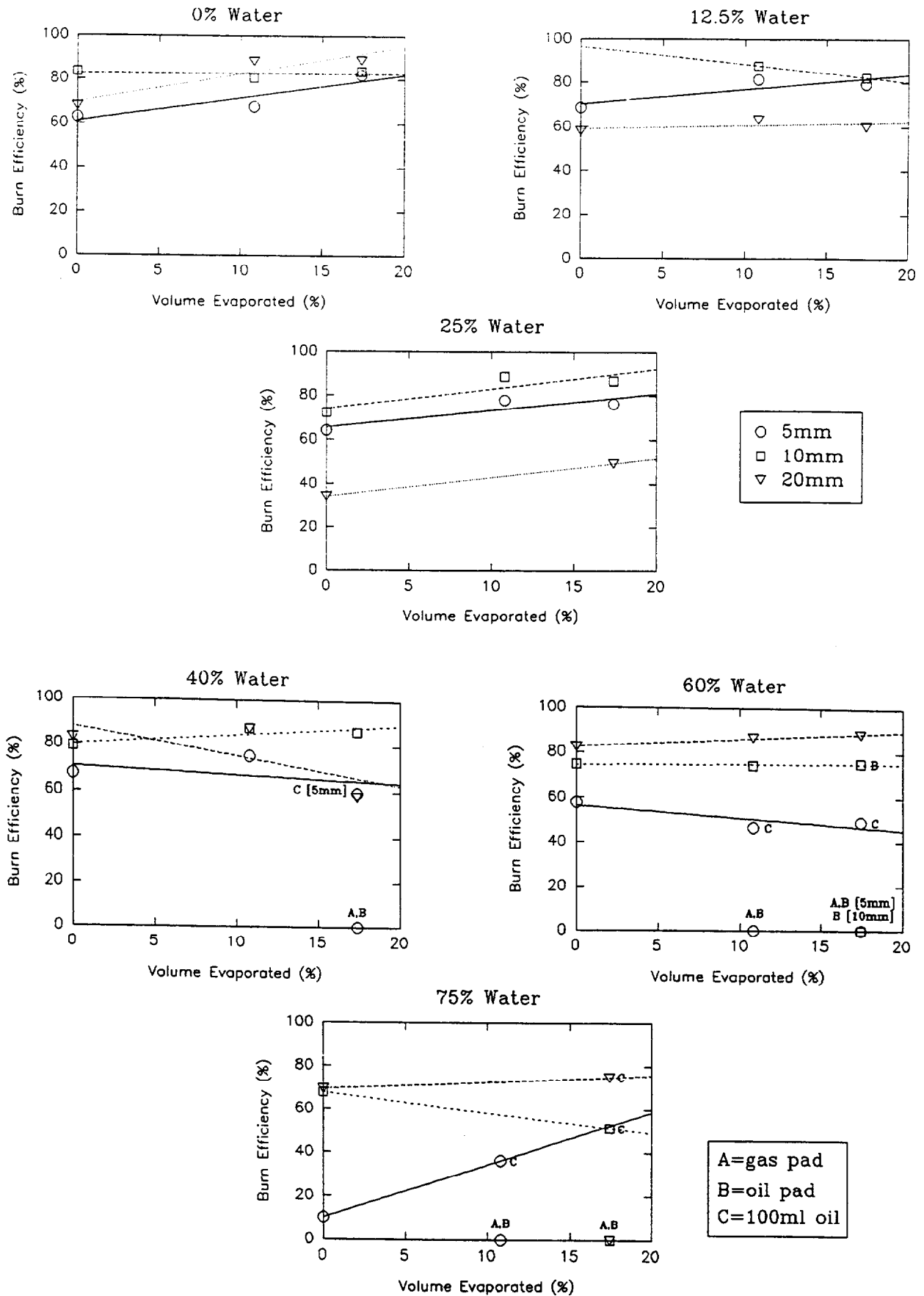


Figure 3.34 Burn efficiency vs. weathering - Alaska North Slope crude

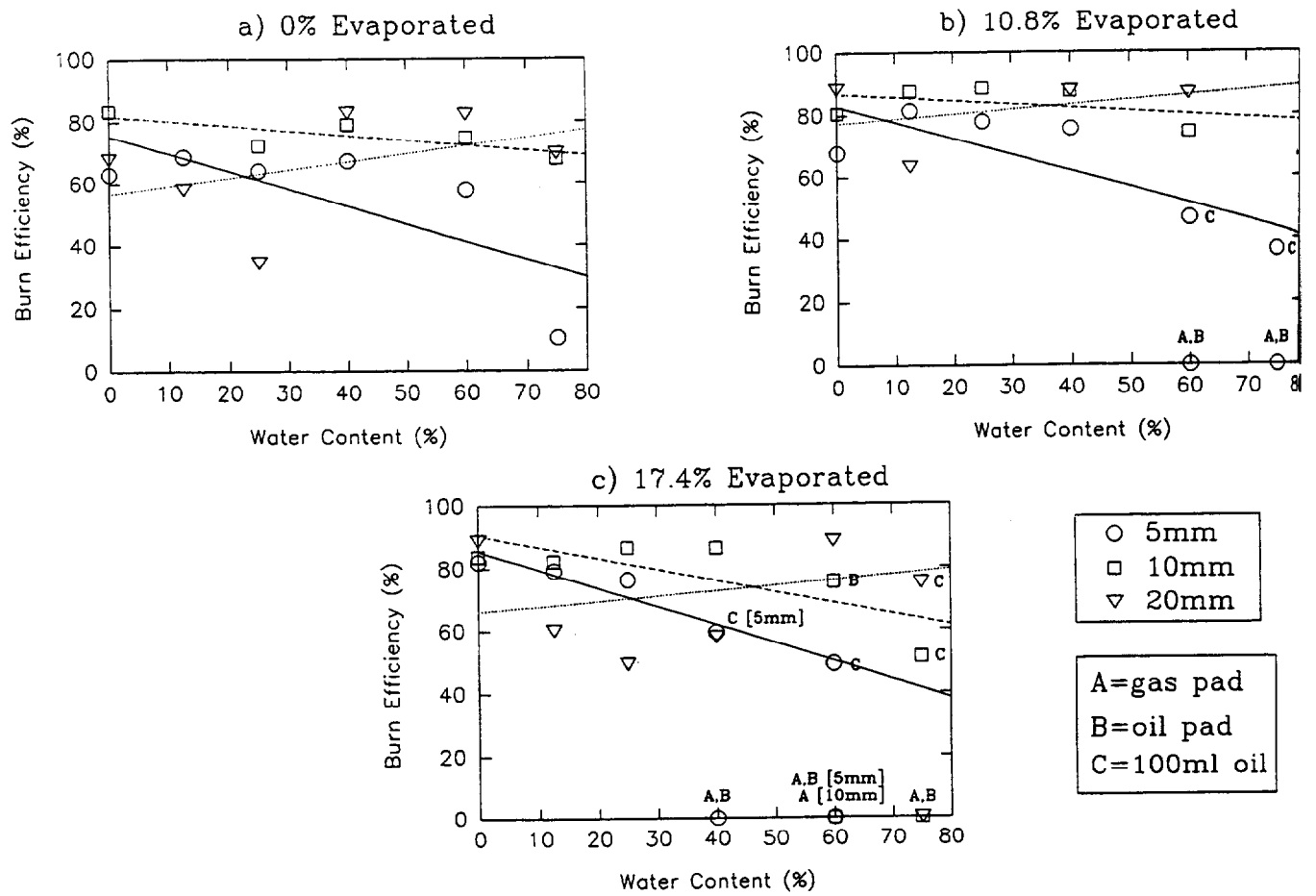


Figure 3.35 Burn efficiency vs. emulsification - Alaska North Slope crude

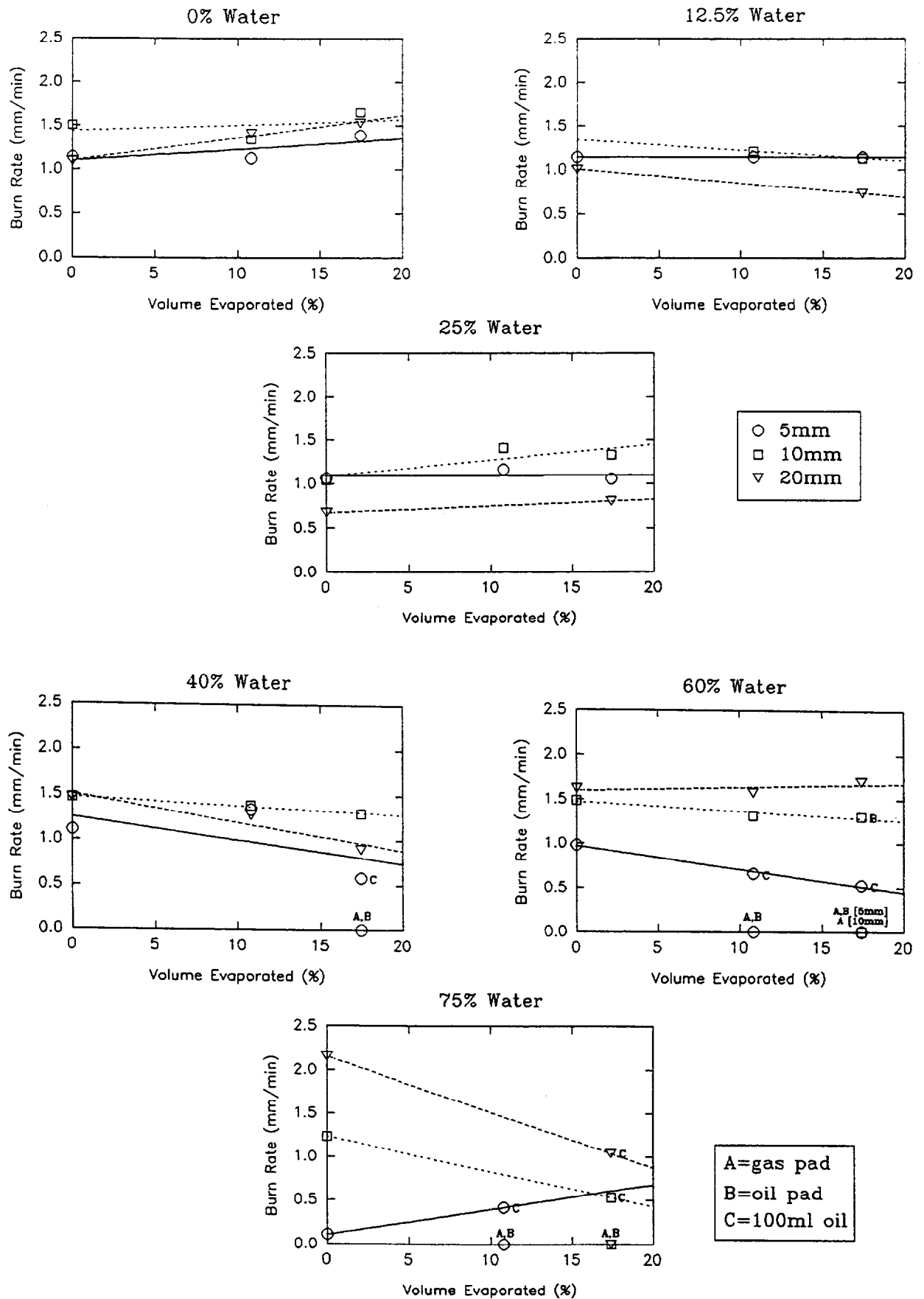


Figure 3.36 Burn rate vs. weathering - Alaska North Slope crude

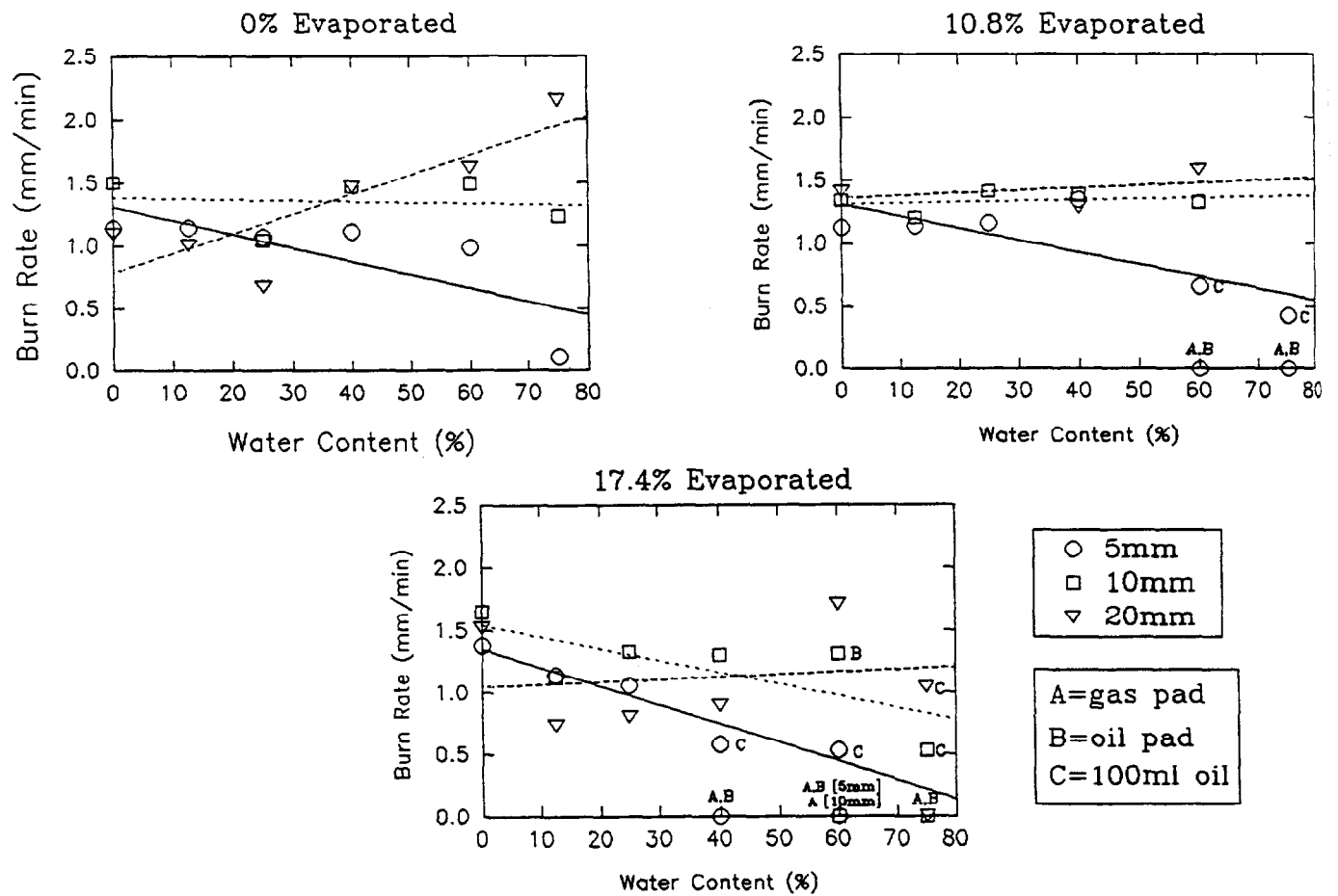


Figure 3.37 Burn rate vs. emulsification - Alaska North Slope crude

3.2.5 Statistical model

A multiple regression analysis was done to study which factors influence central burn parameters (see section 3.2.3). In the analysis, the three crude oils have been treated separately, and then the data have been merged, and an analysis on the total dataset has been done. The total graphical presentation of the analysis is restricted to Statfjord crude oil, but the data from each of the oils, and the three oils together are presented thereafter in tabular form (Table 3.4). In the table the statistical significant factors have been listed.

Figure 3.38 to 3.42 shows the multiple regression models for burn efficiency, burn rate, ignition time, the time for initiation of the intense burn, and the time for the extinction of the burn; all for Statfjord crude oil.

The burn efficiency can be explained by the thickness, the water content and the degree of evaporation (see Table 3.5). Avalon crude deviates somewhat from the other crudes, with more rapid decrease in burn efficiency as water content of the emulsion increases.

The burn rate of all the oil can be explained by the water content when the oils are considered separately. Thickness of the initial oil layer is a significant factor when combined with the water content for Alaska North Slope and Avalon crudes. Evaporation is a significant factor only for Avalon. If data for all the oils are viewed together, evaporation is a significant explanation factor both alone and combined with slick thickness.

The ignition time, the intense burn time and the extinction time for the three oils evaluated separately and evaluated together can be explained with thickness as the central significant explanation factor. It should be noted that the time for the intense burn deviates for Avalon, by the significant explanation factor water. For these three time measurements, the values for the intercepts are not statistically significant. The model for the ignition time in Avalon did not contain any significant parameters.

It can thus be concluded that the emulsions studied have somewhat different burn dynamics, and that the statistical analysis makes it reasonable to assume that this has to do with properties of the emulsions related to the properties of the oils.

Table 3.4 Statistical parameters for the multiple regression models; with emphasis on the statistically significant parameters

BURN EFFICIENCY

PARAMETERS	STATFJORD	ANS	AVALON	ALL OILS
intercept	86.29	82.33	86.92	76.39
thickness	0.31	-	-	0.41
thickness*evaporation	-0.03	-	-	-0.04
water	-0.67	-0.72	-1.54	-0.60
thickness*water	0.03	0.05	0.08	0.02

BURN RATE

PARAMETERS	STATFJORD	ANS	AVALON	ALL OILS
intercept	1.584	1.410	2.204	1.089
thickness*evaporation		-	-	0.002
water	-0.002	-0.016	-0.009	-0.007
thickness*water		-0.002	0.004	0.002
evaporation			-0.008	0.030

IGNITION TIME

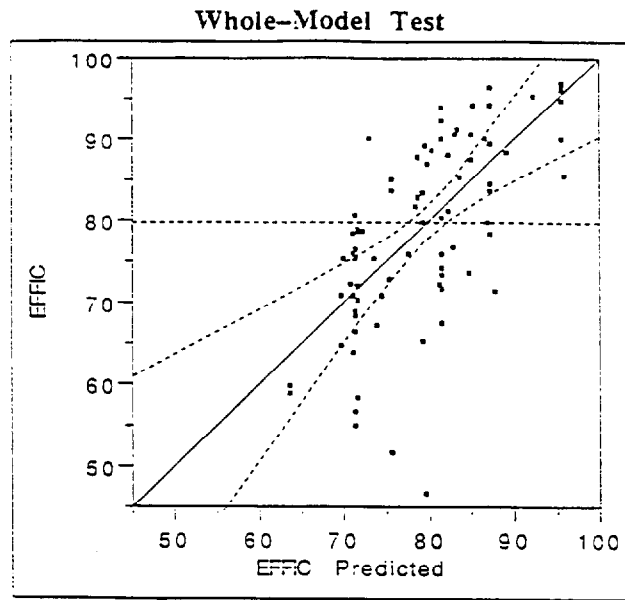
PARAMETERS	STATFJORD	ANS	AVALON	ALL OILS
intercept	18.491 ₁	8.025 ₁	99.897 ₁	40.315 ₁
thickness*evaporation	-0.249			
thickness*evap*water	0.021	0.014	0.019 ₁	0.021

TIME FOR INTENSE BURN

PARAMETERS	STATFJORD	ANS	AVALON	ALL OILS
intercept	-11.576 ₁	-51.613 ₁	-196.602 ₁	52.924 ₁
thickness	32.976	37.419	62.78	32.897
thickness*evaporation	0.691			
water			23.878	
thickness*water	-0.722	-0.433	-0.432	

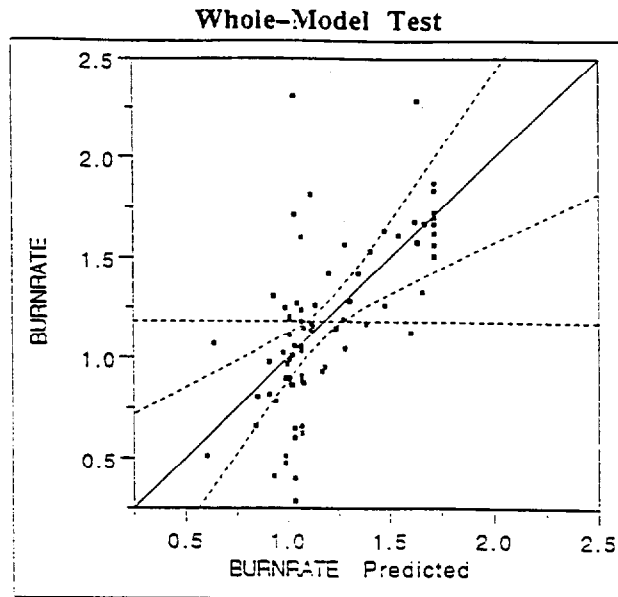
TIME FOR EXTINCTION OF BURN

PARAMETERS	STATFJORD	ANS	AVALON	ALL OILS
intercept	42.573 ₁	3.332 ₁	134.722 ₁	146.395
thickness	30.225	39.55	40.818	29.193
thickness*evaporation	0.747			0.742
thickness*water		-0.446		



Analysis of Variance				
Source	DF	Sum of Squares	Mean Square	F Ratio
Model	7	5534.351	790.622	10.1330
Error	75	5851.833	78.024	Prob>F
C Total	82	11386.184		0.0000

Figure 3.38 Multiple regression models for burn efficiency for Statfjord crude oil.



Analysis of Variance				
Source	DF	Sum of Squares	Mean Square	F Ratio
Model	7	6.373008	0.910430	8.5417
Error	70	7.461060	0.106587	Prob>F
C Total	77	13.834068		0.0000

Figure 3.39 Multiple regression models for burn rate for Statfjord crude oil.

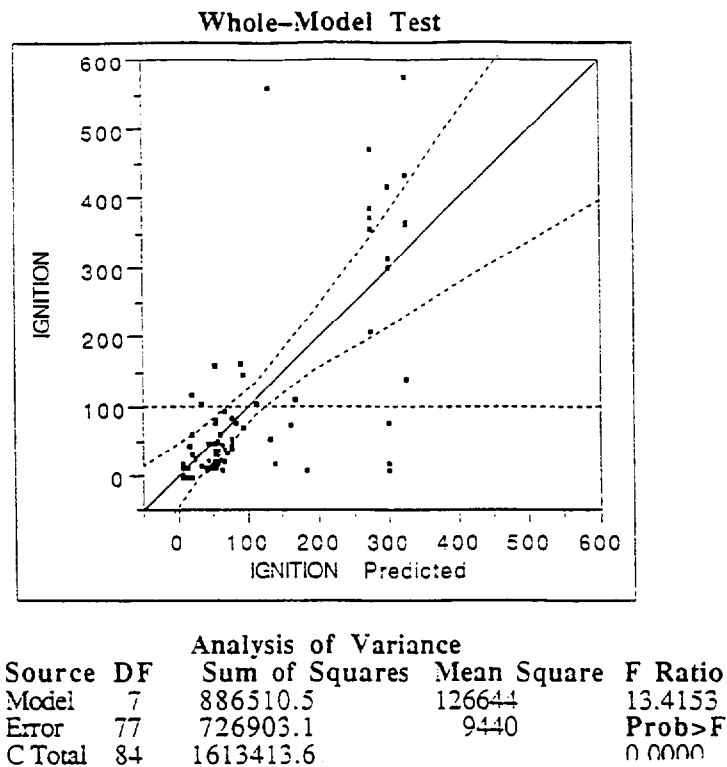


Figure 3.40 Multiple regression models for ignition time for Statfjord crude oil.

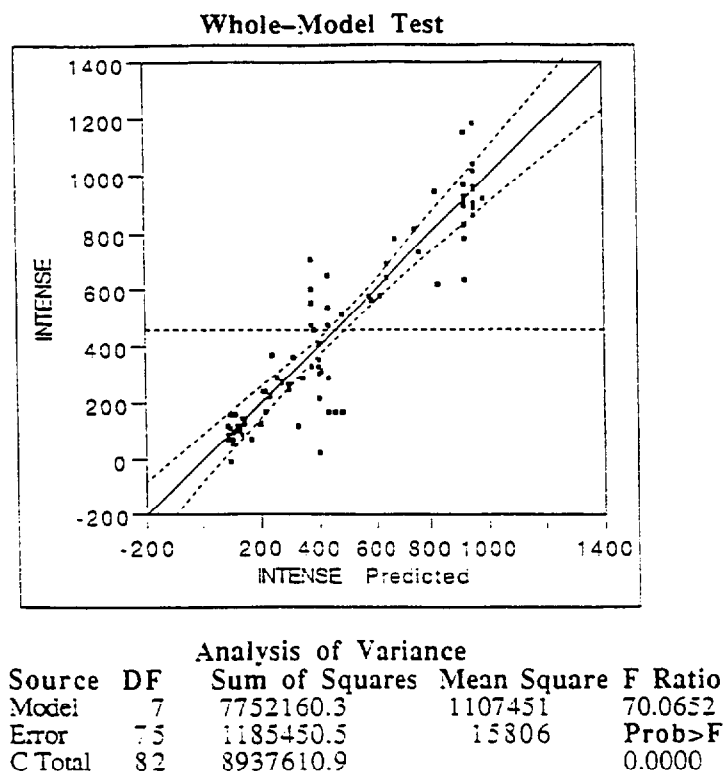
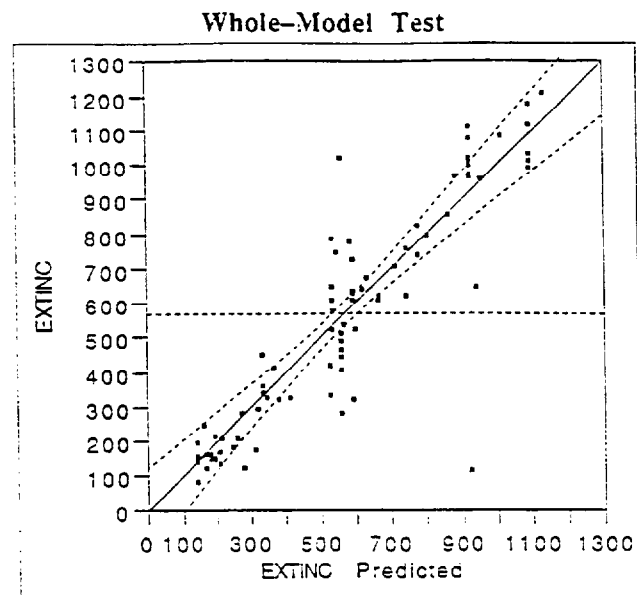


Figure 3.41 Multiple regression models for time for initiation of the intense burn for Statfjord crude oil.



Analysis of Variance				
Source	DF	Sum of Squares	Mean Square	F Ratio
Model	7	7558148.2	1079735	48.8687
Error	76	1679192.1	22095	Prob>F
C Total	83	9237340.2		0.0000

Figure 3.42 Multiple regression models for the time for the extinction of the burn for Statfjord crude oil.

4 LABORATORY STUDIES ON THE LIMITATIONS OF AND IMPROVEMENTS TO EXISTING IGNITION TECHNIQUES

Tests were conducted using emulsions of the most weathered crudes that could not be ignited with a 25 cm² gasoline-soaked sorbent, to determine whether or not gelled crude oil would be a better igniter for emulsions than gelled gasoline. The efficacy of emulsion breaking chemical addition to the slick was also investigated; the chemicals were tested both as applied prior to ignition (to simulate the so-called "break and burn" approach) and as premixed into the igniter fuel prior to gelling. As well, the effects of ferrocene addition to the igniter fuel were tested in some instances.

4.1 Methods

The procedures used for these experiments were identical to those described in Section 3.1.2 above, except that the gasoline-soaked sorbent pad igniter was replaced by a gelled fuel igniter. A 400 ml batch of the gelled fuel (gas, diesel or fresh crude oil) was mixed in a 500 ml glass jar. The gel was created by adding 10 to 15 g of Surefire gelling agent to 400 ml of gasoline (30 g of Surefire was used to gel crude oil). If an emulsion breaker was to be used it was added at a volumetric ratio of 1:30 (breaker:oil). If ferrocene was being used 4% by weight was added to the igniter fuel. The mixture was then sealed in the jar and shaken until set. Approximately 40 ml of igniter fuel was scooped into a tared plastic bag and weighed. The bag was then tied to a crossbar suspended in the fume hood 1.5 m above the water surface. The bag was lit with a propane soldering torch; it subsequently melted as the igniter fuel burned, releasing the gelled fuel to fall onto the slick below. The gelled fuel often extinguished on impact and was relit using the propane torch. This may have been due to the short fall time or possibly to the addition of demulsifier and/or ferrocene to the gelled fuel. In some experiments, where sequential ignition attempts with different igniters were used, the second, and all subsequent, igniters were emptied from the bag onto the emulsion surface, then lit with the propane torch.

For experiments where the addition of emulsion breakers to the slick prior to ignition was studied, two techniques were used. In general, the emulsion breakers were diluted in an equal volume of toluene to permit accurate application by pipette of the normally viscous liquids. For experiments to assess application without mixing either 2 or 4 ml of diluted product were distributed dropwise by pipette evenly over the surface of a 20 mm thick emulsion test slick, then the igniter was released. For experiments to assess application with mixing, the 2 or 4 ml was placed on the test slick and the slick gently stirred with a 2.5 cm wide stick for a period of 2 minutes. Then the igniter was released.

The final series of experiments involved burning 400 ml samples of various gelled fuels (gasoline, fresh Alaska North Slope crude and fresh Statfjord crude) to measure flame temperatures. Some of these burns also involved emulsion breakers and ferrocene additives.

4.2 Results and discussion

4.2.1 Laboratory evaluation of selected techniques

Gelled gasoline dropped from a Helitorch has proven to be a successful igniter for fresh, weathered and slightly emulsified oils. Other techniques, such as pouring fresh oil over weathered oil or dousing the slick with kerosene have also proven to be successful in some cases. The use of gelled gasoline, fresh oil and gasoline or oil soaked sorbent pads were selected as the existing techniques to be tested in the laboratory.

A series of experiments as performed in the laboratory to evaluate the limitations and capabilities of the

existing ignition techniques, these being gasoline or oil soaked sorbent pads, fresh crude oil and gelled gasoline. These techniques were evaluated using three oil types over a range of degrees of evaporation, emulsion water content and slick thicknesses. The results have been plotted in Figures 4.1 and 4.2 as the burn efficiency as a function of degree of evaporation, emulsion water content and slick thickness. These figures also include subsequent attempts using the improved techniques when the existing one failed. For example, with one of the 30.6% evaporated Statfjord emulsions containing 60% water, both the gas soaked pad and the crude oil soaked sorbent pad (denoted as A and B respectively in Figure 4.1) did not provide sufficient heat to cause ignition of the slick. A 1 mm layer of fresh oil (denoted as C in this figure) was required to ignite this oil. The gasoline and oil saturated sorbent pads were limited in their abilities to ignite 19.6 and 30.6% evaporated Statfjord crude with water contents of 60%. Similar trends were found with attempts to ignite evaporated and highly emulsified Alaska North Slope crude. Limited success was achieved in using the gasoline and crude oil saturated sorbent pads as an ignition source.

4.2.2 Recommended improvements

Gelled gasoline, gelled gasoline containing emulsion breakers and direct addition of emulsion breaker to an emulsion slick were the techniques which were found to show most promise in successfully igniting high water content emulsions, and recommended for further evaluation.

Preliminary findings from the Spitsbergen field work in 1992 with gelled gasoline, gelled diesel and gelled crude oil suggested that the use of these compounds as igniters for heavily emulsified oils was worth further investigation. The release of gelled gasoline from a Helitorch was judged to be the most practicable and promising concept upon which to build and make improvements. Gelled gasoline was therefore selected as the existing method to improve upon. Igniters which could be suitably adapted to the Helitorch system were researched and it was found that gelled crude oil would likely be the best candidate. The effectiveness of gelled crude oil as an igniter was therefore investigated using heavily emulsified Alaska North Slope and Statfjord crude oil. As well, the addition of emulsion breakers to the gelled oil mixture or directly to the slick, in an effort to release some free oil for ignition, was tested. Some experiments were also undertaken to investigate ways of enhancing the ignitability of gelled gasoline.

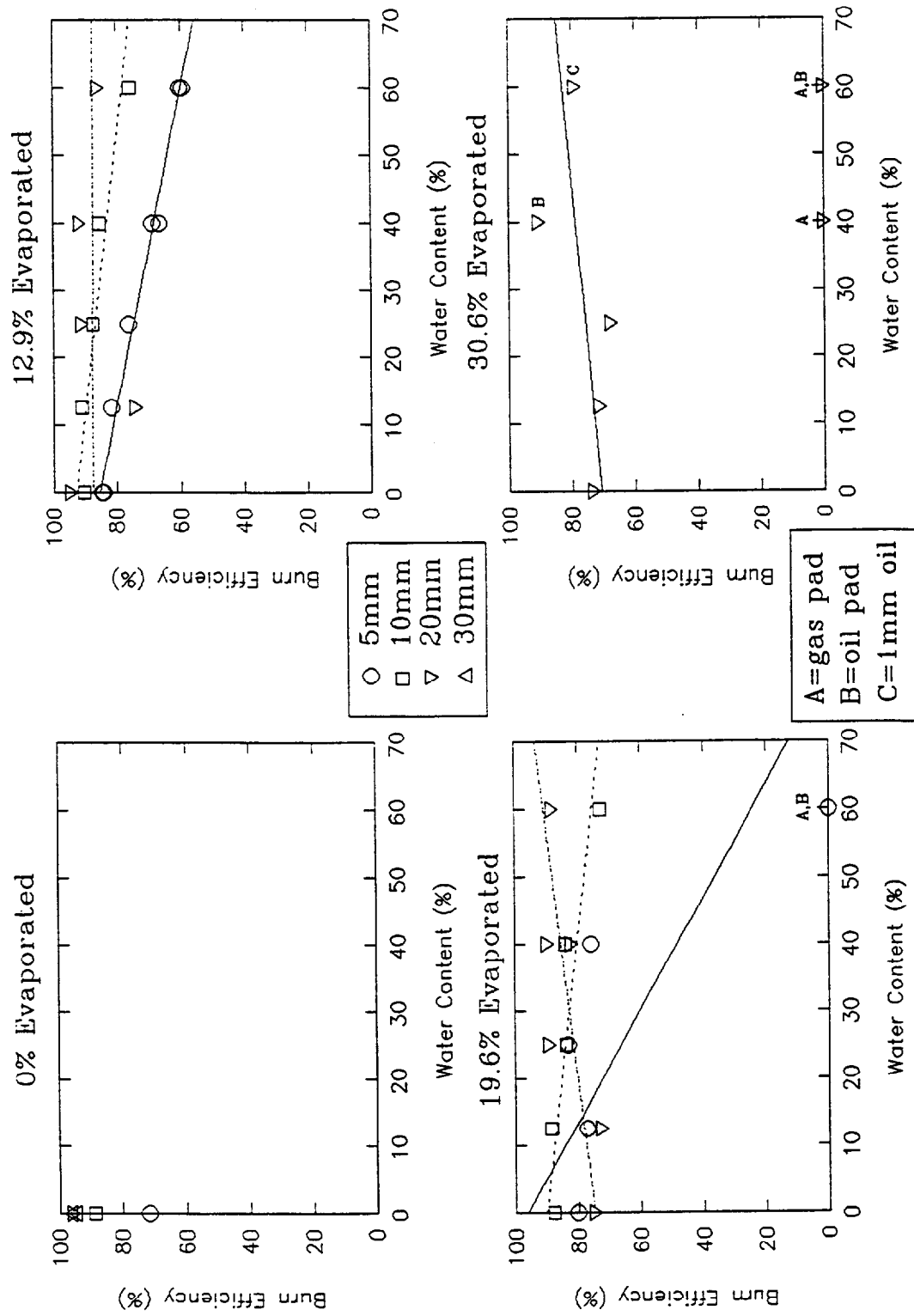


Figure 4.1 Burn efficiency vs. emulsification Alaska North Slope crude

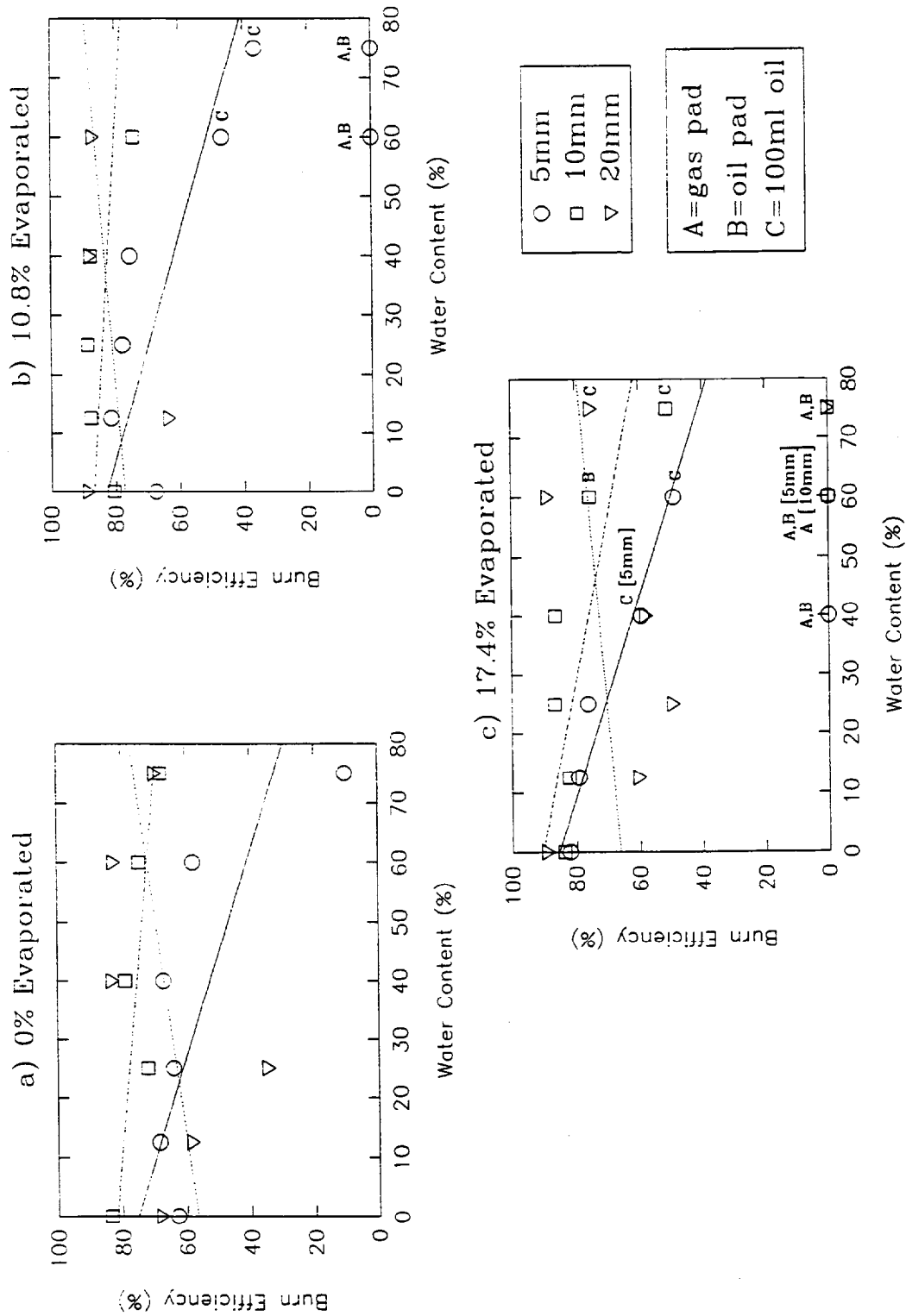


Figure 4.2 Burn efficiency vs. emulsification Statfjord crude

4.2.3 Laboratory tests of igniter capability and enhancements

In this section the results of tests of the capabilities of gelled gasoline to ignite emulsions are presented. In addition, several enhancements to the use of gelled gasoline were researched and tested. These enhancements included combinations of:

- using gelled crude oil instead of gelled gasoline;
- applying emulsion breakers to the slick prior to ignition;
- adding emulsion breakers to the gelled fuel (gasoline or crude) used for the igniter; and,
- adding ferrocene to the gelled fuel.

The data for all the experiments conducted for these purposes with the Avalon crude oil and the Statfjord crude oil are given in Appendix B. (These have been extracted from tables in Appendix A. Although some igniter capability tests were conducted with the Alaska North Slope crude (see Experiments numbers 5.53 through 5.63 in Table 4.1 in the previous section) these are not reported here due to the circumspect behaviour of the crude oil sample (i.e.: it's inability to form a stable emulsion).

4.2.3.1 Gelled gasoline capabilities and limitations

The maximum ignitable water content for an emulsion of a particular crude oil was determined by; first, determining the highest combination of evaporation and water content that could be successfully ignited with a 25 cm² gasoline-soaked pad. The gelled gasoline igniter was then tried on the next higher water content for that degree of evaporation. For the Avalon oil, the 25 cm² gasoline-soaked pad could ignite 25% water, 12.7% evaporated emulsion but not a 40% water emulsion; for the Statfjord crude the gasoline-soaked pad could just barely ignite a 40% water, 30.7% evaporated emulsion; a 25 cm² fresh crude-soaked sorbent pad could. Neither gasoline nor crude-soaked sorbent could ignite a 60% water content emulsion formed with 30.7% evaporated Statfjord crude.

A 32 g ball of burning gelled gasoline could barely ignite a 40% water content emulsion of fresh Avalon oil and a 37 g ball of burning gelled gasoline could not ignite a 40% water content emulsion of 12.7% evaporated Avalon crude. A 21 g ball of burning gelled gasoline failed to ignite a 75% water emulsion created with 30.6% evaporated Statfjord crude.

4.2.3.2 Gelled crude capabilities and limitations

The use of gelled crude as an igniter proved to be somewhat more effective than gelled gasoline for the Statfjord emulsions. In Experiments 4.73 and 4.79, 30 ml of gelled gas could not ignite a 20 mm thick slick of 75% water content Statfjord emulsion but 30 ml of gelled fresh Statfjord crude did. The same test, repeated with Bunker C added to stabilize the emulsion, resulted in failure of the gelled crude igniter and required a layer of fresh crude for successful ignition. The improved efficacy of gelled crude as an igniter over gelled gasoline has been reported by Bech et al. (1992).

4.2.3.3 Emulsion breaker addition to the slick prior to ignition

Several experiments were conducted to determine the effects on ignition potential of pre-ignition application of emulsion breakers to the slick (the so-called "break-and-burn" approach). Two procedures were used: "dropwise" addition whereby the desired amount of diluted emulsion breaker was applied from a pipette at discrete locations; and, "premixed" whereby the slick surface was gently stirred with a stick for two minutes after "dropwise" addition. The chosen igniter was then dropped.

The specific emulsion breakers selected for these experiments were chosen on the basis of a proposed standardized test procedure (Fingas 1993). Results for these experiments may be found in Appendix

C. Four commercially available products were tested with the Statfjord oil: Alcopol 070 PG produced by Allied Colloid; Breaxit OEB-9 produced by Exxon Chemical; Shell 1A1834 produced by Shell Chemical; and, a product developed by Environment Canada now marketed by Cartier Chemical as VYTAC.

All four performed well on the Statfjord crude. Alcopol and Breaxit were chosen for further testing because they performed marginally better and are well-known products in the oil spill response industry. These two products proved effective with 75% water emulsions of fresh Avalon oil, with Alcopol slightly outperforming Breaxit. Both products were not very effective in the test with 75% water emulsions of 12.6% evaporated Avalon crude. Tests of the two products were conducted with Alaska North Slope; however the data was meaningless as the Alaska North Slope would not maintain an emulsion in the test apparatus, even with no breaker added.

The addition of emulsion breakers prior to ignition proved to be a great aid to ignition. For the highly stable Avalon emulsion in Experiment 2.34 a 20 mm thick, 60% water emulsion of fresh Avalon crude could not be ignited with gelled gasoline; the addition of 2 ml of 50/50 Alcopol/toluene mixture to the slick followed by two minutes of gentle mixing permitted ignition by another ball of gelled gasoline and resulted in a 72% burn efficiency. In Experiment 2.37 a 20 mm thick, 40% water emulsion with 12.7% evaporated emulsion was successfully ignited (albeit with 3 igniters) after application and mixing of 2 ml of Alcopol/toluene mixture; an 82% burn efficiency was achieved. Similar results were obtained in Experiment 2.39 with gelled crude igniters. In Experiment 2.40 a 20 mm thick, 60% water emulsion of 12.7% evaporated Avalon crude was successfully ignited by a 60 g gelled gasoline igniter following two applications, premixed, of a total of 5 ml of Alcopol/toluene mix. A 62% burn efficiency resulted.

In the case of the Statfjord crude the pre-ignition application of emulsion breakers proved very effective. In Experiment 4.76 the application and premixing of 2 ml of Alcopol/toluene mixture permitted the ignition of a 20 mm thick, 75% water content emulsion with 30.6% evaporated crude. After this burn was completed it was noted that the residue was herded to the inside edge of the burn ring leaving clear water in the centre. In Experiment 4.77 the test was repeated with the same emulsion stabilized with 10% Bunker C in the oil. A gelled gasoline igniter failed but a gelled crude igniter successfully ignited the treated emulsion. In Experiment 4.78 the procedures used in Experiment 4.77 were repeated (using stabilized oil) except that the emulsion breaker was added dropwise. Gelled gasoline failed to ignite the slick. A 30 g gelled crude igniter succeeded in igniting and burning about ¼ of the surface area of the slick. After this the extinguished, unburned area was stirred and successfully ignited with a gelled crude igniter. The other tests also showed that the pre-ignition addition of Breaxit emulsion breaker also improved the ignition of Statfjord emulsions, particularly those stabilized with Bunker C. In general, Breaxit performed better than Alcopol for the Statfjord emulsions; it could accomplish "dropwise" what Alcopol could "premixed". Overall, the improvement offered by the emulsion breakers were not as dramatic as those achieved with Avalon crude since a gelled crude igniter alone could successfully (although slowly) ignite the 75% water 30.6% evaporated Statfjord crude emulsion.

4.2.3.4 Emulsion breaker addition to the igniter

Based on the success of pre-ignition application of emulsion breakers to the slick, tests were conducted with gelled fuel igniters that had the required dose of emulsion breaker (i.e., 1 ml per igniter) mixed into the fuel prior to gelling. One fact became apparent; the addition of the emulsion breaker changed the behaviour of the gelled fuel igniter dramatically. When the burning igniter hit or was placed on the emulsion surface it would spread out rapidly, carrying flame with it (this could be related to the surface tension flame spreading phenomenon discussed in Section 2.1.5). In Exp. 4_85 a gelled gas igniter containing 1 ml of Breaxit successfully ignited a 75% water emulsion of 30.6% evaporated Statfjord crude. In Experiment 4.86 a plain gelled gasoline igniter failed to accomplish this.

4.2.3.5 Ferrocene addition to the igniter

Although the addition of ferrocene did not seem to raise *in-situ* combustion flame temperatures in the lab burns, it certainly increased flame luminescence and radiation intensity. For this reason tests were conducted with gelled fuel igniters containing 4% ferrocene by weight.

In Experiment 4.86 a 33 g ball of gelled gasoline failed to ignite 20 mm of 75% water, 30.6% evaporated Statfjord crude; a 28 g gelled crude igniter containing ferrocene did successfully ignite the same emulsion.

4.2.3.6 Emulsion breaker plus ferrocene addition to the igniter

Since both emulsion breaker and ferrocene addition to the igniter seemed to offer advantages a number of tests were conducted to test the efficacy of igniters containing both.

In Experiment 2.35 a 30 g gelled crude igniter containing Breaxit and ferrocene failed to fully ignite a 60% water emulsion of fresh Avalon, although the flames lasted for 7 minutes and there was evidence of emulsion breaking occurring. Experiment 4.87 showed that a gelled crude igniter containing 4% ferrocene and 1 ml of Breaxit could ignite a 75% water emulsion of 30.6% evaporated Statfjord crude. In Experiment 4.88 the same igniter successfully ignited the same emulsion stabilized with 5% Bunker C. In Experiment 4.89 the same igniter failed to ignite the same emulsion stabilized with 10% Bunker C; this required a 2 mm layer of fresh crude for ignition.

4.2.3.7 Igniter flame temperatures

Figure 4.3 compares the flame temperatures of different igniter fuels. Experiment 6.1 involved burning 400 ml of gelled gasoline on the water surface in the ring. Experiment 6.2 used 400 ml of gelled gasoline with 4% by weight ferrocene. Experiment 6.3 used 375 ml of gelled, fresh Alaska North Slope crude; Experiment 6.4 involved 350 ml of gelled, fresh Statfjord crude (this initially formed a much smaller diameter blob than the Alaska North Slope oil which explains the initially lower temperatures). Experiment 6.5 used 425 ml of gelled, fresh Alaska North Slope crude with 4% ferrocene; Experiment 6.5 involved the same, but with 15 ml (1 in 30) of Alcopol added. Only the addition of Alcopol, if anything, seems to have affected flame temperatures.

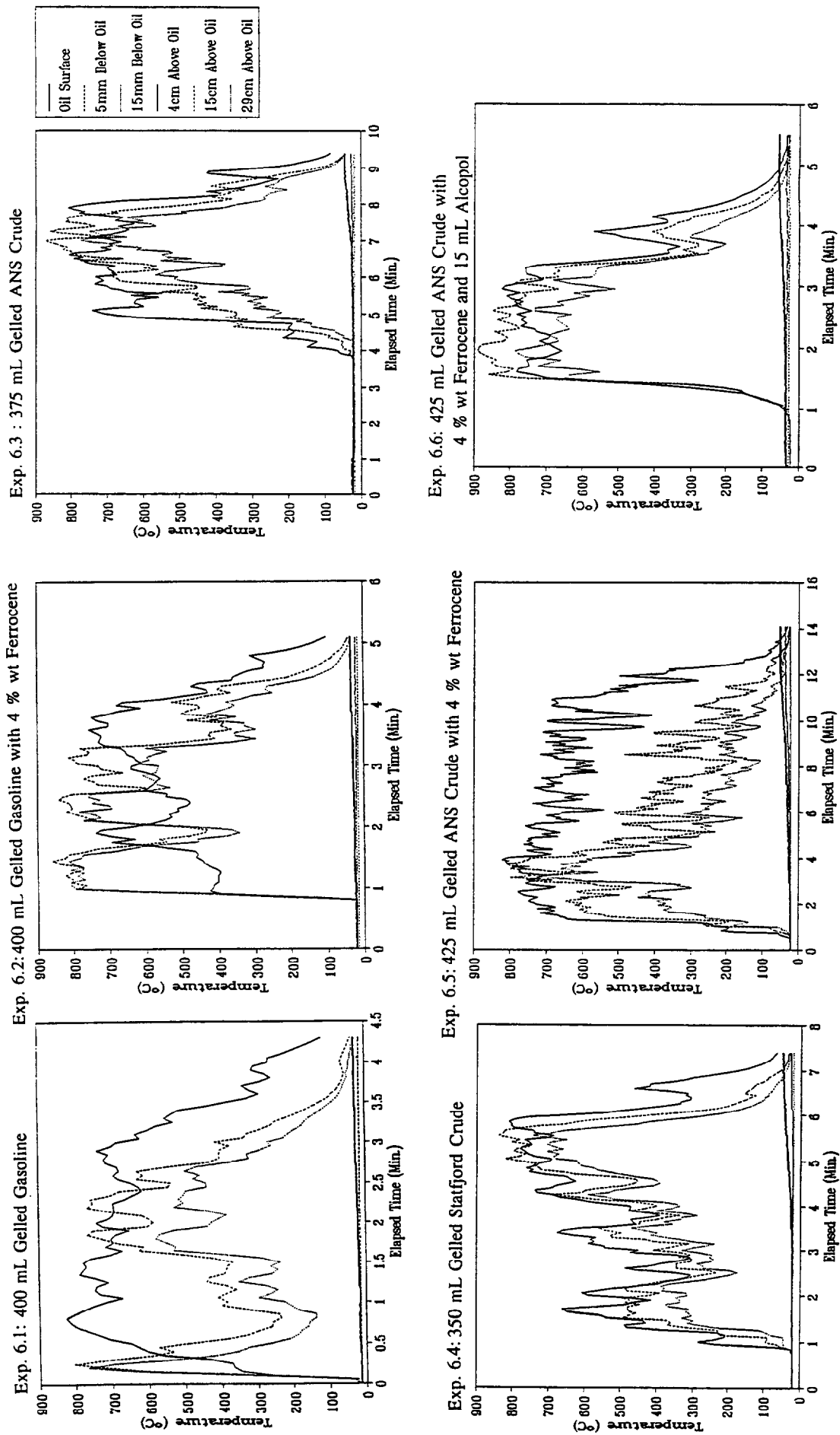


Figure 4.3 Flame temperatures of various gelled fuel igniters

4.2.3.8 Summary

In summary, gelled gasoline igniters were limited to: 40% water emulsions of fresh Avalon; 25% water emulsion of 12.7% evaporated Avalon; and, 60% water emulsions of 30.6% evaporated Statfjord crude. Gelled crude was somewhat more effective, being able to ignite a 75% water content emulsion of 30.6% evaporated Statfjord; gelled crude could not ignite the same emulsion stabilized with 5% Bunker C.

The addition of emulsion breakers and ferrocene to the gelled fuel further improved these capabilities. A gelled crude igniter containing Breaxit and ferrocene almost ignited a 60% water emulsion of fresh Avalon crude. The same type of igniter successfully ignited 75% water content emulsions of 30.6% evaporated Statfjord stabilized with 5% Bunker C; the same emulsion containing 10% Bunker C could not be ignited. The advantages of emulsion breaker addition to the gelled fuel included both enhanced breaking of the emulsion and enhanced flame spreading over the surface of the emulsion; ferrocene addition may improve heat transfer from the flame to the surrounding emulsion.

The most effective method for igniting emulsions was to apply emulsion breaker (and mix it, or allow it time to mix naturally) prior to ignition. This permitted the ignition of 60% water content emulsions of 12.7% evaporated Avalon crude and 75% water content emulsions of 30.6% evaporated Statfjord crude stabilized with 10% Bunker C with a gelled crude oil igniter.

5 FIELD EXPERIMENTS

Meso-scale experiments were carried out on the fjord near Sveagruva Svalbard during the month of May, 1993. The test basins were cut directly into the ice, allowing for open system experiments to be performed. The first series of field experiments was designed to verify the findings from the laboratory experiments concerning the modelling of the emulsion burning process, improvements to the existing igniter technology, and the use of ferrocene during *in-situ* burning (discussed in the next section). The second part of the field experiments was to study the burning of emulsions under dynamic conditions (currents and waves).

5.1 Methods and experimental set-up

This section describes the methods and experimental set-up for the field experiments.

5.1.1 Verification of laboratory results

Two basin sizes were used in this part of the field work: 4 m² circular and square basins, and a 20 m² square basin. The experiments were conducted with Statfjord crude at several states of evaporation and emulsification. The volume of oil used was 200 l for the small basin burns and 2000 l for the large basin burns, giving slick thicknesses of 5 cm and 10 cm respectively.

Twelve small-scale burns were done in the 4 m² basins to study various ignition techniques and to test the recommended improvements to the gelled gasoline igniter.

Two meso-scale burns with 2000 l of emulsion each were conducted in the 20 m² basin during which temperature measurements were made. (In one of these experiments, 0.2% by weight ferrocene was added to the emulsion).

i) improvements to existing ignition techniques

Improvements to the existing igniter technology, (gelled gasoline), were evaluated during a series of 12 small-scale burns. The igniter/additive combinations used were based on the combinations found to have shown most promise during the laboratory tests. The igniters were made by placing 100 ml of fresh Statfjord crude oil into a plastic bag with 6 g of "Surefire" powder (the gelling agent for the Heli-torch fuel). The content could be effectively mixed by squeezing the bags by hand. About ten minutes were required for the Surefire powder to take effect. Two emulsion breakers, Alcopol and Breaxit OEB9 (Exxon) were tested. As well, the effect of varying the concentration of Alcopol in the gelled oil igniter was investigated. The addition of emulsion breaker was done by simply adding the required amount to the oil before adding the gelling agent. In order to test the modified igniters, they were placed directly on the surface of the emulsion and ignited using a propane torch. The igniters were tested individually, during separate burns, and simultaneously, side by side. In all cases, the spreading rate was observed and documented on video.

ii) meso-scale pool burns

Two meso-scale pool burns in the order of 2m³ were conducted with 50% water-in-oil emulsions of Statfjord crude oil, weathered to 25% evaporative loss by volume. Temperature measurements of the underlying water, the slick and flames were made during these two experiments. The thermocouples arrangement used was similar to that used in the small-scale laboratory burns. Temperatures were recorded using data loggers. These experiments were performed to verify some of the emulsion burning processes observed in the laboratory.

For the meso-scale burns, the ignitor used was 100 l of fresh Statfjord crude oil.

Figure 5.1 show the experimental set-up for the 2m³ burns.

Table 5.1 summarizes the field experiments conducted the on Spitsbergen in May of 1993.

Table 5.1: Summary of experiments conducted to study the limitations and improvements of existing ignition techniques for water-in-oil emulsions.

EXP NO.	EVAP %	WATER (%)	VOIUME (l)	IGNITOR TYPE
S1	18	12	200	various types
S2	25	25	200	various types
S3	25	50	200	various types
S7	25	60	200	100 ml gelled oil
S8	25	60	200	gelled oil + 0.5% Alcopol
S9	25	60	200	gelled oil + 4.3% Alcopol
S10	25	60	200	gelled oil + 8.7% Alcopol
S11	25	60	200	gelled oil + 16.7% Alcopol
S12	25	60	200	2 l gasoline
S13	25	50	200	gelled oil + Alcopol or Breaxit
S14	25	50	200	gelled oil + various [Alcopol]
S15	25	60	200	gelled oil + 4.3% Alcopol
L1	25	50	2000	100 l fresh oil
L2	25	50	2000	100 l fresh oil

Note: S=small, L=large

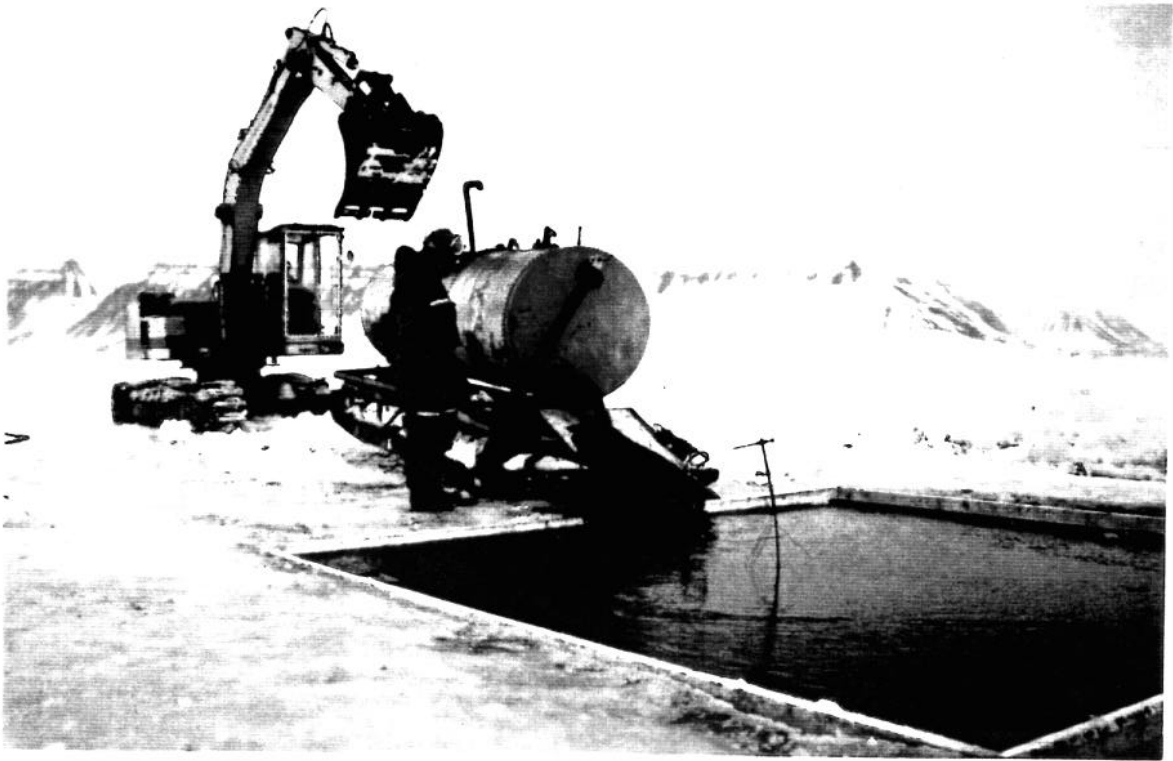


Figure 5.1: Large basin (20 m²) for 2000 l burns

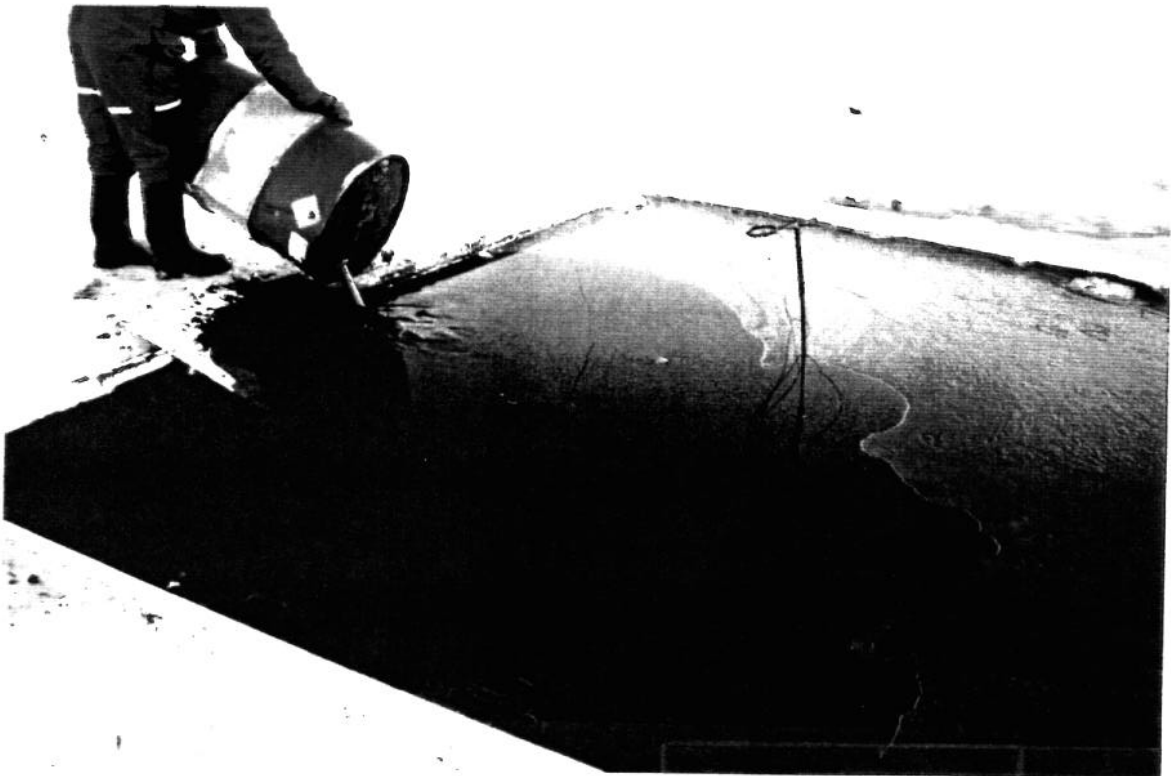


Figure 5.2 Fresh Statfjord crude (100 l) used as igniter

5.1.2 Burning of emulsions under dynamic conditions

Four experiments were performed in the flume basin with currents and waves. A summary of these experiments is given in Table 5.2. Temperatures in the slick, under the slick, and in the flames were continuously recorded as well as wind and current speeds during the first three experiments, using a PC based data acquisition system. The use of ferrocene was studied during the fourth flume experiment. The burn residue was collected, weighed and sampled for further physical-chemical property analysis and toxicity testing.

The recirculating flume basin, designed to study the burning of emulsions against a barrier under dynamic conditions, was fitted with a wave maker capable of generating waves of 5 to 15 cm and a current generator capable of currents of up to 0.3 m/s. The flume is shown in Figure 5.3.

A schematic of the basin is given in Figure 5.4, showing the location of the barrier, wave and current generators, and the water sampling locations. This basin measured 7 m x 16 m with the test area located in the 3 m wide channel. The barrier consisted of an open ended box of 4x4 pieces of wood lined with thin steel sheeting sails. The corners of the flume were rounded using sheets of plywood to facilitate circulation and to limit turbulence. The current and wave generators could be operated remotely using a hydraulic power pack (see Figures 5.5 and 5.6).

Table 5.2: Summary of field experiments to study emulsions burning against a barrier.

EXP NO.	% EVAP	% WATER	Vol. (l)	FERROCENE (%)	IGNITER
F1	18 18	0 12	100 200	0	gas soaked sorbent
F2	18 25	0 25	100 200	0	gas soaked sorbent
F3	18 25	0 50	100 200	0	gas soaked sorbent
F4	18 25	0 50	100 200	≈ 2 0	gas soaked sorbent

Note: F=flume

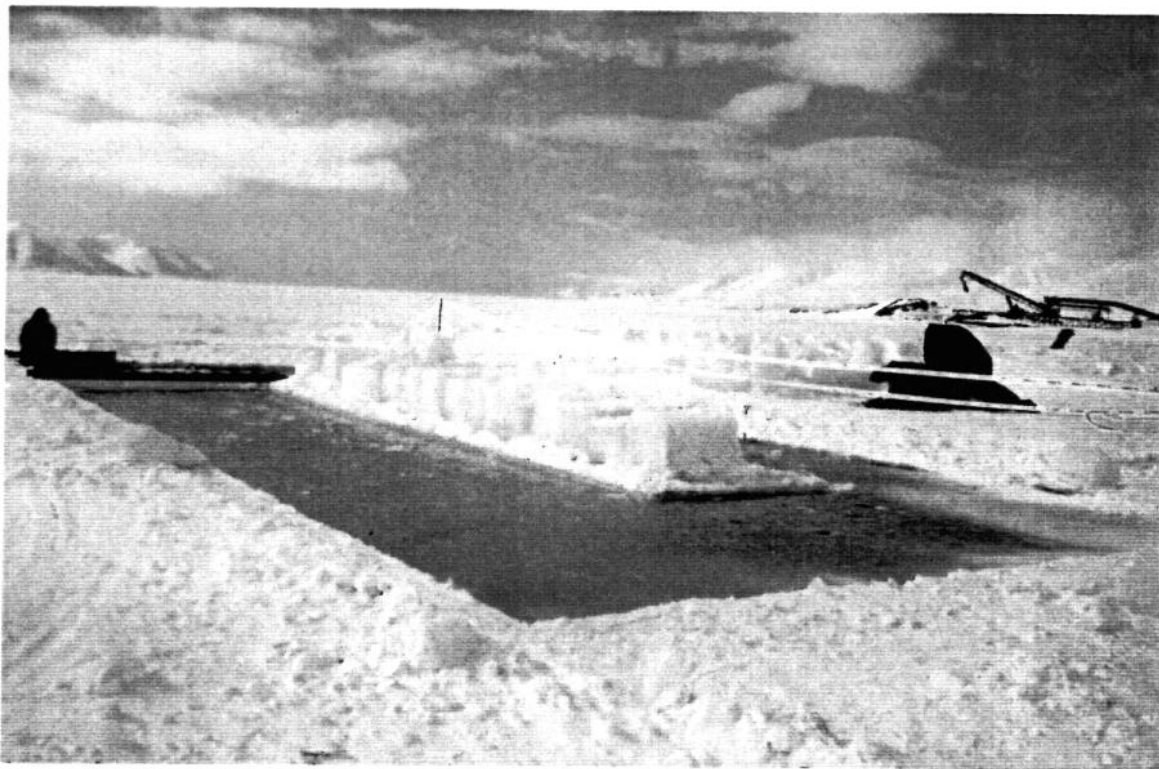


Figure 5.3: Circulating flume tank with current and wave generators

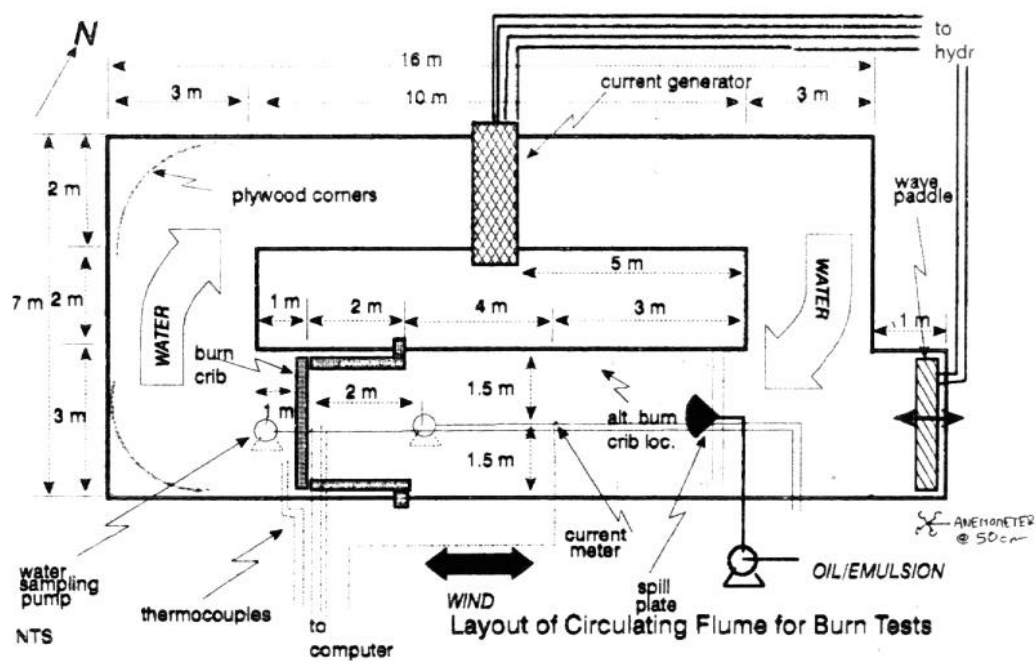


Figure 5.4: Circulating flume schematic



Figure 5.5:
Wave generator



Figure 5.6 Hydraulic power pack

5.2 Results and Discussion

5.2.1 Verification of laboratory results

5.2.1.1 Emulsion burning process

Two large experiments with 2000l each of a 50% w/o emulsion of 25% evaporated Statfjord crude in a contained area of 20 m², were conducted to verify the model developed from the laboratory data, to confirm the laboratory temperature findings and to study the scaling effects on the heat transfer characteristics of burning emulsions. The slick thickness in these experiments was 10 cm which provided a long enough burn to permit recording of data over a sufficiently long steady state burn period. Temperatures in the slick, flames and underlying water were recorded during these experiments. The use of ferrocene was also studied, both for the soot reducing effects of ferrocene, and for any effect that this compound may have on the heat transfer characteristics of the emulsion as well as on the various burns parameters.

The first experiment, L1, was conducted without ferrocene. Due to wind velocities in excess of 10 m/s at the time this experiment was to be initiated, an attempt to ignite the slick failed. The winds remained high for the remainder of the day, and the experiment had to be postponed. The following day most of the slick was covered with a 5 cm layer of snow. Wind speeds ranged from 4 to 5 m/s. Fresh oil was poured over the emulsion slick in order to facilitate ignition. The presence of snow on the slick did not seem to prevent ignition of the emulsion, although some snow remained around the edges of the enclosed area for the first ten minutes. After 15 minutes, only a small amount of snow remained in the upwind corners of the test basin. Eight minutes following ignition, steam could be seen rising from the slick. Some foaming and sporadic burning began to occur around the edges of the slick. After 9 minutes, boiling on the slick surface could be seen. The "microexplosion" phenomena of water droplets bursting in the flames was observed, indicated by sparks near the slick and in the lower flame area. The emulsion water was boiling out of the slick and steam was rising from the emulsion surface. After approximately 28 minutes, small puffs of vapour were released from the slick every few seconds. Foaming over of the slick began at 39 minutes. At this point large areas of the slick would seemingly extinguish. Steam was released, then the area would partially reignite again. Some areas of the slick had burned completely leaving clear areas of water showing through the slick. After 41 minutes, the slick began to extinguish at a rate of roughly 3 m² per minute. At 46 minutes, an increase in the microexplosion phenomena, occurred, signalling the beginning of the intense burn phase. The water beneath the slick was boiling vigorously at this point. Large droplets of boiling water were observed. After 49 minutes the fire was essentially out.

The temperature profiles for experiments L1 and L2 can be seen in figures 5.7 and 5.8 respectively. Flame temperatures recorded 4, 15 and 29 cm above the slick are given in the first graph, while the slick temperature, recorded at the slick surface and 5, 15, 50 and 65 mm below the slick surface are given in the graphs on the lower half of the page.

The flame temperature in experiment L1, ranged from 500 to 850 °C. The flame temperatures with the same emulsion but this time containing 0.20% ferrocene by weight (or 0.40% of the oil by weight) ranged from 400 to 800 °C. More variation in the temperature were recorded during experiment L2. This is likely due to the foaming phenomena, where the slick temporarily extinguishes in some areas, then reignites shortly thereafter. This phenomena was much more pronounced when the emulsion contained ferrocene and occurred earlier in the burn. Foaming usually signalled the beginning of the intense burn phase and the end of the burn. When the emulsion contained ferrocene, the period of foaming lasted much longer than with emulsion containing no ferrocene. However, the entire burn time was shorter when ferrocene was added to the emulsion.

From the temperature curves shown in figures 5.7 and 5.8, it appears that the presence of ferrocene in the emulsion has an impact on the heat transfer characteristics of this slick. In experiment L1, the top portion of the slick reaches a temperature of above 100 °C after approximately 20 minutes indicating that the top layer of the slick no longer contained water at that point. However, temperatures measured at 5 mm below the surface of the slick and lower remained below 100 °C indicating that there was still water present in the vicinity of these thermocouples and that the oil was still emulsified below the burning surface. With the ferrocene burn, the top 5 mm of the slick increased to 100 °C in less than 10 minutes, and the thermocouple located 15 mm below the slick surface recorded temperature of over 100 °C after 20 minutes. This may be an indication that the water evaporated more quickly when ferrocene was mixed with the emulsion than when ferrocene was not present. More radiated heat was noticed during the burn with ferrocene. It may be that more heat is radiated back to the slick, enhancing the rate of increase in temperature in the emulsion and therefore the rate of water vaporization.

5.2.1.2 Ignition improvement experiments

Three types of experiments were carried out to study the effectiveness of the various ignition techniques recommended following the laboratory experiments for the ignition of emulsions with higher water contents. The first series consisted of testing different additive combinations with the gelled oil, including ferrocene and emulsion breakers. One experiment compared the effectiveness of two types of emulsions breakers added to gelled oil, while the third series of experiments, investigated at the effect of varying the concentration of emulsion breaker.

Comparison of different igniter additives:

In the first three experiments, S1, S2, and S3, the effectiveness of four gelled oil igniters were tested simultaneously with three different emulsions. The maximum water content was 50%. The igniters consisted of 100 ml of gelled fresh Statfjord crude with either 6g of ferrocene, 0.5 ml of Alcopol, or both. One igniter, containing gelled oil only was used as a reference. The igniters were placed on the emulsion slick, side by side, approximately 60 cm apart and ignited within seconds of each other using a propane torch.

During experiment S1, the igniter containing the emulsion breaker clearly promoted quicker ignition of the emulsion slick. Beads of water broke out of the slick and were surrounded by relatively water-free oil. This oil was quickly volatilized and the vapours ignited. The igniter containing both Alcopol and ferrocene showed the second fastest flame spreading rate, followed by the igniter containing only ferrocene. The igniter containing no additives was slowest at propagating the fire.

During the second experiment, the wind velocity was quite high, approaching 10 m/s at times. It was therefore difficult to ignite the igniters. Most of them had to be reignited at least once. This did not seem to be dependant on the type of igniter, but rather the strength of the wind at a particular instant over the slick. In this experiment, the igniter containing no additives showed the quickest flame spreading rate, however, this igniter was also in a more sheltered location on the slick than the others. This is believed to be the reason for the more effective ignition. After several minutes, all igniters had successfully ignited an area of the slick. While this experiment did not give conclusive results concerning the use of additive with gelled oil, it does indicate, that even under very windy condition, a gelled oil igniter can successfully ignite a 25% w/o emulsion if it is sufficiently sheltered, and that gelled oil with an emulsion breaker can be effective under windy conditions.

The third experiment with these four igniters, tested their effectiveness in igniting a 50% w/o emulsion. The igniters containing the emulsion breaker clearly enhanced the ignition effectiveness of the gelled oil. The area of the slick with these igniters was completely aflamed after approximately 2 minutes, while the area containing igniters with no emulsion breakers required a longer period of time before the surrounding area was fully ignited.

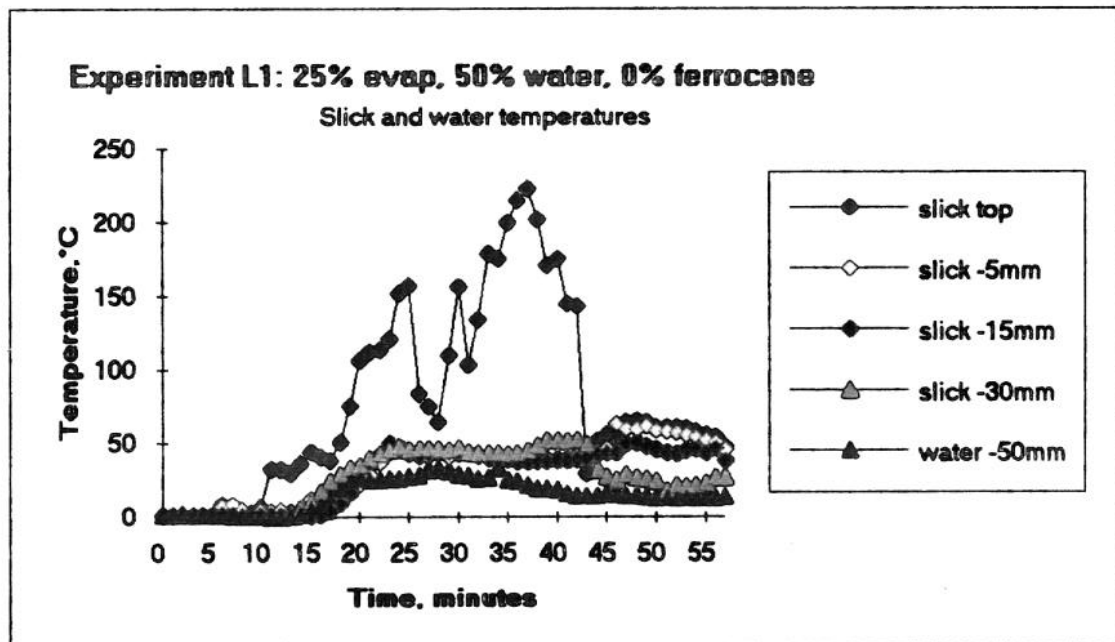
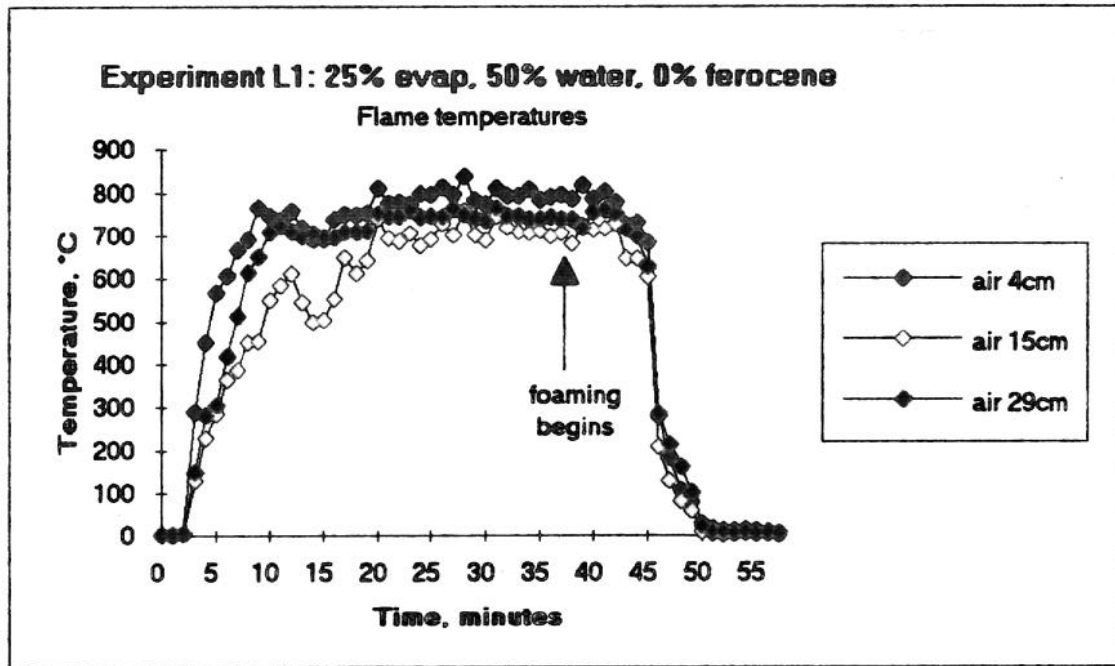


Figure 5.7: Temperature profiles for Experiment L1

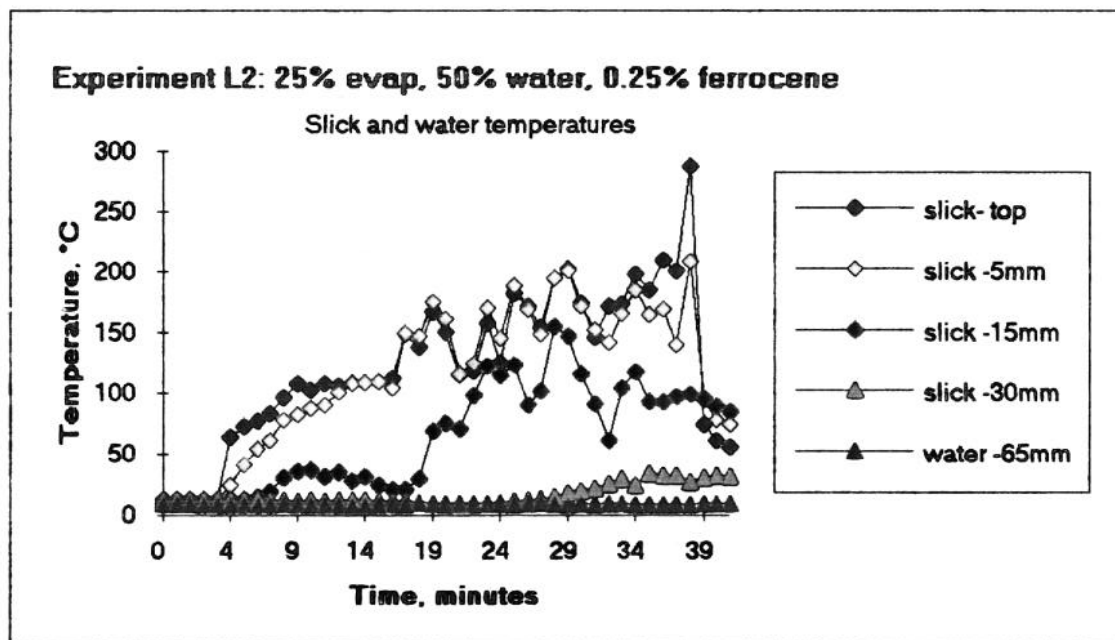
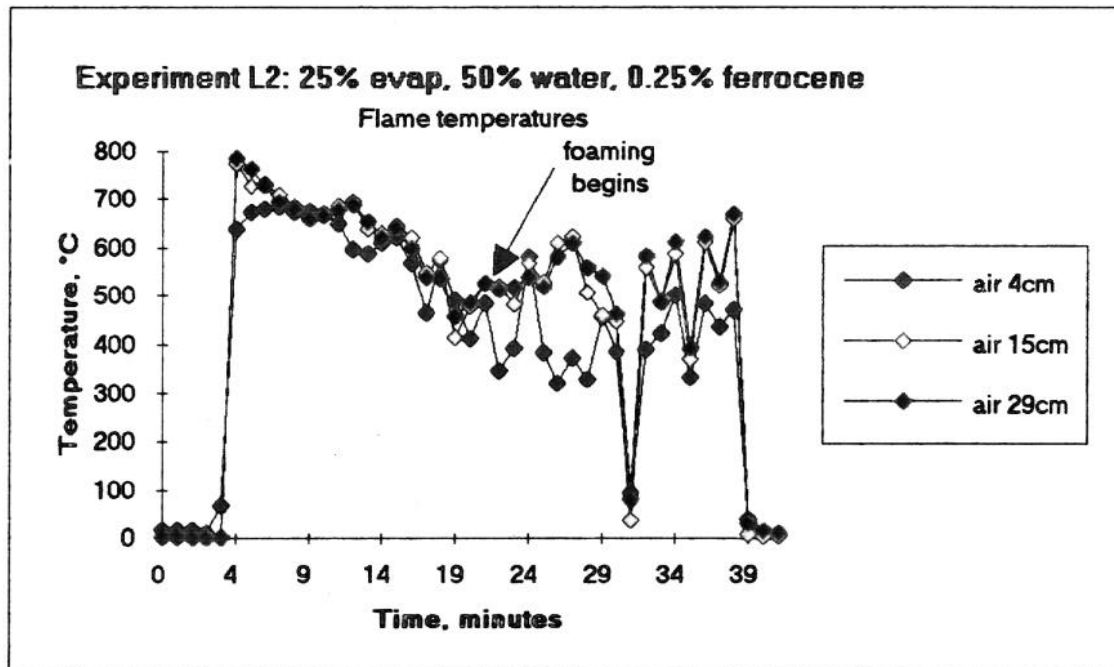


Figure 5.8: Temperature profiles for Experiment L2

Several interesting observations were made during these three igniter experiments. It was noted that in the area surrounding the igniter containing no emulsion breaker, water vapour was seen rising from the emulsion slick as the flames spread out from the igniter. Foaming was also observed as more oil was burned off from the slick surface. These were similar observations to those made during the ignition and burning of emulsions in the laboratory. However in the case of the igniter containing an emulsion breaker, it was evident that the emulsion was physically broken as the igniter burned and spread over the slick. The release of vapour and foaming was not observed during the ignition phase with the gelled oil/demulsifier combination. Instead, free water surfaced and was evaporated leaving a film of free oil on the emulsion surface.

The results from these three experiments clearly demonstrated that the addition of an emulsion breaker to the gelled oil igniters, enhanced the ignitability of an emulsion and increase the flame spreading rate across the slick surface.

Comparison of different emulsion breakers:

In experiment S13, the emulsion breakers Breaxit and Alcopol were compared by adding 5 ml of each to the gelled oil igniters. The igniters were then placed on the surface of a 50% w/o emulsion and ignited with a propane torch.

The flame spreading rate as well as the spreading pattern differed for each of these igniters. Flame spreading around the igniter containing Alcopol was radial, while spreading was more elliptical with the Breaxit igniter. The initial flame spreading rate was higher with Breaxit than with Alcopol. This observation was also made in the laboratory, where for small burns (0.125 m^2), the dropwise addition of Breaxit to the emulsion slick enhanced ignition to a greater extent than did the addition of Alcopol. In this field experiment, 30 seconds following the ignition of the igniters, the surface area burning around the igniter with Breaxit measured 60 cm^2 , while the flame area surrounding the igniter containing Alcopol was 40 cm^2 . After approximately one minute, the flames surrounding both igniters covered approximately the same area. Two minutes following ignition, the section of the slick ignited by the gelled oil with Alcopol exhibited a greater flame spreading rate. Therefore, when comparing these two emulsion breakers, the gelled oil with Breaxit showed quicker flame spreading initially than gelled oil supplemented with Alcopol, however, after two minutes of burning, the flame spreading rate was greater where Alcopol had been used than where Breaxit had been.

These results emphasize two important aspects: firstly, not all emulsion breakers will have the same effect or impact on the ignition of emulsions; and secondly that the emulsion breakers may be oil specific to a certain extent. Also, this field experiment demonstrates the importance of performing full scale testing. While the results from the laboratory gave a good indication of the potential of this ignition technique, it did not give the full picture. For the given scale of these laboratory experiments, the results were correct and validated in the field. Initially, Breaxit did appear to enhance the ignition capability of gelled crude oil to a greater extent than Alcopol. However, it is obvious that larger scale experiments can give additional information which may not be obtained from laboratory experiments.

Effect of varying emulsion breaker concentration:

A series of experiments was conducted to study the effect of varying the concentration of emulsion breaker in the gelled oil. The emulsion breaker Alcopol was used in these experiments. The oil used in these experiments was a 60% w/o emulsion of 25% evaporated Statfjord crude. Following this series of experiments, one experiment was performed with four igniters, ignited simultaneously, and containing the most effective emulsion breaker to gelled oil ratios found in the previous six experiments. This experiment was done with 50% w/o emulsion.

In the first experiment, S7, no emulsion breaker was used with the gelled oil igniter. As the igniter

burned and flames spread to the surrounding emulsion, steam could be seen rising from the slick. After about five minutes, the flames had spread to an area of approximately 2 m^2 . After about 7 minutes, foaming began and the fire briefly extinguish in one area of the slick. Seconds later, foaming ceased and the release oil was reignited by the adjacent area still aflame. After fourteen minutes, boiling of water on the slick surface was observed. After 16 minutes the fire was essentially out. The flames had not spread over the entire surface of the slick.

In the second experiment of this series, S8, the addition of 0.5% Alcopol to the gelled oil was tested. Following ignition of the igniter, foaming around the bag was observed as water was released from the emulsion. Water beaded over the surface of the slick and a thin layer of oil was produced in the vicinity of the igniter. This was much different from observations made during the previous experiment. Without the emulsion breaker, water was released from the slick in the form of steam, while the presence of an emulsion breaker caused the release of water by chemically breaking the emulsion and causing the water to separate from the oil. The emulsion appeared to break shortly after ignition of the gelled oil. The flame spreading rate was much quicker with the emulsion breaker than without. After two and a half minutes, the fire area with the emulsion breaker/gelled oil igniter was approximately 1 m^2 , compared to 0.2 m^2 without the emulsion breaker. Boiling at the water's surface could be seen after two and a half minutes in experiment S8. The violent burn phase occurred five minutes following ignition and the fire was essentially out after 8 minutes. The total burn area was approximately 1.5 m^2 .

The third emulsion breaker tested in this series contained 4.3% Alcopol. One minute following ignition, the area of the slick covered by flame was approximately $14 \times 40 \text{ cm}$ (0.5 m^2). After 1.5 minutes, foaming near the bag was observed, and shortly thereafter, spitting started, caused by the water release from the emulsion and floating on its surface. After approximately four minutes, the flame spreading stalled momentarily, then resumed. This is likely due to the excess amounts of water released onto the emulsion surface by the emulsion breaker, which needed to be evaporated before the flames could continue spreading over the oil film. After approximately 7 minutes, the flame area began to shrink and concentric rings of water on the slick surface were observed. Droplets of water were being released from the emulsion. After nine minutes, a pool of water was present on the slick surface. The fire extinguished after 11 minutes.

In experiment S10, gelled oil with 8.7% Alcopol was tested. One and a half minutes following ignition of this igniter, beads of water were observed on the surface of the emulsion. The flame area after three minutes was approximately 0.06 m^2 , which is considerably less than in experiments S8 and S9 where concentration of 0.5 and 4.3% emulsion breaker respectively, were used with the gelled oil. After four minutes, the flames spread to an area where a layer of relatively water free oil covered the emulsion. Water was seen boiling on the slick surface. Foaming was also noted. The ignited area was 0.25 m^2 at this point. After 5 and a half minutes, the flame area began shrinking back to 0.06 m^2 . After six minutes, a considerable amount of water was observed floating on the slick surface, and by 6 minutes 40 seconds, the fire had extinguished.

A 16.7% emulsion breaker in gelled oil igniter was tested in experiment S11. The flame spread rate over the slick with this combination was slower than all previous concentrations tested. After 3 minutes the aflammed area was approximately 1 m^2 . Four and a half minutes following ignition, foaming and boiling of water on the slick surface could be observed. Ring of free water formed on the slick surface. After five minutes, the flames died down briefly, then flare up again. The fire had nearly extinguished after 6 minutes from what appeared to be an excess of water on the slick surface. At this point, 2 l of gasoline were added to what was left of the fire. This proved to be effective in removing most of the remaining oil in the test enclosure.

The above five experiments gave a good indication of the emulsion breaker concentrations required to effectively ignite a heavily emulsified oil. However, as these experiments were not conducted under the exact wind conditions, another experiment was conducted with four of these igniters tested

simultaneously to confirm the above results.

Experiment S14 simultaneously studied the effect of emulsion breaker concentration in gelled oil using the above tested igniters. All but the igniter with 16.7% Alcopol were chosen for this experiment. Figure 3.19 shows the placement of the four igniters on the slick surface. From top to bottom they contained 0.0, 0.5, 4.3, and 8.7% Alcopol. It is obvious from Figure 3.20 that the presence of an emulsion breaker greatly enhanced the ignition and flame spread over this 50% w/o emulsion. (Note: this second figure has been taken from a different angle than the first). The left hand side of the test slick (with the igniters containing 4.3 and 8.7% Alcopol) was almost completely ignited after approximately 2 minutes while the right hand side of the slick (with the igniters containing 0 and 0.5% Alcopol) had but a small area ignited. In fact, the igniter containing no emulsion breaker had extinguished. The igniter containing 4.3% Alcopol showed the highest ignition and flame spreading rate.

The following general observations have been made regarding the use of emulsion breakers in conjunction with gelled oil:

The results presented above confirm the potential of using gelled oil as an igniter for emulsions and that the addition of certain additives can enhance the effectiveness of this type of igniter. In particular, the use of an emulsion breaker with the gelled oil has proven to be an effective means of igniting otherwise unignitable emulsions using the existing igniter technology (i.e.: Helitorch and gelled gasoline). The emulsion breakers, even in very low concentrations, were capable of breaking the emulsion to the point where enough free oil could be released to sustain *in-situ* combustion.

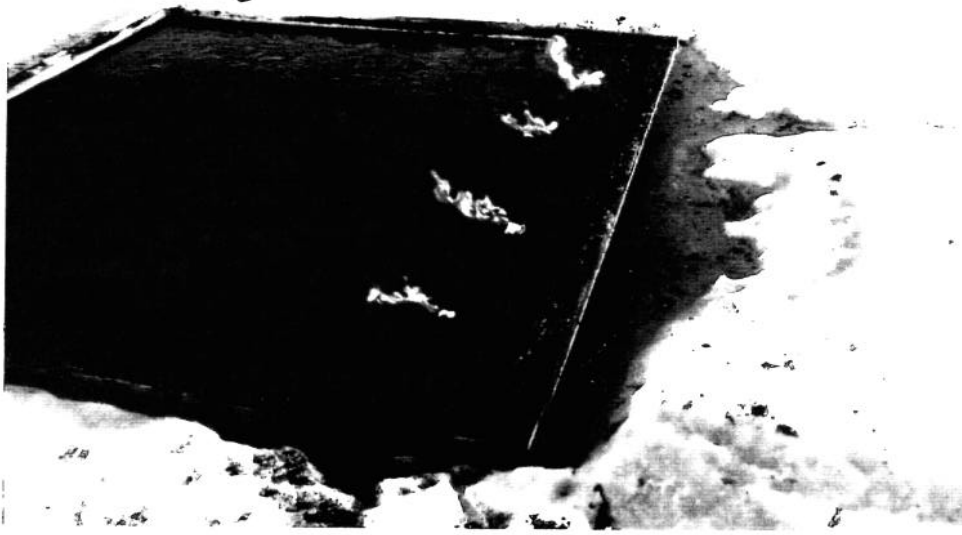
The initial heat requirement of the igniter is reduced when used in combination with an emulsion breaker. Without the emulsion breaker, the igniter must provide sufficient heat to first, heat the emulsion to the boiling point of water in order to release water from the slick, a secondly, heat the oil to its fire point. When an emulsion breaker is used, water is released almost immediately following ignition of the gelled oil, without the requirement for heat input to vaporize the water.

These results indicate that there is an optimum emulsion breaker concentration. There appears to be a saturation point, where an excess amount of emulsion breaker is not only ineffective, but can hinder ignition or flame spreading, as demonstrated in experiments S10 and S11. When a large amount of water was released from the emulsion at once, a layer of water formed on the oil surface. This water must be evaporated before the oil can produce enough vapours for ignition. If too much water is present, the igniter may extinguish before this can ignition occurs.

5.2.2 Burning of emulsions under dynamic conditions

Experiments were conducted in a circulating flume tank to study the ignition, combustion and residue remaining from continuous burning of weathered crude oils and emulsions against a barrier. The main focus of these experiments was to determine whether or not heat radiated from a fire could ignite a high water content emulsion drifting towards the burn, which would otherwise be difficult or impossible to ignite using the Helitorch/gelled gasoline technique. Four experiments were conducted in the flume basin. Temperature measurements were taken during the first three experiments, while the use of ferrocene was studied during the last experiment. Parameters recorded during these experiments were:

- oil/emulsion film temperature
- flame temperature
- water temperature
- smoke emission/density
- amount of residue



Alcopol

0%

0.5%

4.3%

8.7%

Figure 5.9: Placement of igniters on 50% w/o emulsion slick

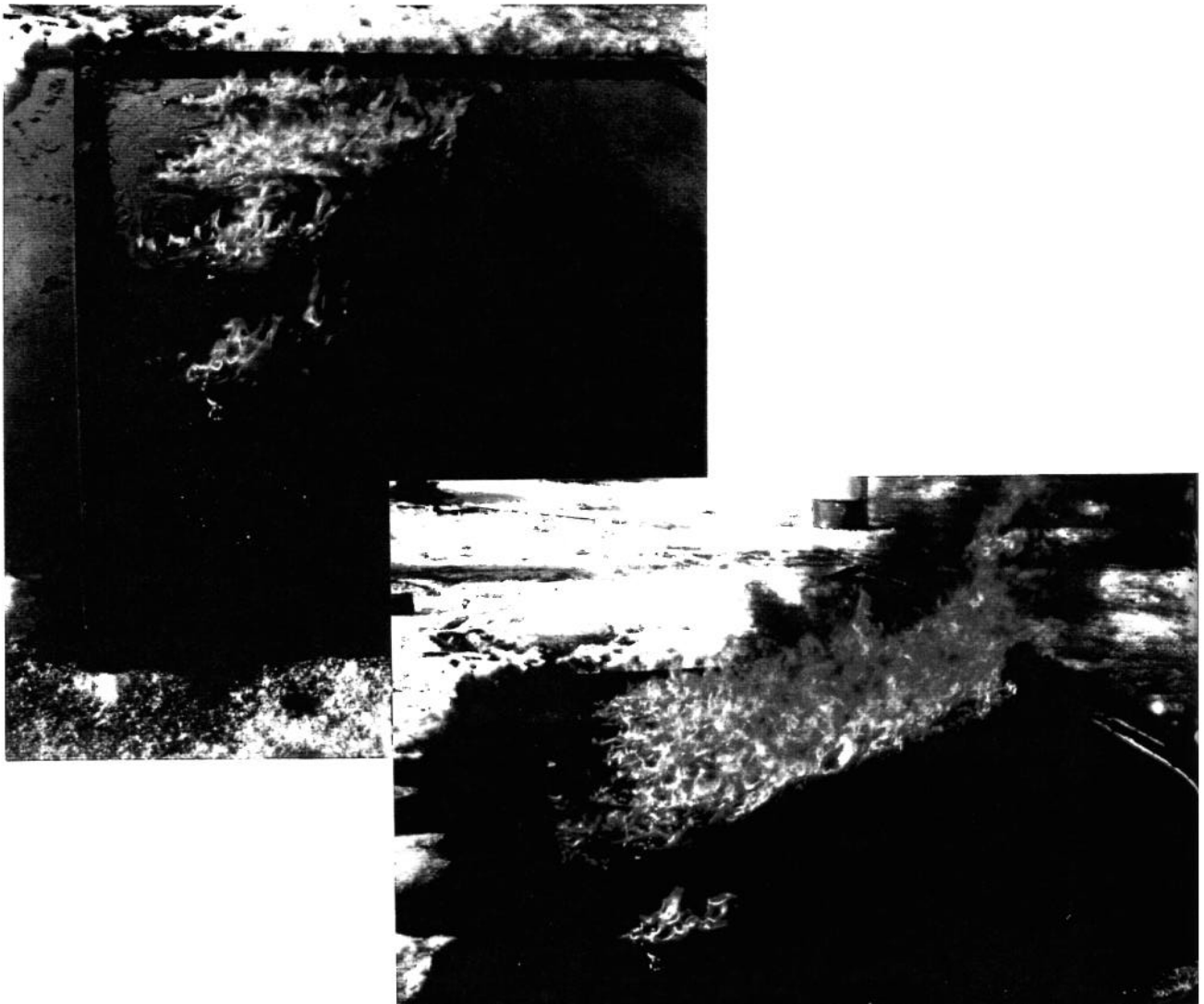


Figure 5.10: Comparison of demulsifier concentration in gelled oil igniters

5.2.2.1 Ignition success

For each of the flume experiments, 100 l of 18% evaporated Statfjord crude oil was placed inside the flume and contained against a fixed barrier. The oil was ignited using a gasoline soaked sorbent pad, and once the flames had spread over the entire slick area, the emulsion was pumped into the basin upstream of the fire. The emulsion was carried into the burning slick by the 0.3 m/s current. In all of the four experiments, the emulsions, ranging from 18 to 50% water in oil, were successfully ignited. The burn area in these experiments measured roughly 6 m². The emulsion was fed into the burning slick at a rate of approximately 15 l/min (see Figure 5.11). Figures 5.12 and 5.13 show an emulsion burning while contained against a barrier in the circulating flume basin.

In experiment F1, a 12.5% w/o emulsion of 18% evaporated Statfjord crude was fed into the burning slick. It was estimated that the ignition time for the forward edge of the emulsion slick was approximately one minute. The approaching cold emulsion was pushed under the slick by the current, where the hot ignited oil warmed the emulsion slick and evaporated the water from the emulsion. Steam was observed rising from the emulsion, followed by the formation of a layer of relatively water free oil which eventually ignited.

A 25% water-in-oil emulsion was ignited in the second flume experiment. As in the first experiment, the hot oil from the ignited slick flowed over the approaching cold emulsion. Larger amounts of steam escaping from the slick were observed during this experiment as water was boiled out of the emulsion. Seven minutes after the start of this experiment, the wave maker was turned on creating waves with an amplitude of approximately 10 cm and a length of 3 to 4 m. The waves did not seem to affect the ignition of the emulsion. It appeared that the heat radiated from the burning slick was sufficient to overcome any negative effect the waves may have had on the ignition of the emulsion.

The third experiment in this series studied the ignition of a 50% w/o emulsion of 25% evaporated Statfjord crude. Typically, an oil at this level of emulsification would be very difficult to ignite using currently available ignition techniques. However, the forward edge of the emulsion drifting into the burning 18% evaporated oil was ignited within one to one and a half minutes. As the hot oil spread over the emulsion, vapour was seen being released from the slick. A distinct edge of the hot oil slick flowing over the cold emulsion was observed and is shown in Figure 5.14. After approximately 11 minutes into this experiment, spitting and foaming of the emulsion slick was observed. The emulsion, pushed under the hot burning slick, began to foam as water was boiled out. Seconds later, the foaming in this area subsided, and that portion of the slick ignited. After roughly 20 minutes, approximately 75% of the slick area had extinguished, with some areas still foaming.

One to two minutes later, parts of the slick reignited again, and flames spread over the entire area of the slick. This phenomena is typical of burns with high water content emulsions and was also observed in the laboratory. During experiment F3, this phenomena lasted for approximately 8 minutes, until in the end only a small area of the slick, around the barrier edge remained burning. This cycle of foaming, extinguishing and reigniting of a slick area can repeat itself several times before the fire is extinguished.

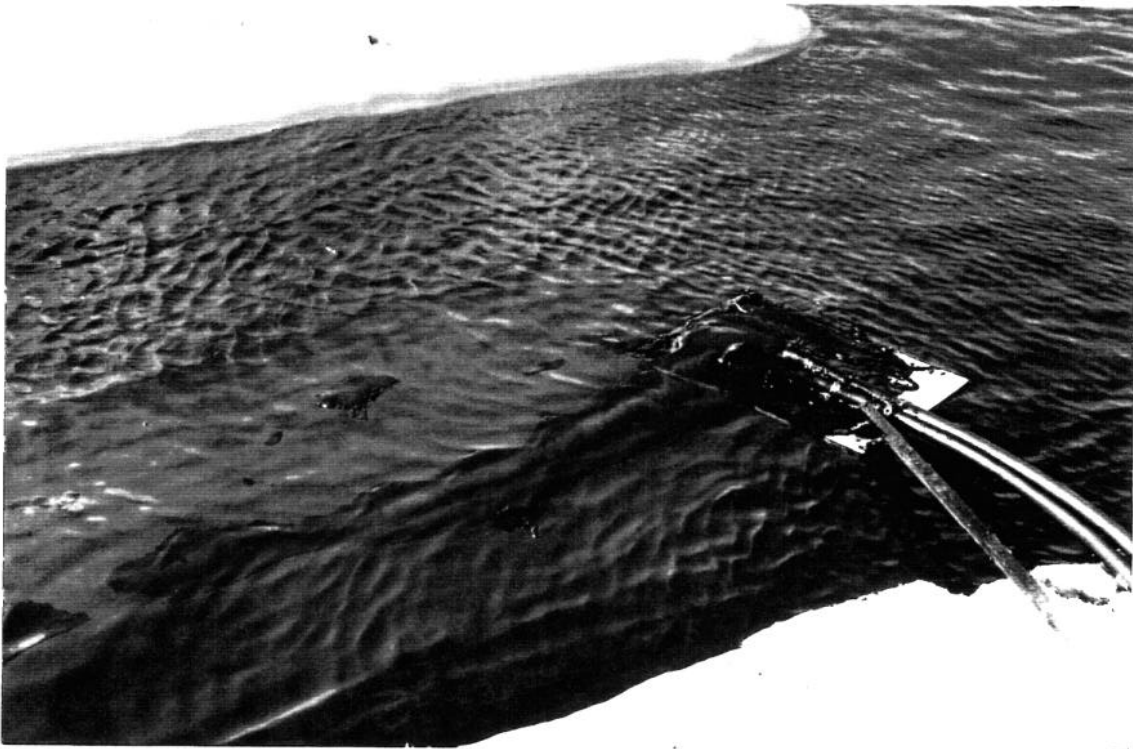


Figure 5.11: Feeding emulsion to the burning slick



Figure 5.12: Burning of emulsion against a barrier

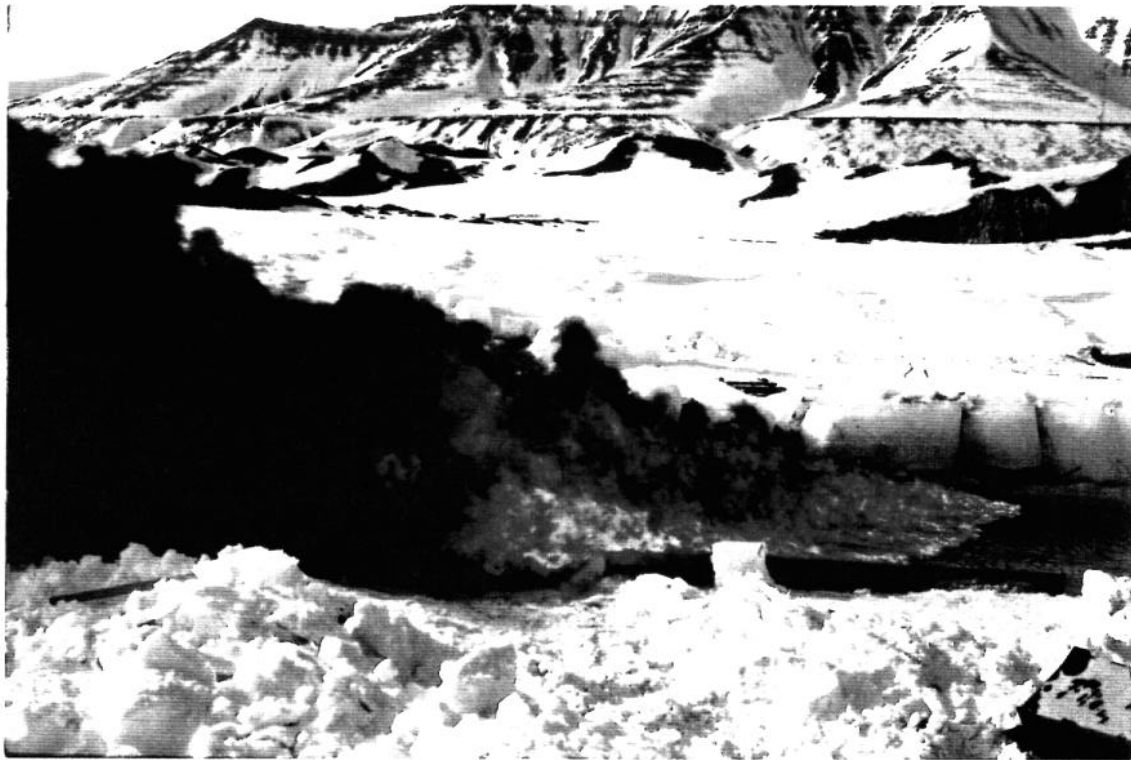


Figure 5.13: Burning of emulsion against a barrier - side view

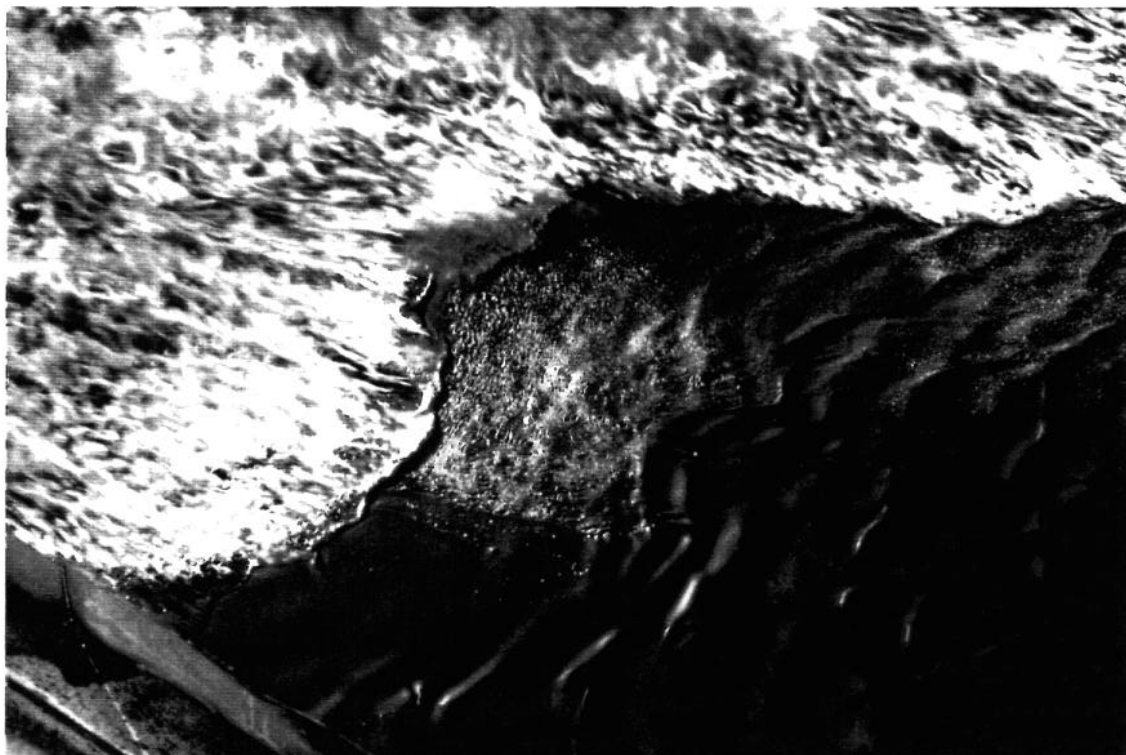


Figure 5.14: Close-up of advancing emulsion drifting into ignited crude oil (Note release of water vapour from edge of ignited slick)

5.2.2.2 Effect on burning process

In order to successfully ignite and burn emulsions, the key step which must be accomplished is that of continually eliminating the water from the emulsion throughout the burn and providing sufficient heat to raise the released oil to above its fire point. Factors influencing this include the water content of the emulsion, the temperature gradient through the slick and the slick thickness. Because of the water present in an emulsion it is theorized that, an emulsified oil will lose heat to the underlying water faster than an unemulsified oil. This is mainly due to the fact that water is not as good an insulator as oil. In addition, as with unemulsified oil, as the slick burns, the thickness decreases and the insulating effect of the emulsion is reduced. When the slick thins to below the minimum thickness which provides enough insulation to permit heating the oil to its fire point, the slick extinguishes. By burning an emulsion against a barrier, the time to reaching this minimum slick thickness is extended as the current continuously pushes the slick against the barrier, maintaining the required slick thickness to sustain burning.

This is in fact what was observed during the three experiments conducted in the flume basin. In the case of pool fires, combustion of oil continues until areas of the slick become too thin to sustain burning. What is often observed is that some of the slick areas will extinguish before others. In the case of a slick burning against a barrier, the burning oil is continuously herded against the barrier where the slick thickness required to sustain combustion can be maintained for a longer period of time. The herded slick is therefore able to burn down to a very small fraction of the original slick area. In these flume experiments, while the emulsion was being fed into the slick an area of approximately 6 to 7 m² were maintained. Once the emulsion was no longer added to the fire, the slick and consequently burn area diminished. As the slick regressed towards the barrier, so did the flame area. The major difference between a pool burn and a burn against a barrier is that as a pool burn approaches the minimum thickness for combustion, the flame area is restricted to areas of the slick thick enough to sustain combustion and which is usually less than the entire slick area. In the case of a burn against a barrier, it is more likely that the flame area will cover the entire slick area which regresses as the oil is consumed, for the duration of the burn than in the case of burning pools of constant surface area. This is due to the fact that the minimum thickness required to sustain burning is maintained for a longer period when burning against a barrier.

The temperature profiles for the flame, slick and underlying water for experiments F2 and F3 are given in Figures 5.15 and 5.16. Flame temperatures were generally in the 500 to 1000°C range for distances of 4 to 29 cm above the slick. Maximum slick temperatures of about 120 °C were recorded. These temperatures tend to be cooler than those recorded during the two meso-scale burns (L1 and L2) however it may be that the slick thermocouples were recording temperature at a slightly lower slick depth during the burns in the flume, since the slick thickness increased once the emulsion was fed to the burn. As well, it was difficult to see and adjust the thermocouples once the slick was ignited.

One disadvantage to burning an emulsion against a barrier in a current or against a towed boom is that the underlying water is continuously replaced and therefore cooled. In a pool burn where the underlying water remains relatively still, increases in temperature can be observed in the water below the slick. However, as the temperature profiles clearly demonstrate, no temperature increases are observed when burning oil in a current. In general the slick temperatures measured below the slick surface during the flume burns were not as high as those recorded during the two meso-scale burns. When comparing these two temperature profiles, the flame temperature in experiment F2 remained much more constant than those in experiment F3. This may be explained by the fact that in the third experiment, a much higher water content emulsion was burned, and that during this burn, the foaming phenomena was much more pronounced than in the previous burns with less emulsified oils. When areas of the slick begin to foam, the flame temporarily subsides, thus reducing the flame temperature. This however does not seem to cause much fluctuation in the slick temperature. The large jump in the slick temperature during

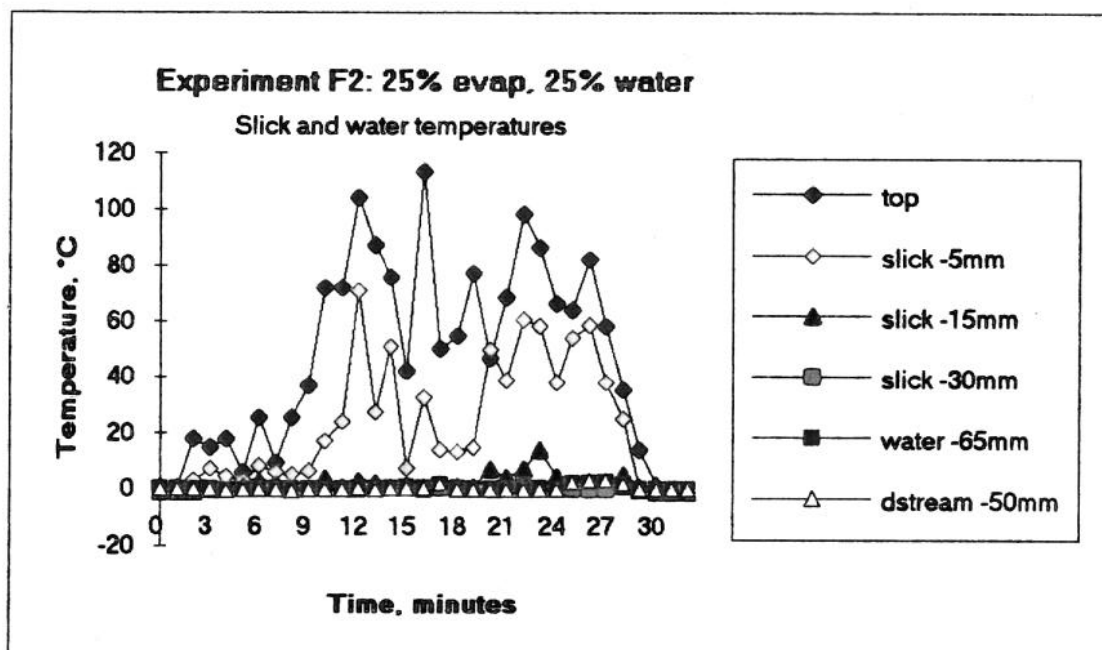
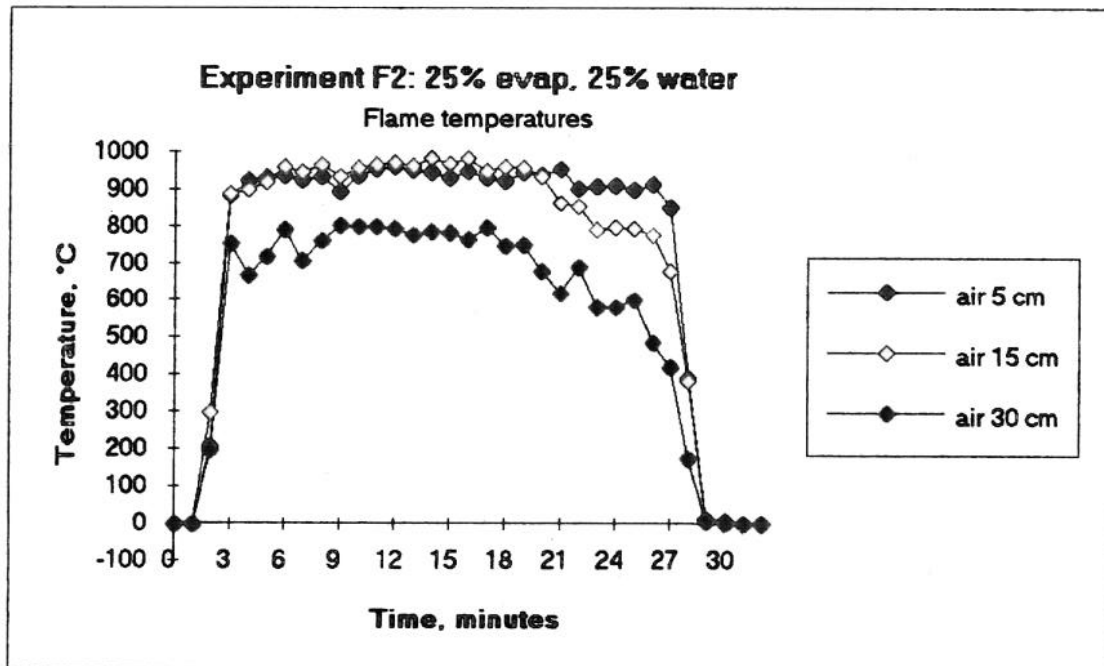


Figure 5.15: Temperature profiles for Experiment F2

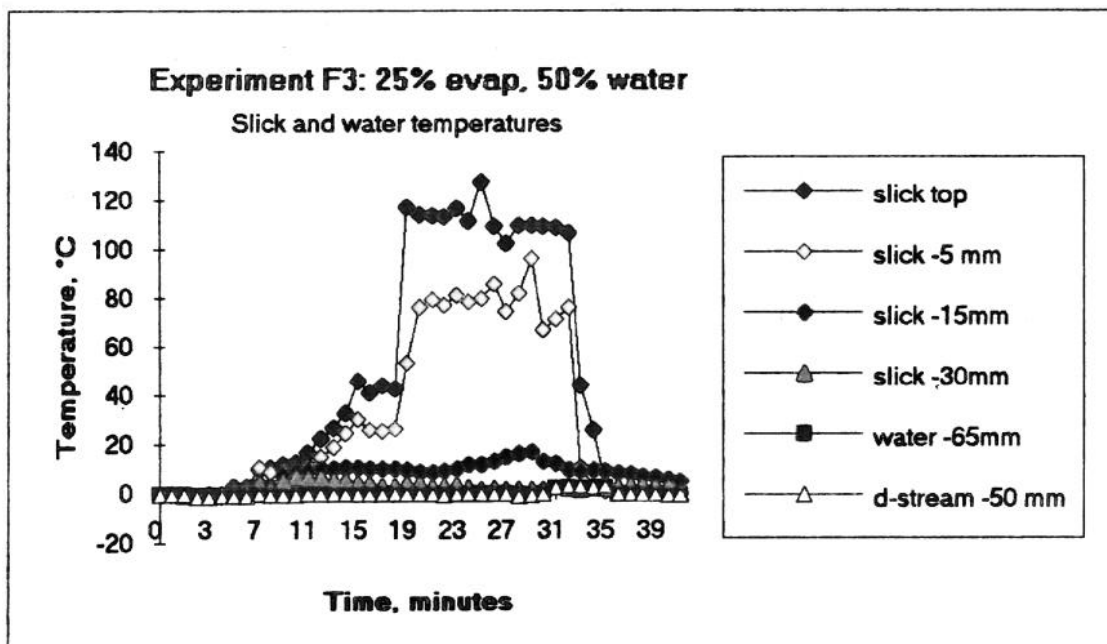
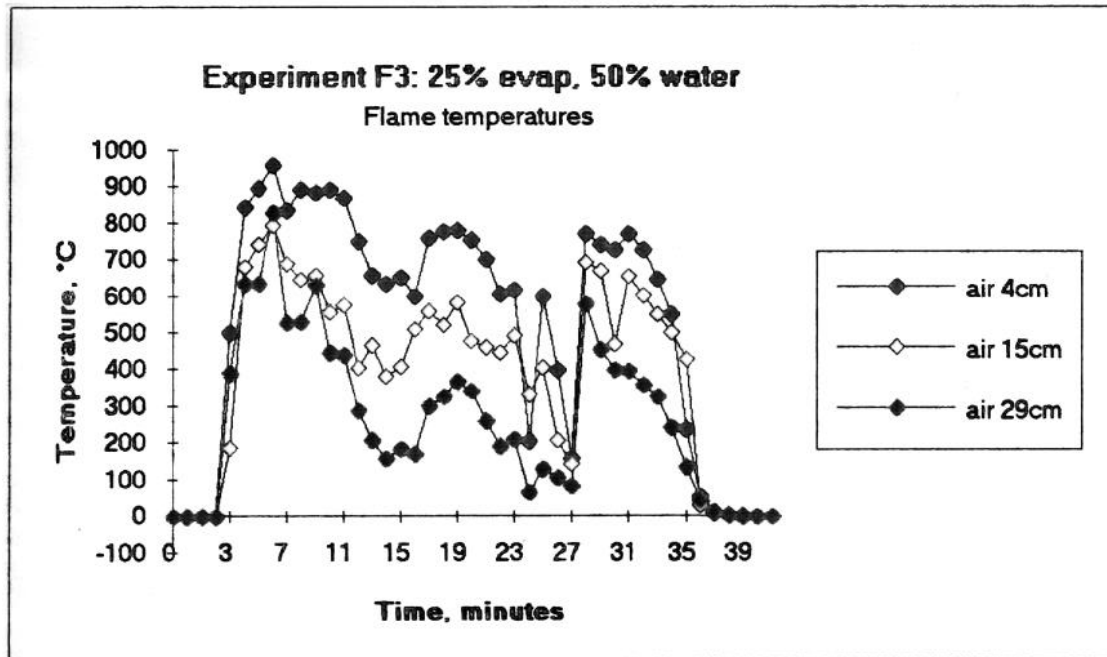


Figure 5.16: Temperature profiles for Experiment F3

experiment F3 was due to the raising of the slick thermocouples, which had become submerged too far below the slick surface once the emulsion collected at the barrier and formed a thicker slick. The variations in the slick temperatures recorded during experiment F2 are mainly due to the presence of waves.

6 EFFECT OF FERROCENE ON *IN-SITU* BURNING OF OILS AND EMULSIONS

6.1 Methods

6.1.1 Preliminary assessment of the use of ferrocene for *in-situ* burning

Some preliminary experiments were performed in Trondheim in February 1993. Visual observations from these experiments showed the use of ferrocene to be very promising as a soot reducing agent. Water was placed in the bottom of cut off drums, then covered with a layer of oil. Experiments using fresh Statfjord crude are shown in Figure 6.1. The drums on the left hand side of these photographs contained oil with approximately 4% ferrocene. The effects of ferrocene on soot reduction were visually impressive. Almost no soot was emitted from oil containing ferrocene.

6.1.2 Quantitative laboratory tests of the smoke reducing effects of ferrocene

Quantitative measurements of the effect of ferrocene on soot production during the burning of crude oil and emulsions were made during the laboratory experiments in Ottawa. A total of 23 laboratory experiments were conducted with ferrocene. Two types of studies were performed: i) the first type consisted of taking soot samples from the fume hood over a period of 5 minutes during the steady state phase of the burn. This type of experiment was done with fresh Avalon crude and with fresh and emulsified Statfjord crude oil. Ferrocene concentrations varying from 0 to 4% wt were used; ii) the second type compared soot production during the initial, steady and intense phases of the burn for fresh Statfjord crude oil containing 0% and 3% wt ferrocene. In all experiments ferrocene was premixed in the test oil or emulsion. The test matrix for each type of experiments is given below:

TYPE I: Soot sampling during steady burn phase

Statfjord crude oil: fresh and emulsified (20% evaporated/25% water)

Ferrocene concentration (% by weight): 0.00, 0.13, 0.25, 0.50, 1.00, 2.00, and 4.00

Avalon crude oil: fresh

Ferrocene concentration (% by weight): 0.00, 0.25, 0.50, 1.20, and 2.35

TYPE II: Soot sampling during initial, steady and intense burn phases

Statfjord crude oil: fresh

Ferrocene concentration (% by weight): 0.00 and 3.00

Sampling periods: initial - between 1.5 and 4 minutes

steady - between 7 and 12 minutes

intense - between 12.5 and end of burn

The laboratory experiments were conducted as described in section 3.1.2. An oil or emulsion volume of approximately three liters was used in each of the experiments with ferrocene resulting in a slick thickness of 29 mm. The average burn time for these experiments was approximately 18 minutes. This provided sufficient time during the steady burn phase to collect representative soot samples.

Soot samples were collected by drawing exhaust from the center of the duct approximately 7.7 m downstream from the fume hood, using a vacuum pump (8 l/min). Samples were drawn through a pre-weighed Watman glass-fibre filter using a 3 mm steel sampling tube and filter holder arrangement (see Figures 6.2 and 6.3). The gas sampling flow rate, temperature and pressure in the duct and sample train were recorded in order to maintain isokinetic conditions during sampling.



Figure 6.1: Preliminary burns with Statfjord crude and ferrocene

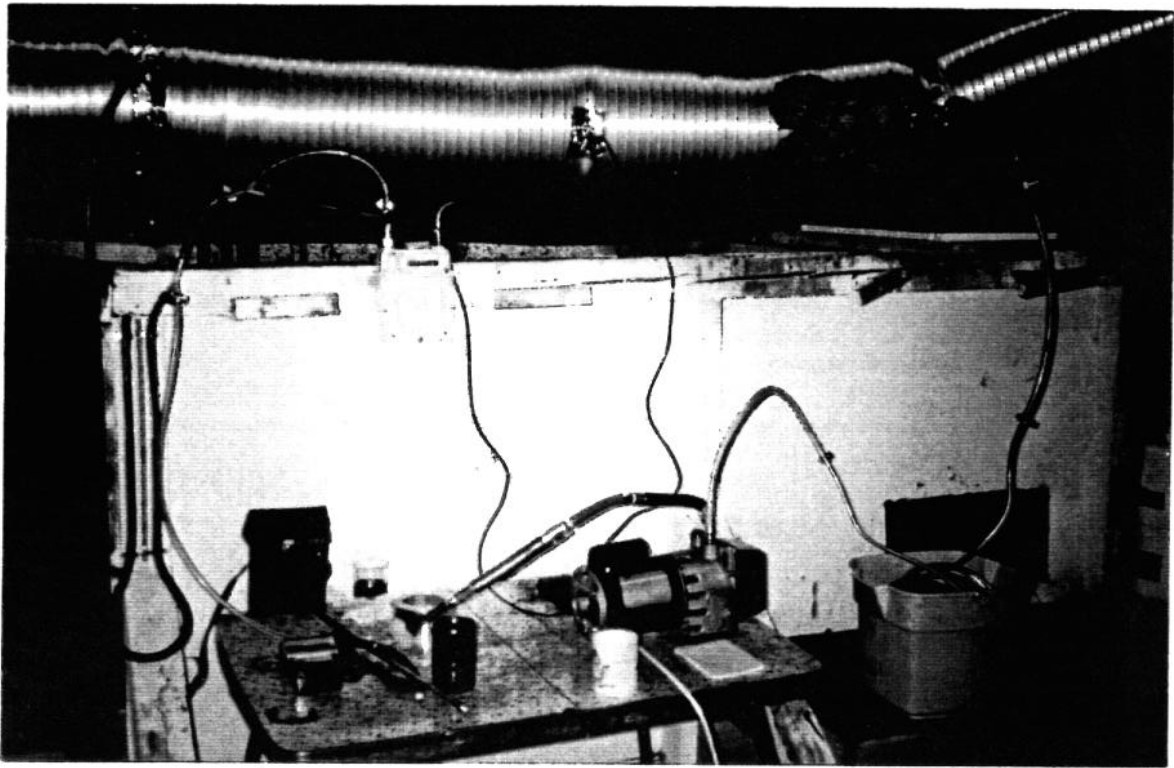


Figure 6.2: Air sampling arrangement

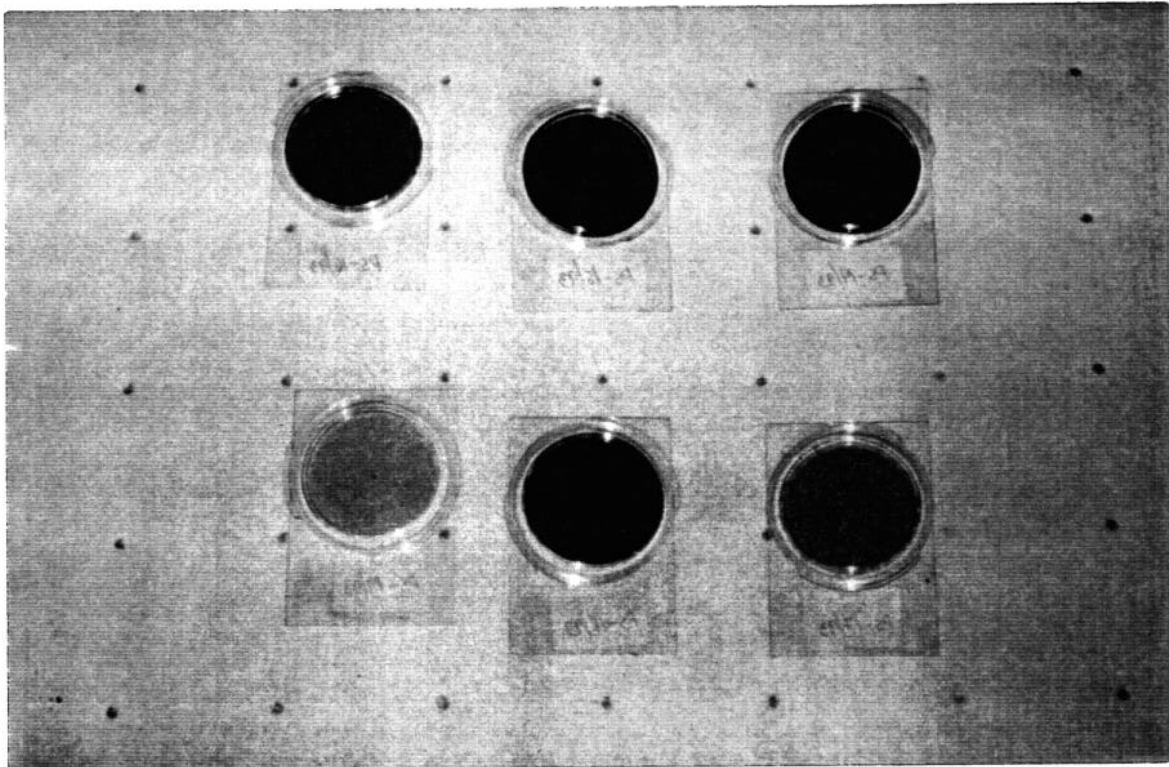


Figure 6.3: Filter samples from experiments 4.29 (top) and 4.30 (bottom)

6.1.3 Field experiments with ferrocene as a soot inhibitor

In order to confirm laboratory findings and to assess the effectiveness of ferrocene under more realistic conditions and scale, field experiments were carried out on Spitsbergen as part of the 1993 experimental field program. The experiments were designed based on the results obtained from the laboratory experiments. Experiments were carried out with Statfjord crude at various degrees of evaporation and emulsification containing varying concentrations of ferrocene. The oil volumes used in these experiments ranged from 200 to 2000 l. A total of nine field experiments were performed involving ferrocene (see Table 6.1).

Table 6.1: Summary of field experiments with ferrocene

EXP NO.	% EVAP	% WATER	VOL. (l)	FERROCENE
F4	18	0	100	≈ 2%
	25	50	200	0%
S1	18	12	200	6g/100ml ignitor
S2	25	25	200	6g/100ml ignitor
S3	25	50	200	6g/100ml ignitor
S4	0	0	200	0.00%
S5	0	0	200	2.00%
S6	0	0	200	0.25%
L1	25	50	2000	0.00%
L2	25	50	2000	0.20%

Note: F=flume, S=small, L=large

The experiment conducted in the flume basin (Exp. F4) consisted of pumping 100 l of 18% evaporated Statfjord crude oil onto the water (see section 5.1.2. for methods and set-up for this experiment). The current generator was turned on so that the oil could be held against the barrier at a constant thickness. Approximately two kilograms of ferrocene were dissolved in gasoline, and the mixture poured over the surface of the oil. The oil was ignited using a gasoline soaked sorbent pad. Once ignition of the entire slick surface was complete, the emulsion was released into the flume.

Three experiments (Exp. S1, S2, and S3) were conducted to study the effectiveness of adding ferrocene and an emulsion breaker (Alcopol) a gelled crude oil igniter. Ferrocene was chosen as a potential additive to this igniter based on the laboratory findings for the igniter experiment described in section 4. Six grams of ferrocene was added to 100 ml of gelled crude oil contained in a small plastic bag. This igniter, along with an igniter containing Alcopol, was used to ignite emulsions with varying degrees of evaporation and emulsification. One bag contained gelled oil only, to serve as a control. The bags were placed on the emulsion and simultaneously ignited.

Three small-scale experiments (Exp. S4, S5, and S6) were performed to investigate the effect of ferrocene concentration in oil on smoke emissions. Based on the laboratory results, indicating that 2% was a near optimum concentration and that even lower concentrations were also highly effective, the concentrations chosen for this experiment were 0.20 and 2%. These experiments were performed in 4 m² circular basins, with 200 l of fresh oil, giving an oil thickness of 5 cm. Fresh oil was chosen for

these experiments because it produces larger quantities of smoke when burned, than an equal volume of emulsion, and would therefore be a better visual indicator of the effectiveness of ferrocene. The following table summarize the experiments performed and some of the observations recorded.

The last two experiments (Exp. L1 and L2) conducted with ferrocene were the meso-scale burns with 2000 l of 25% evaporated, 50 % water-in-oil emulsion of Statfjord crude. These experiments were conducted in a 4.5 x 4.5 m basin (see section 5.1.1). The emulsion thickness was 10 cm. Temperatures in the flame, the slick, and in the water below the slick were measured during both burns. Ferrocene was mixed into the emulsions by adding the ferrocene to the oil tank and recirculating the contents with a gear pump (400 l/min). The igniter used in these experiments was 100 l of fresh Statfjord crude poured over the surface of the emulsion slick.

6.2 Results

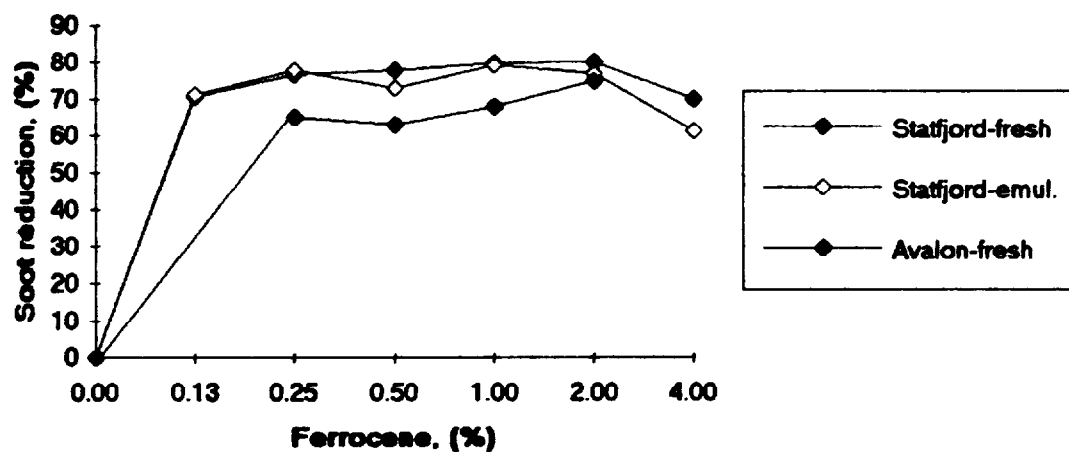
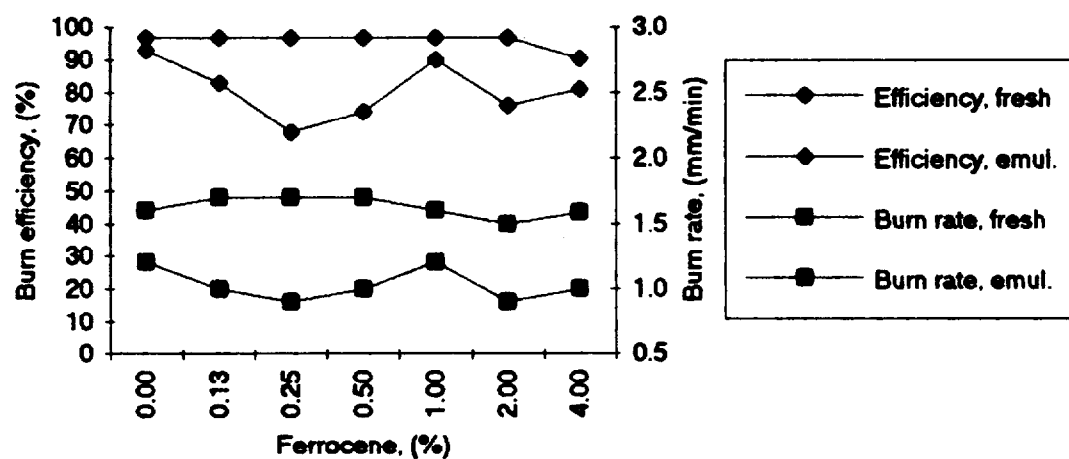
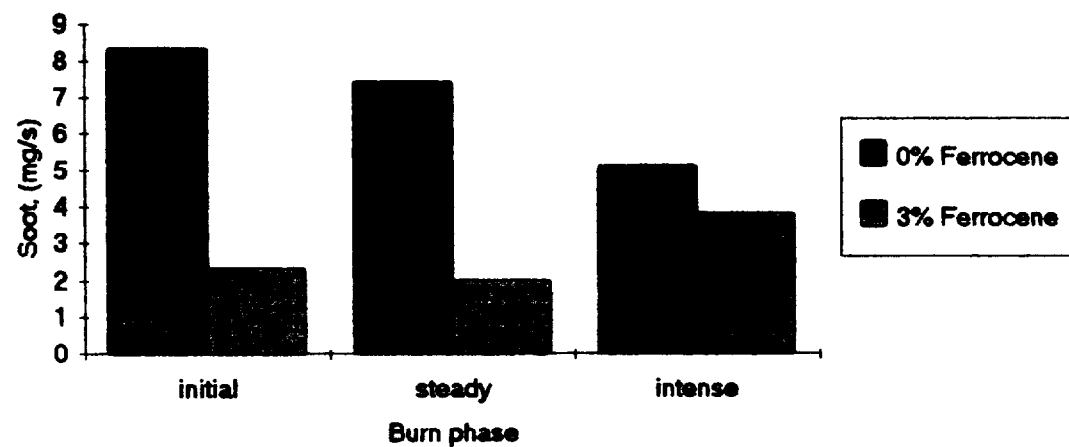
6.2.1 Quantitative assessment of the smoke reducing effects of ferrocene

The results from the laboratory experiments with ferrocene are presented in Figures 6.4 to 6.6. The data for these experiments can be found in Appendix D. The oils used in these experiments were: fresh Avalon crude, fresh Statfjord crude and weathered (20% evaporated by volume), emulsified (25% water-in-oil) Statfjord crude. Their physical properties are given in section 2.

Figure 6.4 depicts the soot reducing effects of ferrocene for each oil as the percentage soot reduction over a sampling period of 5 minutes. Reduction in soot emission varied between 60 and 80%. Ferrocene proved to effectively reduce soot emissions from both fresh and weathered/emulsified oils. Ferrocene was slightly less effective with Avalon crude than with Statfjord crude. It may be that ferrocene is slightly less soluble in Avalon crude than in Statfjord crude, or that it reacts differently to the oils because of the large range of compounds present in oils. It is clear from this figure that a large amount of ferrocene is not required to effectively reduce soot emissions, and that in fact, the highest concentration of ferrocene used, 4% by weight, did not result in the highest reduction of soot. This is consistent with results obtained during previous experiments (Mitchell et al. 1991) where Prudhoe Bay crude oil containing varying concentrations of ferrocene based additives was burned. Measured soot volumes indicated that a concentration of 2% ferrocene were more effective than a concentration of 4%. It is evident that the solubility of ferrocene in a given hydrocarbon (generally about 2% by weight for most hydrocarbon fuels (Mitchell 1990)) will limit the maximum concentration of ferrocene which can be applied. In these experiments, a concentration of 2% ferrocene proved to have the highest soot reducing effect. However, even at concentrations as low as 0.13% ferrocene, soot reduction was as high as 71% for Statfjord crude.

The effect of ferrocene on some of the recorded burn parameters is shown in Figure 6.5. Ferrocene had almost no effect on the burn efficiency and the burn rate of fresh Statfjord crude. A slight decrease in the burn efficiency was observed with 4% ferrocene by weight addition to fresh Statfjord. While the burn efficiency and rate of emulsified Statfjord varied with different ferrocene concentrations, no particular trends were observed.

Two experiments were conducted to study the effect of ferrocene during different phases of the burn. Fresh Statfjord crude oil was used in these experiments with ferrocene concentrations of 0 and 3%. Soot samples were collected during 150 seconds of the initial phase, 300 seconds of the steady phase and during the last 170 seconds (0% ferrocene) and 37 seconds (3% ferrocene) of the intense burn phase. The results are shown in Figure 6.6 which plots the mass of soot collected per second during each burn phase. Soot reductions of 73% during the initial and steady burn phases were observed, however, a reduction of only 25% was recorded during the intense phase. These experiments suggest that the effectiveness of ferrocene decreases towards the end of the burn. The intense burn phase is

Figure 6.4: Soot reducing effect of ferrocene**Figure 6.5: Effect of ferrocene on Statfjord crude burns****Figure 6.6: Effect of ferrocene on different burn phases**

characterised by vigorous burning of the slick and water and oil droplets being ejected into the flames and possibly carried away with the smoke. This might explain the increase in soot collected during the intense phase of these burns (both with and without ferrocene). Further experiments are required to confirm this.

As part of the igniter improvement experiments, ferrocene (4% wt) was added to gelled gasoline and gelled crude oil. It was found that ferrocene had no observable effects of the efficacy of gelled gasoline, but that it did improve the ignitability of gelled crude oil.

6.2.2 Qualitative assessment of the smoke reducing effects of ferrocene

Three types of experiments were conducted with ferrocene in the field: meso-scale in a flume, small scale and meso-scale. During all experiments, the soot emissions from the burning crude was visibly reduced when ferrocene was added to the crude. Ferrocene was also evaluated as a potential igniter additive in the igniter experiments.

In the flume experiment, ferrocene was added to a slick of 18% weathered Statfjord crude by adding a solution of gasoline and ferrocene to the slick surface. This slick was contained by the barrier in the flume. During the first four minutes of the burn, very little smoke was emitted from the burning slick. Four and a half minutes after ignition, a 50% water-in-oil emulsion of 25% evaporated Statfjord crude was pumped into the flume and allowed to drift towards the burning slick in the barrier. This 50% water-in-oil emulsion ignited without any difficulty. The smoke emissions darkened slightly as the approaching emulsion slick was ignited and burned. It was until 20 minutes after ignition that the smoke darkened considerably to a dark grey. It is probable that most of the ferrocene had been consumed at this point.

The purpose of the small scale experiments, conducted in 4 m² circular basin was to visually evaluate of the soot reducing effect of ferrocene on burning crude oil. Some burn parameters were also recorded during these experiments. The following table give some results from the small scale experiments conducted with fresh Statfjord crude in the field.

Table 6.2: Results from small scale field experiments with ferrocene.

Exp No.	Ferrocene (%)	Ignition (s)	Intense (s)	Extinction (s)
S4	0.00	18	735	871
S6	0.25	48	580	750
S5	2.00	45	650	810

The time for the entire oil surface to ignite was longer when the oil contained ferrocene (both at 0.25 and 2.00% by weight concentration levels). This was not observed in the laboratory, however, wind and other environmental factors may have affected the ignition of the oils outdoors. The wind velocity varied between 8 and 10 m/s during the time of these burns. The burns with ferrocene reached the intense burn phase and extinction earlier than the burn without ferrocene. Because of these high winds, there was considerable flames deflection over the down wind edge causing the wall of the basin at that side melt. This combined with the wind herding effect, cause the slick the spread somewhat out of the basin. Because the burn area did not remain constant throughout the burn, it is difficult to accurately compare the times at which the intense phase and extinction occurred during these experiments. More radiant heat was observed during the burns with ferrocene. The smoke plume was less dense during the 2% ferrocene burn than during the 0.25% ferrocene burn, however, the soot reducing effects of the

ferrocene addition were immediately apparent during both burns (see Figure 6.7). Soot emissions increased during the intense phase of the ferrocene burns (as observed in the laboratory), but a visual comparison of smoke plumes during these three experiments indicate that the soot reducing effect of ferrocene is still considerable even at a concentration as low as 0.25% by weight.

The meso-scale experiments conducted with ferrocene added to 2000 l of a 50% water-in-oil emulsions of Statfjord crude are shown in Figures 6.8 and 6.9. Visually, ferrocene appears to have a considerable effect on smoke emissions. The smoke plume in the experiment with ferrocene was light grey and not entirely opaque while the smoke plume in the burn without ferrocene was black and opaque. Very little smoke was emitted at the base of the flame with ferrocene, while the plume darkens at the tip of the longer flames. As in the small-scale burns, more radiant heat was emitted during the burn with ferrocene.

The burn without ferrocene lasted almost 50 minutes, while the burn with ferrocene lasted just under 34 minutes. The burn rate was therefore higher with ferrocene (3 mm/min) than without (2 mm/min); however, as it was difficult to estimate the amount of residue remaining after each burn the efficiency could not be accurately determined.

The foaming phenomena typical of higher water content emulsion burns was more pronounced during the burn with ferrocene. Foaming usually occurs towards the end of the steady burn phase. Typically, part of the slick momentarily extinguishes, foaming is observed as water is boiled out of the emulsion, then flames spread over the area again reigniting the oil. Extinction follows shortly after this foaming effect is observed. Foaming began 24 minutes into the ferrocene burn, while it was observed only after 39 minutes in the burn without ferrocene. This may explain why the ferrocene burn did not last as long as the burn without ferrocene.

Ignition experiments have been described in detail in section 5. Fire spreading rates and relative ease of ignition were observed. Briefly, these experiments demonstrated that the gelled oil igniter with ferrocene resulted in a quicker spreading of the fire than gelled oil alone; however, the emulsion breaker proved to be more effective. It may be interesting to look at the possibility of using ferrocene in an igniter for a soot reducing effect, or to promote combustion once ignition has taken place. This could be an area to investigate more thoroughly.



Figure 6.7: Small-scale burns with ferrocene (top: 0% ferrocene; middle: 0.25% ferrocene; bottom: 2% ferrocene)



Figure 6.8: Experiment L1: 25% evaporated, 50% water-in-oil emulsion, 0% ferrocene



Figure 6.9: Experiment L2: 25% evaporated, 50% water-in-oil emulsion, 0.20% ferrocene

7 BURN RESIDUE

Studies on the fate and behaviour of burn residue have been carried out both on Statfjord crude oil and Alaska North Slope crude. The studies have focused on:

- Fate and behaviour of residue in a current
- Physical properties of the residue
- Toxicity of burn residue

7.1 Methods

7.1.1 Fate and behaviour of residue in a current

In addition to the field experiments conducted, during which the fate and behaviour of burn residue was observed, some small-scale flume experiments were performed in the laboratory. These experiments studied the fate and behaviour of burn residue collected during selected laboratory burn experiments. The residue was selected based on the results of statistical analysis of the burn residue properties. Residues which exhibited unusually high densities or showed a different trend from the rest of the residue data were selected for this study. The table below list the experiments from which residue was chosen along with the initial oil properties and the residue density.

Table 7.1: Burn residue selected for laboratory flume experiments

Exp. No.	Initial oil type (Statfjord crude)	Initial oil density (g/ml)	Residue density (g/ml)
4.01	0% evap/0% water	0.844 at 13°C	0.939 at 12°C
4.24	13% evap/0% water	0.857 at 13°C	0.916 at 24°C
4.33	20% evap/0% water	0.866 at 13°C	0.943 at 22°C
4.56	20% evap/25%water 4% ferrocene	0.908 at 13°C	0.947 at 23°C
4.61	20%evap/25%water 0.5% ferrocene	0.908 at 13°C	0.933 at 22°C
4.71	30% evap/60% water	0.952 at 13°C	0.932 at 22°C

The experiments were conducted in the flume basin shown schematically in Figure 7.1 and 7.2. This basin has been specially designed to create hydrodynamically correct flow in the test portion of the tank. The width of the open channel area used for testing was 30 cm, and was fitted with an adjustable barrier to simulate different draft depths of a boom in water. The tests were conducted with the barrier placed 2, 4 and 6 cm below the water line. The side walls of the test channel were constructed from plexiglass to enable underwater observations to be made throughout the experiments. The barrier was also constructed from plexiglass which permitted the residue behaviour to be observed against the barrier. A small motor mounted in the closed channel parallel to the open channel was used to generate currents ranging from 0.2 to 0.5 m/s.

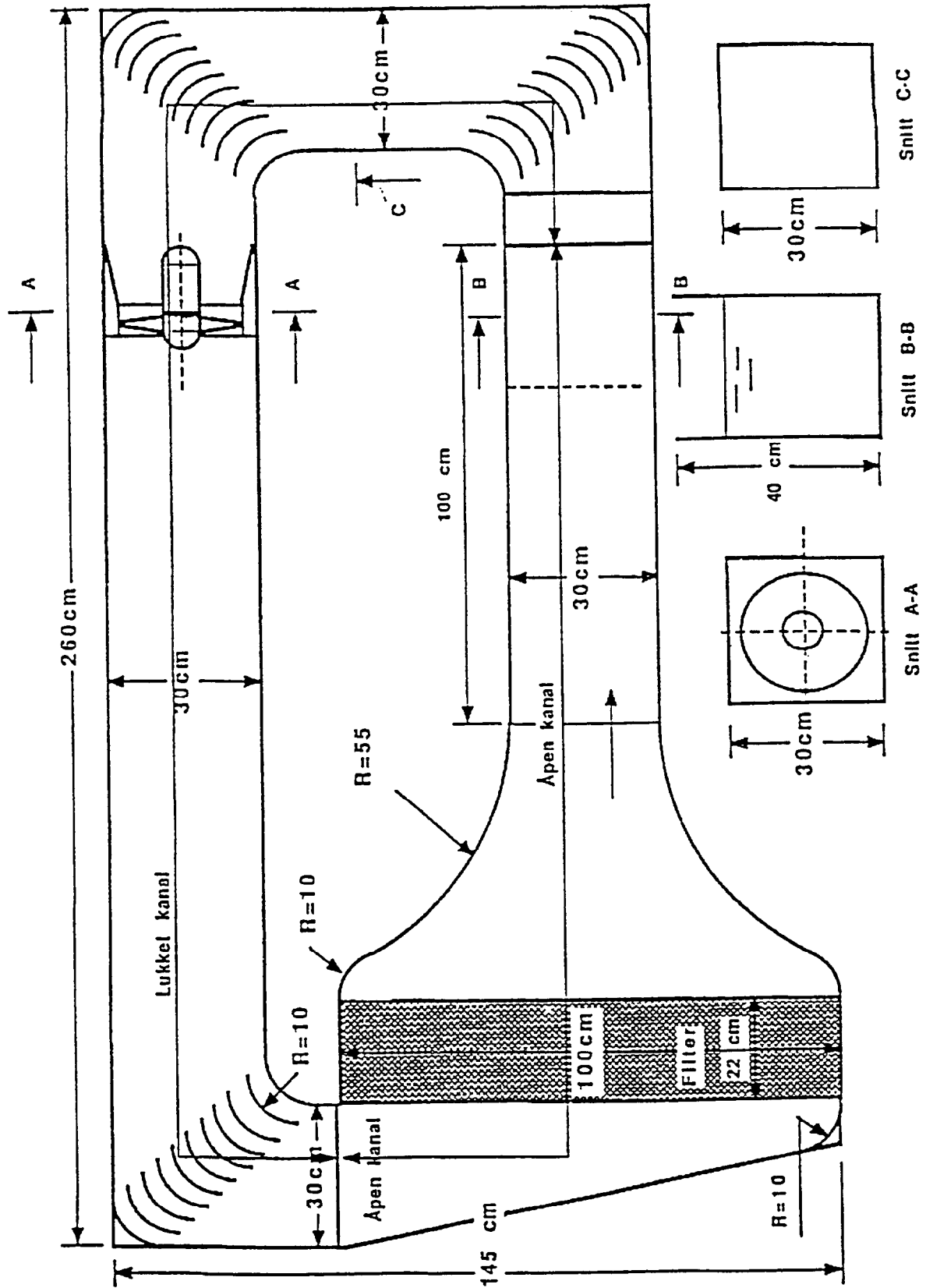


Figure 7.1 Circulating flume for the study of behaviour of residue in a current against a barrier



← view from
downstream end

view from
↓ upstream end

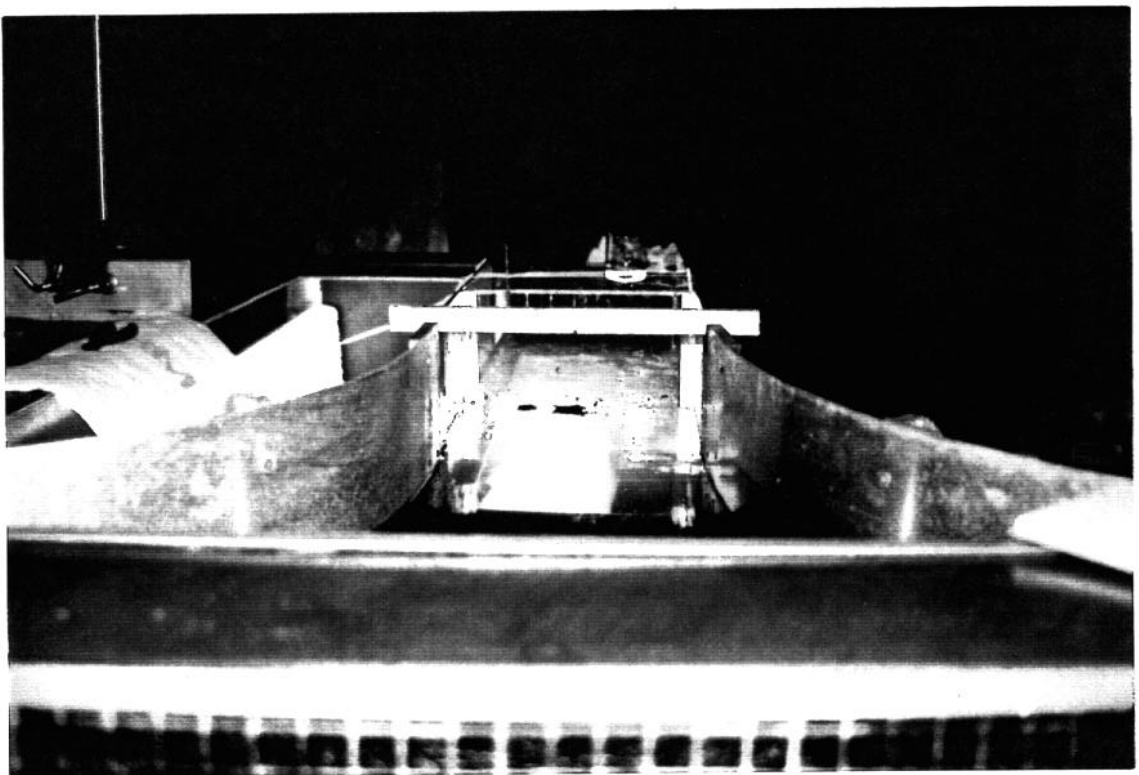


Figure 7.2: Circulating flume with residue

Two samples of the residue collected from each laboratory burn experiment, weighing approximately 5 and 20 g were used in the flume experiments. They were placed together in the flume approximately 30 cm ahead of the barrier and allowed to drift towards the barrier in the current.

The following test matrix was used:

Three barrier depths: 2 cm, 4 cm, 6 cm

Four current speeds: 0.20 m/s, 0.25 m/s, 0.33 m/s, 0.50 m/s

Observation were made with particular attention to buoyancy. The current velocity and barrier depth at which a residue sample was lost beneath the barrier was noted.

Following these experiments, the residue samples were exposed to silt suspended saltwater at a concentration of 25 ppt. The samples were placed in a specially designed box with a separate cell for each residue type. Compressed air was blown through a perforated copper pipe placed at the bottom to the box. This maintained an even distribution of the silt in the seawater and ensured an even exposure of silt to the residue samples. The samples were observed periodically for sinking or any change in buoyancy.

Following the exposure to silt, some of the residue samples were selected for further test in the flume tank, following the same procedures used with the unexposed residue.

7.1.2 Physical-chemical properties of burn residue

The burn residue collected during the small-scale laboratory experiments were analysed for viscosity and density. (Refer to section 2.4 for the analytical methods used to measure these properties). The physical-chemical properties along with the burn parameters were treated statistically as described in section 2.5.

7.1.3 Toxicity of burn residue

Selected burn residue samples from the field experiments were used to determine the toxicity of burn residue produced from the burning of various oils and emulsions. The *Skeletonema* test is used on a routine basis for toxicity evaluation of drilling muds and chemical compounds used in the off-shore industry and is one of three tests prescribed by the Norwegian Pollution Control Authorities and the Paris Commission.

The purpose of this study was to evaluate *in-situ* burn residues for their ability to reduce growth of the marine algae *Skeletonema costatum* during a test period of 72 hours. The test is a standard toxicity test on the marine algae, *Skeletonema costatum*, according to the International Standard ISO/DIS; "Water Quality - Marine algal growth inhibition test with *Skeletonema costatum* and *Phaeodactylum tricornutum*", 1991.

If possible, test results are calculated as the effective concentration of test substance (mg/l) inhibiting algal growth by 50 % (EC₅₀). Calculations are made for growth rates of the algae.

Culture conditions

Incubation	:	20±1°C in continuous light (60-120 µE/m ² /sec).
Stock- and preculture	:	No agitation
Test culture	:	Moderate agitation
Stock culture	:	Weekly re-inoculations to sterile seawater-based growth medium.
Pre-culture	:	3-days culture.
Test cultures	:	Algae inoculated to each flask with preincubated test substance. Algal

- concentrations inoculated: 3×10^3 /ml initial conc., corresponding to measured corrected *in vivo* fluorescence of 6 to 8.
- Control cultures : Algal concentrations inoculated to culture medium without test substance: 3×10^3 /ml initial conc., corresponding to measured *in vivo* corrected fluorescence of 6 to 8.

Test procedure and conditions

- Preincubation : 20 - 24 hrs; Exposure: 72 ± 4 hrs
- Test parameter : *In vivo* fluorescence (Turner fluorometer, model 111) measured daily 0, 24, 48 and 72 h after algal inoculation.
- Test flasks : 250 ml Erlen-Meyer flasks with inverted glass beakers as stoppers.
- Culture medium : Standard seawater-based medium, modified slightly from the medium recommended in the draft ISO Guideline. The natural seawater had a salinity of 34.3 ‰.
- Test substance : Test substance diluted in duplicate at test concentrations in culture medium and preincubated in the dark at $20 \pm 1^\circ\text{C}$ for 20 ± 4 hours with shaking and allowed to stand 1 hour for sedimentation. For substances with moderate to low water-solubility, as in this case, each test concentration was weighed directly into the test vessels in duplicate and each aliquote diluted in 100 ml culture medium. All test flasks were shaken as described above.
- Test concentrations : Given as mg test substance/l culture (test) medium. Test concentrations were chosen in logarithmic series, e.g. 100, 1000, 10 000 and 100 000 mg/l

Preparation of test solutions

The test solutions were prepared by directly adding the test substance to a natural seawater-based culture medium:

The test substances were low water-soluble, with insoluble residues or oil appearing in the culture medium after preincubation (shaking). The content of each test flask was separated in funnels. The supernates/water phases were carefully removed, either by decanting or by pipetting and used for testing.

Measurements and recording

- Fluorescence : *In vivo* fluorescence was measured in each test and control flask after 0, 1, 2 and 3 days after algal incubation, the last measurement 72 ± 4 h after algal inoculation. Measurements were performed in a filter-based fluorometer (Turner, model 111) with an emission wavelength optimal for measurement of chlorophyll A fluorescence. The fluorescence was corrected for blank values and adjusted slit opening factors.
- pH : pH was measured and adjusted before inoculation of algae to provide a pH within the optimum for algal growth (pH 7.5-9.2) for all test concentrations. After the end of the test pH was measured to control potential pH-effects on algal inhibition.

Data treatment

In vivo fluorescence measurements were corrected for blank values and slit opening factors of the fluorometer. Growth rates in each test- and control flask were calculated from the fluorescence data plotting \ln -values of *in-vivo* fluorescence as function of time. Calculations from corrected fluorescence data were performed with the data program MAITEST, designed at SINTEF Applied Chemistry. Calculated growth rates were then treated by the program TOXEDO, developed by the Water Quality

Institute in Copenhagen, to estimate EC-values with 95 % confidence intervals.

Test results

The test results are given as the concentration of test substance causing a median effective inhibition of algal growth rates by 50 % (EC_{50}).

7.2 Results

7.2.1 Fate and behaviour of residue in a current

Observations were made during the field burn experiments conducted in the flume on the fate and behaviour of burn residue. While most of the residue could be contained by the barrier, some was lost, especially in the presence of waves. While some loss of residue beneath the barrier occurred continuously throughout each burn, the majority of the loss occurred toward the end of a burn. In general, the residue remained floating just below the surface of the water. The residue pieces were submerged, with some portion of the residue floating above the waterline. Most of the residue appeared to be quite buoyant, although some was observed circulating around the basin at least 30 cm below the water surface. It was estimated that roughly 25% of the residue sank below the water surface but remained somewhat buoyant and was transported around the flume by the current. During the steady state burn phase, most of this residue which was recirculated around the tank and drifted towards the burning slick could be reignited.

The fate and behaviour of burn residue from several laboratory experiments was studied in an indoor circulating flume. These experiments studied the fate and behaviour of burn residue collected during selected laboratory experiments. The residue samples were selected based on the results from statistical analysis of the burn residue properties. Residue samples which exhibited unusually high densities or showed a different trend from the rest of the residue data were selected for this study.

The following table gives the initial oil properties and density for each residue samples studied. The depth of the barrier and the current velocity are given at which first loss of the residue beneath the barrier occurred (i.e. the lowest current velocity and most shallow least barrier location). Two sample sizes were tested, denoted as "a" and "b". The "a" sample weighed approximately 5 g while the "b" sample weighed approximately 20 g.

Figure 7.3 to 7.6 show the residue samples in the flume basin during selected experiments. In Figure 7.4 the larger piece of residue can be seen on the down stream side of the barrier while the smaller piece remained contained. In most cases, residue which escaped the barrier remained adhered to the barrier and did not flow downstream. The residue particles were very sticky and readily adhered to nearby surfaces.

Experiments with residue exposed to suspended silt for a period of at least 24 hours showed no indications that the density of the residue would increase to the point of causing further sinking.

The residue in these experiments did not seem to have a high tendency to sink, which is consistent with the statistical analysis performed. However, it has long been a subject of discussion whether or not oil will sink due to overwashing and oceanographic conditions. The present study does not falsify nor verify this since the available samples were rather small. It is assumed that this tendency will increase with larger mats of residue to the drag effects on larger volumes of residue. This trend was observed in the flume experiments as the larger residue samples (~ 20 g) were lost beneath the barrier sooner than the smaller samples (~ 5 g). However, when influenced by currents, these experiments indicates that it could be feasible for the residue to escape under a barrier such as a boom or an ice edge if currents are sufficiently strong.

Table 7.2: Barrier depth and current velocity at which burn residue samples were lost beneath the barrier

Exp. No.	Initial oil type (Statfjord crude)	Residue density (g/cm ³)	Barrier depth (cm)	Current velocity (m/s)
4.01a	0% evap/0% water	0.939 at 12°C	2	0.50
4.01b			2	0.33
4.24a	13% evap/0% water	0.916 at 24°C	2	0.50
4.24b			2	0.50
4.33a	20% evap/0% water	0.943 at 22°C	2	0.50
4.33b			2	0.33
4.56a	20% evap/25% water (4.0% ferrocene)	0.947 at 23°C	2	0.33
4.56b			2	0.33
4.61a	20% evap/25% water (0.5% ferrocene)	0.933 at 22°C	2	0.50
4.61b			2	0.33
4.71a	30% evap/60% water	0.932 at 22°C	never	never
4.71b			2	0.33

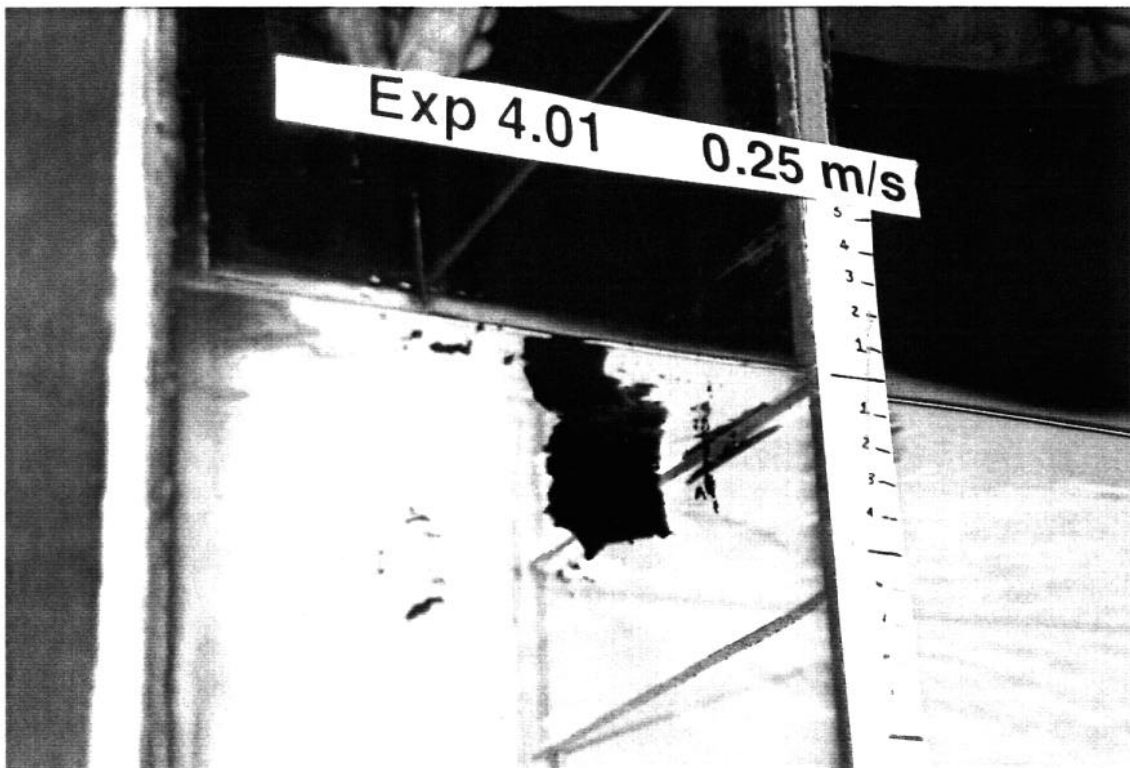


Figure 7.3: Exp. 4.01 - burn residue in flume at 0.25 m/s

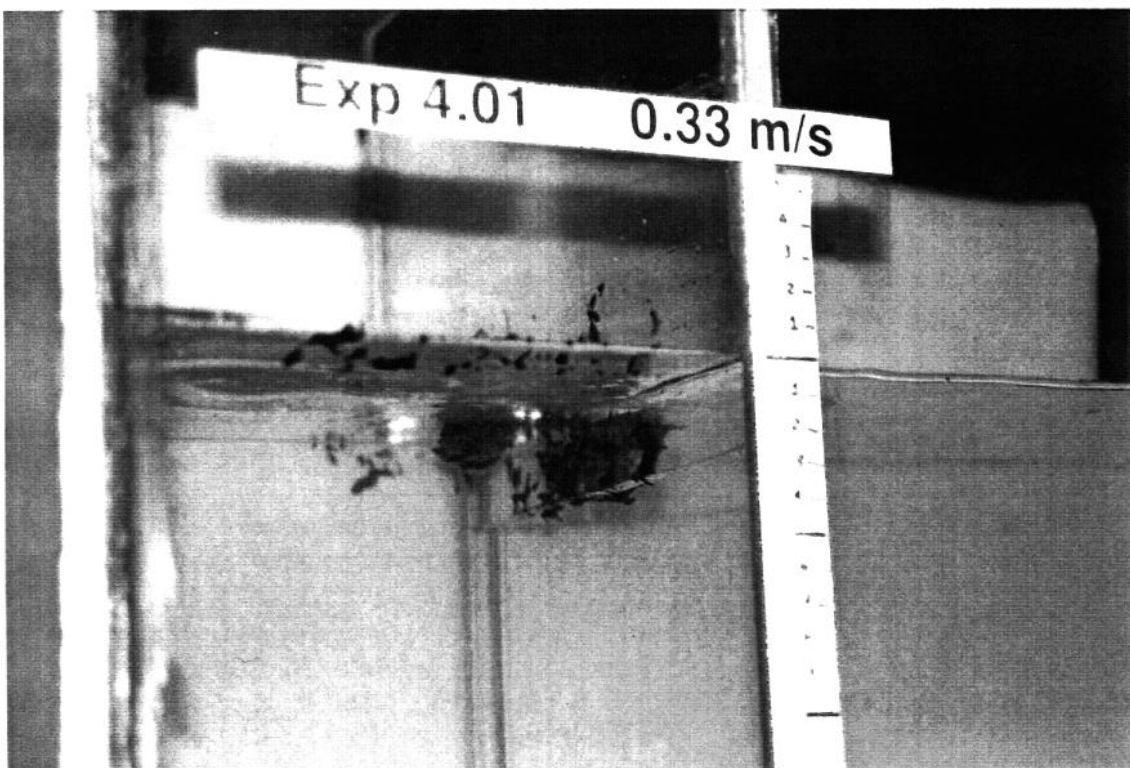


Figure 7.4: Exp 4.01 - burn residue in flume at 0.33 m/s

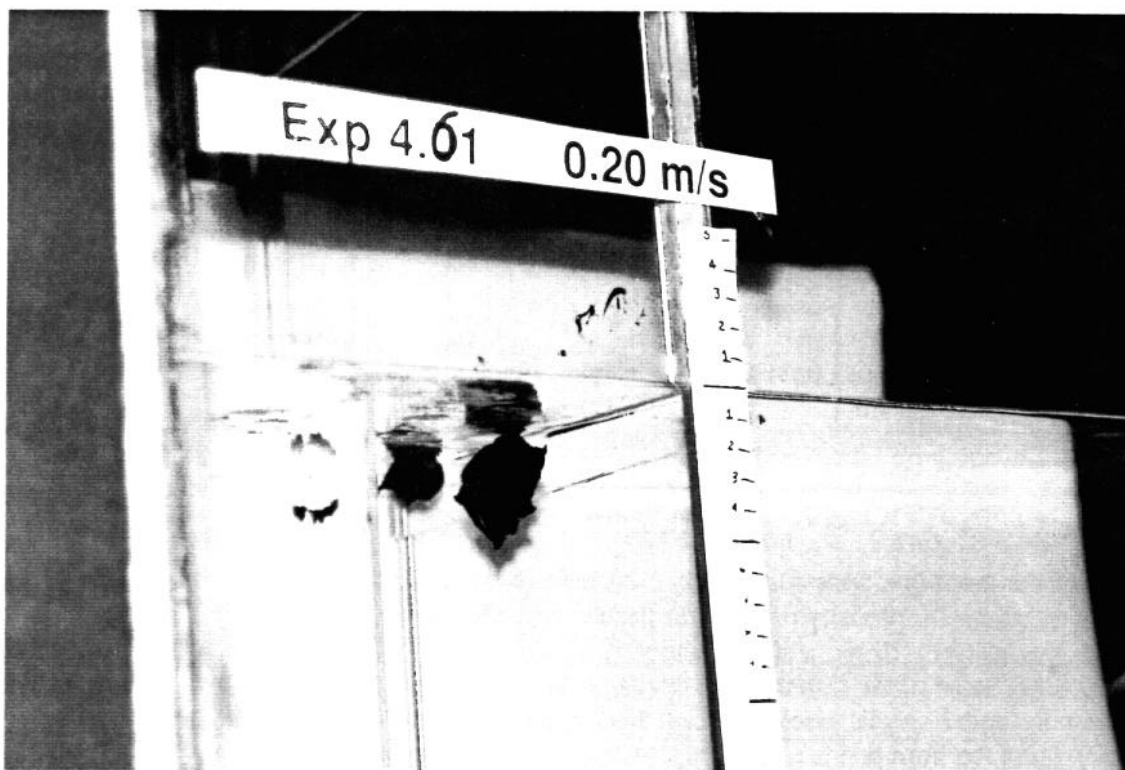


Figure 7.5: Exp. 4.61 - burn residue in flume at 0.2 m/s

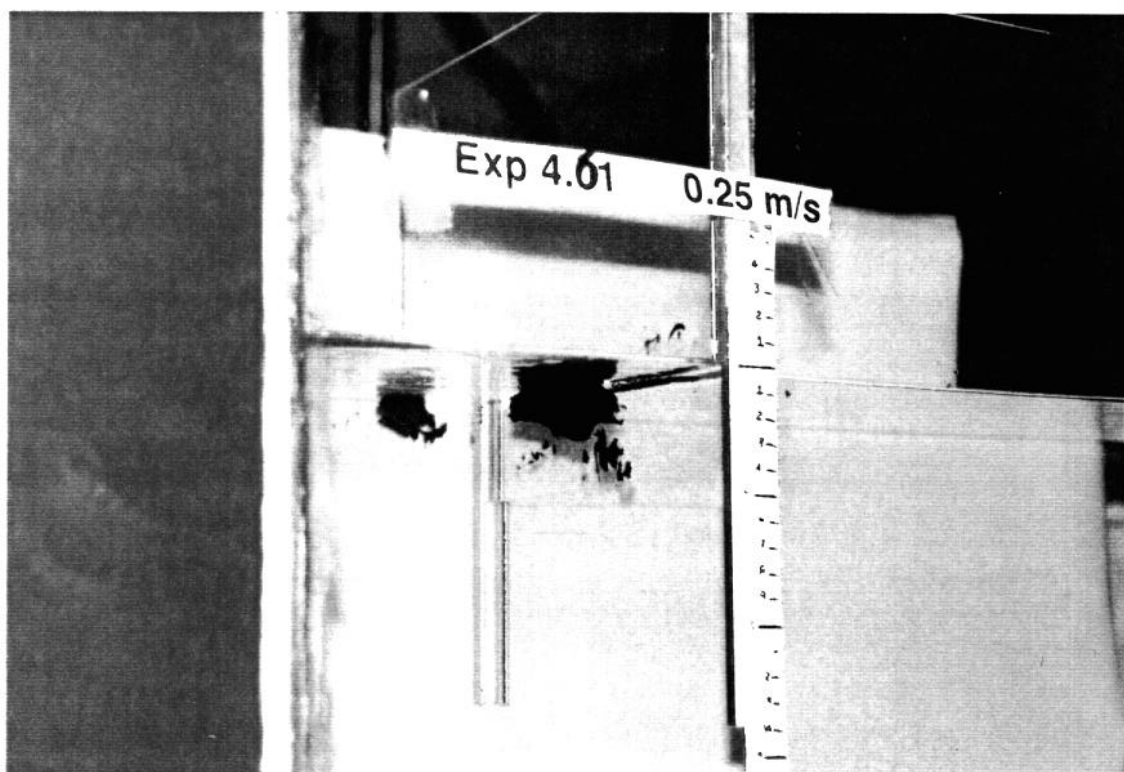


Figure 7.6: Exp.4.61 - burn residue in flume at 0.25 m/s

7.2.2 Physical-chemical properties of burn residue

The data from the physical-chemical analysis of the burn residue and from the burn parameters collected during the small-scale laboratory experiments data have been used for statistical analysis. The question asked was:

How does burn efficiency affect the density and the viscosity of burn residue?

According to the statistical analysis of these data the density of burn residue can be described by the linear correlation:

Density = $0.908 + 0.0003 \times [\% \text{burn efficiency}]$ for Statfjord crude oil

and

Density = $0.942 + 0.0003 \times [\% \text{burn efficiency}]$ for Alaska North slope crude oil

One of the main questions concerning burn residue is whether the residue will sink or not. Based on these equations, the density of the burn residue will not exceed the density of seawater unless the burn efficiency exceeds 100%, which is impossible. This is a statistical evaluation based on approximately 100 burns. Some of the residues will deviate from this linear relationship however, this seems to be the case only under special circumstances. This is an evaluation based strictly on the physical-chemical analysis of the burn residue. The density may however increase further due to other factors, such as adherence of particles.

It was not possible to fit a statistical linear correlation between the viscosity of the burn residue, and the burn efficiency, unless some of the data points were removed (i.e. those from burns with ferrocene).

The physical-chemical properties was determined for some of the burn residue collect during the field experiments. Table 7.3 gives the density of the initial oils and of the residues for selected field experiments. It can be seen from these results that the density of burn residue for oils and emulsions did not exceed that of water. The range of residue densities for these experiments was approximately 0.90 to 0.97 g/cm³. The density and viscosity for some of these samples could not be determined because the residue was extremely thick or hard; however, these samples were buoyant at the time they were collected.

Table 7.3 Density of and viscosity of residue samples from selected field experiments with Statfjord crude oil

Exp. No. (Sample No.)	Density		Viscosity at 13 °C
	initial oil (g/cm ³ at 19°C)	residue (g/cm ³) at (°C)	cP (shear rate)
F1 (R1): 18% evap. and 18% evap./12 % emul.	0,868 0,886	0,919 at 23,7	7,90 x 10 ³ (20 s ⁻¹)
F1 (R2): 18% evap. and 18% evap./12 % emul.	0,868 0,886	hard lump	n.m.
F2 :18% evap. and 25% evap./25 % emul.	0,868 0,935	0,964 at 26,1	5,88 x 10 ³ (4 s ⁻¹)
F3 (R2): 18% evap. and 25% evap./50 % emul.	0,868 0,952	9,957 at 26,5	1,20 x 10 ³ (20 s ⁻¹)
F3 (R3): 18% evap. and 25% evap./50 % emul.	0,868 0,952	0,953 at 26,1	8,58 x 10 ⁰ (40 s ⁻¹)
S1: 18% evap./12 % emul.	0,886		375 x 10 ³ (0,2 s ⁻¹)
S2 (R1): 25% evap./25 % emul.	0,935	0,953 at 24,6	195 x 10 ³ (20 s ⁻¹)
S2 (R2): 25% evap./25 % emul.	0,935	0,945 at 23,6	746 x 10 ³ (0,2 s ⁻¹)
S3: 25% evap./50 % emul.	0,952	0,936 at 23,5	32 x 10 ³ (4 s ⁻¹)
S4 0% Ferrocene 0% evap./0% emul.	0,844	0,938 at 25,2	99,8 x 10 ³ (2 s ⁻¹)
S5 2% Ferrocene 0% evap./0% emul.	0,844	0,918 at 24	8,04 x 10 ³ (20 s ⁻¹)
S6 0.25% Ferrocene 0% evap./0% emul.	0,844	0,929 at 26,1	7,8 x 10 ³ (40 s ⁻¹)
S14 (R1): 25% evap./50 % emul.	0,952	extremely thick	500 x 10 ³ (0,2 s ⁻¹)
S14 (R2): 25% evap./50 % emul.	0,952	0,966 at 21,4	1,52 x 10 ⁶ (0,2 s ⁻¹)
S15 (R2): 25% evap./60 % emul.	0,971	0,899 at 23,5	1,2 x 10 ³ (40 s ⁻¹)
L2: 25% evap./50 % emul.	0,952	0,963 at 24,9	n.m.

R# = residue sample number

evap. = evaporated

emul. = emulsified

7.2.3 Toxicity of burn residue

This toxicity study evaluated *in-situ* burn residues for their ability to reduce growth of the marine algae *Skeletonema costatum* during a test period of 72 hours using a standard toxicity test. If possible, test results were calculated as the effective concentration of test substance (mg/l) inhibiting algal growth by 50 % (EC₅₀). Calculations were made for growth rates of the algae.

Control cultures

Calculated mean values of growth rate for control cultures (ref. table 2): 2.041 d⁻¹ (range 2.036 - 2.049)

Growth rate data, percentage inhibition and EC-values

Table 7.4 shows the estimated EC₅₀ values of algal growth inhibition calculated for the *in-situ* burn residues investigated. The percentage inhibition of nominal concentrations of 100 000 mg/l of each residue is also included in the table.

Table 7.4: Median effective concentrations (EC_{50}) for different *in-situ* burn residues on algae (*Skeletonema costatum*) growth rate inhibition.

<i>In-situ</i> burn experiment	EC_{50} (mg/l)	Growth rate inhibition (%) of nominal concentration of 100 000 mg/l
S1	>> 100 000	21.2
S2	100 945	48.4
S3	5 191	100
S4	1 374	78.3
S5	528	100
F1	>> 100 000	20.0
F2	>> 100 000	20.5
F3	74 913	98.8

The growth rate calculated by linear regression from *in vivo* fluorescence data, the calculated inhibition data and the calculated values for EC_{10} , EC_{50} and EC_{90} with 95 % confidence intervals are shown in Tables 7.5 to 7.12. Graphical presentations of percentage inhibition and EC-estimates are shown in Figures 7.7 to 7.14.

Table 7.5: Inhibition of the growth rates of *Skeletonema costatum* with residue from *in-situ* burn experiment S1.

Concentration (mg/l)	Growth rate	Inhibition of growth rate in percent
Control 1	2.048	-
Control 2	2.047	-
Control 3	2.059	-
Control mean	2.051	0
100.000	1.472	28.2
100.000	2.006	2.2
1000.000	1.418	30.9
1000.000	1.609	21.6
10000.000	1.476	28.1
10000.000	1.523	25.7
100000.000	1.658	19.2
100000.000	1.578	23.1

EC-values were not possible to calculate from the results

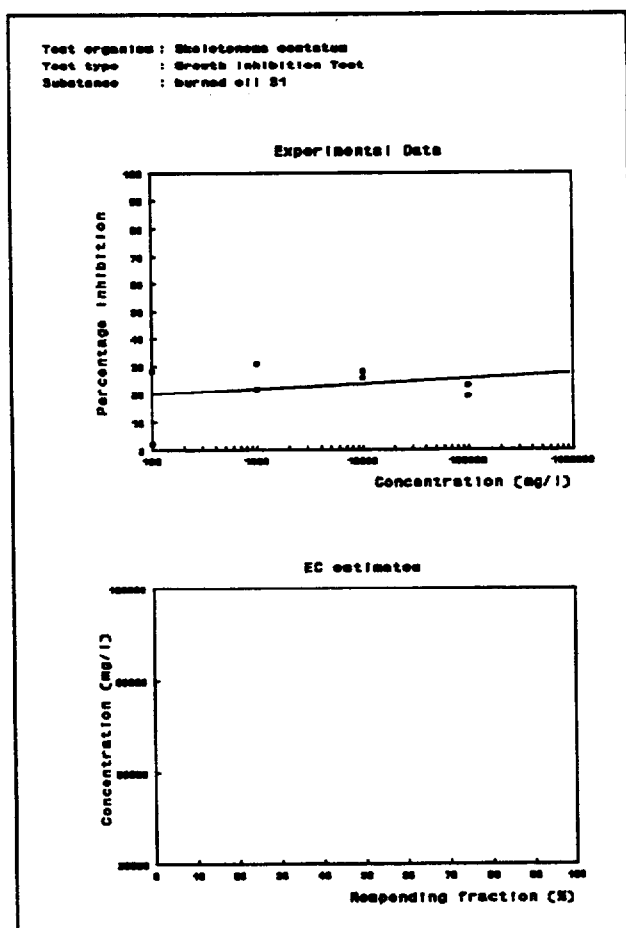


Figure 7.7 Growth inhibition (%) and calculated EC-values for the *in-situ* burn residue S1.

Table 7.6 Inhibition of the growth rates of *Skeletonema costatum* with residue from *in-situ* burn experiment S2.

Concentration (mg/l)	Growth rate	Inhibition of growth rate in percent
Control 1	2.038	-
Control 2	2.036	-
Control 3	2.049	-
Control mean	2.041	0
100.000	1.786	12.5
100.000	1.731	15.2
1000.000	1.319	35.3
1000.000	1.302	36.2
10000.000	1.229	39.8
10000.000	1.255	38.5
100000.000	1.082	47.0
100000.000	1.027	49.7

4 doses and 8 responses have been used during calculations.

EC 10 : 1.35 95 % confidence limits : (0.33 - 3.98)

EC 50 : 100 945 95 % confidence limits : (65 013 - 173 922)

EC 90 : (n.d.) 95 % confidence limits : (n.d.)

Coefficient of determination : 0.792

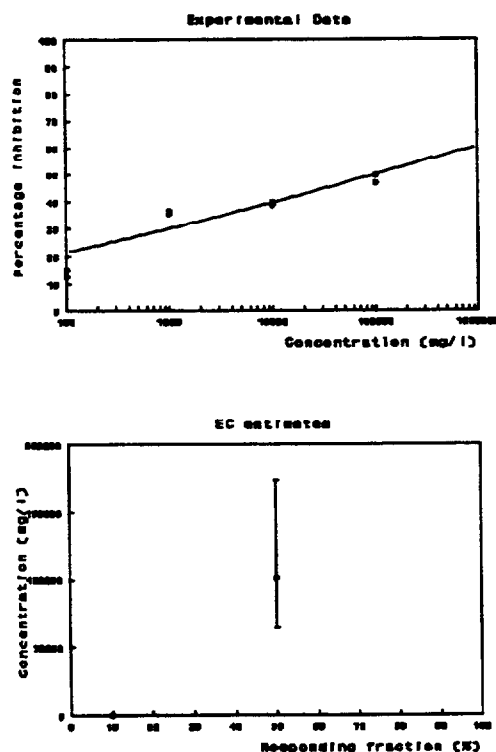


Figure 7.8

Growth inhibition (%) and calculated EC-values for the *in-situ* burn residue S2.

Table 7.7

Inhibition of the growth rates of *Skeletonema costatum* with residue from *in-situ* burn experiment S3.

Concentration (mg/l)	Growth rate	Inhibition of growth rate in percent
Control 1	2.020	-
Control 2	2.018	-
Control 3	2.029	-
Control mean	2.022	0
100.000	1.480	26.8
100.000	1.440	28.8
1000.000	1.452	28.2
1000.000	1.350	33.2
10000.000	0.881	56.4
10000.000	0.818	59.6
100000.000	-0.257	112.7
100000.000	-0.154	107.6

3 doses and 6 responses have been used during calculations.

EC 10 : 3.9 95 % confidence limits : (0.6 - 12.9)

EC 50 : 5 191 95 % confidence limits : (3 150 - 10 140)

EC 90 : n.d. 95 % confidence limits : (n.d.)

Coefficient of determination : 0.829

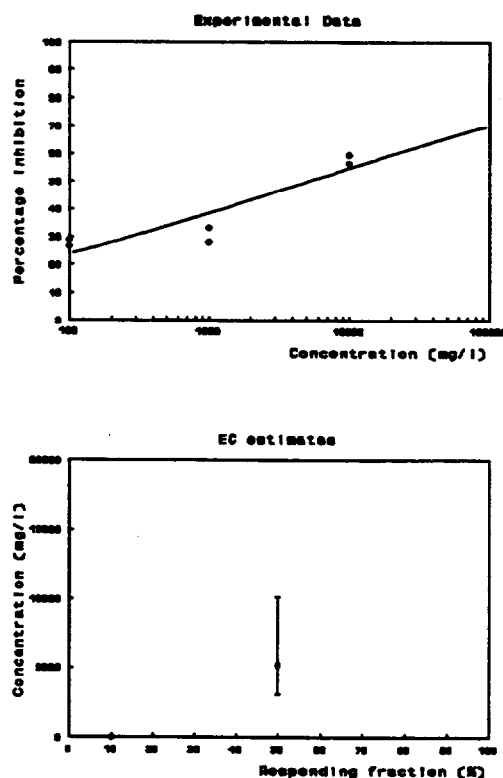


Figure 7.9

Growth inhibition (%) and calculated EC-values for the *in-situ* burn residue S3.

Table 7.8 Inhibition of the growth rates of *Skeletonema costatum* with residue from *in-situ* burn experiment S4.

Concentration (mg/l)	Growth rate	Inhibition of growth rate in percent
Control 1	2.051	-
Control 2	2.050	-
Control 3	2.062	-
Control mean	2.055	0
100.000	1.424	30.7
100.000	1.266	38.4
1000.000	1.355	34.1
1000.000	0.763	62.9
10000.000	0.758	63.1
10000.000	0.914	55.5
100000.000	0.424	79.4
100000.000	0.469	77.2

4 doses and 8 responses have been used during calculations.

EC 10 : 0.487 95 % confidence limits : (0.0 - 13.2)

EC 50 : 1 374 95 % confidence limits : (183 - 6 191)

EC 90 : n.d. 95 % confidence limits : (n.d.)

Coefficient of determination : 0.746

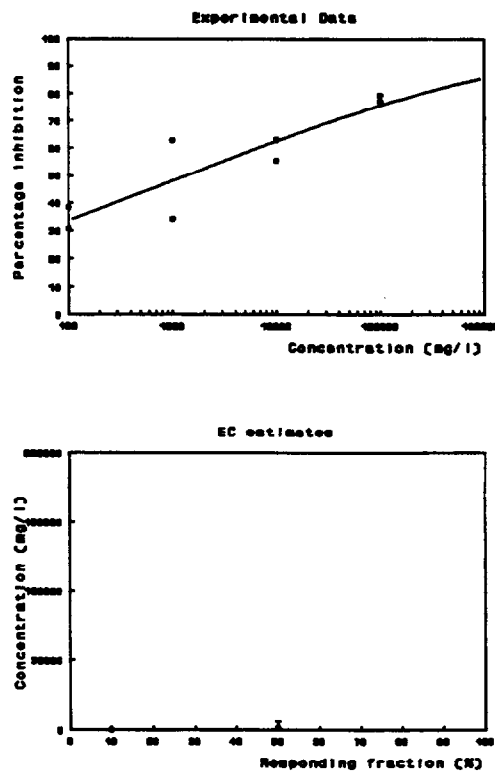


Figure 7.10

Growth inhibition (%) and calculated EC-values for the *in-situ* burn residue S4.

Table 7.9

Inhibition of the growth rates of *Skeletonema costatum* with residue from *in-situ* burn experiment S5.

Concentration (mg/l)	Growth rate	Inhibition of growth rate in percent
Control 1	2.038	-
Control 2	2.036	-
Control 3	2.049	-
Control mean	2.041	0
100.000	1.764	13.6
100.000	1.751	14.2
1000.000	0.350	82.8
1000.000	-0.048	102.4
10000.000	0.141	93.1
10000.000	0.307	85.0
100000.000	-0.018	100.9
100000.000	-0.040	101.9

3 doses and 5 responses have been used during calculations.

EC 10 : 47.3 95 % confidence limits : (15.1 - 98.4)

EC 50 : 528 95 % confidence limits : (302 - 881)

EC 90 : 5 896 95 % confidence limits : (3 108 - 15 384)

Coefficient of determination : 0.864

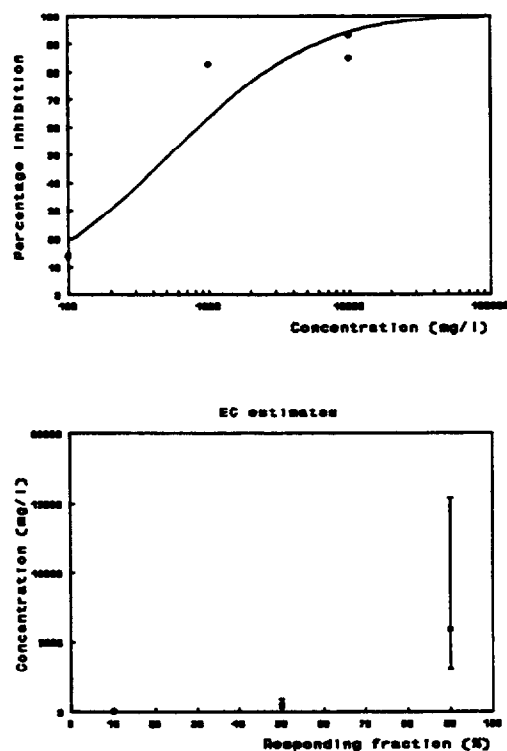


Figure 7.11

Growth inhibition (%) and calculated EC-values for the *in-situ* burn residue S5.

Table 7.10

Inhibition of the growth rates of *Skeletonema costatum* with residue from *in-situ* burn experiment F1.

Concentration (mg/l)	Growth rate	Inhibition of growth rate in percent
Control 1	2.052	-
Control 2	2.050	-
Control 3	2.062	-
Control mean	2.055	0
100.000	1.675	18.5
100.000	1.712	16.7
1000.000	1.704	17.1
1000.000	1.675	18.5
10000.000	1.721	16.2
10000.000	1.707	16.9
100000.000	1.643	20.0

EC-values were not possible to calculate from the results.

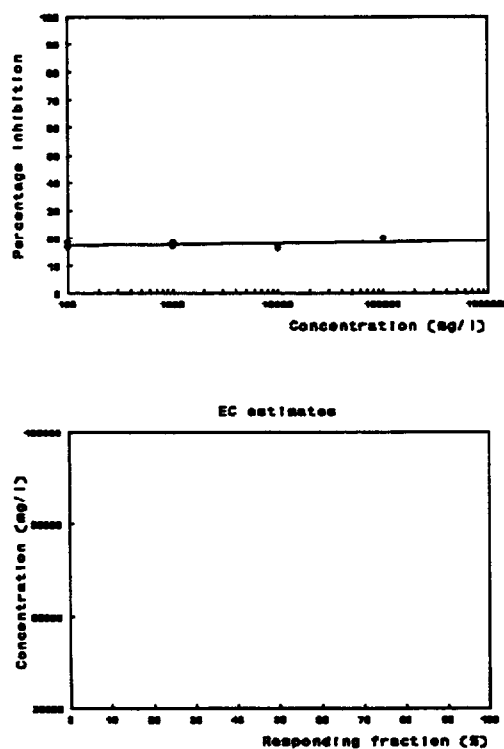


Figure 7.12

Growth inhibition (%) and calculated EC-values for the *in-situ* burn residue F1.

Table 7.11 Inhibition of the growth rates of *Skeletonema costatum* with residue from *in-situ* burn experiment F2.

Concentration (mg/l)	Growth rate	Inhibition of growth rate in percent
Control 1	2.034	-
Control 2	2.033	-
Control 3	2.045	-
Control mean	2.037	0
100.000	1.795	11.9
100.000	1.717	15.7
1000.000	1.727	15.2
1000.000	1.715	15.8
10000.000	1.716	15.8
10000.000	1.718	15.7
100000.000	1.671	18.0
100000.000	1.569	23.0

EC-values were not possible to calculate from the results.

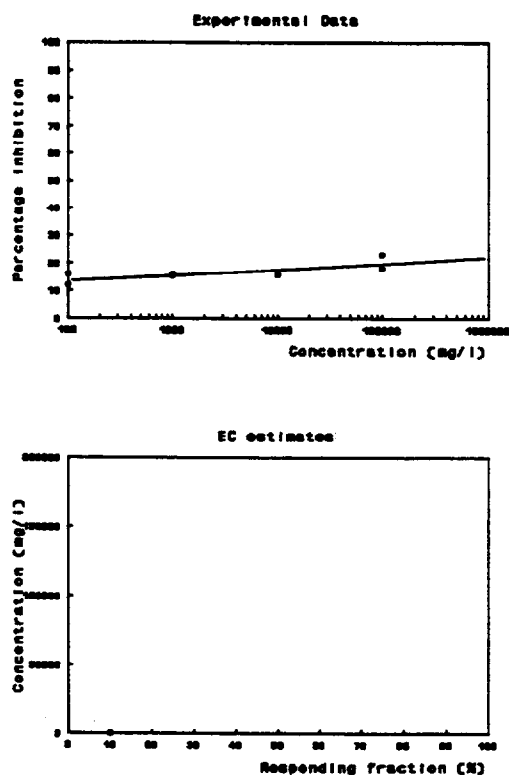


Figure 7.13

Growth inhibition (%) and calculated EC-values for the *in-situ* burn residue F2.

Table 7.12 Inhibition of the growth rates of *Skeletonema costatum* with residue from *in-situ* burn experiment F3.

Concentration (mg/l)	Growth rate	Inhibition of growth rate in percent
Control 1	2.038	-
Control 2	2.036	-
Control 3	2.049	-
Control mean	2.041	0
100.000	1.887	7.6
100.000	1.745	14.5
1000.000	1.660	18.7
1000.000	1.729	15.3
10000.000	1.416	30.6
10000.000	1.256	38.4
100000.000	0.024	98.8

4 doses and 7 responses have been used during calculations.

EC 10 : 134.1 95 % confidence limits : (2.96 - 494.48)

EC 50 : 74 913 95 % confidence limits : (18 785 - 4 600 987)

EC 90 : n.d. 95 % confidence limits : (n.d.)

Coefficient of determination : 0.819

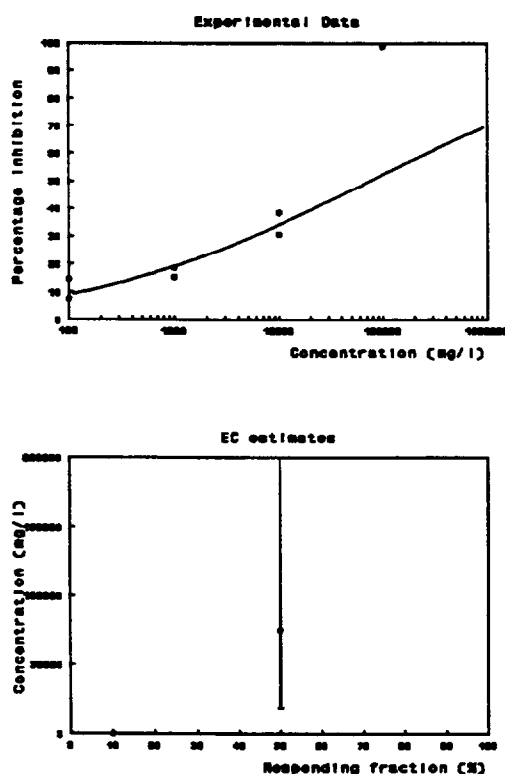


Figure 7.14 Growth inhibition (%) and calculated EC-values for the *in-situ* burn residue F3.

For drilling muds used off-shore the Norwegian State Pollution Control (SFT) operates with cut-off values for *Skeletonema costatum* at an EC_{50} -value of 1000 mg/l (ppm). Thus, while crude oils generally yield EC_{50} -values lower than this cut-off value the residues tested in this study would all, except from the S5 residue, have passed the drilling mud toxicity criteria used for *Skeletonema costatum*. Chemicals used in off-shore operations are evaluated also by additional criteria (volume of discharge, biodegradability and their potential for bioaccumulation) and no fixed cut-off values are used for such compounds. In situations where spilled oil is not possible to be removed by other means it would seem, from a strict marine toxicological point of view, to be an advantage to burn the oil rather than leave the original crude untreated.

The results indicate that there are great differences in the toxicity between the different residues tested. The highest toxicity was found for residue S5, residue S4 being the second most toxic and residue S3 the third most toxic. Residues S4 and S5 originated from the burning of non-evaporated crude oil with no water mixed in. As a comparison an untreated crude oil would normally yield EC_{50} -values on growth rates of *Skeletonema costatum* in the range 10-1000 mg/l depending on the type of oil. Thus, burning has probably reduced or not affected the toxicity of the oil.

The least toxic residues were S1, F1 and F2 with EC_{50} -values $\gg 100\ 000$ mg/l. These and the two remaining residues, S2 and F3, could be characterised as close to non-toxic to *Skeletonema costatum*.

There are indications in the results that increased amounts of water mixed into the oil (water-in-oil emulsions) lead to increased toxicity of the residues after burning of the oil, indicating that toxic compounds are not efficiently burned in the emulsions. This is demonstrated in the difference in toxicity between the residue S3 and S2, S3 being about 20 times more toxic than S2. The residues S4 and S5 both origin from burning of crude oil, the only difference during the burning experiments was the addition of 2% Ferrocene in the S5 experiment. The addition of Ferrocene does not seem to alter the toxicity of the residue significantly.

8 CONCLUSIONS AND RECOMMENDATIONS

8.1 Conclusions

- Some general hypothesis about the processes involved in burning water-in-oil emulsions have been confirmed, those being:
 - i) water must be removed from an emulsion before ignition can occur;
 - ii) water is released from the emulsion layer mainly through evaporation, leaving a layer of essentially water free oil on the slick surface which can be ignited given the proper conditions; and
 - iii) water temperature in w/o emulsion do not exceed approximately 100°C.
- Gelled crude oil can be an effective igniter for w/o emulsions. When water contents exceed 50%, this igniter becomes ineffective. Gelled gasoline is not a very effective igniter for use with emulsions. Ignitibility of an emulsion is predominantly governed by its water content.
- The use of an emulsion breaker with the gelled crude oil igniter enhances ignition and flame spreading. The concentration of emulsion breaker used is a factor in the effectiveness of this additive. Excessive emulsion breaker concentrations can cause the release of an amount of water which is greater than the amount which can be quickly vaporized by the igniter. It is likely that optimum emulsion breaker concentrations varies with the type of oil and the degree of emulsification. The brand of demulsifier can also have an effect on the effectiveness of this technique.
- The present study suggest that the residue is not likely to sink due to inherent properties (i.e. density, etc.), however, flume experiments indicated that when exposed to currents, the residue may be transported under barriers. Adherence of particle such as silt, did not appear to substantially alter the behaviour of the burn residue.
- The residue from burning fresh oil was found to be more toxic than that generated from emulsion burns. Burn residue from w/o emulsions with water contents of 50% was found to be more toxic than residue from a 25% water-in-oil emulsion. Burn residue from evaporated oil and emulsions with water contents of less than 25% were found to be close to non-toxic. The presence of ferrocene did not alter the toxicity of burn residue. These findings are based on the *Skeletonema costatum* toxicity test.
- Emulsions with water content of 50% drifting towards a burning slick (6 m² in area) were successfully ignited in currents speeds of 0.3 m/s and wind velocities of less than 10m/s.
- Ferrocene has proven to be an effective soot reducing agents both in small controlled laboratory burns and in meso-scale field burns of up to 2 m³. Ferrocene concentration as low as 0.13% by weight were found to be effective in the laboratory studies. Field experiments with ferrocene at concentrations as low as 0.2% by wt. showed this compound to effectively reduce soot emissions. It is likely that even lower concentrations of ferrocene could be used and still yield significant reductions in soot production.

8.2 Recommendations for future work

This section presents some recommendations for research in the area of *in-situ* burning, based on the 1993 findings.

Much has been learned about the processes involved in burning oils and emulsions over the course of the last few years. The present study has given some insight into the processes involved in igniting emulsified crude oil and has demonstrated the potential of certain improvements which could be brought to the existing ignition and burning technology. These improvements can help to widen the window of opportunity for the use of *in-situ* burning as a response tool for oil spills on water.

In addition, the use of ferrocene as a soot inhibitor has now been demonstrated in meso-scale experiments and has proven to be effective. The ability to reduce soot emissions from the *in-situ* burning of crude oils can also widen the window of opportunity for the use of this spill clean-up technique, as emissions are one of the main factors retarding the implementation of this method.

These findings would suggest that it is possible to ignite emulsions with water contents greater than 50%. The ultimate goal is to develop the technology to the point where an oilspill can be removed from the sea surface independently of the state of weathering or emulsification, in an environmentally acceptable way. The next step would be therefore, to scale up the 1993 findings and develop these techniques to the point where they can be used on an operational level. For instance, the ignition techniques developed in 1993 can be improved when it comes to sensitivity to environmental factors and the mode of application. Operational studies should also include full scale testing of the igniter/combustion promoter deployment. Thus it is necessary to look into methods of adapting existing application techniques both for igniters and combustion promoters. Work should also focus on the effect of additives on the behaviour of the gelled fuel as this may affect the method of application ultimately used.

The concept of using emulsion breakers to enhance the ignition capabilities of igniters and combined with ferrocene to reduce the smoke emissions should be fine tuned. A product with both combustion promoting and soot inhibiting properties could be a suitable approach to dealing with two of the important problems with using *in-situ* burning as a response tool: ignition of highly emulsified oils and reduction of smoke/soot emissions. Further experiments with ferrocene should also be conducted to investigate the effect of this compound on the emission of other hazardous compounds emitted during the *in-situ* burning of crude oil.

In order to burn oil or emulsions successfully, a certain minimum thickness is required. It has been considered that containment is necessary either naturally (i.e. in ice) or by use of fireproof booms. The fact that emulsions behave completely differently than unemulsified oils in terms of temperature gradients developed through a burning slick, it is likely that the spreading of burning emulsions will be different than that of burning crude oil. Therefore, it would be interesting to look into the possibilities of burning uncontained emulsion slicks on water.

It has also been demonstrated that higher water content emulsions drifting towards burning oil can be ignited. This concept should be further developed to evaluate whether or not it could be used operationally, for instance in combination with a fireproof boom.

9 REFERENCES

- Allen, A.A. 1986. Alaska Clean Seas survey and analysis of air-deplorable igniters. Proceedings of the 9th Annual Arctic Marine Oilspill Program Technical Seminar. Environment Canada, Ottawa.
- Allen, A.A. 1990. Contained controlled burning of spilled oil during the "Exxon Valdez" spill. Proceedings of the 13th AMOP Technical Seminar. Environment Canada, Ottawa.
- Babrauskas, V. 1988. Burning rates. Teh SFPE Handbook of Fire Protection Engineering. pp 2.1-2.15.
- Bech, C.M.B., Sveum, P. and I. Buist. 1991. *In-situ* brenning av emulsjoner (in Norwegian) - STF21F91081.
- Bech, C., Sveum, P. and Buist, I.A. 1992. *In-situ* burning of emulsions: The effects of varying water content and degree of evaporation. Proceedings of the 15th AMOP Technical Seminar, June 10-12, Edmonton, Alta. Environment Canada, Ottawa, Ontario. pp 547-559.
- Bech, C., Sveum, P. and Buist, I.A. 1993. The effect of wind, ice and waves on the in situ burning of emulsions and aged oils. Proceedings of the 16th AMOP Technical Seminar, June 7-9, Calgary, Alta. Environment Canada, Ottawa, Ontario. pp 735-748.
- Blinov, VI and Khudiakov, G.N. 1959. Certain laws governing diffusive burning of liquids. Fire Research Abstracts and Review. Vol 1(1), pp 41-44.
- Brzustowski, T.A. and Twardus, E.M. 1982. A study of the burning of a slick of crude oil on water. Nineteenth Symposium (International) on Combustion. The Combustion Institute, Pittsburgh, PA. pp 847-854.
- Buist, I.A. 1989. Disposal of spilled Hibernia crude oils and emulsions: *In-situ* burning and the "Swirlfire" burner. Proceedings of the 12th AMOP Technical Seminar. Environment Canada, Ottawa.
- Cabioc'h, F. 1993. Last French experiments in order to evaluate the burning possibilities of three water-in-oil emulsions. Proceedings of the 16th AMOP Technical Seminar, June 7-9, Calgary, Alta. Environment Canada, Ottawa, Ontario.
- Daling, P.S. 1994. Personal communication.
- Daling, P.S. and Branvik, P.J. 1988. A study of the Formation and Stability of Water-in-oil Emulsions. Eleventh Arctic and Marine Oilspill Program Technical Seminar, pp 153-170.
- Energetex Engineering. 1977. Ignition and burning of crude oil on water pools under Arctic springtime conditions. Report to Canadian Marine Drilling Ltd. Calgary.
- Energetex Engineering. 1978. Testing of air-deplorable incendiary devices for igniting oil on water. Report to the Department of Fisheries and Environment. Ottawa.
- Energetex Engineering. 1980. Improvement of air-deplorable oil slick igniters. Report to Canadian Marine Drilling Ltd. Calgary.
- Energetex Engineering. 1978. Testing of air-deployable incendiary devices for igniting oil on water. Environment Canada, Ottawa, Ontario. Report No. EPS-4-EC-78-11. 98 p.

Energetex Engineering. 1980b. A study to evaluate the combustibility and other physical and chemical properties of aged oils and emulsions. Report to Environment Canada, Ottawa.

Environment Canada. 1992. A catalogue of crude oil and oil product properties. Report No. EE-144.

Evans, D.D., Walton, W.D., Baum, H.R., Notarianni, K.A., Lawson, J.R. and Tang, H.C. et al. 1992. In situ burning of oil spills: Mesoscale experiments. Proceedings of the 15th AMOP Technical Seminar, June 10-12, Edmonton, Alta. Environment Canada, Ottawa, Ontario. pp 593-657.

Fingas, M. 1993. Personal communication - letter of March 26, 1993 to S. Ross re: emulsion breaker test procedures.

Gåseidnes, K. 1993. Preparation of mousse for oil spill equipment testing. Proceedings of the workshop on Formation and Breaking of Water-in-Oil Emulsions. June 14-15, 1993 Kananskis Village, Alberta, Canada, pp 123-132. Marine Spill Resonse Corporation. Washington, D.C.

Koseki, H. and Mulholland, G.W. 1991. The effect of diameter on the burning of crude oil pool fires. *Fire Technology* 27(1):54-65.

Lee, S.C., D.Mackay, F.Bonville, E.Joner and W.Y. Shiu 1989. A study of the long-term weathering of submerged and overwashed oil. Proceedings of the 12th AMOP Technical Seminar. Environment Canada. Ottawa.

Mackay, D.W., Stiver, W. and Tebeau, P.A. 1983. Testing of crude oils and petroleum products for environmental purposes. Proceedings of the 1983 Oil Spill Conference. Americal Petroleum Institute, Washington, D.C. p 331.

Meikle, K.M. 1981. Incendiary device for oil slick ignition. Proceedings of the 4th Annual Arctic Marine Oilspill Program Technical Seminar. Environment Canada, Ottawa.

Mitchell, J.B.A. 1990. The effectiveness of ferrocene in reduing smoke emission from burning crude oil. Proceeding of the 13th AMOP Technical Seminar. Environment Canada. Ottawa.

Mitchell, J.B.A. and Janssen, E. 1991. The use of additives for smoke reduction from burning pool fires. Proceeding of the 14th AMOP Technical Seminar. Environment Canada. Ottawa.

Ross, S. and Maharaj, S. 1993. Potentially beneficial spill-related effects of chemicals routinely added to crude oils. Proceedings of the 16th AMOP Technical Seminar, June 7-9. Calgary, Alta. Environment Canada, Ottawa, Ontario. pp 123-137.

SAS 1989. JMP Version 2 Software for Statistical Visualization on the Apple MacIntosh. SAS Institute Inc.

S.L. Ross Environmental Research Ltd. and Energetex Engineering. 1986. Decision-making aids for igniting or extinguishing well blowouts to minimize environmental impacts. Environmental Studies Revolving Funds Report Number 051; 95 p.

S.L. Ross Environmental Research Ltd. and Energetex Engineering. 1988. Laboratory studies of the behaviour and fate of waxy crude oil spills. Ontario Environmental Studies Research Fund Report No. 084. 247 p.

S.L. Ross Environmental Research Ltd. 1989. Disposal of spilled Hibernia crude oils and emulsions: *in-situ* burning and the "Swirlfire" burner. Report to Canadian Coast Guard, Ottawa, ON.

S.L. Ross Environmental Research Ltd. 1990. Proceedings of a Workshop to Establish Canadian Marine Oil Spill Research and Development Priorities. Environmental Studies Research Fund Report 106. Calgary.

Spiltec. 1987. Refinement of aerial ignition systems, (test and evaluation of the Helitorch for the ignition of oil slicks). Report to Alaska Clean Seas, Anchorage Alaska.

Sveum, P. and I. Buist. 1991. Personal communication.

Twardawa, P. and G. Couture. 1980. Incendiary devices for the *in-situ* burning of oil spills. Proceedings of the 3rd Annual Arctic Marine Oil Spill Program Technical Seminar. Environment Canada, Ottawa.

Twardus, E.M. and Brzustowski, T.A. 1981. The burning of crude oil spilled on water. Archivum Combustionis 1(1/2):49-60.

Wakamiya, W., Petty, S.E., Boiarski, A. and Putnam, A. (Pacific Northwest Laboratory). 1982. Combustion of oils on water: An experimental program. U.S. Department of Energy Report No. NBM/1002. U.S. Department of Energy, Washington, DC. 95 p.

APPENDIX A

LABORATORY BURN RESULTS

Description of acronyms use in tables describing laboratory burn experiments in Appendix A:

Exp. No.	- experiment number to permit cross-referencing to other data files; Avalon = series 2, Statfjord = series 4 and Alaska North Slope = series 5
Vol. Evap.	- volume percent loss to evaporation of the parent oil used to create the emulsion.
Water Content	- volume percent water in the emulsion as created in the bucket/impeller mixer; note that for some unstable oil/water combinations this may be an overestimate of actual water content at ignition.
Burn Eff.	- the mass percent of the oil (i.e., excluding emulsified water) added to the ring, not recovered from within the ring after the burn = (mass of oil added - mass recovered)
Burn Rate	- the regression rate of oil burning from the emulsion slick (i.e., mm of oil per minute) ,= (mass of oil added - mass of residue)/(extinction time - ignition time).
Mass Oil	- the mass of oil added to the test pan (excluding emulsified water).
Mass Residue	- the mass of residue recovered from the test pan including emulsion water, if any; it was assumed that successful burns involved the breaking of the emulsion and that the residue was composed primarily of unburnt oil. Visual observations confirmed this.
Vol. Emul.	- the volume of emulsion added to the test pan for the burn.
Thickness	- the calculated (volume/area) of emulsion added to the test pan for the burn.
Ignition	- the ignition time for each burn (time to "full involvement") defined as the time for the flames to cover the entire slick surface.
Extinction	- the elapsed time to extinguishment of the burn.
Ignition Source	- the type of ignition that finally resulted in successful ignition of the candidate emulsion; s.g. = 25 cm ² gasoline-soaked sorbent pad; f.c. = fresh (i.e., unweathered crude added on top of emulsion - 100 or 200 mL - mass noted in Comments column); g.g = gelled gasoline; g.g.f. = gelled gasoline with 4 wt% ferrocene added; g.g.f.b. = gelled gasoline with 4 wt% ferrocene and emulsion breaker (brand and application techniques noted in Comments); n.r. = not recorded; n.a. = not applicable (i.e., no technique was successful in igniting the oil).

Avalon Crude Oil (Series 2)

Burn Results for Tasks 1, 2, and 3

Exp. No	Vol. Evap (%)	Water Content (%)	Burn Eff. (%)	Burn Rate (mm/min)	Mass Oil (g)	Mass Res. (g)	Vol. Emul. (ml)	Thickness (mm)	Ignition (s)	Intense (s)	Extinguishment (s)	Ignition Source	Comments
Exp2_1	0.0%	0.0%	74.5%	n.a.	461.5	117.6	522.7	4.9	25	149	n.r.	s.g.	s.g.=25 cm ² gas pad
Exp2_2	0.0%	0.0%	89.3%	1.317	928.5	99.4	1051.5	9.8	25	382	423	s.g.	f.c.=fresh Avalon crude
Exp2_3	0.0%	0.0%	75.6%	1.005	1843.1	449.5	2087.3	19.4	19	860	895	s.g.	g.g.=gelled gas(napalm)
Exp2_4	12.7%	0.0%	73.9%	1.422	465.4	121.3	520.6	4.8	39	169	190	s.g.	g.g.f.=napalm(4%wt. ferrocene)
Exp2_4a	12.7%	0.0%	76.8%	1.306	463.4	107.6	518.3	4.8	32	182	202	s.g.	g.g.f.b.=g.g.f.+1 ml brexit/30 g.g.f.)
Exp2_5	12.7%	0.0%	88.3%	1.440	940.3	109.6	1051.8	9.8	31	337	391	s.g.	n.r.=not recorded
Exp2_6	12.7%	0.0%	74.3%	0.952	1867.6	479.3	2089.0	19.4	35	905	945	s.g.	n.a.=not applicable(residue>mass oil or n.r.)
Exp2_7	20.6%	0.0%	79.3%	1.326	457.9	95	506.5	4.7	68	206	237	s.g.	
Exp2_8	20.6%	0.0%	90.2%	1.194	896.1	87.5	991.3	9.2	58	420	476	s.g.	
Exp2_9	20.6%	0.0%	72.5%	0.939	1771.0	487.1	1959.1	18.2	52	971	997	s.g.	
Exp2_10	0.0%	25.0%	76.3%	0.407	341.6	81.1	515.8	4.8	60	448	448	s.g.	
Exp2_11	0.0%	25.0%	6.7%	0.033	699.2	652.3	1055.8	9.8	43	909	909	s.g.	
Exp2_12	0.0%	12.5%	82.5%	0.749	404.0	70.68	522.9	4.9	40	223	315	s.g.	
Exp2_13	0.0%	12.5%	52.9%	0.533	808.0	380.4	1045.8	9.7	34	455	530	s.g.	
Exp2_14	0.0%	12.5%	59.5%	0.570	1290.4	522.9	1670.1	15.5	58	865	890	s.g.	
Exp2_15	0.0%	0.0%	79.6%	2.106	1753.9	357.2	1986.3	4.5	41	101	143	s.g.	
Exp2_16	12.7%	0.0%	78.2%	2.550	1866.6	406.2	2087.9	4.7	73	107	160	s.g.	
Exp2_17	20.6%	0.0%	83.1%	2.172	1826.8	308.5	2020.8	4.6	100	130	205	s.g.	
Exp2_18	0.0%	25.0%	n.a.	n.a.	1307.3	1426.6	1974.0	4.5	257	never	490	s.g.	
Exp2_19	12.7%	12.5%	79.7%	1.154	403.9	82.1	516.4	4.8	430	496	602	s.g.	
Exp2_20	12.7%	12.5%	89.5%	0.792	834.5	88	1066.7	9.9	159	630	740	s.g.	
Exp2_21	12.7%	12.5%	67.3%	0.652	1614.5	527.8	2063.9	19.2	140	never	1167	s.g.	
Exp2_22	20.6%	12.5%	82.5%	0.705	398.5	69.65	503.8	4.7	23	220	308	f.c.	85.27g
Exp2_23	20.6%	12.5%	48.5%	0.507	806.6	415	1019.7	9.5	26	448	498	f.c.	111.5g
Exp2_24	20.6%	12.5%	73.4%	0.665	1522.5	404.5	1924.8	17.9	25	n.r.	1052	f.c.	83.1g
Exp2_25	0.0%	40.0%	n.a.	n.a.	271.1	91.7	511.7	4.8	64	n.r.	128	s.g.	Emulsion unstable-disregard
Exp2_25-A	0.0%	40.0%	n.a.	n.a.	274.9	563.3	518.8	4.8	64	n.r.	128	f.c.	84.7g
Exp2_25-B	0.0%	40.0%	n.a.	n.a.	1104.4	2092.5	2084.6	19.4	10	n.r.	136	f.c.	136
Exp2_26	0.0%	40.0%	n.a.	0.394	358.0	88.5	531.0	4.9	15	n.r.	100	f.c.	164.8g
Exp2_28a	12.7%	25.0%	86.4%	0.454	695.7	94.55	1037.6	9.6	43	284	422	f.c.	163.4g
Exp2_28b	12.7%	25.0%	51.1%	0.305	1392.5	681.6	2076.8	19.3	23	never	149	f.c.	251g
Exp2_29a	12.7%	25.0%	44.5%	0.270	1329.6	738.4	1961.1	18.2	33	1343	1363	f.c.	78.2g
Exp2_30	20.7%	25.0%	84.6%	0.493	660.2	101.6	973.8	9.1	27	never	63	f.c.	159.97g
Exp2_31a	20.7%	25.0%	75.0%	0.489	347.3	86.9	512.3	4.8	33	601	707	f.c.	156.9g
Exp2_32	20.7%	25.0%	n.a.	n.a.	1073.8	1863	1979.8	18.4	16	321	356	f.c.	162.2g
Exp2_33a	12.7%	40.0%	85.1%	0.550	1346.3	200.93	2541.2	20.2	never	never	1075	f.c.	262.9g
Exp2_33b	12.7%	40.0%	46.5%	0.266	1381.8	739.7	2608.2	20.8	34	1154	0	f.c.	91.8g
Exp2_31-A	0.0%	40.0%	n.a.	n.a.	1367.1	1391	2580.3	20.5	28	never	480	f.c.	164g/l
Exp2_31-B	0.0%	40.0%	72.1%	0.500	917.5	255.7	2597.7	20.7	270	760	923	g.c.f.b.	81.5g
Exp2_32-A	0.0%	40.0%	54.6%	0.279	869.3	395	2461.2	19.6	212	g.g.	n.a.	g.g.	32g
Exp2_32-B	0.0%	40.0%	73.6%	0.609	885.0	233.75	2505.7	19.9	n.r.	g.g.	n.a.	g.g.	32g
Exp2_33-A	0.0%	40.0%	82.2%	0.700	1386.0	246.51	2584.0	20.6	19	919	1075	g.c.f.	200 ml
Exp2_33-B	0.0%	40.0%	55.9%	0.425	1339.0	590.6	2496.3	19.9	18	never	433	g.c.f.	30g(2 ml alcopol/toluene-2 min. mix)
Exp2_33-C	0.0%	40.0%	78.3%	0.694	1389.7	329.3	2590.9	20.6	34	1175	1008	g.c.f.b.	166.8g
Exp2_34a	0.0%	60.0%	62.4%	0.493	842.3	317	2355.5	18.7	never	never	615	g.c.f.b.	40.8g
Exp2_34b	0.0%	60.0%	57.5%	0.401	877.3	372.6	2453.2	19.5	28	n.r.	923	g.g.	166g(2 ml alcopol/toluene-2 min. mix)
Exp2_35	0.0%	60.0%	67.9%	0.393	884.7	284	2474.0	19.7	113	660	871	g.g.	50g(2 ml alcopol/toluene-2 min. mix)

Statfjord Crude Oil (Experiment 4)

Burn Results for Tasks 1, 2, and 3

Exp. No	Vol. Evap (%)	Water Content (%)	Burn Eff. (%)	Burn Rate (mm/min)	Mass Oil (g)	Mass Res. (g)	Vol. Emul. (ml)	Thickness (mm)	Ignition Intense (s)	Extinction (s)	Ignition Source	Comments
Exp4_48	19.6%	75.0%	n.a.	n.a.	535.9	2127.3	2475	20	never	never	f.c.(78.6g+165.6g)	350 ml Bunker C to stabilize emulsion
Exp4_49	19.6%	40.0%	n.a.	n.a.	1331.8	?	2563	20	150	614	s.g.	210 ml Bunker C
Exp4_50	19.6%	40.0%	52.00%	0.64	661.3	317.4	1273	10	180	457	s.g.	+Bunker C
Exp4_51	19.6%	60.0%	n.a.	n.a.	878.4	952	2536	20	never	never	s.g.	+Bunker C
Exp4_52	19.6%	40.0%	65.77%	0.89	1272.4	435.6	2449	19	165	683	s.g.	+Bunker C
Exp4_53	19.6%	60.0%	47.15%	0.30	899.7	475.5	2597	21	never	never	s.g.	160 ml Bunker C
Exp4_54	19.6%	60.0%	n.a.	n.a.	862.0	1050.2	2488	20	562	1029	s.c.	5% by wt. Bunker C
Exp4_55	19.6%	25.0%	92.72%	1.22	2356.5	171.5	3628	29	53	1038	s.g.	4% by wt. ferroccene
Exp4_56	19.6%	25.0%	80.74%	0.98	2485.2	478.6	3826	30	86	1198	s.g.	68.2g ferroccene
Exp4_57	19.6%	25.0%	76.18%	0.89	2403.8	572.7	3701	29	53	1187	s.g.	400 ml gelled gasoline
Exp4_58	0.0%	0.0%	96.68%	n.a.	278.4	9.24	330	3	1	200	n.r.	400 ml gelled fresh Statfjord
Exp4_59	0.0%	0.0%	78.80%	n.a.	321.3	68.1	381	3	35	n.r.	s.g.	37.3g ferroccene
Exp4_60	19.6%	25.0%	90.44%	1.21	2394.5	228.91	3687	29	58	1044	s.g.	17.1g ferroccene
Exp4_61	19.6%	25.0%	73.75%	1.01	2372.6	622.7	3653	29	44	999	s.g.	8.5g ferroccene
Exp4_62	19.6%	25.0%	68.00%	0.91	2361.9	755.8	3637	29	47	1018	s.g.	4.26g ferroccene
Exp4_63	19.6%	25.0%	72.12%	0.89	2396.4	668.1	3690	29	50	1123	s.g.	3.09g ferroccene
Exp4_64	19.6%	25.0%	94.22%	1.13	2344.0	135.5	3609	29	48	1126	s.g.	11.7g ferroccene
Exp4_65	0.0%	0.0%	94.49%	n.a.	286.6	15.8	340	3	1	88	400 ml gelled gas	13.3g ferroccene
Exp4_66	0.0%	0.0%	89.94%	n.a.	343.6	34.55	407	3	119	200	400 ml gelled crude	
Exp4_67	30.6%	0.0%	73.20%	0.84	2188.6	586.53	2484	20	65	923	s.g.	
Exp4_68	30.6%	12.5%	71.24%	1.32	1912.5	550	2481	20	95	629	s.g.	
Exp4_69	30.6%	25.0%	67.72%	0.80	1661.9	536.4	2515	20	106	864	s.g.	
Exp4_70a	30.6%	40.0%	n.a.	n.a.	0.0					97	s.g.	
Exp4_70b	30.6%	40.0%	90.41%	1.04	1339.4	128.5	2534	20	113	743	s.g.	
Exp4_71a	30.6%	60.0%								87	s.g.	
Exp4_71b	30.6%	60.0%	79.04%	0.43	739.6	155	2099	17	10	752	s.c.	130 ml
Exp4_71c	30.6%	60.0%								150	f.c.	21.4 g
Exp4_72a	30.6%	75.0%								135	g.g. = gelled gas	154.38 g
Exp4_72b	30.6%	75.0%	71.28%	1.09	295.5	84.87	1342	11	24	129	g.c.=gelled crude	30 ml
Exp4_73a	30.6%	75.0%								163	f.c.(ANS)	25.4g
Exp4_73b	30.6%	75.0%	70.83%	1.20	569.8	166.2	2587	21	142	142	g.g.	19.4g
Exp4_74a	30.6%	75.0%								never	g.g.	26.2g
Exp4_74b	30.6%	75.0%								never	g.g.	179.7g(5% by wt. Bunker C)
Exp4_74	30.6%	75.0%	65.12%	0.53	269.7	94.1	1225	10	10	190	f.c.	167.5ml(5% by wt. Bunker C)
Exp4_75	30.6%	75.0%	55.53%	0.62	554.8	246.7	2519	20	20	289	f.c.(ANS)	18.8g(2ml alcopolitoluene-1 min. mix)
Exp4_76	30.6%	75.0%	57.03%	0.42	561.6	241.3	2550	20	81	498	g.g.	25.3g(2ml alcopolitoluene-3 min. mix)
Exp4_77	30.6%	75.0%	64.30%	0.50	532.5	190.1	2418	19	210	581	g.c.	29.8g(2ml alcopolitoluene-dropped)
Exp4_78	30.6%	75.0%	76.77%	2.32	541.2	125.69	2457	20	421	518	g.c.	24.7g+33.9g
Exp4_79	30.6%	75.0%	79.42%	1.26	573.9	118.1	2606	21	439	635	g.g.+g.c.	29.6g
Exp4_80	30.6%	75.0%	72.42%	0.93	588.3	162.25	2671	21	365	613	g.g.	21.3g (2 ml alcopolitoluene)
Exp4_81	30.6%	75.0%	58.80%	0.68	573.6	236.3	2604	21	370	638	g.g.	28.8g(2ml unimixed, 3ml brexit/10luene mixed)
Exp4_82	30.6%	75.0%	71.20%	0.92	538.8	155.2	2446	19	390	562	g.c.	29.98g(2 ml brexit/10luene, unimixed)
Exp4_83	30.6%	75.0%	n.a.	n.a.	532.5	n.r.	2418	19	360	735	g.c.	29.98g(2 ml brexit/10luene, unimixed)
Exp4_84	30.6%	75.0%	79.02%	1.62	586.8	123.1	2664	21	580	610	g.c.(4%ferrocene)=g.c.f.	30.73g(2 ml brexit/10luene, unimixed)
Exp4_85	30.6%	75.0%	78.73%	1.27	523.7	111.4	2378	19	474	650	g.g.	28.72g(2 ml brexit/10luene, unimixed)
Exp4_86	30.6%	75.0%	69.20%	1.07	562.7	173.3	2555	20	315	515	g.c.(4%ferrocene)=g.c.f.	28.3g(bag placed not dropped)
Exp4_87	30.6%	75.0%	76.33%	1.73	532.6	126.1	2418	19	375	721	same as above g.c.f.b.	crude has 1 ml brexit/30 ml oil
Exp4_88	30.6%	75.0%	81.03%	1.73	563.7	106.6	2559	20	304	447	same as above g.c.f.b.	5% Bunker C
Exp4_89	30.6%	75.0%	75.66%	0.66	553.4	134.7	2513	20	10	365	f.c.(200 ml)	10% Bunker C

Statfjord Crude Oil (Experiment 4)

Burn Results for Tasks 1, 2, and 3

Exp. No	Vol. (%)	Evap (%)	Water Content (%)	Burn Eff. (%)	Burn Rate (mm/min)	Mass Oil (g)	Mass Res. (g)	Vol. Emul. (ml)	Thickness (mm)	Ignition (s)	Intense (s)	Extinction (s)	Ignition Source	Comments
Exp4_01	0.0%	0.0%	0.0%	71.85%	1.14	393.9	110.9	467	4	1	115	165	s.g.	s.g.=25 cm ² gas pad f.c.=fresh crude oil
Exp4_02	0.0%	0.0%	0.0%	88.78%	1.70	856.6	96.1	1015	9	1	253	296	s.g.	
Exp4_03	0.0%	0.0%	0.0%	95.81%	1.69	1719.7	72.1	2038	19	1	585	644	s.g.	
Exp4_04	0.0%	0.0%	0.0%	96.56%	1.59	2662.3	91.5	3154	29	15	1021	1085	s.g.	
Exp4_05	0.0%	0.0%	0.0%	90.47%	1.59	2654.4	253	3145	29	15	970	1013	s.g.	
Exp4_06	0.0%	0.0%	0.0%	96.98%	1.53	2654.4	80.1	3145	29	5	1046	1117	s.g.	100.3g ferrocene
Exp4_07	0.0%	0.0%	0.0%	96.93%	1.64	2627.2	80.66	3113	29	3	958	1027	s.g.	50.2g ferrocene
Exp4_08	0.0%	0.0%	0.0%	97.36%	1.75	2633.0	69.6	3120	29	1	898	972	s.g.	25.2g ferrocene
Exp4_09	0.0%	0.0%	0.0%	97.09%	1.72	2631.2	76.54	3118	29	0	901	983	s.g.	12.7g ferrocene
Exp4_10	0.0%	0.0%	0.0%	96.76%	1.69	2658.8	86.25	3150	29	2	915	1008	s.g.	6.3g ferrocene
Exp4_11	12.9%	12.9%	12.5%	81.59%	1.65	473.2	87.1	631	5	23	127	153	s.g.	3.25g ferrocene
Exp4_12	12.9%	12.9%	12.5%	91.06%	1.55	923.7	82.6	1232	10	24	274	327	s.g.	
Exp4_13	12.9%	12.9%	12.5%	74.00%	1.06	1900.9	494.2	2535	20	26	703	787	s.g.	
Exp4_14	12.9%	12.9%	0.0%	84.12%	1.60	527.8	83.8	616	5	20	154	175	s.g.	
Exp4_15	12.9%	12.9%	0.0%	90.41%	1.63	1023.9	98.2	1195	10	14	296	331	s.g.	
Exp4_16	12.9%	12.9%	0.0%	94.69%	1.44	2170.8	115.3	2533	20	13	738	807	s.g.	
Exp4_17	12.9%	12.9%	25.0%	76.17%	1.30	396.5	94.5	617	5	23	108	152	s.g.	
Exp4_18	12.9%	12.9%	25.0%	87.39%	1.21	782.2	98.6	1217	10	16	288	332	s.g.	
Exp4_19	12.9%	12.9%	25.0%	91.03%	1.44	1732.1	155.4	2736	22	17	573	626	s.g.	
Exp4_20	12.9%	12.9%	40.0%	91.63%	1.28	1282.7	107.38	2495	20	15	468	528	s.g.	
Exp4_21	12.9%	12.9%	40.0%	85.33%	1.83	642.9	94.3	1250	10	14	139	181	s.g.	
Exp4_22	12.9%	12.9%	40.0%	66.77%	1.15	327.1	108.7	636	5	20	66	126	s.g.	
Exp4_23	12.9%	12.9%	40.0%	68.87%	1.19	329.6	102.6	641	5	21	75	127	s.g.	
Exp4_24	12.9%	12.9%	0.0%	84.81%	2.30	1862.1	282.8	2173	5	33	99	142	s.g.	
Exp4_25	12.9%	12.9%	60.0%	85.69%	1.29	883.6	126.43	2577	21	10	252	337	s.g.	
Exp4_26	12.9%	12.9%	60.0%	75.84%	0.99	431.7	104.3	1259	10	28	211	211	s.g.	
Exp4_27	12.9%	12.9%	60.0%	60.25%	0.68	214.1	85.1	625	5	40	83	146	s.g.	
Exp4_28	12.9%	12.9%	60.0%	59.42%	0.68	216.1	87.7	630	5	54	95	159	s.g.	
Exp4_29	0.0%	0.0%	0.0%	95.11%	n.a.	3099.9	151.5	3673	29	21	874	n.r.	s.g.	3% by wt. ferrocene
Exp4_30	0.0%	0.0%	0.0%	86.07%	1.61	3183.9	443.6	3772	30	2	930	967	s.g.	
Exp4_31	19.6%	19.6%	0.0%	80.27%	1.35	535.7	105.7	619	5	37	124	212	s.g.	
Exp4_32	19.6%	19.6%	0.0%	87.80%	n.a.	1077.8	131.5	1245	10	n.r.	n.r.	n.r.	s.g.	
Exp4_33	19.6%	19.6%	0.0%	74.72%	0.97	2180.8	551.2	2518	20	47	953	978	s.g.	
Exp4_34	19.6%	19.6%	12.5%	77.16%	1.28	456.2	104.2	602	5	65	170	217	s.g.	
Exp4_35	19.6%	19.6%	12.5%	88.47%	1.19	886.1	102.4	1172	9	50	277	415	s.g.	
Exp4_36	19.6%	19.6%	12.5%	72.53%	0.95	1855.5	509.8	2449	19	51	790	833	s.g.	
Exp4_37	19.6%	19.6%	25.0%	89.02%	1.18	1589.6	174.6	2447	19	47	585	710	s.g.	
Exp4_38	19.6%	19.6%	25.0%	83.88%	1.16	750.4	121	1155	9	42	232	342	s.g.	
Exp4_39	19.6%	19.6%	25.0%	83.24%	1.59	404.4	67.8	623	5	50	102	167	s.g.	
Exp4_40	19.6%	19.6%	40.0%	89.68%	1.17	1318.2	136.1	2537	20	72	525	629	s.g.	
Exp4_41	19.6%	19.6%	40.0%	84.01%	1.05	636.1	101.7	1224	10	83	250	363	s.g.	
Exp4_42	19.6%	19.6%	40.0%	75.75%	0.80	322.4	78.2	621	5	105	126	254	s.g.	
Exp4_43	19.6%	19.6%	60.0%	88.11%	1.03	873.7	103.9	2522	20	80	372	469	s.g.	
Exp4_44	19.6%	19.6%	60.0%	72.72%	0.83	432.9	118.1	1250	10	80	150	288	s.g.	
Exp4_45a	19.6%	19.6%	60.0%	n.a.	n.a.	0.0	n.a.	n.a.	5	never	never	116	s.g.	
Exp4_45b	19.6%	19.6%	60.0%	n.a.	n.a.	213.5	297.3	616	5	never	never	0	s.c.	
Exp4_46	19.6%	19.6%	70.0%	80.10%	0.88	694.1	136.1	2672	21	78	375	425	s.g.	
Exp4_47	19.6%	19.6%	40.0%	82.09%	1.07	1102.2	197.4	2177	17	80	336	545	s.g.	

Table IV - Alaska North Slope Crude Oil
Task #1 In-Situ Burn Results

Exp. No	Vol. Evap (%)	Water Content (%)	Burn Eff. (%)	Burn Rate (mm/min)	Mass Oil (g)	Mass Res. (g)	Vol. Emul. (ml)	Thickness (mm)	Ignition (s)	Intense (s)	Extinction (s)	Ignition Source	Comments
Exp5_1	0%	0%	62.0%	1.14	400.0	148.4	455.6	4	19	111	144	s.g	s.g = 25cm ² soaked gas pad
Exp5_2	0%	0%	83.4%	1.50	1164.1	192.79	1325.9	11	13	316	379	s.g	s.c = 25 cm ² soaked crude ANS pad
Exp5_3	0%	0%	67.8%	1.09	2180.0	705.1	2494.3	20	11	754	784	s.g	f.c = 100 ml of fresh crude ANS
Exp5_4	0%	12.5%	68.6%	1.14	508.2	159.42	681.5	5	22	148	195	s.g	g.g = gelled gas(napalm)
Exp5_5	0%	12.5%	n.a.	n.a.	1052.5	n.r.	1369.9	11	13	240	384	s.g	n.r = not recorded
Exp5_6	0%	12.5%	58.0%	1.00	1914.8	804.91	2492.4	20	16	497	643	s.g	n.a = not applicable
Exp5_7	0%	25.0%	64.0%	1.07	445.0	160.11	675.7	5	20	123	171	s.g	
Exp5_8	0%	25.0%	72.1%	1.04	847.1	236.7	1288.4	10	18	218	347	s.g	
Exp5_9	0%	25.0%	34.3%	0.68	1426.6	937.3	2166.5	17	15	343	424	s.g	
Exp5_10	0%	40.0%	67.2%	1.11	339.8	111.82	645.1	5	33	123	149	s.g	
Exp5_11	0%	40.0%	78.0%	1.47	870.1	140.6	1272.0	10	18	184	220	s.g	
Exp5_12	0%	40.0%	82.8%	1.47	1351.3	232.07	2565.1	20	21	373	453	s.g	
Exp5_13	0%	60.0%	57.8%	0.98	225.6	95.27	642.5	5	28	91	103	s.g	
Exp5_14	0%	60.0%	74.6%	1.49	437.4	111.2	1245.5	10	24	128	148	s.g	
Exp5_15	0%	60.0%	82.2%	1.62	897.6	159.4	2555.9	20	27	243	285	s.g	
Exp5_16	0%	75.0%	10.2%	0.11	140.4	126	639.6	5	40	never	113	s.g	
Exp5_17	0%	75.0%	67.7%	1.23	283.2	91.4	1290.2	10	25	100	113	s.g	
Exp5_18	0%	75.0%	69.4%	2.16	585.3	172.82	2575.3	20	28	110	131	s.g	
Exp5_19	10.8%	0%	67.8%	1.12	588.6	189.7	649.0	5	33	209	220	s.g	
Exp5_20	10.8%	0%	80.8%	1.34	1108.0	214.7	1221.6	10	20	355	371	s.g	
Exp5_21	10.8%	0%	88.3%	1.41	2253.7	283	2484.8	20	21	725	784	s.g	
Exp5_22	10.8%	12.5%	81.3%	1.14	488.8	87.2	588.2	5	50	191	226	s.g	
Exp5_23	10.8%	12.5%	87.7%	1.21	980.2	120.8	1235.1	10	36	317	411	s.g	
Exp5_24a	10.8%	12.5%	63.3%	n.a.	1994.0	731.7	2512.6	20	n.r.	n.r.	411	s.g	
Exp5_24b	10.8%	12.5%	n.a.	n.a.	1945.7	n.r.	2451.7	20	58	607	717	s.g	
Exp5_25	10.8%	25.0%	77.8%	1.16	410.5	91	603.5	5	60	197	205	s.g	
Exp5_26	10.8%	25.0%	88.5%	1.41	841.1	98.64	1238.5	10	50	291	328	s.g	
Exp5_27	10.8%	25.0%	n.a.	1.89	1697.7	n.a.	2495.7	20	50	524	524	s.g	
Exp5_28	10.8%	40.0%	75.5%	1.34	334.1	82	614.0	5	95	173	194	s.g	
Exp5_29	10.8%	40.0%	87.5%	1.38	673.2	84	1237.1	10	75	273	289	s.g	
Exp5_30	10.8%	40.0%	87.8%	1.28	1358.5	166	2496.3	20	60	471	550	s.g	
Exp5_31	10.8%	60.0%	48.8%	0.68	234.1	125	645.3	5	18	95	105	f.c	100 ml
Exp5_32	10.8%	60.0%	74.3%	1.32	449.0	115.4	1237.6	10	114	213	247	s.g	
Exp5_33	10.8%	60.0%	88.6%	1.58	918.3	123	2531.0	20	70	300	335	s.g	
Exp5_34b	10.8%	75.0%	36.4%	0.42	148.0	92.85	643.8	5	18	75	85	s.g	
Exp5_35	17.4%	0%	82.1%	1.38	598.0	105.6	643.0	5	47	220	229	s.g	
Exp5_36	17.4%	0%	83.8%	1.65	1068.0	176.34	1187.8	9	43	307	331	s.g	
Exp5_37	17.4%	0%	88.6%	1.53	2281.0	253	2490.2	20	54	710	747	s.g	
Exp5_38	17.4%	12.5%	79.3%	1.14	488.2	100.82	608.1	5	75	222	252	s.g	
Exp5_39	17.4%	12.5%	82.3%	1.13	861.3	170	1199.4	10	82	421	458	s.g	
Exp5_40	17.4%	12.5%	60.1%	0.73	1993.8	790.7	2475.1	20	83	875	933	s.g	
Exp5_41	17.4%	25.0%	78.4%	1.06	459.2	108.4	688.4	5	80	228	263	s.g	
Exp5_42	17.4%	25.0%	88.6%	1.33	815.2	108.3	1188.6	9	82	332	368	s.g	
Exp5_43	17.4%	25.0%	49.4%	0.81	1715.2	888	2498.8	20	71	none	619	s.g	
Exp5_44	17.4%	40.0%	59.5%	0.58	333.8	135.25	607.4	5	23	163	201	f.c	100 ml
Exp5_45	17.4%	40.0%	88.4%	1.30	682.9	93.07	1242.5	10	247	459	483	s.g	
Exp5_46	17.4%	40.0%	57.9%	0.90	1390.0	584.7	2529.1	20	235	678	703	s.g	
Exp5_47	17.4%	60.0%	49.2%	0.53	228.5	118	623.6	5	24	104	135	f.c	100 ml
Exp5_48	17.4%	60.0%	75.5%	1.31	448.6	110	1227.2	10	189	280	334	s.c	
Exp5_49	17.4%	60.0%	88.4%	1.71	911.3	105.8	2487.2	20	167	280	413	s.g	
Exp5_50	17.4%	75.0%	n.a.	n.a.	148.0	n.r.	637.7	5	22	96	100	f.c	100 ml
Exp5_51	17.4%	75.0%	51.3%	0.53	279.1	138	1218.9	10	18	70	158	f.c	100 ml
Exp5_52	17.4%	75.0%	74.6%	1.04	580.6	148	2535.5	20	31	111	249	f.c	100 ml
Exp5_53a	17.4%	75.0%	70.6%	3.05	580.1	170.6	2533.4	20	324	350	394	g.c	36g placed
Exp5_54	17.4%	75.0%	77.8%	1.87	583.4	129.6	2547.8	20	344	403	484	g.c	28 1g(dropped in one lump)
Exp5_55	17.4%	75.0%	79.7%	1.86	585.6	114.8	2469.7	20	464	507	584	g.c	31 8g(2ml brexitholene-no mix)
Exp5_56	17.4%	75.0%	78.4%	1.38	579.0	119.2	2528.3	12	168	292	342	g.c	33g(2ml brexitholene-2 min. mix)
Exp5_57	17.4%	75.0%	82.7%	1.34	578.1	69.73	2515.9	20	218	347	404	g.c	34 5g(2ml alcopd/toluene-2 min. mix)
Exp5_58	17.4%	75.0%	78.8%	1.25	588.4	125	2569.4	20	170	309	363	g.c	32 1g(2ml alcopd/toluene-2 min. mix)
Exp5_59	17.4%	75.0%	73.2%	1.31	559.7	150.2	2444.0	19	257	360	420	g.c	28 5g(4% ferrocene by weight)
Exp5_60	17.4%	75.0%	52.7%	1.44	588.1	269	2481.0	20	252	310	390	g.c	30g(1ml brexitholene-no mix)
Exp5_61	17.4%	75.0%	100.0%	1.71	579.7	n.r.	2531.3	20	108	160	288	g.c	
Exp5_62	17.4%	75.0%	79.1%	1.48	580.4	121.4	2534.4	20	178	292	340	g.c	
Exp5_63	17.4%	75.0%	75.3%	1.36	576.6	142.4	2518.0	20	208	300	375	g.c	32g(1ml brexitholene-no mix)

APPENDIX B
IGNITION EXPERIMENT RESULTS

Description of acronyms use in tables describing laboratory burn experiments in Appendix B:

Exp. No.	- experiment number to permit cross-referencing to other data files; Avalon = series 2, Statfjord = series 4 and Alaska North Slope = series 5
Vol. Evap.	- volume percent loss to evaporation of the parent oil used to create the emulsion.
Water Content	- volume percent water in the emulsion as created in the bucket/impeller mixer; note that for some unstable oil/water combinations this may be an overestimate of actual water content at ignition.
Burn Eff.	- the mass percent of the oil (i.e., excluding emulsified water) added to the ring, not recovered from within the ring after the burn = (mass of oil added - mass recovered)
Burn Rate	- the regression rate of oil burning from the emulsion slick (i.e., mm of oil per minute) = (mass of oil added - mass of residue)/(extinction time - ignition time).
Mass Oil	- the mass of oil added to the test pan (excluding emulsified water).
Mass Residue	- the mass of residue recovered from the test pan including emulsion water, if any; it was assumed that successful burns involved the breaking of the emulsion and that the residue was composed primarily of unburnt oil. Visual observations confirmed this.
Vol. Emul.	- the volume of emulsion added to the test pan for the burn.
Thickness	- the calculated (volume/area) of emulsion added to the test pan for the burn.
Ignition	- the ignition time for each burn (time to "full involvement") defined as the time for the flames to cover the entire slick surface.
Extinction	- the elapsed time to extinguishment of the burn.
Ignition Source	- the type of ignition that finally resulted in successful ignition of the candidate emulsion; s.g. = 25 cm ² gasoline-soaked sorbent pad; f.c. = fresh (i.e., unweathered crude added on top of emulsion - 100 or 200 mL - mass noted in Comments column); g.g = gelled gasoline; g.g.f. = gelled gasoline with 4 wt% ferrocene added; g.g.f.b. = gelled gasoline with 4 wt% ferrocene and emulsion breaker (brand and application techniques noted in Comments); n.r. = not recorded; n.a. = not applicable (i.e., no technique was successful in igniting the oil).

IGNITION TEST RESULTS

Avalon Crude Oil (Series 2)

Exp. No	Vol. Evap (%)	Water Content (%)	Burn Eff. (%)	Burn Rate (mm/min)	Mass Oil (g)	Mass Res. (g)	Vol. Emul. (ml)	Thickness (mm)	Ignition (s)	Intense (s)	Extinction (s)	Ignition Source	Comments
Exp2_31a	20.7%	25.0%	84.6%	0.493	660.2	101.6	973.8	9.1	27	never	63	f.c.	91.8g
Exp2_31b	20.7%	25.0%	75.0%	0.489	347.3	86.9	512.3	4.8	33	never	707	f.c.	104g
Exp2_32	20.7%	25.0%									356	f.c.	171.8g
Exp2_33a	12.7%	40.0%	n.a.				1979.8	18.4	16	never	212	f.c.	81.5g
Exp2_33b	12.7%	40.0%							212	g.g.	n.a.	g.g.	165.4g
Exp2_31-A	0.0%	40.0%							n.r.	g.g.	n.a.	g.g.	32 g
Exp2_31-B	0.0%	40.0%							n.r.	g.g.	n.a.	g.g.	30g(2 ml alcopol/toluene-2 min. mix)
Exp2_31-C	0.0%	40.0%	85.1%	0.550	1346.3	200.93	2541.2	20.2	19	never	1075	g.g.	200 ml
Exp2_32-A	0.0%	40.0%							n.r.	g.g.	433	g.g.f.	32 g
Exp2_32-B	0.0%	40.0%	46.5%	0.266	1381.8	739.7	2608.2	20.8	18	never	0	f.c.	166.8g
Exp2_33-A	0.0%	40.0%							34	never	480	f.c.	172.9g
Exp2_33-B	0.0%	40.0%							28	n.r.	615	g.c.f.b.	40.8g
Exp2_33-C	0.0%	40.0%	n.a.				2580.3	20.5	never	never	never	g.g.	166g(2 ml alcopol/toluene-2 min. mix)
Exp2_34a	0.0%	60.0%							20.7	never	never	g.g.	43g
Exp2_34b	0.0%	60.0%	72.1%	0.500	917.5	255.7	2597.7	20.7	270	760	923	g.g.	50g(2 ml alcopol/toluene-2 min. mix)
Exp2_35	0.0%	60.0%	54.6%	0.279	869.3	395	2461.2	19.6	270	n.r.	1110	g.c.	30g(brexit + ferrocene)
Exp2_36	0.0%	60.0%	73.6%	0.609	885.0	233.75	2505.7	19.8	98	571	626	g.g.	39g(ferrocene) + dropwise
Exp2_37	12.7%	40.0%	82.2%	0.700	1388.0	246.51	2584.0	20.6	180	780	1006	g.g.	37g(alcopol-2 min. mix)
Exp2_38	12.7%	40.0%	55.9%	0.425	1339.0	590.6	2496.3	19.9	300	1175	1194	g.g.	36g(ferrocene + alcopol + mix)
Exp2_39	12.7%	40.0%	76.3%	0.694	1389.7	329.3	2590.9	20.6	700	1140	1475	g.c.	39g(alcopol-2 min. mix)
Exp2_40	12.7%	60.0%	62.4%	0.493	842.3	317	2355.5	18.7	480	960	1009	g.c.	36g(alcopol-2 min. mix)
Exp2_41	12.7%	60.0%	57.5%	0.401	877.3	372.6	2453.2	19.5	256	790	880	g.c.	44g(ferrocene-alcopol-mix)
Exp2_42	12.7%	60.0%	67.9%	0.393	884.7	284	2474.0	19.7	113	660	871	g.c.	many attempts

g.g.=gelled gas(napalm)
g.g.f.=napalm(4%wt. ferrocene)
g.g.f.b.=g.g.f.+1 ml brexit/30 g.g.f.
n.r.=not recorded
n.a.=not applicable(residue>mass oil or n.r.)

Statfjord Crude Oil (Series 4)

Exp. No	Vol. Evap (%)	Water Content (%)	Burn Eff. (%)	Burn Rate (mm/min)	Mass Oil (g)	Mass Res. (g)	Vol. Emul. (ml)	Thickness (mm)	Ignition (s)	Intense (s)	Extinction (s)	Ignition Source	Comments
Exp4_72a	30.6%	75.0%	71.28%	1.09	295.5	84.87	1342	11	24	never	150	g.g.=gelled gas g.c.=gelled crude f.c.(ANS)	21.4 g
Exp4_72b	30.6%	75.0%								80	135	g.g.	154.38 g
Exp4_72c	30.6%	75.0%	70.83%	1.20	569.8	166.2	2587	21	142	never	163	g.g.	30 ml
Exp4_73a	30.6%	75.0%								176	325	g.c.	25.4g
Exp4_74a	30.6%	75.0%								never	142	g.c.	19.4g
Exp4_74b	30.6%	75.0%								never	427	g.c.	26.2g
Exp4_74	30.6%	75.0%	65.12%	0.53	269.7	94.1	1225	10	10	135	190	f.c.	179.7g(5% by wt. Bunker C)
Exp4_75	30.6%	75.0%	55.53%	0.62	554.8	246.7	2519	20	20	30	289	f.c.(ANS)	167.5ml(5% by wt. Bunker C)
Exp4_76	30.6%	75.0%	57.03%	0.42	561.6	241.3	2550	20	81	225	498	g.g.	18.8g(2ml alcopol/toluene-1 min. mix)
Exp4_77	30.6%	75.0%	64.30%	0.50	532.5	190.1	2418	19	210	480	581	g.c.	25.3g(2ml alcopol/toluene-3 min. mix)
Exp4_78	30.6%	75.0%	76.77%	2.32	541.2	125.69	2457	20	421	313	518	g.c.	29.8g(2ml alcopol/toluene-dropped)
Exp4_79	30.6%	75.0%	79.42%	1.26	573.9	118.1	2606	21	439	479	635	g.c.	24.7g+33.9g
Exp4_80	30.6%	75.0%	72.42%	0.93	588.3	162.25	2671	21	365	300	613	g.c.+g.c.	29.6g
Exp4_81	30.6%	75.0%	58.80%	0.68	573.6	236.3	2604	21	370	546	638	g.c.	21.3g(2 ml alcopol/toluene)
Exp4_82	30.6%	75.0%	71.20%	0.92	538.8	155.2	2446	19	390	562	617	g.c.	29.98g(2 ml brexit/toluene, unmixed)
Exp4_83	30.6%	75.0%	n.a.									g.c.(4%ferrocene)=g.c.f.	29.98g(2 ml brexit/toluene, unmixed)
Exp4_84	30.6%	75.0%	79.02%	1.62	586.8	123.1	2664	21	580	660	735	g.g.	30.73g(2 ml brexit/toluene, unmixed)
Exp4_85	30.6%	75.0%	78.73%	1.27	523.7	111.4	2378	19	474	610	650	g.g.	28.72g(2 ml brexit/toluene, unmixed)
Exp4_86	30.6%	75.0%	69.20%	1.07	562.7	173.3	2555	20	315	336	515	g.c.(4%ferrocene)=g.c.f.	28.3g(bag placed not dropped)
Exp4_87	30.6%	75.0%	76.33%	0.53	532.6	126.1	2418	19	375	721	792	g.c.(4%ferrocene)=g.c.f.	crude has 1 ml brexit/30 ml oil
Exp4_88	30.6%	75.0%	81.09%	1.73	563.7	106.6	2559	20	304	415	447	same as above g.c.f.b.	5% Bunker C
Exp4_89	30.6%	75.0%	75.68%	0.66	553.4	134.7	2513	20	10	365	413	f.c.(200 ml)	10% Bunker C

APPENDIX C
EMULSION BREAKER EXPERIMENT RESULTS

EMULSION BREAKER TESTING

EMULSION BREAKING--ALCOPOL-070 PG

Flask	Emulsion Volume (ml)	Demulsifier Added (ul)	Height Oil I. (mm)	Height Oil F. (mm)	Mass Grad Cyl. - M (g)	M+ Tol (g)	M+ Tol+ Oil (g)	Mass Bkr M' (g)	M+ Sample (g)	M+ Samp+ Tol (g)	Transmitt (%)	Absorbance	Conc In Beaker	Conc In Grad Cyl	Mass Oil Grad Cyl (g)	Mass Oil/ gram Sample	Sample (% Water)
1	20	0	8	7	130.25	150.83	152.34	112.25	114.47	176.74	43	0.3665	0.0008	0.0207	0.4562	0.3021	0.6979
2	20	40	8	4	131.95	152.37	153.54	112.10	114.22	172.89	15.1	0.8210	0.0018	0.0456	0.9838	0.8408	0.1592
3	20	20	8	4	122.71	143.81	144.93	112.00	114.47	209.16	29.7	0.5272	0.0011	0.0418	0.9280	0.8285	0.1715
4	20	8	8	5	133.01	153.68	154.75	112.07	114.63	169.07	13.4	0.8729	0.0019	0.0370	0.8934	0.7508	0.2492
5	20	4	8	5	131.75	152.52	153.57	112.02	114.30	170.58	36.2	0.4413	0.0010	0.0216	0.4721	0.4496	0.5504
6	20	4	8	6	134.11	155.09	156.01	112.09	114.39	160.71	19	0.7212	0.0016	0.0284	0.6220	0.6761	0.3239
7	10	10	4	2	130.10	150.10	151.18	112.07	114.42	170.12	17.7	0.7520	0.0016	0.0355	0.7491	0.6936	0.3064

75% WATER - 25% OF 30.6% EVAP STATFORD

EMULSION BREAKING--BREAKIT OE

Flask	Emulsion Volume (ml)	Demulsifier Added (ul)	Height Oil I. (mm)	Height Oil F. (mm)	Mass Grad Cyl. - M (g)	M+ Tol (g)	M+ Tol+ Oil (g)	Mass Bkr M' (g)	M+ Sample (g)	M+ Samp+ Tol (g)	Transmitt (%)	Absorbance	Conc In Beaker	Conc In Grad Cyl	Mass Oil Grad Cyl (g)	Mass Oil/ gram Sample	Sample (% Water)
1	20	0	8	5	132.74	154.46	155.18	117.62	120.53	156.48	14.3	0.8447	0.0018	0.0232	0.5215	0.7243	0.2757
2	20	40	8	5	131.48	150.43	151.37	117.52	119.60	152.27	12.5	0.9031	0.0020	0.0316	0.6278	0.6679	0.3821
3	20	20	8	5	129.82	149.49	150.86	117.57	119.30	174.03	23	0.6383	0.0014	0.0446	0.9380	0.6846	0.3154
4	20	8	8	5	131.63	154.09	155.53	117.64	118.41	141.12	15.8	0.8013	0.0018	0.0532	1.2722	0.8835	0.1165
5	20	4	8	4	131.25	153.05	154.54	117.52	118.41	142.31	12	0.9208	0.0020	0.0554	1.2897	0.8656	0.1344
6	20	2	8	4	133.71	155.41	156.68	117.59	118.78	150.88	19.2	0.7167	0.0016	0.0431	0.9895	0.7791	0.2209
7	10	10	4	2	129.71	151.00	151.62	117.68	119.42	169.70	44.8	0.3487	0.0008	0.0222	0.4864	0.7845	0.2155

75% WATER - 25% OF 30.6% EVAP STATFORD

EMULSION BREAKING--SHELL LA 18

Flask	Emulsion Volume (ml)	Demulsifier Added (ul)	Height Oil I. (mm)	Height Oil F. (mm)	Mass Grad Cyl. - M (g)	M+ Tol (g)	M+ Tol+ Oil (g)	Mass Bkr M' (g)	M+ Sample (g)	M+ Samp+ Tol (g)	Transmitt (%)	Absorbance	Conc In Beaker	Conc In Grad Cyl	Mass Oil Grad Cyl (g)	Mass Oil/ gram Sample	Sample (% Water)
1	20	0	8	4	132.72	154.53	155.30	117.44	122.34	159.02	15	0.8239	0.0033	0.0247	0.5578	0.7214	0.2756
2	20	40	8	4	131.56	152.73	153.66	117.59	120.72	154.34	4.9	1.3098	0.0029	0.0313	0.6915	0.7435	0.2665
3	20	20	8	4	129.83	150.48	151.48	117.48	119.84	178.80	23	0.6383	0.0014	0.0350	0.7577	0.7577	0.2423
4	20	8	8	5	131.62	149.83	151.26	117.52	119.36	152.65	7.1	1.1487	0.0025	0.0453	0.8905	0.627	0.3773
5	20	4	8	4	131.30	152.89	153.83	117.52	120.41	185.51	23.9	0.6402	0.0014	0.0316	0.7114	0.7568	0.2432
6	20	2	8	4	133.74	155.31	155.75	117.46	122.05	165.42	16.6	0.7799	0.0017	0.0161	0.3537	0.8039	0.1961
7	10	10	4	3	129.71	148.77	149.08	117.55	126.47	189.30	16.6	0.7799	0.0017	0.0120	0.2323	0.7495	0.2505

75% WATER - 25% OF 30.6% EVAP STATFORD

EMULSION BREAKING--ENV. CANADA DEMOUSSIFIER

Flask	Emulsion Volume (ml)	Demulsifier Added (ul)	Height Oil I. (mm)	Height Oil F. (mm)	Mass Grad Cyl. - M (g)	M+ Tol (g)	M+ Tol+ Oil (g)	Mass Bkr M' (g)	M+ Sample (g)	M+ Samp+ Tol (g)	Transmitt (%)	Absorbance	Conc In Beaker	Conc In Grad Cyl	Mass Oil Grad Cyl (g)	Mass Oil/ gram Sample	Sample (% Water)
1	20	0	8	4	132.74	155.05	156.88	117.56	119.66	175.78	10.9	0.9626	0.0021	0.0569	1.3733	0.7504	0.2006
2	20	40	8	4	131.49	154.00	155.44	117.71	118.53	153.26	23.2	0.5346	0.0012	0.0505	1.2083	0.8391	0.1609
3	20	20	8	4	129.81	151.34	153.14	117.75	119.20	162.35	11.5	0.9393	0.0021	0.0623	1.4530	0.8072	0.1928
4	20	8	8	4	131.64	153.37	155.25	117.59	119.19	196.38	26	0.5850	0.0013	0.0637	1.5036	0.7998	0.2002
5	20	4	8	4	131.30	152.12	153.50	117.60	118.62	166.92	33.7	0.4724	0.0010	0.0494	1.0902	0.7913	0.2057
6	20	2	8	5	133.76	154.95	156.85	117.79	119.48	186.31	18	0.7447	0.0016	0.0652	1.5046	0.7918	0.2082
7	10	10	4	2	129.72	152.70	153.19	117.61	119.85	142.32	26.9	0.5702	0.0012	0.0128	0.3015	0.6152	0.3648

75% WATER - 25% OF 30.6% EVAP STATFORD

EMULSION BREAKER TESTING

EMULSION BREAKING--ALCOPOL-070 P-8

75% WATER - 25% FRESH AVALON

Flask	Emulsion Volume (ml)	Demulsifier Added (ul)	Height Oil I. (mm)	Height Oil F. (mm)	Mass Grad Cyl. - M (g)	M + Tol. (g)	M + Tol. Oil (g)	Mass Bkr. M' (g)	M' + Sample (g)	M' + Sample Tol (g)	Transmitt. (%)	Absorbance	Conc In Beaker	Conc In Grad Cyl.	Mass Oil Grad Cyl. (g)	Mass Oil/gram Sample	Sample (% Water)
1	20	0	14	13	130.26	150.50	150.99	111.73	113.57	146.71	19.9	0.7011	0.0004	0.0069	0.1439	0.2037	0.7063
2	20	40	14	6	132.02	153.51	154.20	112.11	114.13	165.55	9.8	1.0088	0.0011	0.0276	0.6124	0.8075	0.1125
3	20	20	14	6.5	122.70	144.73	145.47	112.00	113.51	150.41	11.2	0.9508	0.0009	0.0233	0.5305	0.7168	0.2832
4	20	8	14	6.5	133.04	153.74	154.36	112.05	113.80	146.56	13.5	0.8697	0.0008	0.0144	0.3080	0.4967	0.5033
5	20	4	14	9	132.11	152.40	152.90	111.98	113.72	163.57	20.9	0.6799	0.0003	0.0097	0.2021	0.4042	0.5958
6	20	2	14	9	134.08	154.35	155.21	112.06	113.74	161.62	16.8	0.7747	0.0006	0.0159	0.3339	0.3983	0.6117
7	10	10	7	3	130.12	150.45	150.96	112.12	114.62	162.67	10.3	0.9872	0.0010	0.0199	0.4152	0.8140	0.1860

EMULSION BREAKING--BREAKIT OEB-9

75% WATER - 25% FRESH AVALON

Flask	Emulsion Volume (ml)	Demulsifier Added (ul)	Height Oil I. (mm)	Height Oil F. (mm)	Mass Grad Cyl. - M (g)	M + Tol. (g)	M + Tol. Oil (g)	Mass Bkr. M' (g)	M' + Sample (g)	M' + Sample Tol (g)	Transmitt. (%)	Absorbance	Conc In Beaker	Conc In Grad Cyl.	Mass Oil Grad Cyl. (g)	Mass Oil/gram Sample	Sample (% Water)
1	20	0	14	14	130.14	151.41	152.35	114.59	117.74	176.85	19.9	0.7011	0.0004	0.0072	0.1607	0.1709	0.8291
2	20	40	14	6	131.93	152.68	153.81	114.83	116.33	175.18	8.5	1.0706	0.0012	0.0479	1.0478	0.9272	0.0728
3	20	20	14	6	122.84	144.06	144.87	114.80	116.23	162.56	11.5	0.9393	0.0009	0.0300	0.6601	0.8149	0.1851
4	20	8	14	13	133.00	153.44	154.73	115.00	116.43	150.87	14.3	0.8447	0.0007	0.0173	0.3749	0.2906	0.7091
5	20	4	14	9	131.70	152.41	153.43	115.01	116.92	171.97	15.3	0.8153	0.0006	0.0186	0.4052	0.3972	0.6028
6	20	2	14	13	134.06	154.91	155.59	114.93	117.09	173.12	21.8	0.6615	0.0003	0.0077	0.1666	0.2450	0.7550
7	10	10	7	6	130.07	151.51	152.34	114.99	116.44	159.75	19.6	0.7077	0.0004	0.0121	0.2687	0.3238	0.6762

EMULSION BREAKING--ALCOPOL-070

75% WATER - 25% of 12.69% evap. AVALON

Flask	Emulsion Volume (ml)	Demulsifier Added (ul)	Height Oil I. (mm)	Height Oil F. (mm)	Mass Grad Cyl. - M (g)	M + Tol. (g)	M + Tol. Oil (g)	Mass Bkr. M' (g)	M' + Sample (g)	M' + Sample Tol (g)	Transmitt. (%)	Absorbance	Conc In Beaker	Conc In Grad Cyl.	Mass Oil Grad Cyl. (g)	Mass Oil/gram Sample	Sample (% Water)
1	20	0	14	14	130.19	151.59	152.24	113.62	116.55	162.79	18.6	0.7305	0.0005	0.0071	0.1571	0.2417	0.7583
2	20	40	14	11	131.93	151.43	152.30	113.82	116.74	160.30	10.3	0.9872	0.0010	0.0154	0.3139	0.3608	0.6392
3	20	20	14	11	122.71	142.80	143.36	113.91	115.81	145.63	16.8	0.7747	0.0006	0.0087	0.1802	0.3218	0.6782
4	20	8	14	14	133.00	153.83	154.64	113.80	116.07	145.90	13.4	0.8729	0.0008	0.0102	0.2207	0.2735	0.7275
5	20	4	14	14	134.06	154.53	155.03	113.89	116.46	141.54	15.5	0.8097	0.0006	0.0062	0.1302	0.2603	0.7397
6	20	2	14	14	121.65	142.09	142.88	113.97	116.52	145.32	12.2	0.9136	0.0009	0.0099	0.2094	0.2051	0.7349
7	10	10	7	5	130.05	150.20	150.58	113.90	116.01	158.84	20.9	0.6799	0.0003	0.0069	0.1416	0.3227	0.6273

EMULSION BREAKING--BREAKIT OEB-9

75% WATER - 25% of 12.69% evap. AVALON

Flask	Emulsion Volume (ml)	Demulsifier Added (ul)	Height Oil I. (mm)	Height Oil F. (mm)	Mass Grad Cyl. - M (g)	M + Tol. (g)	M + Tol. Oil (g)	Mass Bkr. M' (g)	M' + Sample (g)	M' + Sample Tol (g)	Transmitt. (%)	Absorbance	Conc In Beaker	Conc In Grad Cyl.	Mass Oil Grad Cyl. (g)	Mass Oil/gram Sample	Sample (% Water)
1	20	0	14	14	130.22	150.68	151.49	113.60	115.65	147.70	16.4	0.7852	0.0006	0.0090	0.1910	0.2358	0.7612
2	20	40	14	10	131.93	151.58	152.42	113.79	115.54	156.45	14.7	0.8327	0.0007	0.0160	0.3277	0.3902	0.6098
3	20	20	14	11	122.73	141.40	142.12	113.78	115.26	150.76	17.2	0.7645	0.0005	0.0127	0.2467	0.3427	0.6573
4	20	8	14	13	133.15	154.82	155.94	113.74	115.58	158.59	15.8	0.8013	0.0006	0.0143	0.3263	0.2914	0.7086
5	20	4	14	13	131.71	151.67	152.29	113.66	116.31	164.86	18.1	0.7423	0.0005	0.0088	0.1804	0.2910	0.7090
6	20	2	14	14	121.69	141.64	143.08	113.61	115.80	145.52	9.6	1.0177	0.0011	0.0149	0.3185	0.2212	0.7288
7	10	10	7	5	130.15	149.57	150.84	113.70	115.56	151.45	8.5	1.0706	0.0012	0.0235	0.4867	0.3832	0.6188

APPENDIX D
RESULTS FROM LABORATORY BURN
EXPERIMENTS WITH FERROCENE

Results from Stafford crude burns with ferrocene

Stafford crude oil: 0% evaporation, 0% water, 29 mm slick

EXP No.	Ferrocene (%)	Soot (g)	Reduction (%)	Burn Eff. (%)	Burn rate (mm/min)	Ignition (s)	Intense (s)	Extinction (s)
4.05	4	0.74	70.0	90	1.6	15	970	1013
4.06	2.00	0.49	80.2	97	1.5	5	1046	1117
4.07	1.00	0.50	79.8	97	1.6	3	958	1027
4.08	0.50	0.55	77.7	97	1.7	1	898	972
4.09	0.25	0.58	76.5	97	1.7	0	901	983
4.10	0.13	0.73	70.4	97	1.7	2	915	1008
4.04	0.00	2.47	0.0	97	1.6	15	1021	1085

Stafford crude oil: 20% evaporation, 25% water, 29mm slick

EXP No.	Ferrocene (%)	Soot (g)	Reduction (%)	Burn Eff. (%)	Burn rate (mm/min)	Ignition (s)	Intense (s)	Extinction (s)
4.56	4	0.47	61.2	81	1	86		1220
4.57	2	0.28	76.9	76	0.9	53	1166	1187
4.60	1	0.25	79.3	90	1.2	58	937	1044
4.61	0.5	0.33	72.7	74	1	44	975	999
4.62	0.25	0.27	77.7	68	0.9	47	840	1018
4.63/64	0.13	0.35	71.1	83	1	49	845	1125
4.55	0	1.21	0.0	93	1.2	53	644	1038

Stafford crude oil: 0% evaporation, 0% water, 29 mm slick

EXP No.	Ferrocene (%)	Soot (g)	Reduction (%)	Burn Eff. (%)	Burn rate (mm/min)	Ignition (s)	Intense (s)	Extinction (s)
4.29	0.00	1.25						
4.29	0.00	2.22						
4.29	0.00	0.86		95	1.9	21	874	920
4.30	3.00	0.34	72.8					
4.30	3.00	0.60	73.0					
4.30	3.00	0.14	83.7	86	1.9	2	930	967

Exp 4.29 0% Ferrocene			Exp 4.30 3% Ferrocene			
Time frame	Total soot (g)	Soot (mg/s)	Time frame	Total soot (g)	Soot (mg/s)	Reduction (%)
1:30-4:00	1.25	8.3	1:30-4:00	0.34	2.3	72.3
7:00-12:00	2.22	7.4	7:00-12:00	0.6	2.0	73.0
12:30-15:20	0.86	5.1	12:30-16:07	0.14	3.8	25.5

Results from Avalon crude burns with ferrocene

Avalon crude oil: 0% evaporation, 0% water, 29 mm slick

EXP No.	Ferrocene (%)	Soot (g)	Reduction (%)	Burn Eff. (%)	Burn rate (mm/min)	Ignition (s)	Intense (s)	Extinction (s)
1.8	2.35	0.55	74.5				540	834
1.4	2.35	0.57	73.6				480	1038
1.5	1.2	0.68	68.5					990
1.6	0.5	0.79	63.4				480	980
1.7	0.25	0.75	65.3				420	930
1.3	0	2.16	0.0				810	1032